Synergism from combination of platinum drugs and selected phytochemicals in colorectal cancer

Hana Faisal Bali

A thesis submitted in fulfillment of the requirements for the

Degree of Doctor of Philosophy

Discipline of Biomedical Science

Faculty of Medicine

University of Sydney, Australia

March, 2018

Declaration

I, the author of the thesis, declare that none of the material in this thesis has been previously submitted by me or any other candidate for any degree to this or any other university.

Hana Faisal J Bali

Acknowledgement

Submission of a PhD thesis is not a simple task and this thesis is the product of the support from a network of people (Thanks God).

I would like to express my sincere gratitude to my supervisor Associate Professor Dr Fazlul Huq for his support, guidance, encouragement and motivation. At all stages in my research project I benefited from his advice and his careful editing contributed enormously to the production of this thesis. It would never have been possible for me to take this work to completion without him, he has assisted me in building on both my experience and my confidence in my own abilities.

I would like to thank my Auxiliary Supervisor Associate Professor Dr Philip Beale for his support during the project.

Also, I would like to thank King Abdullah Scholarship Scheme which sponsored me and gave me this great opportunity to do such an exciting project and have a very rewarding experience.

Also, a special thank you to Dr Jun Qing Yu for all your invaluable help, for being so approachable, for encouraging me, helping in the lab and being a very nice to me during my hard time.

Furthermore, I would like to thank the Australian Proteome Analysis Facility (APAF) for the proteomic assistance. And thank you to all my friends in the laboratory Meher, Zynab, Laila, Abir, Safi, Anwar, Nur, Muhammed, Yahya and everyone else I met along the way!

I would like also to acknowledge the heart-felt love and prayers from my Father. And thank you to my husband Fahad Othman for his continual support, patience, faith, kindness and love throughout my journey. Thank you too to my rest of my family and my family in-law for their understanding of not being with them when they need me.

Finally, I like to say thank you to my friends **Lily Qassem, Nur Alawi, Nwal AL-Zahrani** for their support and help. My friend's encouragement was instrumental to the completion of this thesis.

DEDICATION

With a heart filled with love, happiness and gratitude, I would like to dedicate this thesis

To the fond memory of my mother Refqa Ali Abu Al-jud

To my loving father Faisal Jafar Bali

To my love Fahad Asaad Othman and my angels Lujin, Asaad & Abdulellah.

Contents

ABSTRACT

Colorectal cancer is the second most leading cause of death among all reported cancer mortality. Chemotherapy is the treatment of choice to treat metastasized colorectal cancer patients. Combined administration of drugs having different mechanism of actions has been demonstrated better efficacy than conventional monotherapy. Epidemiological data suggests that consumption of phytochemicals has a great impact in prevention and treatment of colorectal cancer. In this study four phytochemicals including curcumin, colchicine, EGCG and taxol were combined with cisplatin and oxaliplatin in a binary mode at three different concentrations and sequence of administrations against four different colorectal cancer cell lines (HT-29, CACO-2, LIM-1215 and LIM-2405). When oxaliplatin is combined with curcumin or EGCG, the cytotoxic outcome is more synergistically effective than the combination of cisplatin with either phytochemicals in a binary combination. However, cisplatin in combination with colchicine showed greater synergism than that of oxaliplatin with colchicine. Observed synergisms of the combinations were found to be correlated with platinum–DNA binding and cellular accumulations of platinum. DNA damage study indicated that antagonistic combinations were less damaging towards DNA. Proteomic study revealed eleven proteins which displayed significant changes in expression following different drug treatments which were: NPM, ACTB, TBB5, HSP7C, K2CB, GSTP1, GRP78, PSB6, COF1, IDHC and K1C18. Among these proteins NPM and ACTB was considered as antiapoptotic whereas IDHC and K1C18 believed to be proapoptotic.

Abbreviation

ACTB	Actin cytoplasmic 1 protein
6-gin	6-gingerol
AAS	Atomic absorption spectroscopy
Abs	Absorption
ADCD	Autophagy dependent cell death
APAF	Australian Proteomic Analysis Facility
CARM1	Coactivator-associated arginine methyltransferase
CI	Combination indices
Cis	Cisplatin
COF1	Cofilin-1
Col	Colchicine
CRC	Colorectal cancer
CT	Computed tomography
Cur	Curcumin
DACH	Diaminocyclohexane
Dm	Median effect dose
Dm	Medium effect dose
DMF	Dimethylformamide
DMSO	Dimethyl sulfoxide
D_p	Concentration of phytochemical
D_{pt}	Concentration of platinum
DTT	Dithiothreitol
EB	Emulsifying buffer
ED_{50}	median effective dose in 50% of the cell kill
ED_{70}	median effective dose in 70% of the cell kill
ED_{90}	median effective dose in 90% of the cell kill
EDTA	Ethylenediaminetetraacetic acid
EGCG	Epigallocatechin-3-gallate
ERCC1	Excision repair cross-complementing group 1
fa	Affected fraction by the dose
FAP	Familial adenomatous polyposis
FDG-PET	Fluorodeoxyglucose-positron emission tomography
GRP78	78 kDa glucose-regulated protein
GSTP1	Glutathione S transferase P 1
HNPCC	Hereditary nonpolyposis colorectal cancer
HSP7C	Heat shock cognate 71 kDa protein
IC_{50}	Concentration required to kill half of the cells
ICD	Immunogenic cell death
IDHC	Isocitrate dehydrogenase [NADP] cytoplasmic
IEF	Iso-electric focusing
IL	Interleukin

IPG	Immobilized pH gradient
K1C18	Keratin, type I cytoskeletal 18
K2CB	Keratin, type II cytoskeletal 8
LDCD	Lysosome dependent cell death
m	Exponent defining shape of the dose effect curve
MALDI	Matrix Assisted Laser Desorption Ionisation
MMR	Mismatch repair
MPT	Mitochondrial permeability transition
mQ	Ultrapure water
MRI	Magnetic resonance imaging
MS	Mass spectrometry
NaOH	Sodium hydroxide
NER	Nucleotide excision repair
NF-κB	Nuclear factor kappa B
NPM	Nucleolar phosphoprotein B23
Nrf2/Keap1	Nuclear factor erythroid 2-related factor 2/ kelch-like ECH-associated protein-1
OD	Optical density
Ox	Oxaliplatin
PAGE	
PBS	Phosphate-buffered saline
Phyt	Phytochemical
PI	Isoelectric points
PRMT1	Protein arginine methyl-transferase
PSB6	Proteasome subunit beta type-6
Pt	Platinum
r	Reliability coefficient
RCD	Regulated cell death
ROS	Reactive oxygen species
RPMI	Roswell Park Memorial Institute
SDS	Sodium dodecyl sulfate
TAE	Tris-acetate-EDTA
Tax	Taxol
TBB5	Tubulin beta chain
TNF	Tumour necrosis factor
TOF	Time of flight-mass
VEGF	Vascular endothelial growth factor

LIST OF FIGURES

LIST OF TABLES

1 INTRODUCTION

Preamble: Cancer is the main health concern all around the world. Cancer research UK (2014) reports 14.1 million new cases diagnosed, which make it one of the most devastating diseases of our time. This number will increase because of ageing and growth of world population and increasing adaptation to sedentary lifestyle. Colorectal cancer is the second most cancer affecting people in Australia and third (1.23 million) worldwide after the lung (1.61 million) and breast (1.38 million) cancer according to cancer council NSW (2017). More than 41265 new cases of colorectal cancer were detected and around 15903 colorectal cancer deaths occurred in year 2014 worldwide according to the statistical study from the cancer research. Chemotherapy is still in the main stream of the management of colorectal cancer along with surgery and radiotherapy. Platinum drugs such as: oxaliplatin, cisplatin and carboplatin have been extensively used as chemotherapy in treating variety of cancers including colorectal cancer. Specially, oxaliplatin has been incorporated in standard combination therapy of advanced stages of colorectal cancer. In this study oxaliplatin and cisplatin have been combined with selected phytochemicals with the aim of maximizing the antitumour activity without increasing the side effects against colorectal cancer models. This chapter provides brief overview on cancer with special focus on colorectal origin, selected phytochemicals and aim of the present study.

1.1 Hallmarks of cancer

Cancer cells exhibit six hallmarks in their physiology. These are growth signal autonomy, inhibitory signals insensitivity, death programmed cell (apoptosis), metastasis and tissue invasion, sustained angiogenesis (formation of new blood vessels), and limitless replicative potential. In addition, two consequential characteristics genome instability and mutation and tumour-promoting inflammation are currently regarded as enabling attributes of cancer (Hanahan and Weinberg 2011). Carcinogenesis is a multistep process that requires accumulation of several mutations.

1.2 Types of cancer

Currently, over 200 types of cancer have been classified (Chambers, Groom et al. 2002). They are classified either by their tissue of origin or location of first development in the body. Approximately 80- 90% of cancers are classified as carcinomas. Cancer originated from mesoderm cells (such as bone, muscle) is called sarcomas, and cancers of glandular tissue (breast) are named adenocarcinomas (Ying, Dey et al. 2016). Blood cancer is known as leukaemia (liquid cancer), while cancer in lymphatic system is called lymphoma (solid cancer). Based on the anatomical site cancer can be names as lung, breast, ovarian, prostate, brain, pancreatic, oral, colorectal cancer, testicular and so on. Cancers of different origins have distinct features. For example, skin cancer has many characteristics that differ from lung cancer. Whereas ultraviolet radiation from the sun can easily target skin, cigarette smoke can target the cells of the lungs.

1.3 Common causes of cancer

Genetic factors, ageing and hormonal imbalances are regarded as three major internal factors (beyond any control) responsible for cancer. Various external factors such as environment, lifestyle (eg. smoking causes lung cancer, alcohol consumption can cause liver cancer), diet (excessive meat consumption can cause colon cancer), toxic chemicals (eg. benzopyrene in cigarette smoke), radiation (eg. excessive exposure to UV radiation from sun causes skin cancer), viruses (eg. Papilloma virus causes cervical cancer) are also found to be linked to cause various cancers (Stewart and Wild 2017).

1.1 Cell cycle

The trillions of cells that constitute the human body maintain a balance between cell death and division. Both normal and cancer cells multiply themselves through the cell cycle process. The steps and different phases of cell cycle are showed in the Figure 1.1

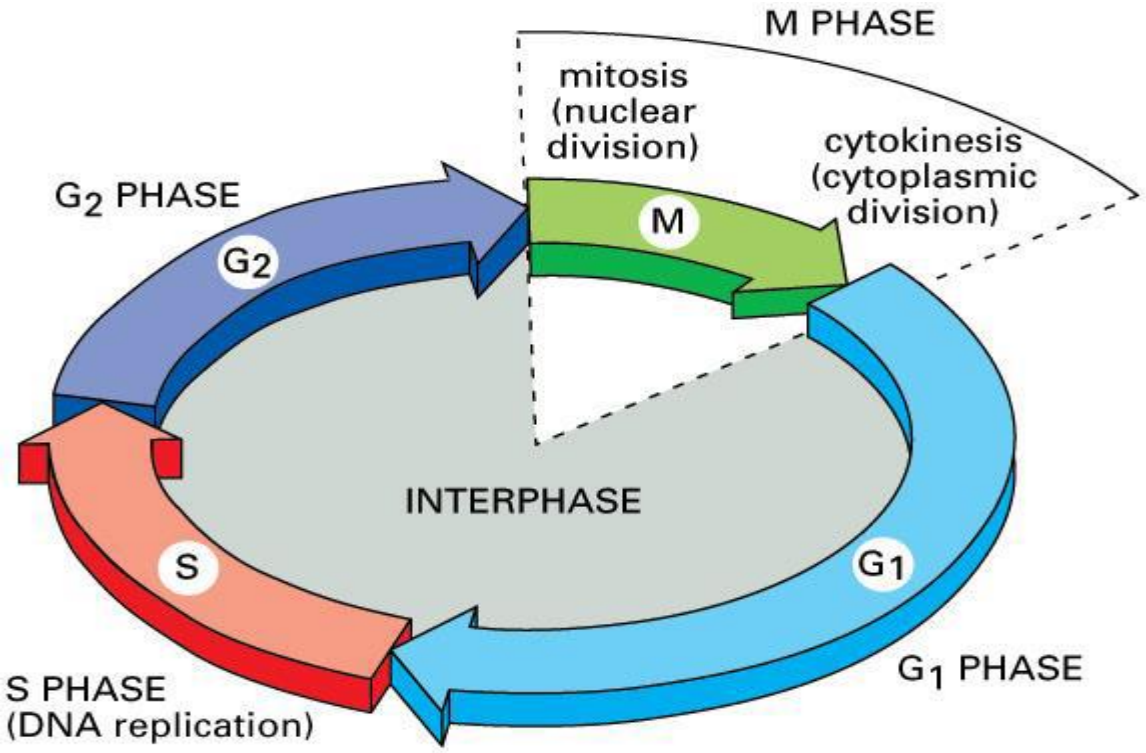

Figure 1.1: The phases of Cell Cycle (Alberts 2002)

There are five steps in overall cell cycle process which are G0, G1, S, G2, and M (Mattanovich, Dragosits et al. 2015). The cells in G0 or resting phase are not yet ready to divide. The length of this stage varies from hours to years depending on cell types. In the G1 phase, the cell prepares to reduce by increasing the production of RNA and protein. This phase lasts twelve to thirty hours and is followed by the phase S. Throughout the phase S, the cell duplicates its DNA, and the purpose of replication is so that the cell division will have the right amount of DNA. This phase continues 6 to 20 hours. The G2 phase is the period right before cell division. During this period, which lasts 2-10 hours, RNA and protein are synthesized. During this phase the fidelity of DNA replication is determined and errors corrected. The last phase is called the M phase or the mitosis that lasts only 30-60 minutes and during which the cell separates

into two new cells. Throughout the cycle there are check-points that regulate progression through the cycle ensuring that each step takes place only once and in the right sequence. The cell must make commitment at the G1 check point to continue into the S-phase, the DNA making step or to halt at G1 and wait until situations are more suitable for cell duplication to happen. Once the commitment is made the cell automatically goes through S, G2 and M to return to G1. If the cell is blocked at S, G2 or M check points it dies. The G1 and S check points are regulated by many gene proteins such as p53, pRb, p15, p16 and cyclins A, D, E and cdk 2, 4 (Ross, Stagliano et al. 2001).

1.4 Cell proliferation

There is a precise balance in normal cells between growth restraining and promoting signals such that proliferation happens only when it is required (Roos, Thomas et al. 2016). The balance shifts when increased numbers of cells are required, such as injury healing and normal tissue turn over. There is slight systematic overlay between the parts inducing proliferation and apoptosis. Somewhat, the two processes are attached at numerous levels across the individual molecular factors responsible for coordinating cell growth. Proliferations of cells in these processes happen in controlled manner and terminate when they are not at all longer needed. However, the process disrupts in tumour cells, and cell proliferation continually occurs and some loss of differentiation also originates (Evan and Vousden 2001).

1.5 Cell death

Cell death is an autonomous and inevitable process of eukaryotes. Broadly cell death can be classified into accidental or regulated. Accidental cell death occurs due to severe exposure of cells with physical, chemical or mechanical stresses e.g. high pressure, extreme pH or shear forces. In contrast, regulated cell death is based on specific molecular signals which can be modulated (Galluzzi, Bravo-San Pedro et al. 2016). Morphologically cell death can be categorized into three types: Type I, Type II and Type III.

Type I cell death is also called apoptosis which is characterized by cell shrinkage, pyknosis, karyorrhexis and membrane blebbing. Type II cell death is also known as autophagy which is manifested by vacuolization, phagocytic uptake and lysosomal degradation. Type III cell death or necrosis is demonstrated by cellular swelling and premature membrane damage (Galluzzi, Vitale et al. 2018). Recent updated classification of different types of cell death recommended by nomenclature committee of cell death is given in figure 1.2.

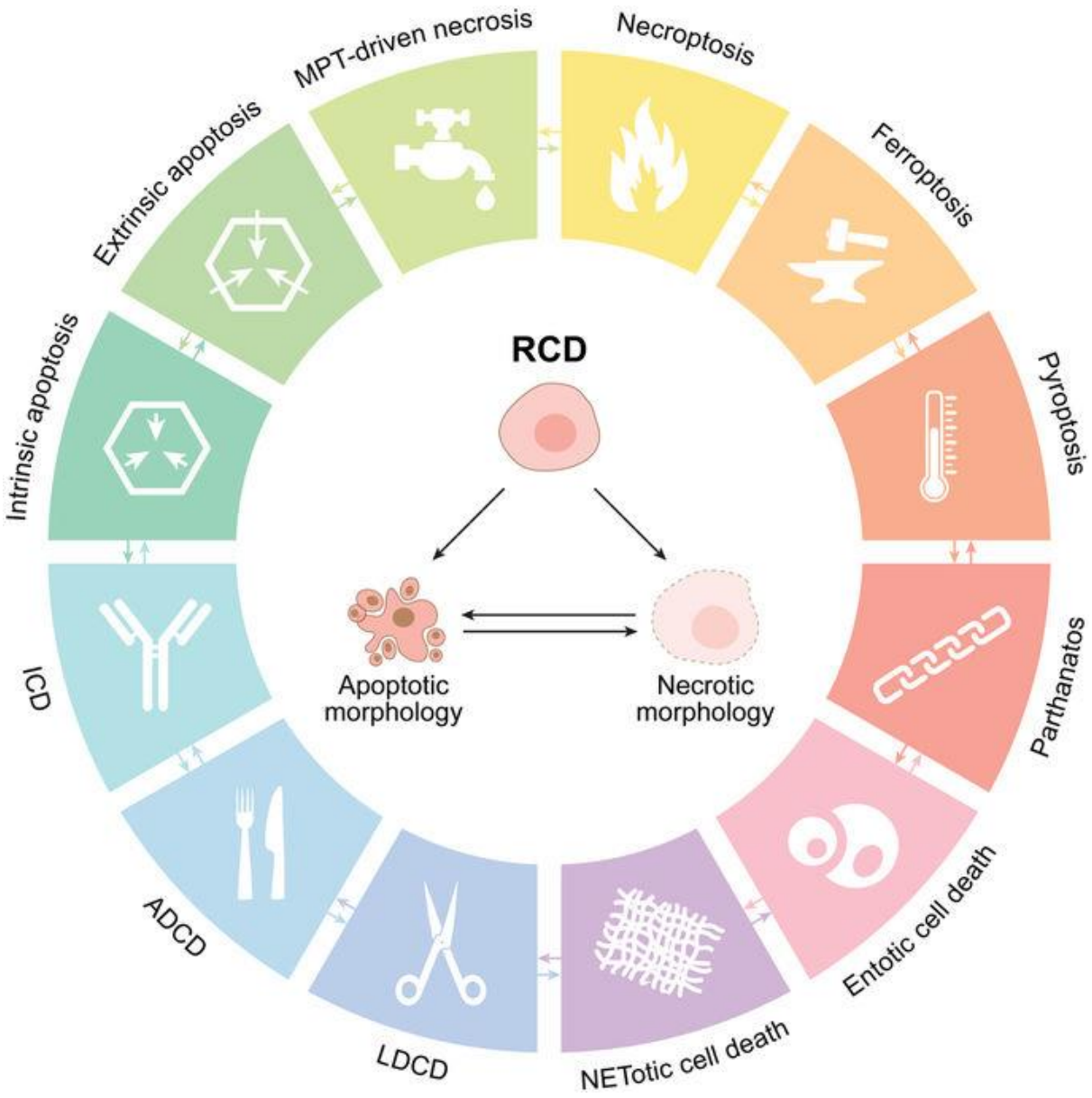

Figure 1.2: Classification of cell death [where RCD= regulated cell death; ICD= immunogenic cell death; ADCD= autophagy dependent cell death; LDCD= lysosome dependent cell death; MPT= mitochondrial permeability transition, adapted from (Galluzzi, Vitale et al. 2018)]

1.6 Oxidative stress and cancer

Life is unimaginable without oxygen and production of reactive oxygen species (ROS) is a continual process in human body. ROS is the byproduct generated from the metabolism of molecular O_2, which includes superoxide ($O_2^{\bullet}$) and hydroxyl radical

(HO•) and nonradical hydrogen peroxide (H_2O_2). The organelle where most of ROS is generated is mitochondria, during ATP synthesis through oxidative phosphorylation. One or two electron reduction instead of four electrons leads towards the formation of $O_2^{\bullet}$ or H_2O_2 which later transformed into other ROS. Cytochrome *P*-450 enzymes and oxidases (peroxisomal, NADPH and xanthine) enzymes can also cause the production of ROS (Mao and Huang 2014, Kumar, Ghosh et al. 2017).

However, increased level of ROS is harmful for the cells and can initiate various disease processes. A homeostasis of ROS in the human body is maintained by several antioxidant systems working simultaneously (Rahal, Kumar et al. 2014). Major antioxidant systems working in human body are: catalases, thioredoxin system, glutathione peroxidases, peroxiredoxins, eosinophil peroxidases and myeloperoxidases. An imbalance in this in vivo homeostasis process cause to the effect called 'oxidative stress'. Generation of oxidative stress is dependent on the available molecular oxygen in the cell, physical or chemical external stimuli and type of the cell/tissue or organ (Sies, Berndt et al. 2017).

Oxidative stress can initiate and maintain the progression of cancer in multiple ways: cause DNA damage and increase the mutagenicity (Gupta, Patel et al. 2014); promote cell survival and proliferation by increasing transcriptional activity (Sies, Berndt et al. 2017); exert prosurvival functions by activating ERK/MEK and PI3K/AKT signal transduction pathways (Oh and Mouradian 2017); and by enhancing invasiveness and metastasis (K Auyeung and K Ko 2017).

Master regulators of oxidative stress are responsible for controlling stimulation/inhibition of redox signalling cycles and to modulating the integrate activity of redox sensing systems. Molecular redox switches which act as master regulators and control diverse biological activities involve mainly Nrf2/Keap1 (nuclear factor

erythroid 2-related factor 2/ kelch-like ECH-associated protein-1) and NF-κB (nuclear factor kappa B) pathway.

When cells undergo stressed conditions whether intrinsic or extrinsic, human body automatically cope the situation via Nrf2-Keap1 pathway dependent antioxidant response. During normal physiologic situations, Keap1 acts as an adaptor of Cul3-based E3 ligase and consequently stimulates Nrf2 degradation. Stimulation of the Nrf2/Keap1 pathway is protective, but over activation can be destructive. With the exposure of extreme oxidative stress, Nrf2 is restricted in the nucleus and regulate carcinogenesis (Kensler, Wakabayashi et al. 2007). After translocating from the nucleus, Nrf2 recruits other transcriptional devices including CREB binding protein (CBP), coactivator-associated arginine methyltransferase (CARM1) and protein arginine methyl-transferase (PRMT1).

NF-κB is a transcription factor having multiple subunits which can stimulate the gene expressions associated with inflammation and immune responses. When cells are exposed to oxidative stress, the inhibitory subunit of the NF-κB inhibitor (IκB) is released and then binds with tumour necrosis factor (TNF) receptor and interleukin (IL)-1 receptor, proceed towards inflammatory response.

1.7 Colorectal cancer (CRC)

CRC is the outcome of successive pathologic changes which alter normal colorectal epithelium into invasive carcinoma. In case of CRC, most of the tumours are found in the distal large intestine while comparatively lesser frequency is observed in proximal regions. CRC usually originate on the intestinal wall as polyps which are benign in nature, but become malignant later on. Initially CRC develops locally into the deeper

layers of the bowel wall and subsequently spread from there to the lymph nodes. And in advanced cases (late stages), it could spread to other organs (Figure 1.3).

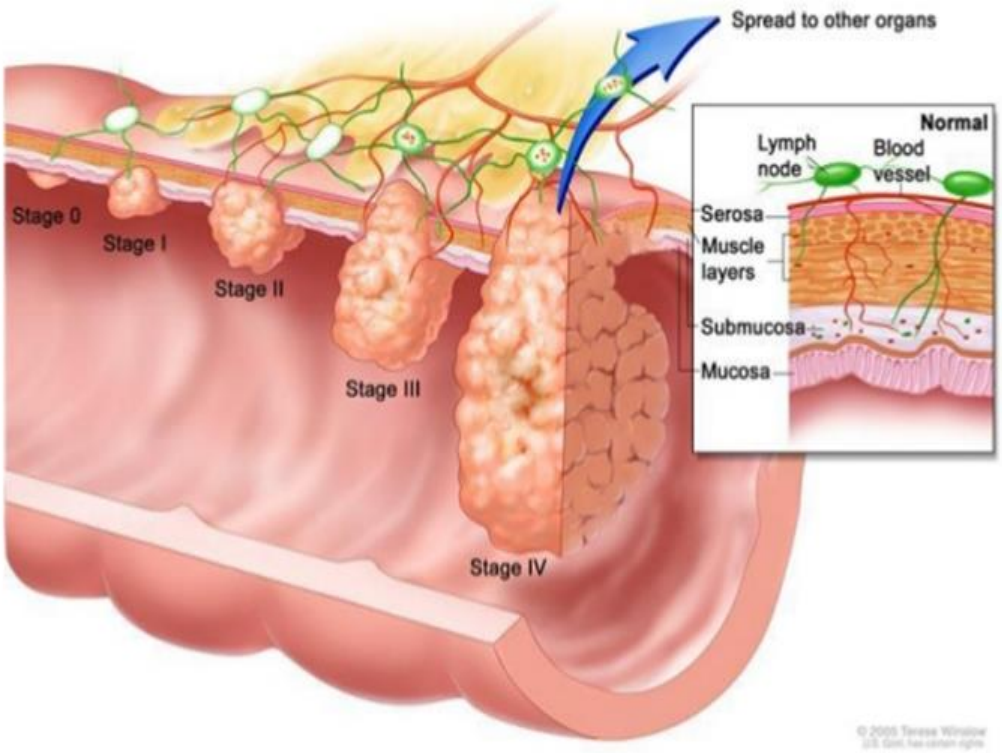

Figure 1.3: Initiation and progression of CRC (reproduced from bowelcanceraustralia.org)

1.7.1 Global incidence and mortality of CRC

Among all different types of cancer, CRC is in third position in respect to commonly diagnosed malignancy and in fourth position in respect to mortality throughout the world. There are approximately 1.4 million new cases and around 0.7 million mortality stated in last GLOBOCAN report (Ferlay, Soerjomataram et al. 2015). The incidence of CRC is higher in developed countries, comprising 75% of all cases compared to lower income regions of the world. Almost 60% of all mortality cases from CRC are from the countries of higher income. However, fast progression in both CRC incidence

and death rate are currently evident in several mid income countries of East Europe, Asia and South America. But, decrease or stability in the new diagnosis and death has been achieved in United States and Oceania regions.

1.7.2 Aetiology of CRC

The exact causes of colorectal cancer are not known, but it has been reported that it needs several mutations in different genes to cause colorectal cancer. Mutation of genes could be categorized into inherited or acquired gene mutations. Epidemiological studies revealed that approximately fifteen percent of CRC occur due to inherited gene mutations (Kinzler and Vogelstein 1996). The most common causes of inherited gene mutations are familial adenomatous polyposis (FAP) and hereditary nonpolyposis colorectal cancer (HNPCC). Human with FAP usually develop 100 to 1000s of adenomas or adenomatous polyps at the age of 30 or more. APC gene is responsible for FAP which is in fact a tumor suppressor gene and mutation of it causes to form benign polyps in the colon. Later on, malignant cancer could develop in one or more of these polyps. In contrast, mutation of HNPCC genes which allow DNA repair is responsible for hereditary nonpolyposis colorectal cancer or Lynch syndrome. Examples of such are MLH1, MSH2, MLH3, MSH6, and PMS1 (Lynch, Smyrk et al. 1996). 2-3% of total CRC is the outcome of the mutation of HNPCC genes.

Most CRC is the consequence of acquired gene mutations which are associated with a number of risk factors, such as: high consumption of red meat, heavy alcohol drinking, obesity, old age, less exercise, inflammatory bowel disease, type-II diabetes, race and ethnicity (Singh, Singh et al. 2014). However, the diets high in vegetables, fruits, and whole grains have shown a decreased risk of colorectal cancer.

1.7.3 Pathogenesis of CRC

After a long term research on the different stages of CRC, Vogelstein suggested a model of colorectal carcinogenesis that is linked with explicit genetic events with changing tissue morphology (Fearon and Vogelstein 1990). This pathogenetic framework through which a normal mucosa is transformed into malignant lesions is called adenoma–carcinoma sequence. Wnt/β-catenin pathway displays a significant role in the initial phase of CRC carcinogenesis. Mutation of the APC gene is a key determinant which stimulates the Wnt pathway through β-catenin. Detail molecular signalling pathways associated with colorectal cancer pathogenesis are vividly depicted in figure 1.5.

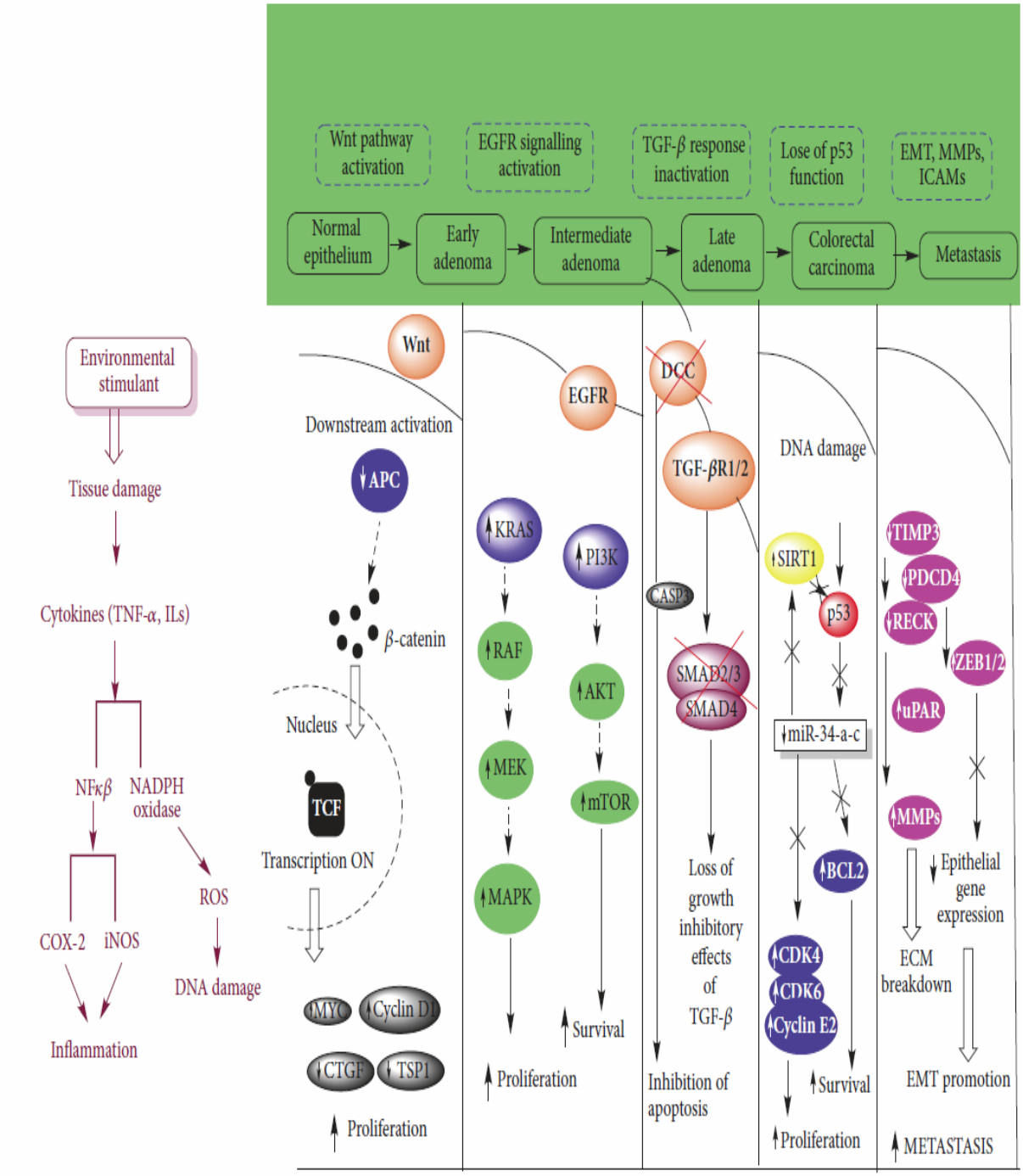

Figure 1.4: Molecular signal transduction pathways involved in CRC pathogenesis [Adapted from(Alam, Almoyad et al. 2018)]

1.7.4 Stages of CRC

In earlier days, CRC was classified by using Dukes method from Dukes A to Dukes D depending on the tumour metastasis. However, clinicians diagnose CRC by combining 'TNM staging' and 'Grade' system (Obrocea, Sajin et al. 2011). In TNM classification, T indicates tumour; N refers to node and M is meant for metastasis. Clinicians diagnose the patient by scanning the question- is there any evidence of tumour and how many layers for determining T. Similarly, for determining N or M: has the tumour disseminated to lymph node or other organs and how much. Grade of CRC is identified from 1 to 4 depending on the differentiation from normal cells and tissues. The higher the grade the worse is the prognosis. CRC staging system adopted by oncologists of USA is given in figure 1.5.

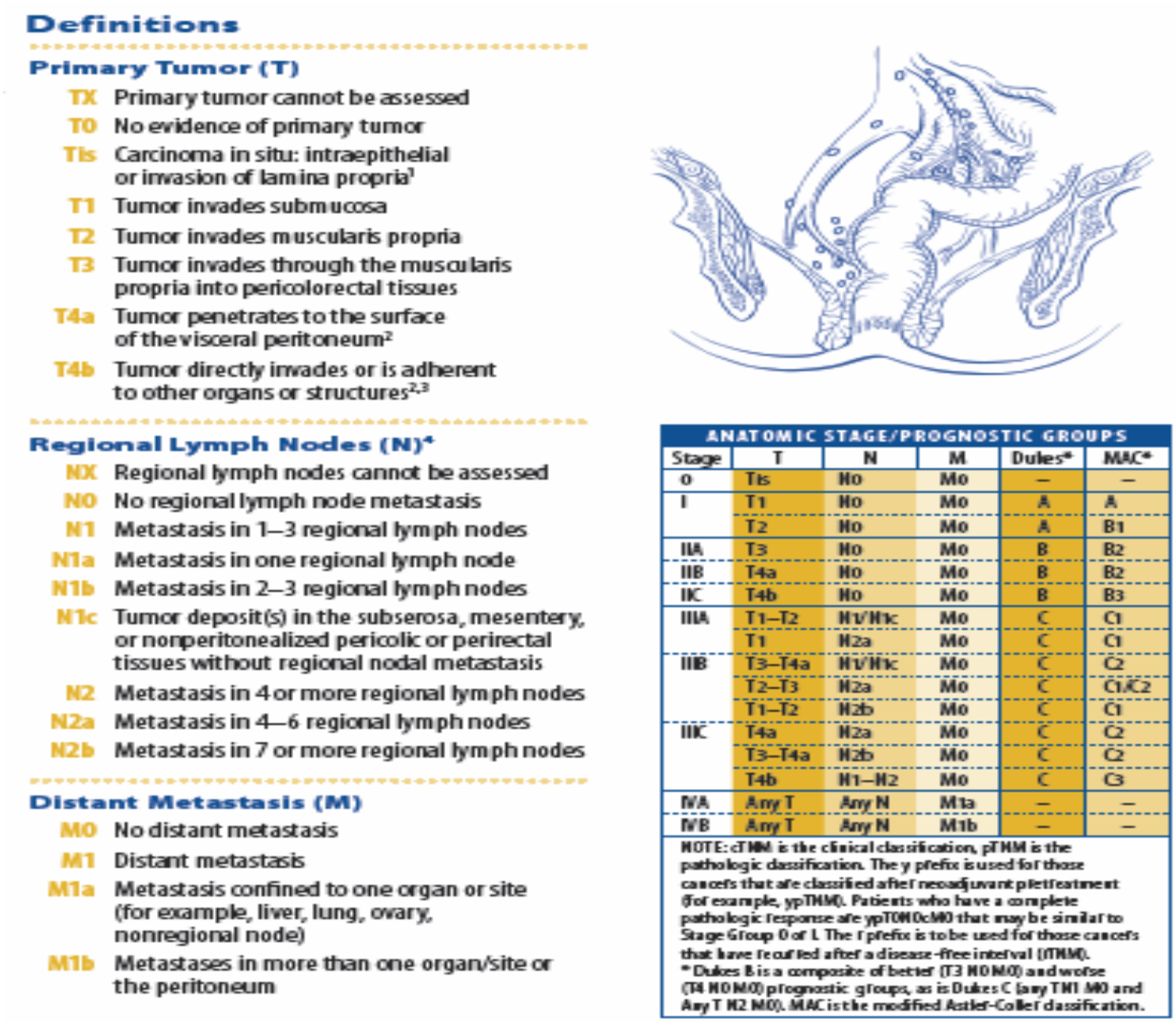

Definitions

Primary Tumor (T)

- TX Primary tumor cannot be assessed
- T0 No evidence of primary tumor
- Tis Carcinoma in situ: intraepithelial or invasion of lamina propria[1]
- T1 Tumor invades submucosa
- T2 Tumor invades muscularis propria
- T3 Tumor invades through the muscularis propria into pericolorectal tissues
- T4a Tumor penetrates to the surface of the visceral peritoneum[2]
- T4b Tumor directly invades or is adherent to other organs or structures[2,3]

Regional Lymph Nodes (N)[4]

- NX Regional lymph nodes cannot be assessed
- N0 No regional lymph node metastasis
- N1 Metastasis in 1–3 regional lymph nodes
- N1a Metastasis in one regional lymph node
- N1b Metastasis in 2–3 regional lymph nodes
- N1c Tumor deposit(s) in the subserosa, mesentery, or nonperitonealized pericolic or perirectal tissues without regional nodal metastasis
- N2 Metastasis in 4 or more regional lymph nodes
- N2a Metastasis in 4–6 regional lymph nodes
- N2b Metastasis in 7 or more regional lymph nodes

Distant Metastasis (M)

- M0 No distant metastasis
- M1 Distant metastasis
- M1a Metastasis confined to one organ or site (for example, liver, lung, ovary, nonregional node)
- M1b Metastases in more than one organ/site or the peritoneum

ANATOMIC STAGE/PROGNOSTIC GROUPS

Stage	T	N	M	Dukes*	MAC*
0	Tis	N0	M0	–	–
I	T1	N0	M0	A	A
	T2	N0	M0	A	B1
IIA	T3	N0	M0	B	B2
IIB	T4a	N0	M0	B	B2
IIC	T4b	N0	M0	B	B3
IIIA	T1–T2	N1/N1c	M0	C	C1
	T1	N2a	M0	C	C1
IIIB	T3–T4a	N1/N1c	M0	C	C2
	T2–T3	N2a	M0	C	C1/C2
	T1–T2	N2b	M0	C	C1
IIIC	T4a	N2a	M0	C	C2
	T3–T4a	N2b	M0	C	C2
	T4b	N1–N2	M0	C	C3
IVA	Any T	Any N	M1a	–	–
IVB	Any T	Any N	M1b	–	–

NOTE: cTNM is the clinical classification, pTNM is the pathologic classification. The y prefix is used for those cancers that are classified after neoadjuvant pre-treatment (for example, ypTNM). Patients who have a complete pathologic response are ypT0N0cM0 that may be similar to Stage Group 0 or I. The r prefix is to be used for those cancers that have recurred after a disease-free interval (rTNM).
* Dukes B is a composite of better (T3 N0 M0) and worse (T4 N0 M0) prognostic groups, as is Dukes C (any T N1 M0 and Any T N2 M0). MAC is the modified Astler-Coller classification.

Figure 1.5: CRC staging system proposed by American joint committee of cancer

1.7.5 Diagnosis and management of CRC

Common symptoms of CRC are abdominal pain, rectal bleeding, irritable bowel syndrome, constipation or diarrhoea (Vega, Valentín et al. 2015). Physicians usually diagnose CRC by computed tomography (CT) scan, magnetic resonance imaging (MRI) or ultrasonography. In addition, recently developed technique

fluorodeoxyglucose-positron emission tomography (FDG-PET) scan is now gaining popularity among the doctors for CRC diagnosis.

Like all other cancers, primary treatment methods of CRC are: surgery, cryosurgery, stereotactic body radiation therapy, radiofrequency ablation and chemotherapy. Surgery is a gold standard for the treatment of localized colorectal cancer. In most of newly diagnosed cases (80%) required surgery. The principles of this surgery are isolation the tumor, removal of all tissue having cancer cells, removal of regional lymph nodes, and maintain the organ function. Cryosurgery is mainly used when cancer cells metastasize to liver of CRC patients. The probe perfused with liquid nitrogen to produce an ice ball within the liver having predictable thermal zones ranging from –40°C to 0°C. Tumour cells die at –20°C to –40°C due to the disruption of the cell membranes (Pathak, Jones et al. 2011).

Radiotherapy can be used alone or with surgery and chemotherapy. Stereotactic body radiation therapy provides accurate delivery of a very high dose of radiation to tumour cells, sparing normal adjacent tissues (Nosher, Ahmed et al. 2015). In contrast, radiofrequency ablation therapy utilizes an electrode probe to kill cancer cells. A thin electrode probe is placed within the metastasized organ under ultrasound control. After positioning the tip array, an electrical current is applied (in the range of 350–500 kHz), generating heat (80–100°C) that kills the cancer cells (Nosher, Ahmed et al. 2015).

Chemotherapy is the treatment of choice for advanced stages of CRC when tumours have been metastasized into other organs of the body. Examples of FDA approved drugs to treat colorectal cancer are capecitabine, oxaliplatin, 5-fluorouracil, irinotecan and trifluridine. Combination therapy with FOLFOX (5-fluorouracil, leucovorin plus oxaliplatin) and FOLFIRI (5-fluorouracil, leucovorin plus irinotecan) is the most

popular due to their high efficacy (Souglakos, Androulakis et al. 2006, Wang, Dong et al. 2015).

1.8 Platinum metal based chemotherapy

Serendipitous discovery of cisplatin during 1970s explore a new horizon of the treatment of cancer using platinum metals. Several thousands of platinum antitumour drugs have been designed and it is hard to find a cancer hospital today which is not using platinum based drugs. Among all platinum analogues only cisplatin, oxaliplatin and carboplatin are used globally by the clinicians. Nedaplatin has been locally approved to be used in the clinic as anticancer drug in Japan, while lobaplatin has approved for China and heptaplatin in Korea. Since cisplatin and oxaliplatin has been used in this study in combination with selected phytochemicals against colorectal cancer models brief description on cisplatin and oxaliplatin is given in following sections.

1.8.1 Cisplatin

Chemically cisplatin is cis-diamminedichloroplatinum (II) which was discovered by Peyrone in 1845 as Peyrone's salt. But antitumour activity of cisplatin was unknown until Barnett Rosenberg identified during conducting experiments to measure the effect of electrical currents on the cell growth of the bacteria Escherichia coli (Muggia, Bonetti et al. 2015). Afterward, Hill's group has carried out the first clinical studies which reported to demonstrate cisplatin efficacy against several human malignancies, and it get the first approved for clinical use in the USA in 1978.

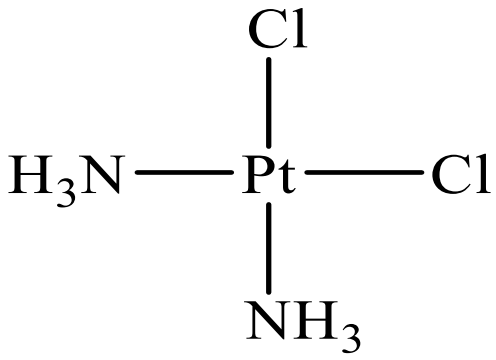

Figure 1.6: Chemical structure of cisplatin

Cisplatin has shown the highest successful rates and it is the preferred therapy for many cancers such as testicular, urothelial, lung, and gynecological. Specifically, successful application of cisplatin has resulted testicular cancer as the most curable solid tumour (Amidi, Hosseini et al. 2017). Besides, cisplatin is also given during the treatment of metastatic tumours such as: breast cancer, melanoma, prostate cancer and mesothelioma.

1.8.1.1 Mechanism of action of cisplatin

Cisplatin is usually administered through intravenous injection. After entering into cells from blood into the cells, aquation of cisplatin takes place which converts cisplatin into its active form. In this aquation process chloride groups are being replaced by water molecules due to lower concentration of chlorine inside the cell compared to extracellular fluid. The generated active species then binds with RNA, DNA and proteins. But cytotoxicity is the outcome of Pt–DNA binding, predominantly bifunctional and monofunctional adducts (Zamble and Lippard 2006). Cisplatin binds to the N(7) position of adenine or guanine bases, forming primarily 1,2-d(GpG) and 1,2-d(ApG) intrastrand cross-links which is about 90% of total DNA adducts. The rest

of the adducts are due to 1,3-d(GpNpG) intrastrand, interstrand and protein-DNA cross-links (Lepre and Lippard 1990, Comess and Lippard 1993).

DNA damage that is caused thorough binding of cisplatin is then recognized by downstream proteins which activate various signalling pathways leading towards cell death unless the damage is repaired. The important proteins that recognize the DNA damage caused by cisplatin binding and involved in apoptotic programmed cell death are: Casp-8, Fas/FasL, p53, ATR, Chk2, MAPK and c-Abl. Schematic representation of the subsequent events causing tumour cell death is given in figure 1.7.

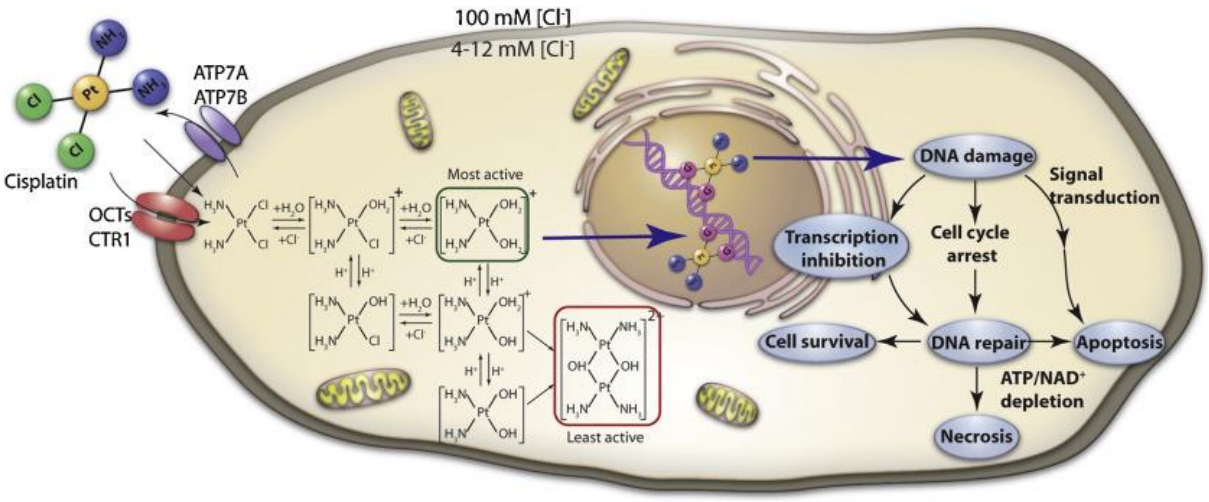

Figure 1.7: Mechanism of action of cisplatin [Adapted from(Ma, Xiao et al. 2015)]

1.8.1.2 Limitations of cisplatin

The major limitation of cisplatin as anticancer drug is its numerous adverse effects and drug resistance. Administration of cisplatin into cells does not only kill the tumour cells but also other highly proliferating normal cells without showing any selectivity. The most common side effects are nephrotoxicity, ototoxicity, gastrotoxicity, immunosuppression and hypersensitivity (Wilmes, Bielow et al. 2015).

Drug resistance, particularly during the relapse of cancer is another aspect which served to limit the use of cisplatin against cancer. Mechanism of cisplatin resistance could be attributed to increased drug efflux from the cell, decreased uptake into the cell, increased deactivation through glutathione and increased DNA repair by nucleotide excision repair (NER) and mismatch repair (MMR) proteins (Galluzzi, Vitale et al. 2014). Among NER proteins the most important for cisplatin resistance is the mutation of excision repair cross-complementing group 1 (ERCC1), whereas *mutS* homolog 2 and *mutS* homolog 1 are from MMR proteins (Aebi, Kurdi-Haidar et al. 1996, Friboulet, Olaussen et al. 2013).

1.8.2 Oxaliplatin

Oxaliplatin is a third generation platinum drug having a bulky diaminocyclohexane (DACH) moiety and the oxalate as leaving group. Chemical name of oxaliplatin is (trans-R,R-1,2-diaminocyclohexane)oxalateplatinum(II) and its chemical structure is shown in figure 1.8. Due to the presence of oxalate in its structure, oxaliplatin undergoes rapid hydrolysis to give its reactive metabolite.

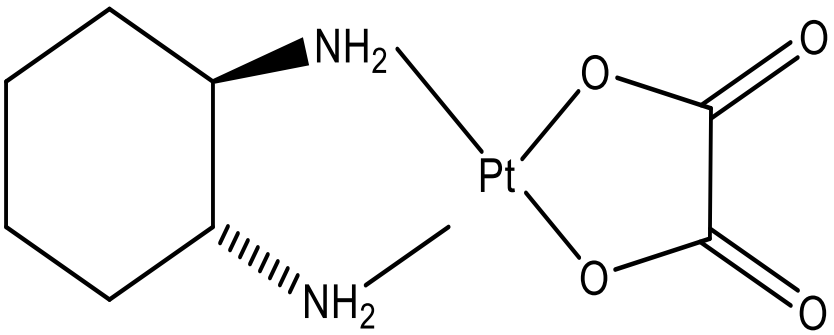

Figure 1.8: Chemical structure of oxaliplatin

The activity profile of oxaliplatin is similar to cisplatin and carboplatin but shows sensitivity towards those cancers where the later drugs prove to be resistant. Moreover,

oxaliplatin is significantly active against colorectal cancer and it has been used in clinic in combination with 5-fluorouracil, folinic acid and capecitabine (Perego and Robert 2016).

1.8.2.1 Mechanism of action of oxaliplatin

Alike to cisplatin and carboplatin, primary target of oxaliplatin is DNA, particularly N (7) of purine nucleotides and it forms both intra- strand, inter-strand and DNA-protein cross-links. However, oxaliplatin is more potent than other approved platinum drugs and it requires fewer adducts to produce same effects (Cvitkovic 1998). Although inter-strand adducts play a significant contribution in cisplatin cytotoxicity, but it is proved to be less important in regards to the mode of action of oxaliplatin (Zwelling, Anderson et al. 1979, Woynarowski, Faivre et al. 2000). Although it is obvious that oxaliplatin cause to form DNA-protein cross links and results into disruption of enzymes as well as other proteins, those cross links are not associated with the killing of tumour cells. Moreover, in contrast to cisplatin the formed monoadducts of DNA from binding with the bio-transformed metabolites of oxaliplatin do not show any lethality towards cancer cells (Di Francesco, Ruggiero et al. 2002).

DNA lesions from binding with metabolites of oxaliplatin cause to trigger downstream proteins to enter into the pathways for programmed cell death. It includes the activation of caspase-3, followed by translocation of Bax into mitochondria and release of cytochrome-C in cytoplasm (Arango, Wilson et al. 2004). Due to significant cytotoxicity of oxaliplatin towards cisplatin resistant cells, it has been presumed that oxaliplatin adducts are unique which can not be recognized by MMR proteins (Alcindor and Beauger 2011). In addition to DNA-lesion mediated apoptosis, oxaliplatin can also cause apoptotic cell death by inhibiting DNA and RNA synthesis, initiating

immunogenic reactions (Fischel, Formento et al. 2002, Todd and Lippard 2009, Tesniere, Schlemmer et al. 2010). Figure 1.9 summarizes the important mode of action of oxaliplatin (DNA lesion mediated cell death).

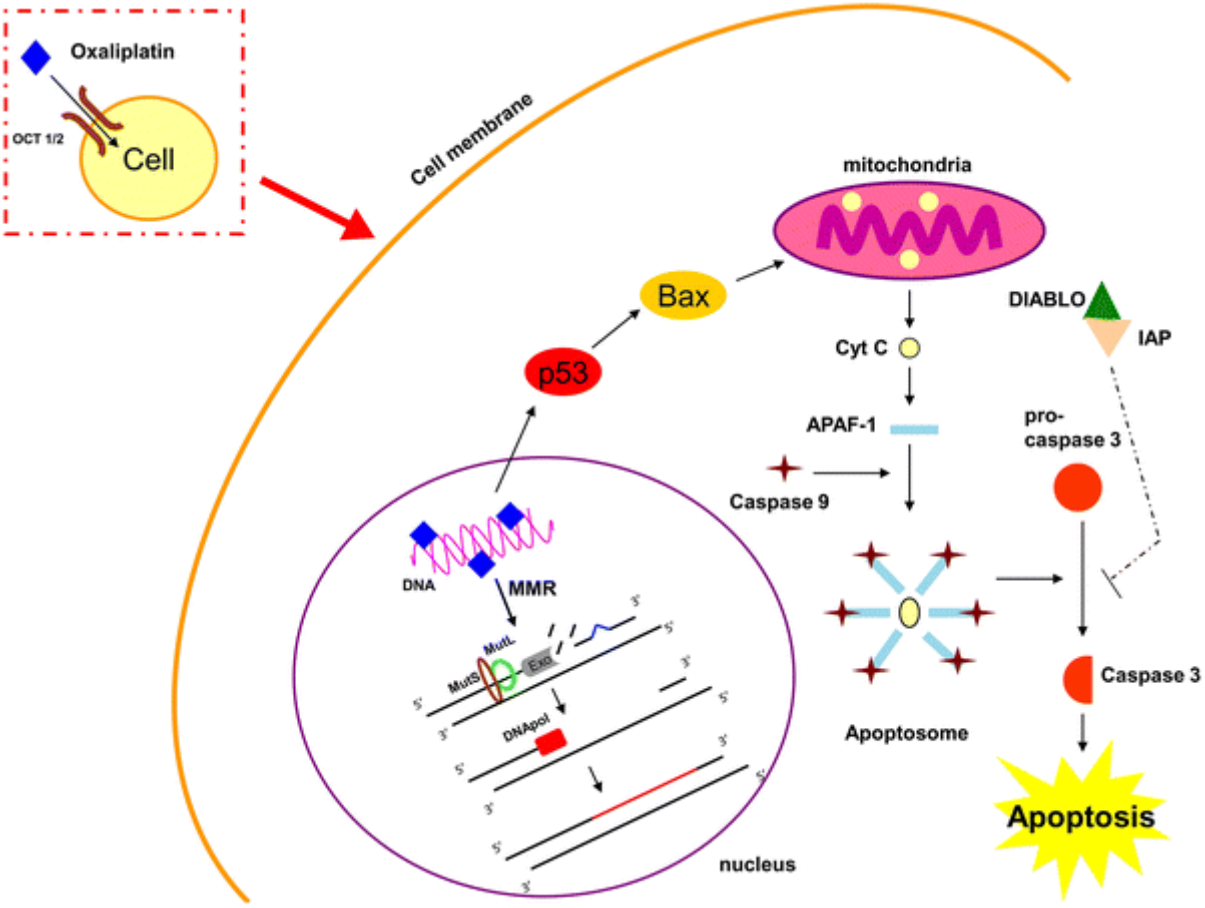

Figure 1.9: DNA-lesion mediated apoptotic pathway for oxaliplatin action

1.8.2.2 Limitations of oxaliplatin

Although the mode of action and activity profile of all platinum drugs are similar but oxaliplatin shows different toxicity profile than other platinum drugs. The major side effects produced from the administration of oxaliplatin are: gastrointestinal toxicity, haematological toxicity and neuropathy (Tesniere, Schlemmer et al. 2010).

Several studies have been proved that oxaliplatin is less prone to resistance compared to other platinums. However oxaliplatin is not devoid of drug resistance. Elevated

expression of glutathione through γ-glutamyl transpeptidase is the principal mechanism of oxaliplatin resistance. Additionally, decreased uptake of oxaliplatin via mutation in copper transporter proteins has also been indicated for oxaliplatin resistance.

1.9 Combination therapy

Co-administration of two or more drugs to treat a disease in a better way with improved efficacy or lowering toxicity is known as combination therapy. It is now gaining popularity among clinicians to combat many diseases including cancer, arthritis, diabetes, hypertension and other cardiac diseases, hyperlipidaemia, alzheimer's disease, microbial and fungal infections (Gudzune, Monroe et al. 2014, Sitbon, Jaïs et al. 2014, Matsunaga, Kishi et al. 2015, Maruthur, Tseng et al. 2016, Beganovic, Luther et al. 2018). Only in USA there are about ten thousands clinical trials on combination therapy are continuing against neoplasia, infections, diabetes, autoimmune, cardiovascular and nervous system disorders.

1.9.1 Combination therapy to combat cancer

Combination therapy is used against cancer to increase efficacy of individual drugs used at reduced doses with minimal side effects. Combined therapy can chemosensitize cells though additive or synergistic effects and thus minimize the possibility for development of drug resistance or overcome acquired drug resistance. The concept of combined chemotherapy was first postulated by Emil Frei in 1965 against acute leukaemia. The study on the children showed that POMP combination regimen comprising of prednisone, 6-mercaptopurine, methotrexate and vincristine offered significantly higher success rate over single therapy (FREI, KARON et al. 1965). Due to the success of POMP regimen, subsequently a number of studies have been

conducted using different types of drugs against variety of cancers. For instance, sabutoclax with minocycline against pancreatic cancer (Quinn, Dash et al. 2015), carboplatin and paclitaxel against ovarian cancer (Ozols, Bundy et al. 2003). Combined treatment regimens FOLFOX and FOLFIRI are being used in the management of advanced stages of colorectal cancer. Recently newer techniques in combination therapy have been introduced, such as: restrictive combinations and drug repositioning. Restrictive combination involves planned dosing and drug administration to selectively kill the cancer cells without causing any effects towards normal cells. To fulfil the purpose, combined therapy advantageously use the minor differences exists between malignant and normal cells, i.e. the absence of a target (deficiency of p53), or by the manifestation of a target (surface marker) (Bayat Mokhtari, Homayouni et al. 2017). Drug repositioning is the strategy where present therapeutic agent primarily employed against non-cancerous conditions is being used for management of cancer (Chong and Sullivan Jr 2007).

Mokhtari et al, reviewed the pathways through which combination therapy provide better efficacy against cancer with limited side effects. The mentioned important pathways are antioxidant pathways and phytochemicals; hypoxia and carbonic anhydrase inhibitors; epigenetics and histone deacetylases inhibitors; autocrine growth factor pathways and serotonin receptor inhibitors; angiogenesis and vascular endothelial growth factor (VEGF) inhibitors; apoptotic cell death and agents targeting apoptosis (Bayat Mokhtari, Homayouni et al. 2017).

1.9.2 Phytochemicals in combination chemotherapy

Many of the phytochemicals can act as antioxidants and thus give chemopreventive (blocking the initiation step of carcinogenesis) effects to combat cancer. Epidemiological studies (more than 200) suggest that higher consumptions of fruits and vegetables which are the major sources of antioxidant phytochemicals can implicate in reducing the incidence of cancer (Willett and Trichopoulos 1996). Phytochemicals can protect the cells from oxidative DNA damage from the interactions of reactive oxygen species (ROS) being generated continuously inside the cell. Moreover they can regulate various transcription factors including nuclear factor erythroid 2-related factor 2 (Nrf2), nuclear factor kappa B (NFκB), beta catenin and TGF-β (Russo 2007).

Studies from the combinations of chemotherapeutic drugs and phytochemicals in clinical settings result into synergistic effects in many instances in various cancers. (Block, Koch et al. 2008, Panahi, Saadat et al. 2014). Paclitaxel has been approved by FDA in combination with carboplatin to treat ovarian cancer. A number of phytochemicals in combination with other chemotherapeutic drugs have been investigated and entered into clinical trials, such as resveratrol, EGCG, curcumin, quercetin, genistein and daidzein. Our group has been published a significant number of research articles showing the combined effect of platinum drugs and phytochemicals against ovarian cancer (Yunos, Beale et al. 2011, Mazumder, Beale et al. 2012, Nessa, Beale et al. 2012, Al-Eisawi, Beale et al. 2013, Huq, Yu et al. 2014, Huq 2015, Arzuman, Beale et al. 2016). In this project, the study has been extended in colorectal cancer models to find out the combined effect of selected phytochemicals and platinum drugs.

1.10 Phytochemicals used in this study

1.10.1 Curcumin

Curcumin is the main active ingredient of turmeric (*Curcuma longa*) which is indigenous to Asia and commonly used as spices in preparing different dishes. Although turmeric is familiar component of kitchen, traditional healers of Asian countries have been using it since 500 BC for the treatment of various diseases (Gupta, Sung et al. 2013, Deogade and Ghate 2015). Curcumin constitutes 2-5% of the total contents of turmeric which is orange-yellow in colour and water insoluble. Chemically, it is a polyphenol and known as diferuloylmethane which is shown in figure 1.10.

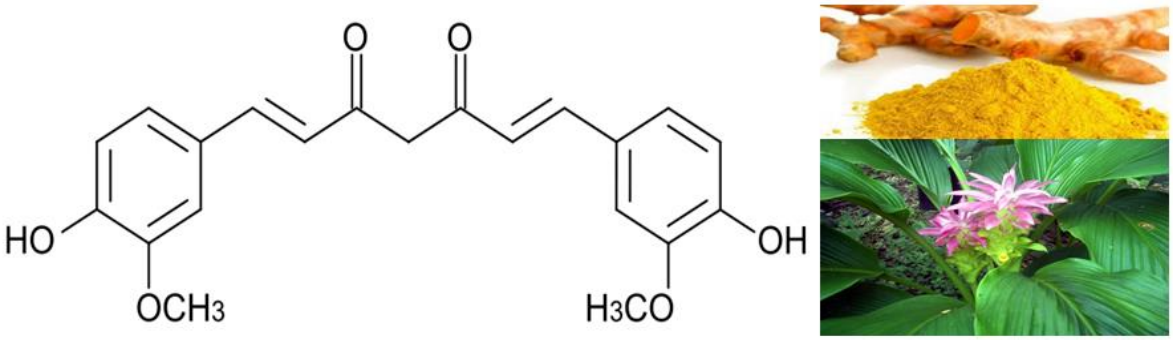

Figure 1.10: Curcumin and its botanical source

A diverse range of biological activities is shown by curcumin, such as: antibacterial, antifungal, antioxidant, anti-inflammatory, cholesterol lowering as well as anticancer (Patil, Jayaprakasha et al. 2009, Prasad, Gupta et al. 2014). Owing to the above mentioned bioactivities curcumin has been proven to be beneficial in various diseases (Kocaadam and Şanlier 2017). Figure 1.11 pictorially describes the potential uses of curcumin in different disease conditions and its molecular targets obtained from various *in vitro* and *in vivo* studies.

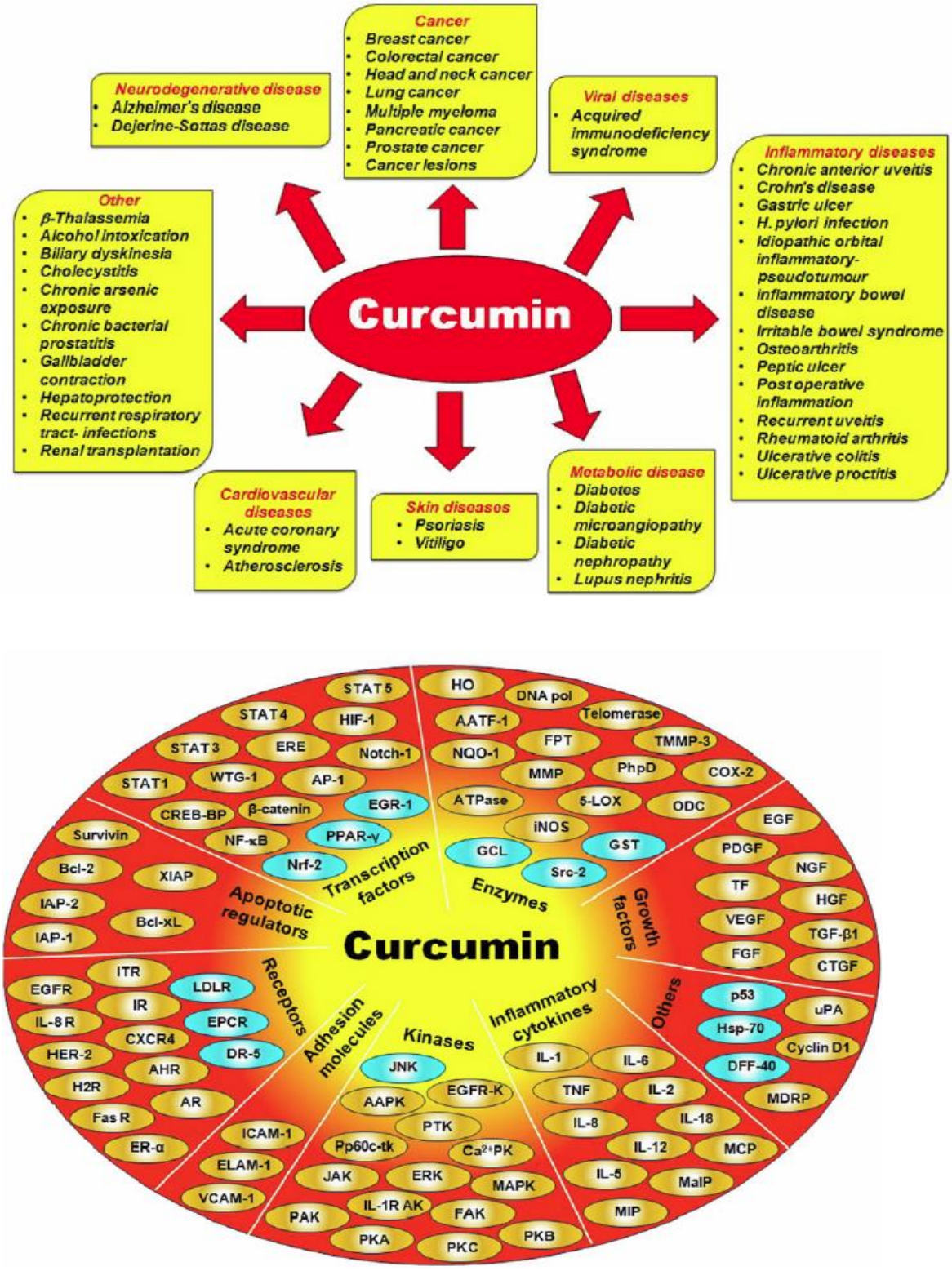

Figure 1.11: Benefits of curcumin in different diseases and its molecular targets [Adapted from(Kunnumakkara, Bordoloi et al. 2017)]

1.10.2 Colchicine

Colchicine is an alkaloid extracted from the plants meadow saffron (*Colchicum autumnale*) or glory lily (*Gloriosa superba*). The medicinal uses of rhizome of colchicum have been traced back to 550 AD in ancient Egypt against rheumatism. In early 1900s colchicine was isolated and named as active ingredient of colchicum, applied against gout management in France (Mandhare and Banerjee 2016). Colchicine has been indicated in other clinical conditions, such as: familial Mediterranean fever, Behcet's disease, pericarditis, coronary artery diseases, cirrhosis and Sweet's syndrome (Leung, Yao Hui et al. , Larocque, Ovadje et al. 2014). But the compound has low therapeutic index and cautiously prescribed in the patients having kidney problems.

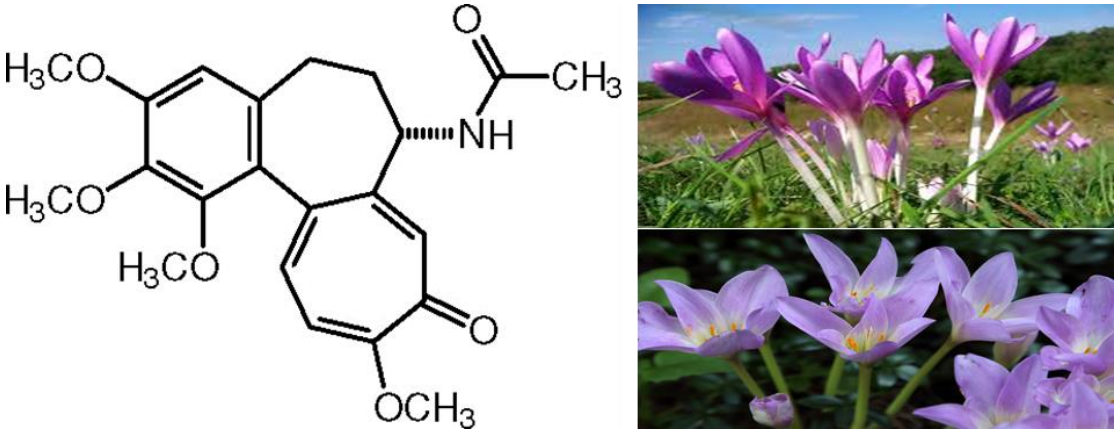

Figure 1.12: Colchicine and its botanical source

Colchicine has also shown anticancer activities by inhibiting tubulins and polymerization of microtubules. Depolymerization of microtubules happen through inhibition of lateral contacts between protofilaments (Bhattacharyya, Panda et al. 2008). From a recent clinical trial, it has been suggested that colchicine could be used in the treatment of everolimus-induced oral ulcers (Ropert, Coriat et al. 2017). A number of synthetic analogues of colchicine have also been synthesized and found to be active against multiple cancers including: lung, colorectal, prostate, ovarian and breast

(Blakey, Westwood et al. 2002, Mandhare and Banerjee 2016). Established anti-inflammatory mechanism of colchicine is given in figure 1.13.

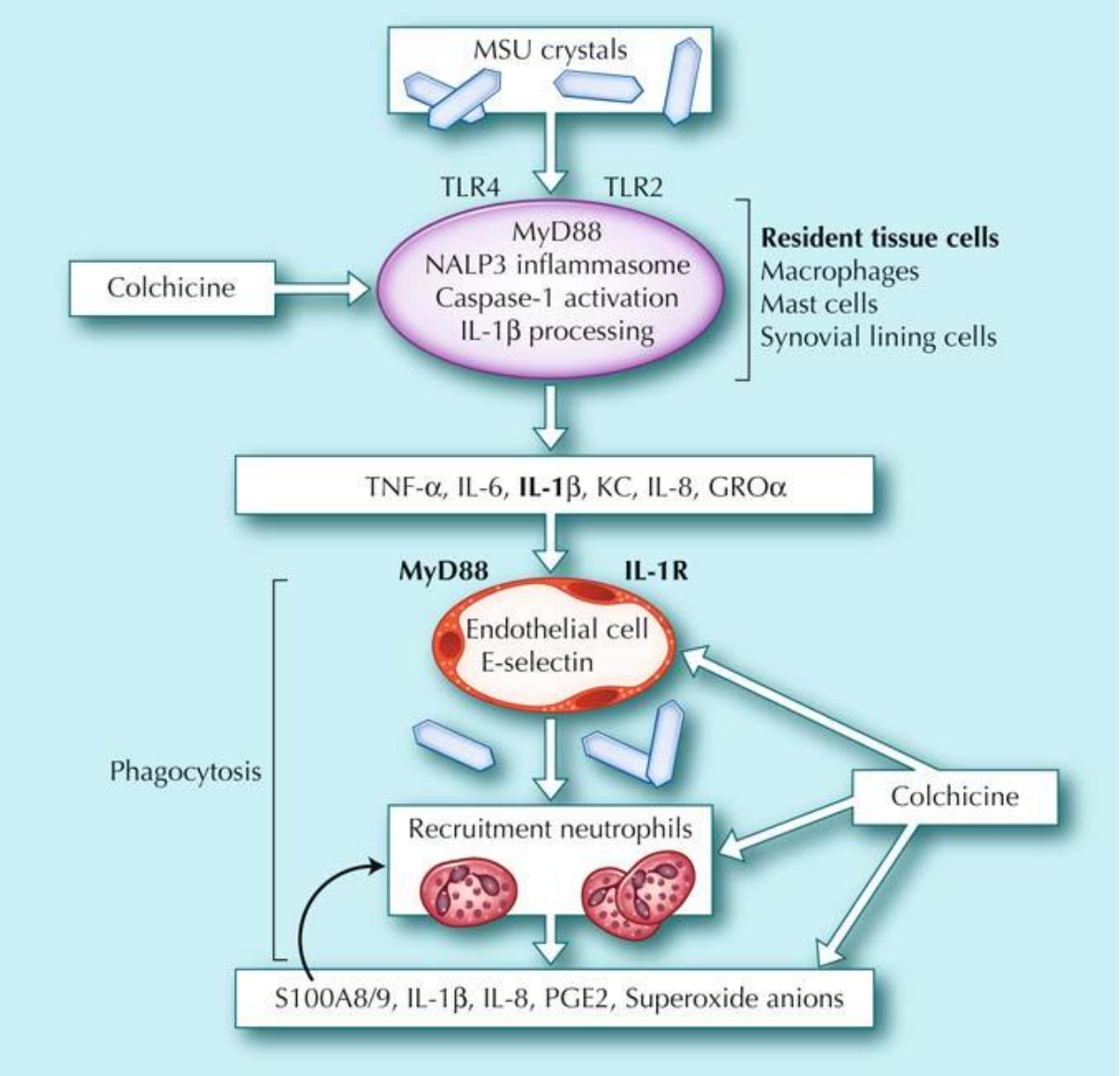

Figure 1.13: Anti-inflammatory action of colchicine [Adapted from (Nuki 2008)]

1.10.3 EGCG (Epigallocatechin-3-gallate)

EGCG is a catechin, belongs to large polyphenol class which is found in green tea (derived from dried fresh leaves of the plant *Camellia sinensis*). Traditional healers of China and India used green tea as a stimulant, diuretic, astringent, antiflatulent and cardio tonic (Chopade, Phatak et al. 2008). EGCG was first isolated by Michiyo Tsujimura in 1929 in Japan along with other three catechins from green tea (Rady, Mohamed et al. 2017). Structurally (Figure 1.14), it is a flavone-3-ol having 8 hydroxyl groups, which renders EGCG as bioactive compound with diverse range of functions including: antioxidant, anti-inflammatory, lipid lowering, antitumour and antidiabetic.

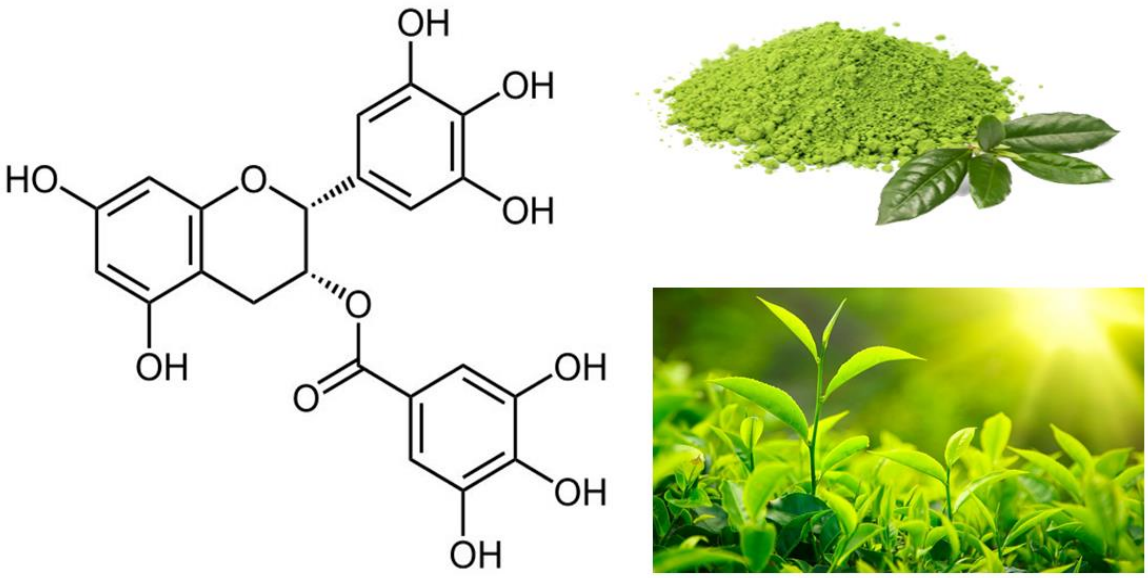

Figure 1.14: EGCG and its botanical source

Anticancer potential of EGCG has been evidenced from a huge number of *in vitro* cancer-related molecular targets and *in vivo* model studies (Nagle, Ferreira et al. 2006, Rady, Mohamed et al. 2017). The molecular targets identified from those studies which are thought to be associated with anticancer action of EGCG have been shown in figure 1.15.

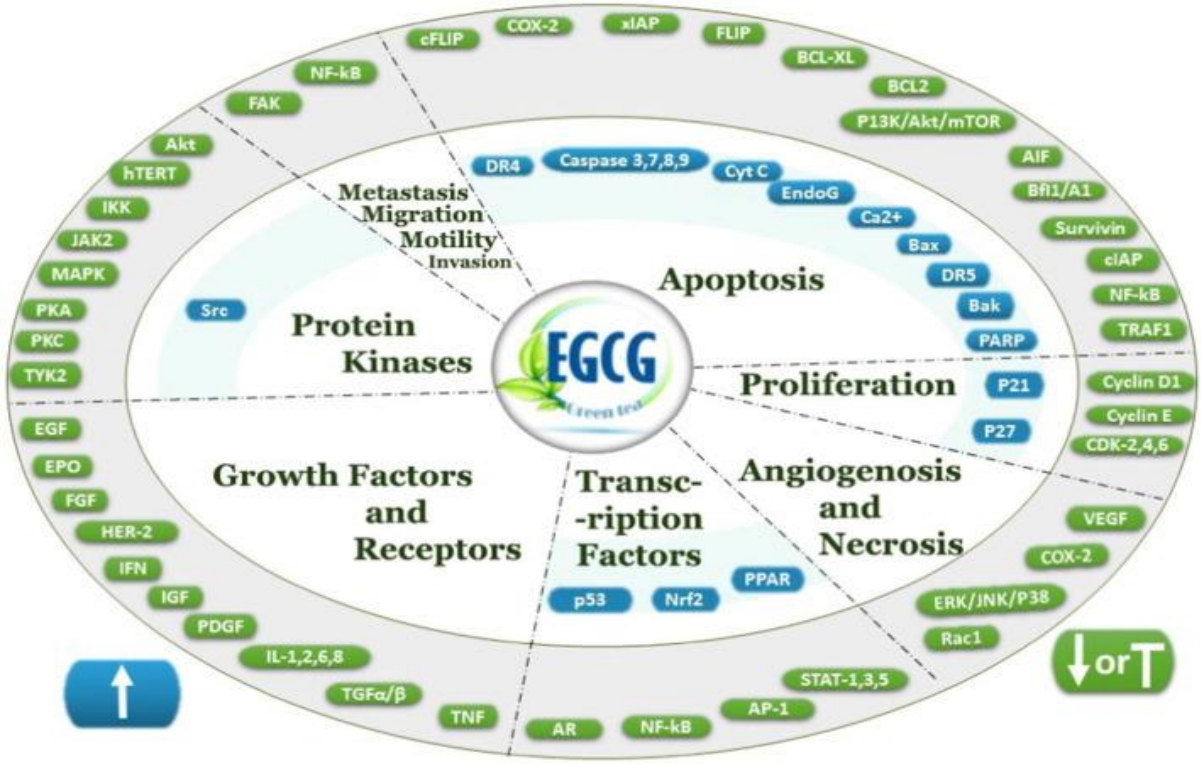

Figure 1.15: Molecular targets of EGCG linked with its antitumour activity [Adapted from Rady et.al. 2017]

1.10.4 6-gingerol

It is a pungent phenolic constituent, obtained from the rhizomes of ginger (*Zingiber officinale*) and constitutes the most abundant contents of that. Ginger has a long history (5000 years back) of being an important ingredient of traditional medicines of China and Asia in the treatment of cataract, arthritis, constipation, and digestive disorders (Edwards, Rocha et al. 2015). Traditional use of ginger relies on the activity of gingerols. 6-gingerol has anticancer, neuroprotective, anti-inflammatory and anti-oxidant effects (Zeng, Zong et al. 2015).

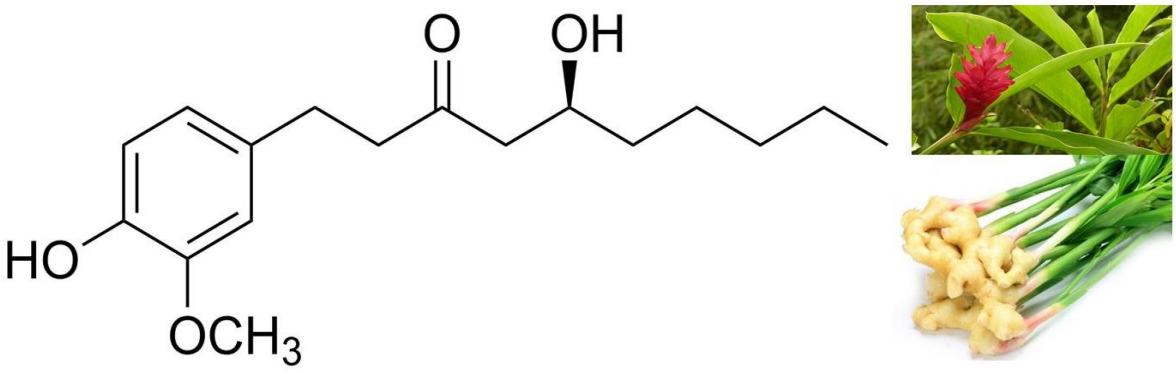

Figure 1.16: 6-gingerol and its botanical source

Antitumour activity of 6-gingerol has been observed in many studies e.g. cell growth arrest and apoptosis against colon cancer (Lee, Cekanova et al. 2008) and pancreatic cancer (Park, Wen et al. 2006), inhibition of angiogenesis and metastasis against breast cancer (Kim, Min et al. 2005, Lee, Seo et al. 2008) and ROS mediated cell death against lung cancer (Nigam, Bhui et al. 2009). Molecular targets for antitumour activity of 6-gingerol have been reported as NF-κB, IL-8 and VEGF. Proposed mechanism for the anticancer action of 6-gingerol mediated through NF-κB pathway is shown in figure 1.17.

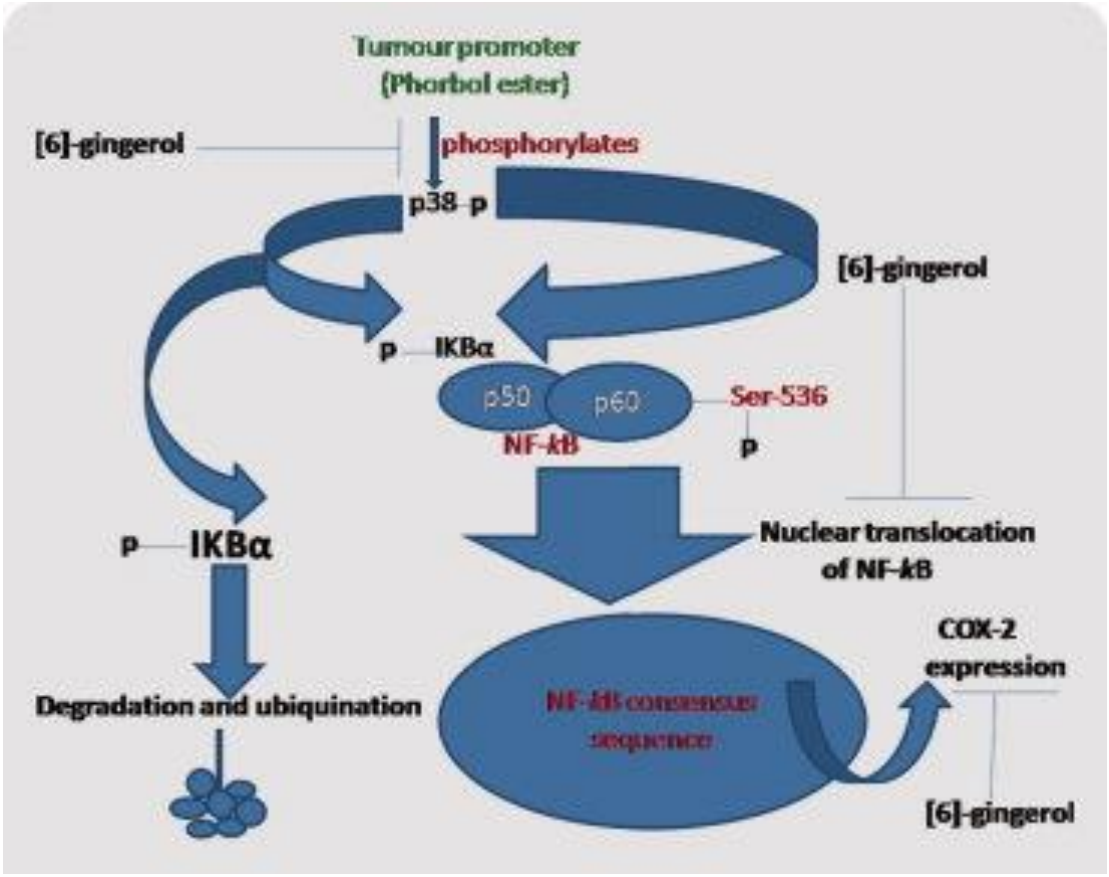

Figure 1.17: NF-κB mediated anticancer action of 6-gingerol [Adapted from (Oyagbemi, Saba et al. 2010)]

1.10.5 Taxol

Taxol (Figure 1.18) was isolated from Pacific yew tree (*Taxus brevifolia*) and named in 1967. However, the antitumour activity of the crude extracts of the plant collected by Arthur Barclay in 1962 was identified during the natural compounds screening program conducted by National Cancer Institute, USA. After around 30 years, it was renamed as paclitaxel and patented by Bristol-Myers Squibb and got approval for ovarian cancer in 1992, breast cancer 1994 and lung cancer in 1999 (Weaver 2014). Taxol kills the cancer cells by promoting the assembly of microtubules and mitotic arrest (Runowicz, Wiernik et al. 1993). It can also bring cell apoptotic cell death via binding with Bcl-2 (Haldar, Chintapalli et al. 1996). However, paclitaxel also suffers with drug resistance

and adverse effects at higher doses. The major side effects are allergic reactions, loss of hair, neutropenia, peripheral neuropathy, myalgia, arrhythmia, nausea and mucositis.

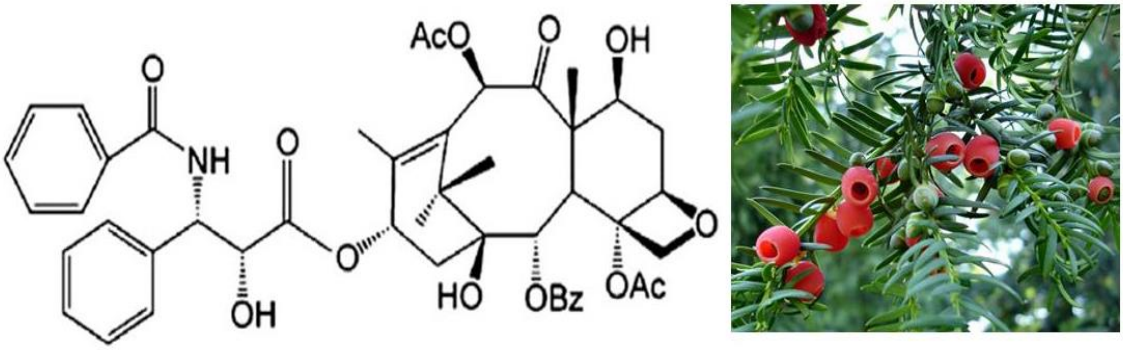

Figure 1.18: Taxol and its botanical source

1.11 Aim of the present study

Colorectal cancer is one of the leading causes of mortality and morbidity from cancer around the globe. For the treatment of advanced stages of CRC, chemotherapy is the first-line treatment. However, existing treatment strategies of metastasized CRC are greatly suffered by side effects, resistance or high cost. Phytochemicals are usually cheap, devoid of adverse effects and a many of them possess antitumour activities. Combination of tumour active phytochemicals with platinums might provide a better option of combating CRC with lesser toxicity and overcome drug resistance. The primary objective of the present study is to find out the combined drug effects from the binary combinations of platinums (cisplatin and oxaliplatin) and selected phytochemicals against CRC as a matter of sequence of addition and concentration. Mechanistic studies have been carried out to get the insights behind the combined drug effects. The specific aims of the present study were:

- Determination of the cytotoxicity of platinum drugs (cisplatin and oxaliplatin) and selected phytochemicals (curcumin, colchicine, EGCG, 6-gingerol and taxol) against

four different colorectal cancer models (HT-29, Caco-2, Lim-1215 and Lim-2405 cell lines)

- ❖ Investigation on binary sequenced drug effects from the combinations of platinums and phytochemicals of choice against the mentioned colorectal cancer models
- ❖ Investigation on the damage to the DNA caused by the selected drug combinations through DNA damage study using Agar gel electrophoresis
- ❖ Determination of cellular accumulation of platinums from selected drug combinations
- ❖ Determination of Pt–DNA binding levels from the selected drug combinations
- ❖ Proteomic study to identify the proteins responsible for combined drug actions

2 EXPERIMENTAL

Preamble: This chapter details the methodology used in the present study which are well-established and have been used in the host laboratory for last twenty years. Before starting the combination study between platinum drugs (cisplatin/oxaliplatin) with phytochemicals (colchicine, curcumin, EGCG, 6-gingerol and taxol), cytotoxicity of the individual compounds were determined against four colorectal cancer cell lines (HT-29, CACO-2, LIM-1215 and LIM-2405). The binary combination study was carried out and the combined effect was determined as a function of concentration and sequence. The mechanisms behind the combined effect were also investigated through study of interactions with the DNA extracted from the drug treated cells, cellular accumulation, platinum-DNA binding study. Finally proteomic study was conducted to reveal the proteins associated with the combined drug effects.

2.1 Reagents and equipment

The important chemicals and instruments used for the different studies carried out in the present study are listed in Table 2.1. All of the selected phytochemicals: colchicine (Col), curcumin (cur), epigallocatechin-3-gallate (EGCG), 6-gingerol (6-gin) and taxol (Tax) were purchased from Sapphire Bioscience, Pty. Ltd., Australia.

2.2 Preparation of the stock solution of platinums and phytochemicals

Stock solutions of the compounds were prepared in the beginning of this study to be used later on for the determination of cytotoxicity, combination study and other mechanistic studies. Ethanol was used as a solvent for dissolving the phytochemicals Mixture of DMF and mQ water was used to dissolve the platinum drugs. Information relating to the prepared stock solution of the compounds is tabulated in Table 2.2.

Table 2.1: List of the important equipment and reagents used in the study

Equipment/ Material	Purchased Source
96-well plates, cell culture flask, cisplatin, phosphate buffered saline (PBS), 3-[4,5-dimethylthiazol-2yl]-diphenyl tetrazolium bromide (MTT), trypsin, hepes, sodium hydroxide (NaOH) dimethyl sulfoxide (DMSO), tris base, tris-HCl, disodium salt of ethylene diamine tetraacetic acid, boric acid, acetic acid and ethidium bromide, triton-X (t-octylphenooxypolyethoxyethanol) and sodium azide	Sigma-Aldrich Pty Ltd, NSW, Australia
Foetal calf serum, roswell park memorial institute (RPMI) 1640 media, 200 mM L-glutamine and sodium bicarbonate,	Thermo Trace Pty Ltd Melbourne, Australia
Microplate Reader (iMark™ Version 1.04.02E), TC-10 automated cell counter, PROTEAN i12 isoelectric focusing (IEF) cell, criterion dodeca cell (Serial: 561BR 01908), chemidoc XRS system (Serial: 720BR1508), criterion TGX precast gel, bromophenol blue (161-0404), bovine serum albumin (BSA) (1.44 mg/mL), protein assay standard II kit (500-0007), dye reagent concentrate (500-0006), protean plus overlay agarose, coomasie G-250 stain, wicks and gels for 1st dimensional electrophoresis [ReadyStrip IPG strip of 11 cm long, 3.3 mm wide, 3-10 NL (nonlinear) pH gradient and 0.5 mm thick gel], carrier ampholytes (163-1112), iodoacetamide, 10 X tris/glycine buffer and mineral oil	Bio-Rad, Australia
CO_2 incubator	SANYO, Japan
Varian-Cary UV spectrophotometer, Atomic absorption spectrophotometer (AAS),	Varian, Inc., Australia
EZ-10 spin column genomic DNA minipreps KIT	Astral Scientific Pty. Ltd., Australia
Kodak Gel Logic 100 imaging system (GL 100)	Eastman Kodak Company, USA
1,4-Dithiothreitol (DTT), urea, glycerol, agar and thiourea	Merck chemicals, Australia
Protease inhibitor cocktail tablets	Roche Applied Science, Australia
CHAPS (3[(3-Cholamidopropyl)dimethylammonio]-1-propanesulfonate	Calbiochem, Germany
DeStreak reagent	GE Healthcare Bio-sciences AB, Sweden
Glycerol and sodium dodecyl sulfate (SDS)	MP Biomedicals, LLC, France

Table 2.2: Concentrations of the stock solutions used in the study

Compound	Molecular weight	Concentration (?g/5mL	Solvent
Cis	300	1 mM (0.0015)	1 mL DMF+ 4 mL DMF
Ox	397.29	1 mM (0.0019)	1 mL DMF+ 4 mL DMF
Cur	368.38	10 mM (0.018)	Ethanol
EGCG	458.37	10 mM (0.022)	Ethanol
Col	399.43	1 mM (0.002)	Ethanol
6-gin	294.39	10 mM (0.014)*	Ethanol
Tax	853.93	1 mM (0.004)	Ethanol

* indicates mL instead of g, because the compound is liquid

2.2 Cell lines

Amongst the four colorectal cancer cells used in the present study two cell lines (HT-29 and CACO-2) were got from Dr. Mu Yao of Endocrinology department from The University of Sydney. Other two cell lines: LIM-1215 and LIM-2405 were purchased from Cell Bank of Australia.

2.3 Cell culture and cytotoxicity study

2.3.1 Recovery of frozen cancer cells

Cryovial containing the desired cell line was taken out from the liquid nitrogen tank and thawed very rapidly (less than 1 min) using preheated 37°C water bath available in the host laboratory. The vial was swirled gently in water bath until 80% of the ice gets melted. The vial was then transferred into laminar air flow cabinet and the contents were dissolved with 9 mL of 10% RPMI media (pre-warmed) in a centrifuge tube. The tube was then spun at 2000 rpm for 5 minutes. The clarity of the supernatant and visibility of the cell pellet was checked. Fresh medium (2 mL) was added after discarding the old medium without disturbing the cell pellet. The cell pellet was

resuspended thoroughly in the fresh medium using pipette and then transferred into a cell culture flask having 8 mL of medium. The flask was kept in an incubator (37°C, 5% CO_2) for the cells to grow.

2.3.2 Subculturing technique

Subculturing of the cells was conducted to make sure that cells are healthy are actively growing, by breaking the bonds between the cells and also with the substrate (plastic or glass surface) where the cells were grown. Usually enzymes (trypsin, dispase or collagenase) are used to break the cellular glue. There are two types of subculturing method: monolayer and adherent. Monolayer subculturing method was used in the present study. Initially, cells having 80-90% confluence, grown in corning cell culture flask (25 cm^2) was taken out from the incubator and checked for any contamination under microscope. The old medium was discarded using sterile pipette and then washed with PBS, followed by addition of trypsin. The corning cell culture flask was kept in incubator for 3 min. The effect of the trypsinization was checked under microscope and confirmation was made from the detachment of cells from the substrate as well as rounding up. RPMI media was added by vigorous pipetting and cell suspension was transferred into new flask. The corning cell culture flask containing the cell suspension was incubated at desired atmosphere (37°C, 5% CO_2) and allowed the cells to grow. For maintenance of cell lines the technique was repeated twice a week to make sure that cells were growing in logarithmic phase. Cells were counted periodically and necessary dilution was done. For 10 tomes dilution, 9 mL of the cell suspension was discarded and another 9 mL of fresh medium was added to the cell.

2.3.3 Composition of cell culture media

10% foetal calf serum in RPMI media was used for culturing HT-29, CACO-2, LIM-1215 and LIM-2405 cell lines. To prepare the media; 100 mL of FCS, 20 mL of hepes, 20 mL of $NaHCO_3$, 10 mL of glutamine and 0.5 mL of NaOH were added with 200 mL of RPMI solution. The exact concentration of each ingredients of cell culture media used in the study is listed in Table 2.3.

Table 2.3: Components of Cell culture media

Component	**Concentration**
RPMI 1640	5 X
FCS	10%
Hepes	1 M
$NaHCO_3$	5.6%
Glutamine	200 mM
NaOH	Saturated

2.3.4 Preparation of PBS

To prepare 2 L of PBS solution, 1800 mL of milli Q water was taken in a 2L volumetric flask and 19.2 g of PBS powder was added. PBS powder was dissolved into water by gentle stirring. pH of the solution was adjusted to 7.3 using 1 M of HCl. Finally, the volume of the solution was made up to 2L by addition of mQ water carefully and sterilized by filtration.

2.3.5 Preparation of trypsin solution

Initially, 0.02 g of ethylene diamine tetra-acetic acid (EDTA) was measured and dissolved in 1 mL of mQ water in a 100 mL volumetric flask. 10 mL of trypsin (2.5%) was then added and the final volume was made to 100 mL by addition of 89 mL of PBS. The mixture was mixed thoroughly by tilting the volumetric flask and then sterilized by filtration.

2.3.6 Cell counting and seeding

In the cell culture, concentration of cells was quantified using counter slide, trypan blue and automated cell counter (T10 Bio-Rad). 10 µL of cell suspension was taken and mixed with equal volume of trypan blue. It was then added on the both sides of counting slide. Finally, the slide was inserted and the counting was recorded.

In most of the cases 96-well plates were used and 100 µL of cell suspensions were added into each well. The cell concentration was approximately 2 X 10^5 cells/mL of suspension. For seeding purpose, 96-well plates were placed in 5% CO_2 incubator at 37°C for 24 h after addition of cell suspensions into the well.

2.3.7 Preservation of cell lines

The cell lines were preserved using cryopreservation technique which involve the use of cryoprotective agents: such as ethylene glycol, polyvinyl pyrrolidine, DMSO, glycerol. In this study DMSO was used as a cryoprotective agent and cell lines were stored below -130°C using nitrogen tank. Briefly the technique involved the harvesting of the cells at late log phase having concentration 3 X 10^6 cells/mL. The cells were spun for 3000 rpm for 3 min to get the cell pellet. The supernatant was decanted and the pellet was resuspended using 10% FCS. Equal volume of cell suspension was added with 20% DMSO (2 mL DMSO + 8 mL of 10% FCS) to obtain the desired concentration of 10% DMSO. The mixture was then aliquoted into different prelabelled cryovials.

2.3.8 Cellular viability assay

Viability of cells can be determined by three major techniques i.e. imaging, flow cytometry and microplate assays. In this study MTT reduction assay, was used to

quantify the viable cells which is the most popular microplate assay and provides a measure of viable cells in a quantitative manner. Dehydrogenase enzymes present in metabolically active cells can reduce tetrazolium salts and produce purple coloured formazan which can be quantified using spectrophotometer.

During preparation of MTT solution, required amount of MTT powder was measured and dissolved in 500 mL of RPMI medium (serum free) to make desired concentration of 1 mg/mL. The powder was dissolved into the medium through moderate shaking and avoiding from sunlight for 1 hour to make sure that every particle mixed properly. The solution was then sterilized by filtration and aliquoted into 50 mL tubes (covered with aluminium foil), kept into refrigerator.

During assay, 96-well plate was taken out from the incubator and the medium was discarded. 50 µL of MTT solution was added to each well and incubated again for 4 h. After discarding the MTT solution from the 96-well plate, 150 µL was added into each well (Abdullah, Huq et al. 2003). The optical density (OD) was recorded from a microplate reader (iMark) at 595 nm. The percentage of viable cells was obtained from the following formula:

$$\frac{\text{OD of compound or drug-treated cells}}{\text{OD of control}}$$

2.3.9 Estimation of cells killing

The cytotoxicity of the compounds tested in this study was expressed as a measure of concentration required to kill half of the cells (IC_{50}) value. It was determined from the dose response curve constructed from the plot of drug concentration versus percentage of viable cells. Each experiment was carried out for minimum four times to obtain statistically significant results.

2.4 Binary sequenced combination study

The main objective of the present study was to find out the combined drug effects from the combinations of platinums and phytochemicals. Drugs were combined with the idea that mechanisms of cell killing applied in combination would be different and would facilitate cancer cell killing more efficiently with reduced side effects. Drugs were combined at a constant ratio of their IC_{50} values and combined effects were determined from dose response curves and combination indices.

2.4.1 Addition of drugs

IC_{50} values obtained from the cytotoxicity study of the individual compounds used as a pilot for designing combination study. Drugs were added alone and in combinations at three different concentrations and sequences. During combination drugs were added at a constant ratio based on their IC_{50} values. Molar ratios of added combined drugs in different cell lines are shown in Table 2.4.

96-well plate seeded with 100 µL of cells in each well (at least 24 h before) was taken out from the incubator and placed inside the laminar air flow cabinet for drug addition. The wells intended for single drug addition, was added with 100 µL of respective drugs. The wells intended for combined drug addition, was added with 50 µL of each selected

drugs (Alshehri, Beale et al. 2011). The wells intended for serve as control, was added with 100 μL of medium. Three different sequences namely: bolus or 0/0 (platinum and phytochemical added at the same time); 0/4 (platinum drug added first and phytochemical 4 h later) and 4/0 (phytochemical added first and platinum 4 h later) were used for combined drug addition. A model for combination study design is shown in Figure 2.1. MTT reduction assay was done to obtain percentage of viable cells after 72 h of drug addition and incubation in 5% CO_2 incubator.

Table 2.4: Summary of the molar concentration ratios between platinum compounds (Cis and Ox) and phytochemicals (Cur, EGCG, Col and taxol), while administered in combination to the human colorectal cancer CACO-2, HT-29, LIM-1215, and LIM-2405 cell lines

Cell lines	**Drug Combination**			
	Cis+Cur	**Cis+EGCG**	**Cis+Col**	**Cis+Tax**
CACO-2	0.814	0.424	0.0072	17.3
HT29/219	0.298	0.208	0.0017	10
LIM1215	0.239	0.512	0.003	14.75
LIM2405	0.597	0.135	0.0023	3.25
	Ox+Cur	**Ox+EGCG**	**Ox+Col**	**Ox+Tax**
CACO-2	0.128	0.0444	0.092	1.813
HT29/219	0.029	0.018	0.025	0.94
LIM1215	2.18	9.7	0.010	0.401
LIM2405	0.910	0.206	0.002	0.131

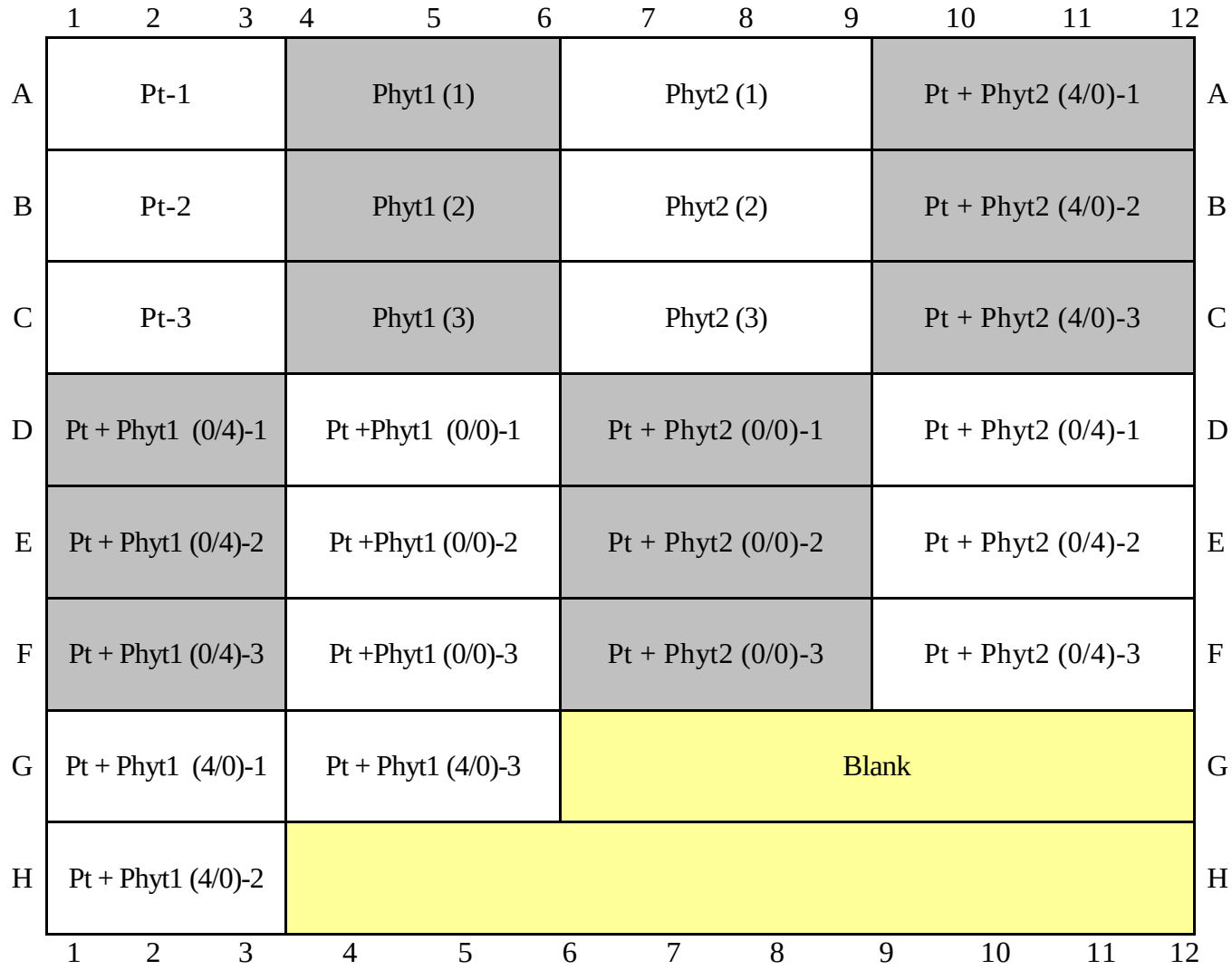

Figure 2.1: Combination study design for the addition of drugs in a 96 well plate, where Pt=platinum drug; Phyt1=phytochemical 1; Phyt2=phytochemical 2; 1=five times diluted IC_{50} concentration; 2=IC_{50} concentration and 3=five times higher IC_{50} concentration

2.4.2 Determination of combined drug action

The nature of combined drug action was determined from dose response curves and combination indices. Dose response curves were obtained by plotting the concentration of drugs against cell survival fractions. Qualitative measure of combined drug actions

can be obtained from dose response curves and it provides visually appealing presentation of the results.

In contrast, combination indices (CI) represent the quantitative measure of combined drug action, which is more accurate and reliable. The values indicate the nature of combined drug action i.e. a value less than 1 refers to synergistic combined effect, a value greater than 1 refers to antagonistic combined effect and a value 1 refers to additive combined drug effects. CI values were calculated by using the software Calcusyn which calculates the combined drug effects through Chou-Talalay method (Chou and Talalay 1984).

Chou-Talalay initially develops the formula to describe enzyme kinetics but now is being modified and extensively used for determination of combined drug effects (Ashton 2015, Zhang, Fu et al. 2016, Anastasiadi, Polizzi et al. 2018). CI correlates dose and effects in a simplest possible form and can be calculated for binary combination using the following equation

$$CI = \frac{D_{pt}}{D_{ptz}} + \frac{D_p}{D_{pz}}$$

Where, D_{pt} refers to concentration of platinum drug required for z% cell kill while in combination; D_p refers to concentration of phytochemical required for z% cell kill in combination; D_{pt} refers to concentration of platinum drug required for z% cell kill while applied alone; D_p refers to concentration of phytochemical drug required for z% cell kill while applied alone. Dz can be determined from the formula

$Dz= D_m [f_a/(1-f_a)]_{1/m}$

Where D_m refers to median effect dose; fa refers to affected fraction by the dose and m refers to exponent of dose response curve

2.5 Cellular accumulation of platinum

2.5.1 Addition of drugs and cell collection

Based on the combined drug effects few combinations were selected for this study to gather the link between combined drug action and cellular accumulation of platinum inside the cell. Combinations of platinums and phytochemicals producing synergistic/additive/antagonistic effects in HT-29 and CACO-2 cell lines were only selected for this study. Selected combinations are shown is Table 2.5. For cellular accumulation study, stock solutions of the compounds were again prepared (Cis: 1mM; Oxa: 0.63 mM; Cur: 0.71 mM; EGCG: 5.09 mM; Col: 1.23 mM and Tax: 1.16 mM). Exponentially growing HT-29 and CACO-2 colorectal cancer cells in 4.75 mL 10% FCS/RPMI medium (cell density = 50 x 10^4 cells mL-1) were seeded into cell culture dishes and allowed to attach overnight. While drugs were added in combination, 125 µL of each selected drugs were added to the cells. But in case of Cis and Ox alone treatment 125 µL of drug and 125 µL of each medium were added. Then the culture dishes were incubated for 24 h at 37°C, 5% CO_2 incubator. Cells were collected as shown in Figure 2.2.

Table 2.5: Combinations selected for cellular accumulation study

Cell	Sample	Combined action
HT-29	Cis	Not applicable
HT-29	Cis & Cur (4/0)	Additive
HT-29	Cis & EGCG(0/0)	Synergistic
HT-29	Ox	Not applicable
HT-29	Ox & Cur (0/0)	Synergistic
HT-29	Ox & Cur (4/0)	Synergistic
HT-29	Ox & EGCG(0/0)	Synergistic
HT-29	Ox & Col (0/4)	Additive
HT-29	Ox & Tax (4/0)	Antagonistic
CACO-2	Cis	Not applicable
CACO-2	Cis & Cur (0/0)	Additive
CACO-2	Cis & EGCG (0/0)	Additive
CACO-2	Ox	Not applicable
CACO-2	Ox & Cur (0/0)	Synergistic
CACO-2	Ox & EGCG (0/0)	Synergistic
CACO-2	Ox & Col (0/4)	Additive
CACO-2	Ox & Tax (4/0)	Antagonistic

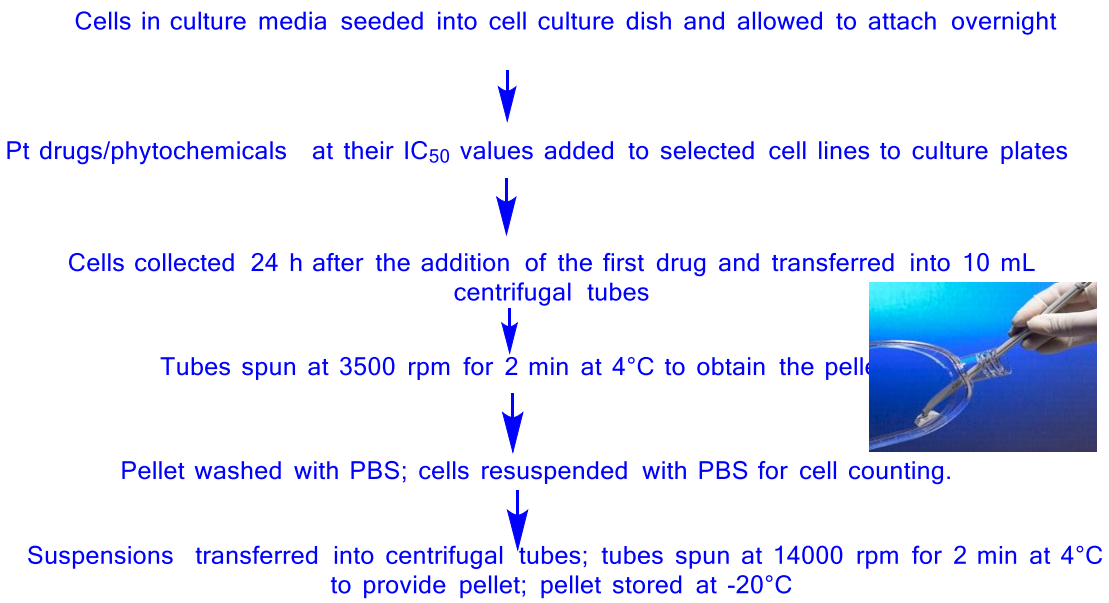

Figure 2.2: Flow diagram showing cell collection methodology

2.5.2 Accumulated platinum content estimation

1% triton –X 100 solution was made by dissolving required amount of triton X-100 in mQ water. In each prelabelled cell pellet, 0.5 mL of freshly prepared triton-X solution was added. Cell lysis was done very carefully using sonicator held on ice for about half an hour. The lysed cells were then spun in a large capacity refrigerated centrifuge at 14,000 rpm for 2 min. The supernatant was then taken for further determination of platinum contents using AAS.

Platinum standard solution used in the assay was prepared by mixing 0.001 mL of concentrated Pt standard solution (970 ppm) with 9.999 mL of 0. 1 M of HCl. Calibration curve was generated by loading serially diluted platinum standard solution using auto sampler (Abdullah, Huq et al. 2003). At least three different individual

experiments were conducted for each sample.

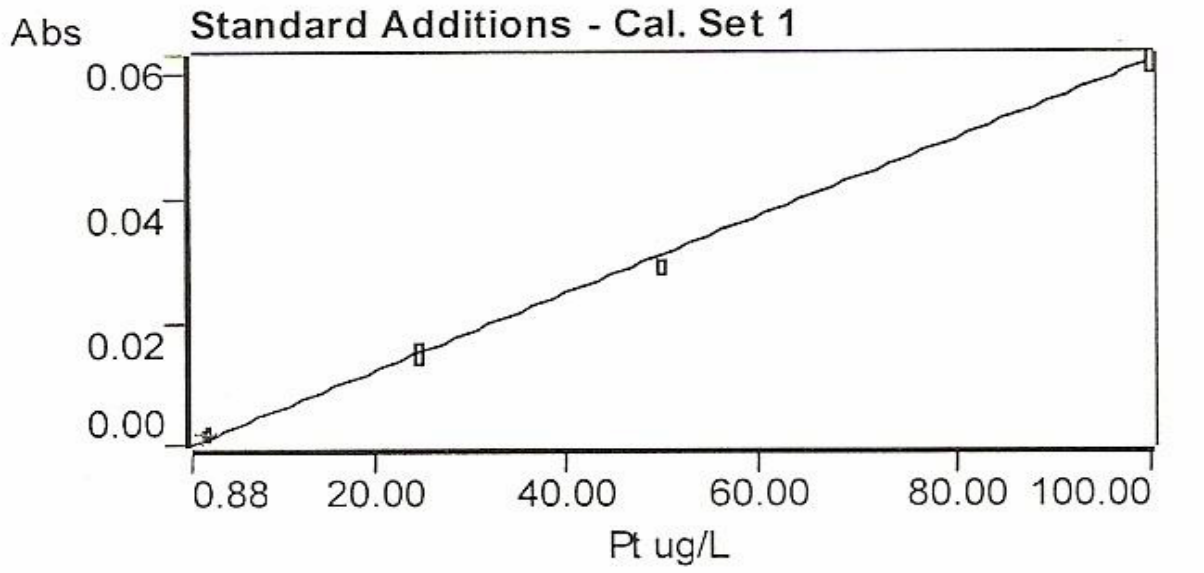

Figure 2.3: Calibration curve used in AAS assay for determination of platinum

2.6 Platinum–DNA binding

The study was also designed to reveal the link between the combined drug actions and binding of DNA with platinums. Drugs were added to the cells using the same combined treatments and same methodology as described in previous section (2.6.1). The final concentrations of the drugs used in the study are presented in Table 2.6.

Table 2.6: Final concentration of drugs applied to cells in platinum-DNA binding study

Drugs	**Single drug**	**Drugs in combination**
Cis	50	25
Ox	38	19
Cur	Not applicable	17
Col	Not applicable	127
EGCG	Not applicable	29.47
Tax	Not applicable	29

After collection of cells as pellets as portrayed in figure 2.3, pure genomic DNA was isolated from the cells with the use of EZ-10 spin column minipreps KIT. The method described in the booklet provided with the kit was exactly followed to extract the DNA. Flow chart of the entire procedure is given in figure 2.4. Concentration of DNA was quantified by following the equation: DNA concentration = Absorbance of DNA at 260 nm x 50 ng/μL.

After extracting DNA, 200 μL of each sample was injected into AAS using auto sampler to determine the extent of platinum-DNA binding. Each sample underwent into minimum three times individual experiment to obtain the statistically significant results.

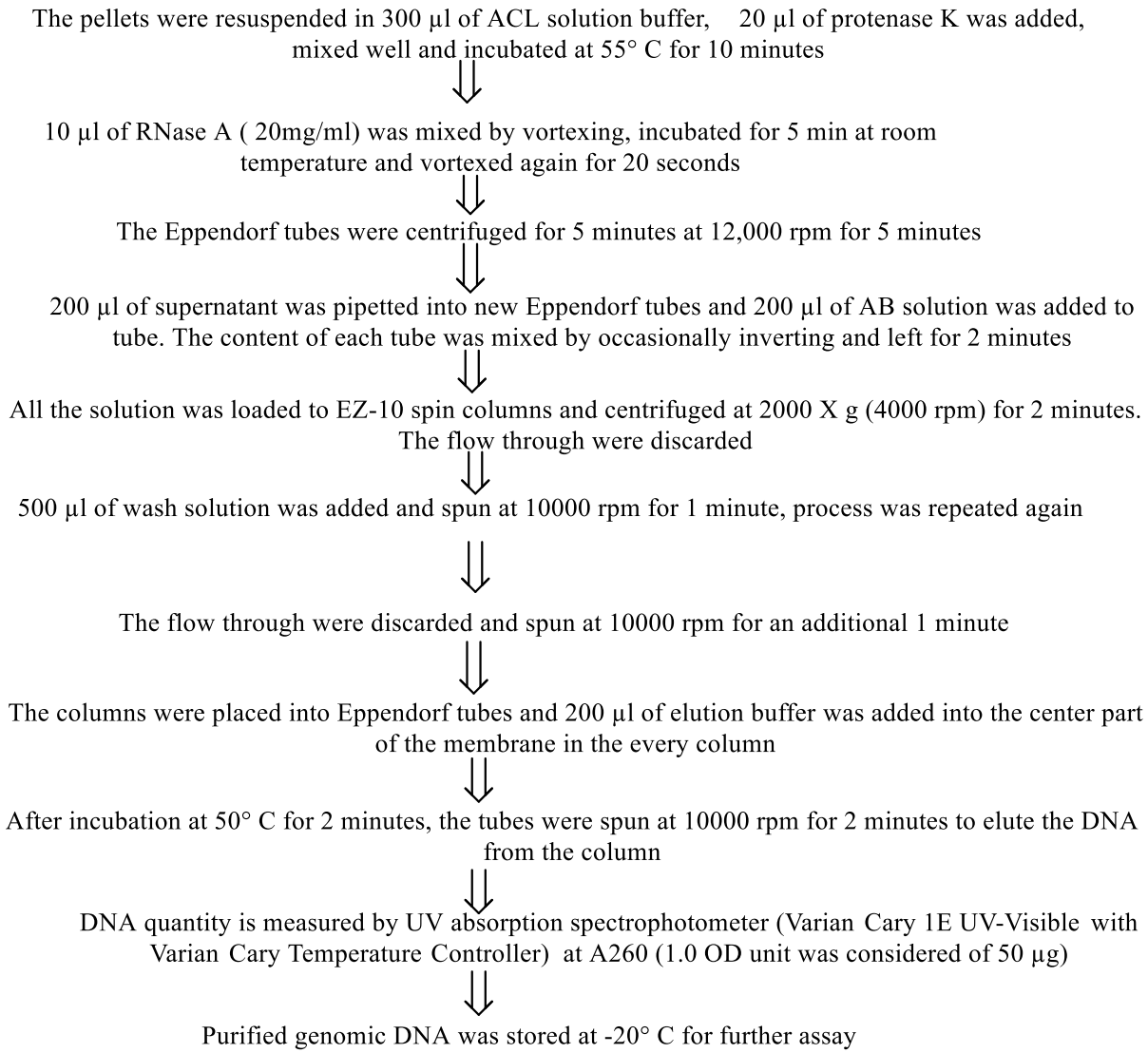

Figure 2.4: DNA extraction protocol

2.7 Study of interaction with DNA

Agar gel – electrophoresis study was carried out to gather the information relating to the interactions of the combinations with DNA. The aim of this study is to get the mechanistic insight relating to the combined drug action and damage to the DNA. Final concentration of the added drugs used in this study was same as tabulated in Table 2.6. Drugs were added by following the same technique as described in section 2.6.

Cell collection methodology as well as DNA extraction techniques have already been described in section 2.6 and 2.7. Agar gel-electrophoresis was conducted on all phytochemicals and platinums as single drug and seven combinations in DNA obtained from HT-29 cells. Moreover, six combinations were selected along with all single drug treatments for study with DNA obtained from CACO-2 cells.

Before starting agar gel electrophoresis, Tris-acetate-EDTA (TAE) buffer was freshly prepared. Initially 50 X TAE stock buffer (50 mL) was made by stirring 12.11 g of Tris base, 2.85 mL of glacial acetic acid and 0.93 g of EDTA in 47.15 mL of mQ water. Then it was diluted to 1 X TAE working buffer by measuring 40 mL of 50 X TAE and making the final volume up to 2 L using mQ water. 2 g of agarose gel powder was weighed and dissolved in 200 mL of working buffer using microwave. 125 µL of ethidium bromide was then added and mixed thoroughly to the gel. Prepared gel was then solidified on the tray (with comb in appropriate place). After 45 minutes, in each side of the electrophoresis chamber was added with 250 µL of ethidium bromide. Entire gel was dipped into the electrophoresis chamber using TAE working buffer. Estimated volume of DNA sample (measured as corresponding to 0.2 µg of DNA) was mixed with required volume of mQ water to make the total of 18 µl, followed by mixing with 2 µl of bromophenol blue chromatogram. Finally, each DNA sample was loaded into the well and electrophoresis was conducted for 120 min at 120 V. Image of the gel with DNA bands was visualized using UV lamp and Kodak Gel Logic (Huq, Yu et al. 2004).

2.8 Proteomic study

At the end of this study, proteomics was conducted with the aim of identifying the key proteins associated with the cytotoxicity of the single and combined drug administration. Only HT-29 and CACO-2 cancer cells were chosen for this study with

few selected treatments (alone and in combination). HT-29 cell line was treated with Ox alone, Col alone, EGCG alone, Ox+Col (0/4) and Ox+EGCG (0/0). In contrast, CACO-2 cell line was treated with Ox alone, Cur alone and Ox+Cur (0/0). Images of the gels obtained from drug treated HT-29 and CACO-2 colorectal cancer cells was matched and compared with the untreated gels of the same lines. The expression of the various proteins were compared with treated and untreated gels, hence the proteins responsible for cytotoxicity/combined drug action were identified. A pictorial diagram demonstrating the different steps of proteomic study is present in figure 2.5.

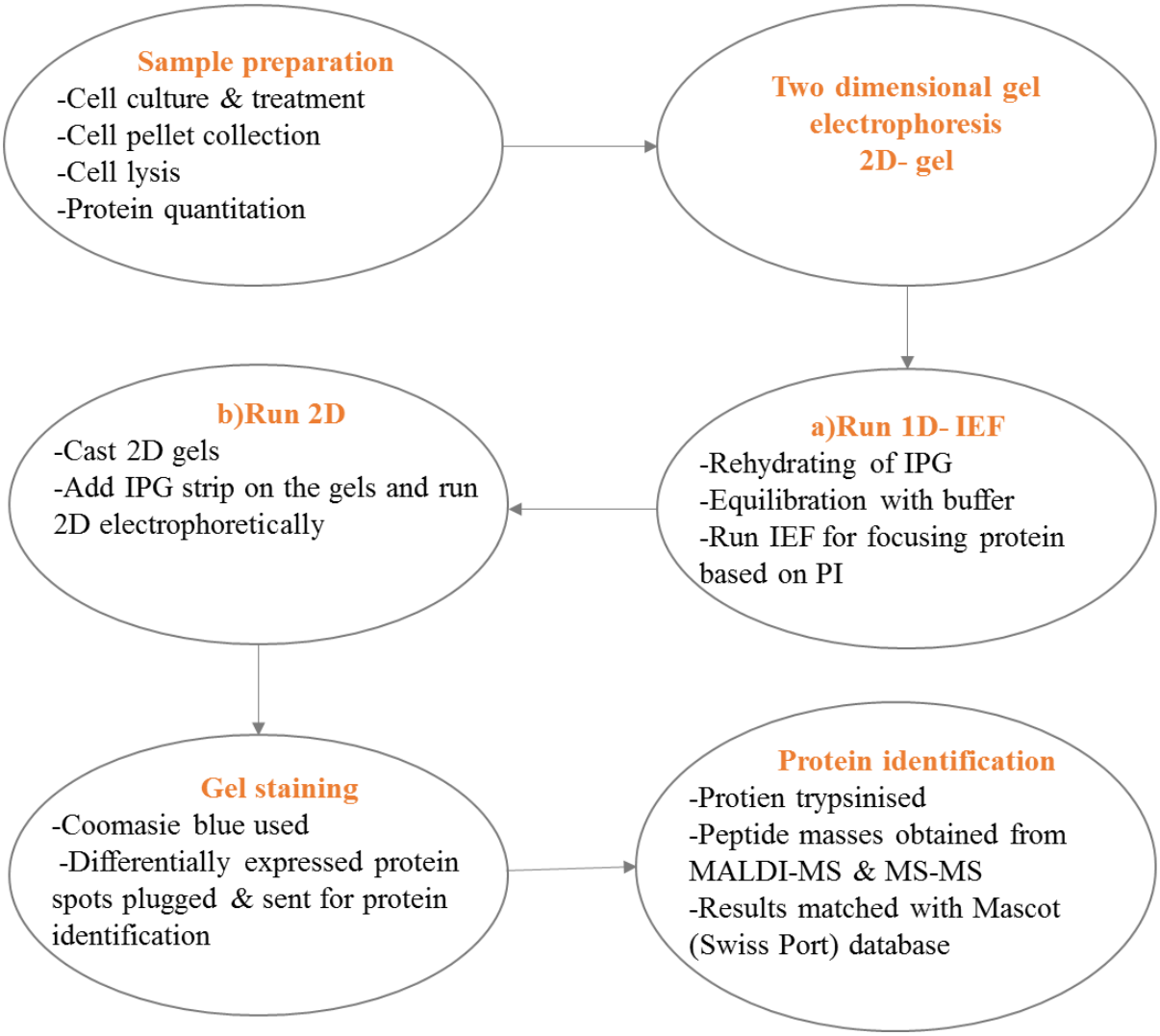

Figure 2.5: Summary of different steps carried out in proteomic study

2.8.1 Drug addition in colorectal cells

HT-29 and CACO-2 colorectal cells were sub cultured into large corning surface cell culture flask (175 cm^2) for proteomic study. Exponentially growing cells were harvested and seeded into 50 cm^2 culture dishes having 4.25 mL of medium and incubated for cell to grow with 80 percent confluence. After the incubation period, prelabelled culture dishes were added with drugs. For single drug additions: 0.375 mL of drug and 0.375 mL of medium; for combined drug additions: 0.375 mL of each drug; and for control 0.75 mL of medium was added. After the addition of drugs, the culture dishes were transferred into the 5% CO_2 incubator for 24 h.

2.8.2 Preparation of cell pellet

Cell collection methodology was similar to that described in figure 2.2, except that cell collections were done from large culture dishes instead of small culture dishes. Since the volume was greater, 50 mL tubes were used instead of 10 mL tubes and 5 mL PBS was used for washing in place of 2 mL.

2.9.3 Lysis of cells and protein content determination

Cell lysis was performed by following the established protocol in the host laboratory using the freshly prepared buffer composed of urea, thiourea, CHAPS, DTT and protease inhibitor tablets (Al-Eisawi, Beale et al. 2016). Exact composition of the lysis buffer and detail method for measuring the protein concentration is provided in Appendix –I.

2.8.3 Separation of individual proteins

2-D gel electrophoresis was conducted to separate the proteins initially on the basis of isoelectric points (pI) and subsequently as a function of molecular weight. pI based separation was performed in first dimension through iso-electric focusing (IEF) on

immobilized pH gradient (IPG) strips. In addition, second dimensional separation of the proteins was accomplished through polyacrylamide electrophoresis (PAGE) gels. Coomasie blue was used to stain the gels and 0.05% sodium azide solution was used for gel preservation (Salvato, Carvalho et al. 2012). Figure 2.6 shows the sample of IPG strip and other instruments used in 1D electrophoresis. The detail procedure of gel electrophoresis is provided in Appendix-1.

Figure 2.6: IPG strip and PROTEAN IEF system used in the study

2.8.4 Protein gel image analysis

Proteins spots on gels were analysed using updated version of Melanie software. Minimum two gels obtained from the same treatment were used for accuracy and precision. Initially the gel images were imported into the software and arranged into separate groups and classes. In this study 10 matched groups were created which

belonged to two different classes. Figure 2.7 illustrates the matched classes and groups created in this study. During analysis of spots, two spots were selected as marker spots which were found to be present in every gel for the matched groups and class. Then the matching of the spots was performed through Melanie software. Change in fold of a protein by 1.5 or more was considered as significant in the study. Statistical test was performed by analysis of variance method (ANOVA) and a value of 0.05 was cut off point.

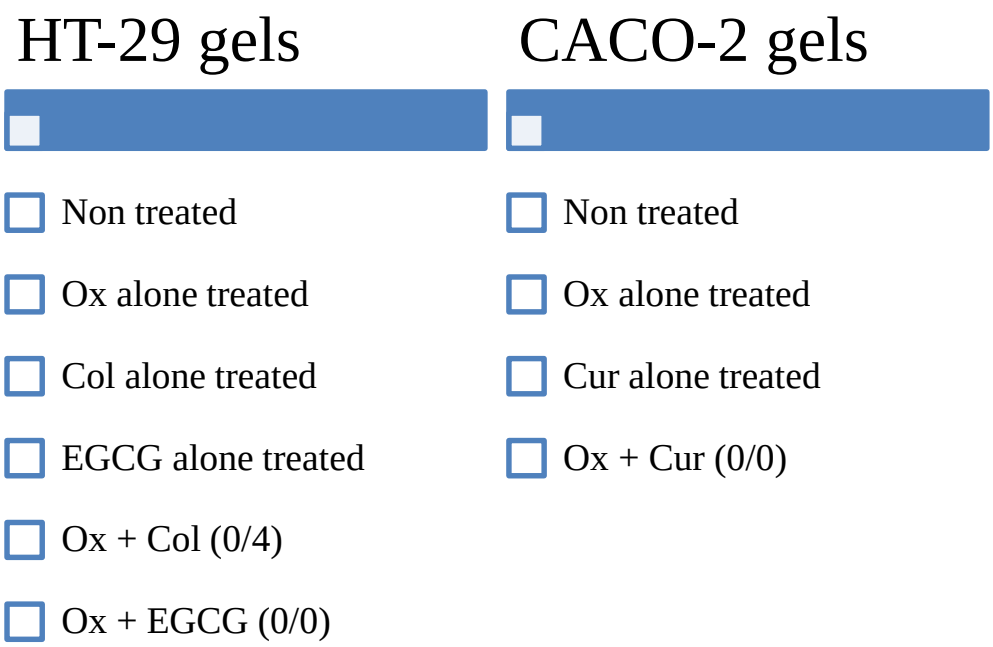

Figure 2.7: Matched classes and groups in proteomic study

2.8.5 Determination of protein identity

Selected protein spots were excised from the gels and sent to Australian Proteomic Analysis Facility (APAF), located at Macquarie University, Sydney, Australia for protein characterisation and identification. Matrix Assisted Laser Desorption Ionisation mass spectrometry (MALDI-MS) was employed with an Applied Biosystems 4800

Proteomics Analyser to determine the identity of selected proteins. The detail of experimental is given in Appendix I.

3 RESULTS

Preamble: Colorectal cancer is one of the most dreaded diseases of our time and chemotherapy stands as frontline treatment in metastasized advanced level of CRC. The objective of this study was to look for the phytochemicals which give synergism with platinum drugs against colorectal cancer models. This chapter consists of the results obtained from the cytotoxicity of platinum compounds and phytochemicals investigated in this study either alone or in combination against four different colorectal cancer cell lines (HT-29, CACO-2, LIM-1215 and LIM-2405). Results of the mechanistic studies e.g. cellular accumulation, platinum DNA binding, DNA damage and proteomics will also detailed in this chapter.

3.1 Antitumour activity of the compounds alone

Cytotoxicity of the individual compound was determined using MTT reduction assay against four colorectal cancer cell lines. The result of the cytotoxicity of the compounds has been described here in terms of dose response curves and IC_{50} values. Obtained IC_{50} values were further used in designing the plan for combination study.

3.1.1 HT-29 cell line

Figure 3.1 gives the cell survival versus concentration plots for platinum drugs: Cis, Ox and phytochemicals: Tax, Col, Cur, EGCG, and 6-gin as applied to the human colorectal cancer cell line HT-29.

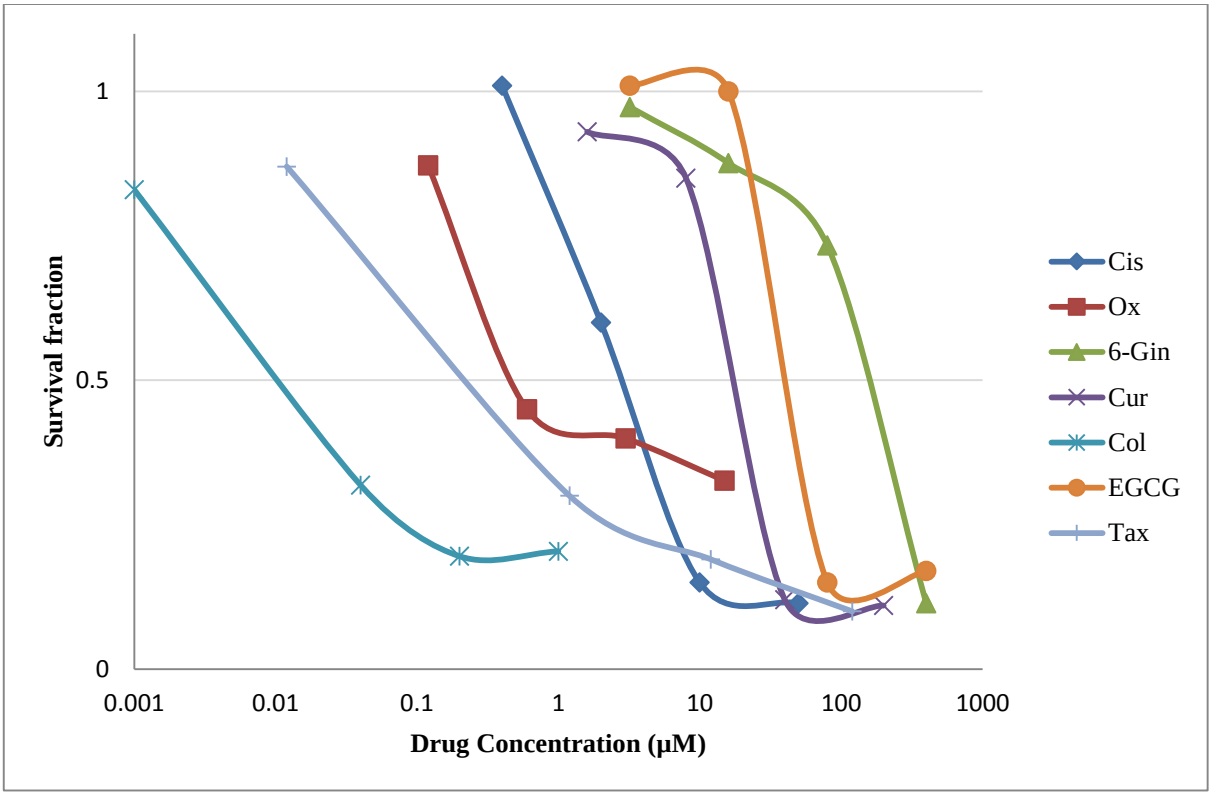

Figure 3.1 : Dose response curves for the tested compounds as applied to the human colorectal cancer cell line HT-29.

It can be seen that the most active compound against the colorectal cancer cell line HT-29 is Col followed by Tax and the least active compound is 6-gin. Among the platinum drugs, the oxaliplatin is more active than cisplatin against the cell line.

3.1.2 CACO-2 cell line

Figure 3.2 gives the cell survival versus concentration plots for platinum drugs: Cis, Ox and phytochemicals: Tax, Col, Cur, EGCG, and 6-Gin as applied to the human colorectal cancer cell line CACO-2.

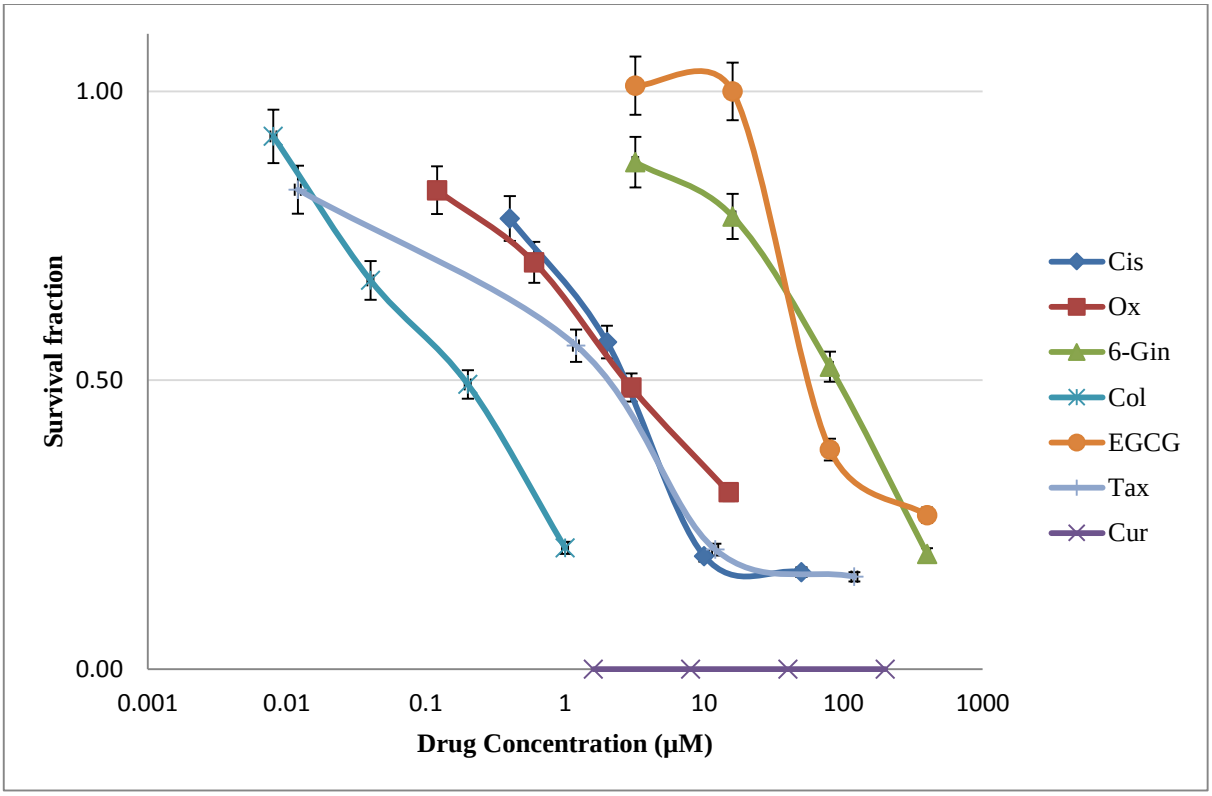

Figure 3.2 : Dose response curves for the tested compounds as applied to the human colorectal cancer cell line CACO-2

It can be seen that the most active compound against the colorectal cancer cell line CACO-2 is Col followed by Tax and the least active compound is 6-gin. Among the platinum drugs, the Ox is more active against the cell line than Cis.

3.1.3 LIM-1215 cell line

Figure 3.3 gives the cell survival versus concentration plots for platinum drugs: Cis, Ox and phytochemicals: Tax, Col, Cur, EGCG, and 6-Gin as applied to the human colorectal cancer cell line LIM-1215.

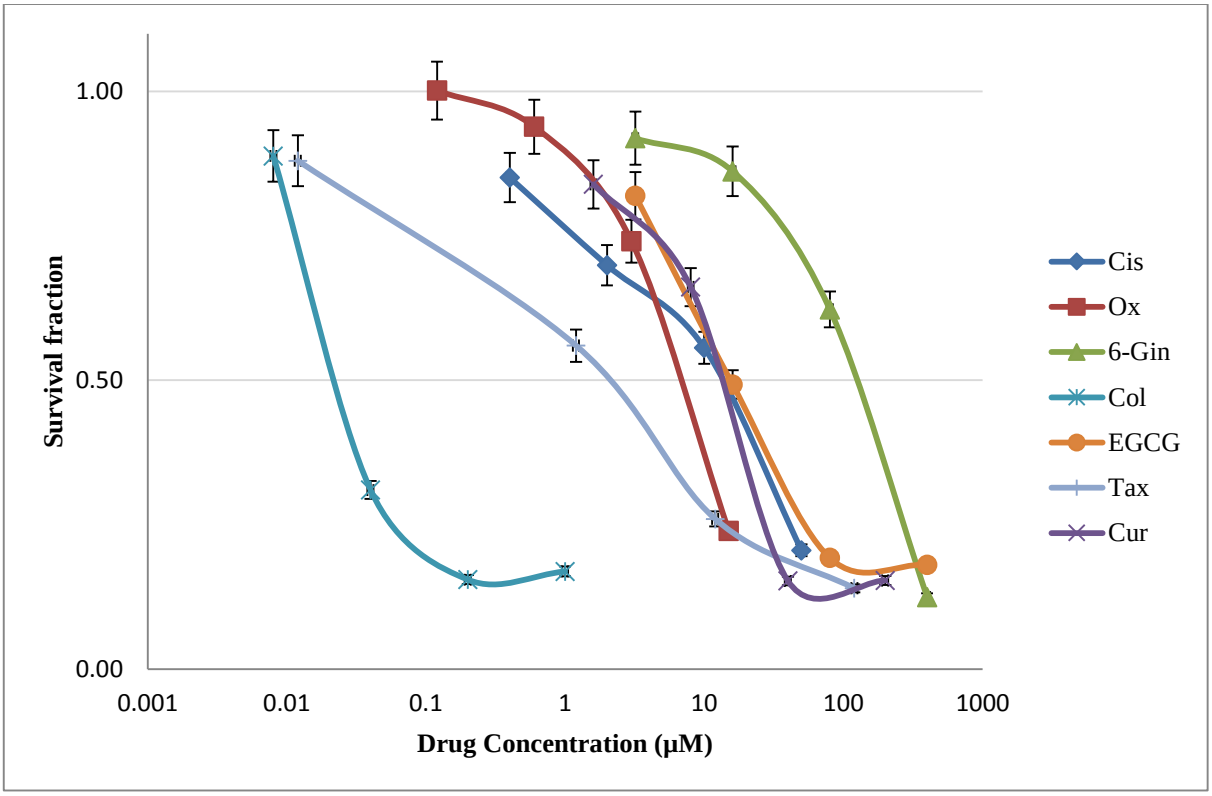

Figure 3.3: Dose response curves for the tested compounds as applied to the human colorectal cancer cell line LIM-1215.

It can be seen that the most active compound against the colorectal cancer cell line LIM-1215 is Col followed by Tax and the least active compound is 6-Gin. Among the platinum drugs, the Ox is more active than Cis against the cell line.

3.1.4 LIM-2405 cell line

Figure 3.4 gives the cell survival versus concentration plots for platinum drugs: Cis, Ox and phytochemicals: Tax, Col, Cur, EGCG, and 6-gin as applied to the human colorectal cancer cell line LIM-2405.

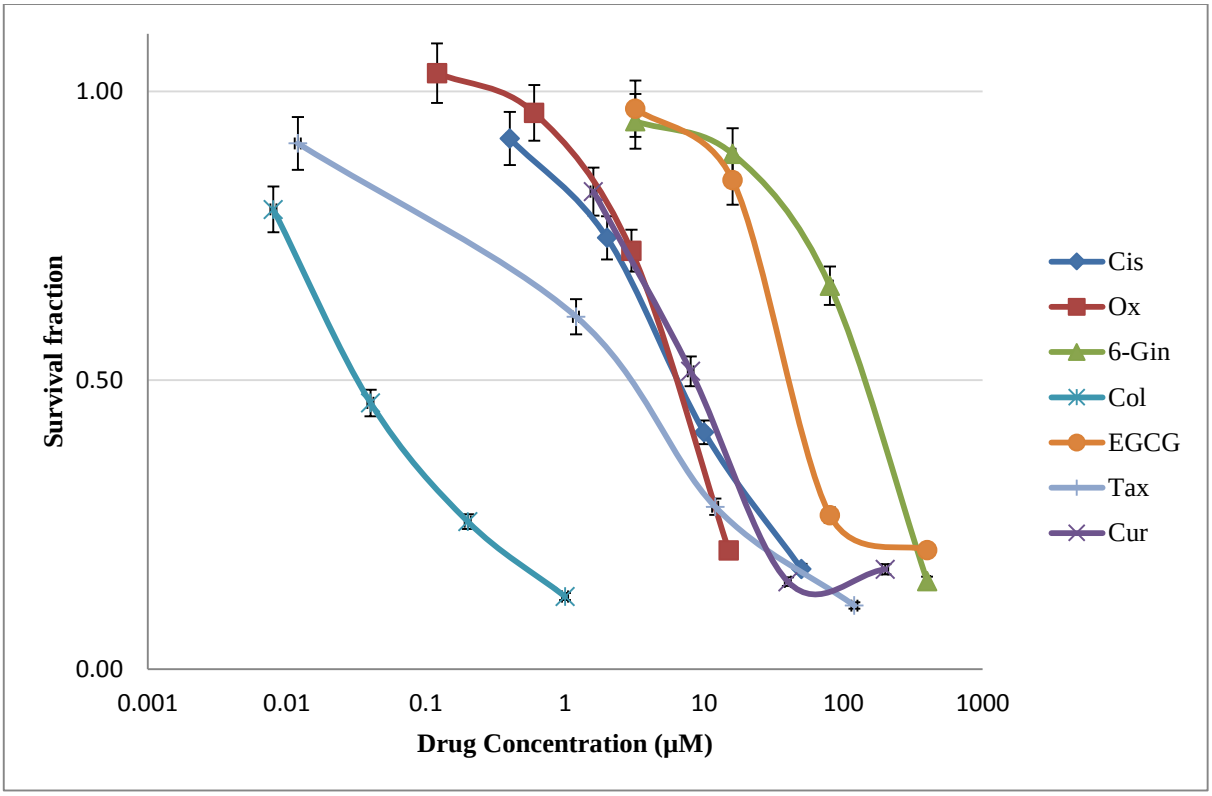

Figure 3.4**:** Dose response curves for the tested compounds as applied to the human colorectal cancer cell line LIM-2405

It can be seen that the most active compound against the colorectal cancer cell line LIM-2405 is Col followed by Tax and the least active compound is 6-Gin. Among the platinum drugs, the cisplatin is more active than oxaliplatin against the cell line.

3.1.5 Summary of IC_{50} values

Table 3.1 gives a summary of IC_{50} values of the compounds platinums: cisplatin (Cis), oxaliplatin (Ox) and phytochemicals: taxol (Tax), colchicine (Col), curcumin (Cur), epigallocatechin-3-gallate (EGCG), and 6-gengirol (6-Gin) as applied to the cell lines HT-29, CACO-2, LIM-1215 and LIM-2405. Figure 3.5 gives a graphical representation of the IC_{50} values of the studied compounds (except 6-Gin which showed very large values in all cell lines).

Table 3.1: Summary of the IC_{50} values (μM) for Cis, Ox, 6-Gin, Cur, Col, EGCG and Tax as applied to HT-29, CACO-2, LIM-1215 and LIM-2405 human colorectal cancer cell lines

Cell lines	Platinum drug		Phytochemical				
	Cis	Ox	Col	Cur	EGCG	Tax	6-Gin
HT-29	5.00±0.00	0.47±0.00	0.01±0.00	17.25±0.02	28.40±0.04	0.50±0.00	146.46±0.27
CACO-2	26.02±0.05	2.72±0.00	0.19±0.00	21.20±0.02	61.30±0.1	2.50±0.00	116.96±0.21
LIM-1215	7.49±0.02	1.25±0.00	0.02±0.00	31.30±0.06	14.60±0.02	1.00±0.02	147.39±0.29
LIM-2405	4.98±0.01	7.60±0.01	0.01±0.00	8.30±0.01	37.00±0.05	1.50±0.2	161.89±0.37

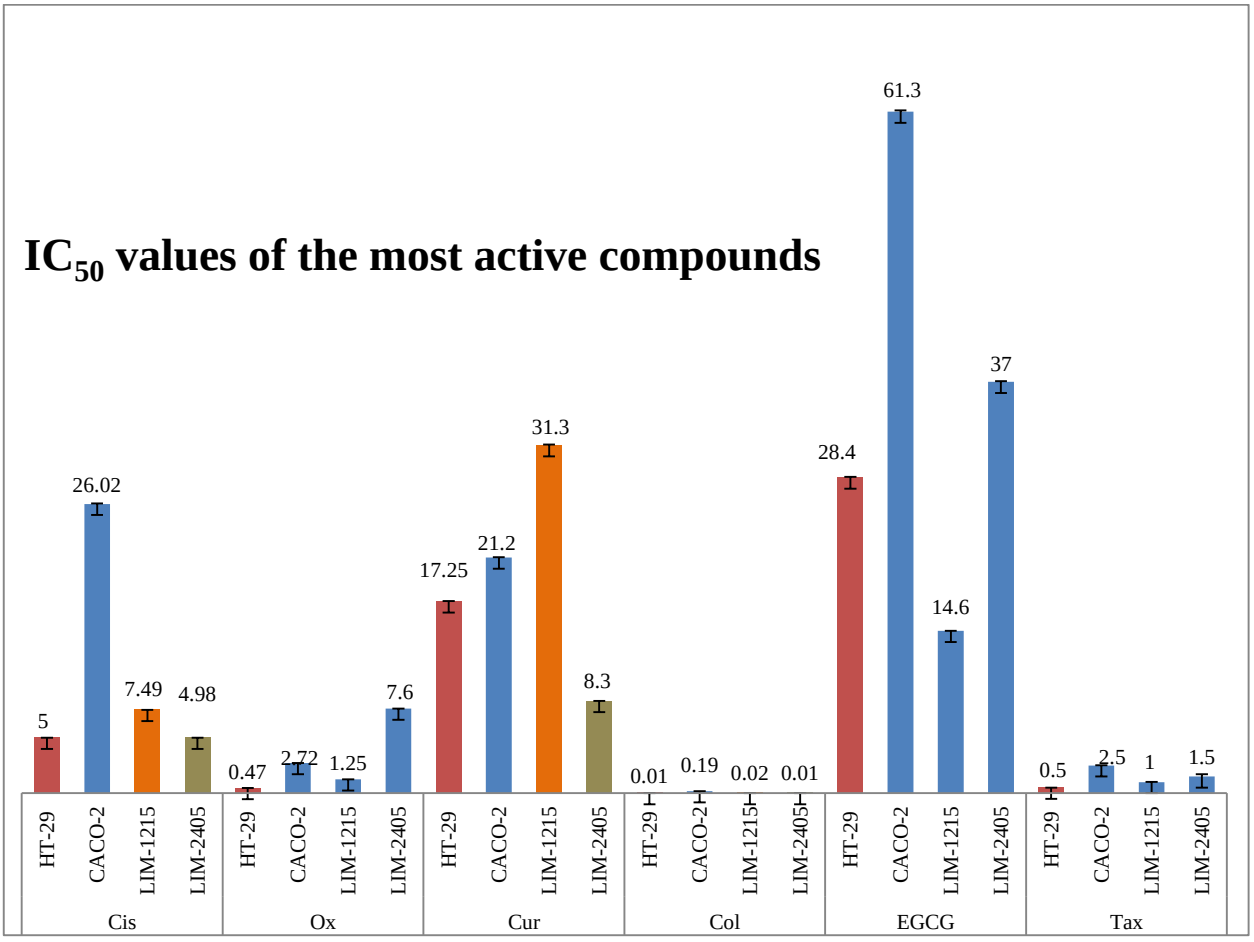

Figure 3.5: IC_{50} values (μM) for Cis , Ox, Cur, Col, EGCG and Tax as applied to HT-29, CACO-2, LIM-1215 and LIM-2405 human colorectal cancer cell lines

It can be seen that colchicine is the most potent compound in all four colorectal cancer cell lines which is followed by taxol then oxaliplatin. The exact order of antitumour activity from highest to lowest in different colorectal cancer cell lines was as follows:

HT-29: Col>Ox>Tax>Cis>Cur>EGCG>6-Gin

CACO-2: Col>Tax>Ox>Cur>Cis>EGCG>6-Gin

LIM-1215: Col>Tax>Ox>Cis>EGCG>Cur>6-Gin

LIM-2405: Col>Tax>Cis>Ox>Cur>EGCG>6-Gin

These results are discussed in more detail in the next chapter.

3.2 Drugs in Combination

After the determination of the IC_{50} values, studies on drug combination were carried out to investigate whether the combined action of the drugs was synergistic, additive or antagonistic. Since 6-gin showed very low antitumour activity in all selected colorectal cancer cell lines with IC_{50} values greater than 100 μM, the phytochemical was not considered for combination study. Dose response curves and combination indices were used as measures of the combined drug action in this study.

3.2.1 Dose response curves

3.2.1.1 Combinations between platinum drugs and phytochemicals in HT-29 cell line

Table 3.2 gives the dose effect values (affected cell fractions) at three different concentrations of Cis and phytochemicals added alone and in combination according to three different sequences of administration (Cis/Phytochemical h): (0/0 h), (0/4 h), and (4/0 h) to HT-29 cell line. Figures 3.6 -3.9 represent the corresponding dose response curves.

From the dose response curve (Figure 3.6), it can be said that 4/0 addition of Cis with Cur against HT-29 cell line produced greater cell kill whereas 0/4 addition of the same was the least effective. Bolus addition of Cis with Col displayed highest cytotoxicity against HT-29 cell line while 4/0 addition did the lowest in the same cells (Figure 3.7). When Cis was combined with EGCG, bolus addition caused greater cell kill whereas 0/4 sequence of addition was the least effective (Figure 3.8). In contrast, when Cis was combined with Tax, bolus addition produced greater cell kill whereas 4/0 administration was the least effective against HT-29 cell line (Figure 3.9).

Table 3.2: Cell fractions affected by drug treatments (Cis and phytochemicals) alone and in combination against HT-29 cell line

Effects observed at different concentrations (µM) of drugs administered alone				
Cis (µM)	**Effect**			
0.4	0.09 ± 0.01			
4	0.54 ± 0.12			
40	0.85 ± 0.05			
Cur (µM)	**Effect**	**Col (µM)**	**Effect**	
1.38	0.11 ± 0.03	0.001	0.21 ± 0.09	
13.8	0.61 ± 0.05	0.01	0.49 ± 0.07	
137.98	0.90 ± 0.06	0.07	0.71 ± 0.04	
EGCG (µM)	**Effect**	**Tax (µM)**	**Effect**	
1.92	0.08 ± 0.06	0.04	0.001 ± 0.02	
19.2	0.33 ± 0.03	0.4	0.51 ± 0.10	
192	0.86 ± 0.01	4	0.88 ± 0.08	
Effects observed at different concentrations (µM) of drugs administered in combination				
Concentration		**Sequence and drug effect**		
		(0/0 h)	(0/4 h)	(4/0 h)
Cis	**Cur**	**Effect**	**Effect**	**Effect**
0.2	0.69	0.31 ± 0.10	0.4 ± 0.04	0.28 ± 0.02
2.0	6.9	0.55 ± 0.03	0.59 ± 0.09	0.53 ± 0.04
20.0	68.99	0.87 ± 0.05	0.89 ± 0.08	0.87 ± 0.08
Cis	**Col**			
0.2	0.0005	0.743 ± 0.07	0.745 ± 0.07	0.803 ± 0.06
2.0	0.0047	0.744 ± 0.04	0.828 ± 0.07	0.825 ± 0.08
20.0	0.047	0.745 ± 0.14	0.924 ± 0.06	0.8852 ± 0.02
Cis	**EGCG**			
0.2	0.96	0.31 ± 0.03	0.4 ± 0.04	0.28 ± 0.01
2.0	9.6	0.55 ± 0.05	0.59 ± 0.02	0.53 ± 0.03
20.0	96	0.87 ± 0.01	0.89 ± 0.08	0.87 ± 0.07
Cis	**Tax**			
0.2	0.02	0.001 ± 0.11	0.001 ± 0.14	0.001 ± 0.10
2.0	0.2	0.337 ± 0.09	0.3873 ± 0.04	0.3345 ± 0.05
20.0	2	0.9036 ± 0.13	0.8977 ± 0.09	0.8833 ± 0.08

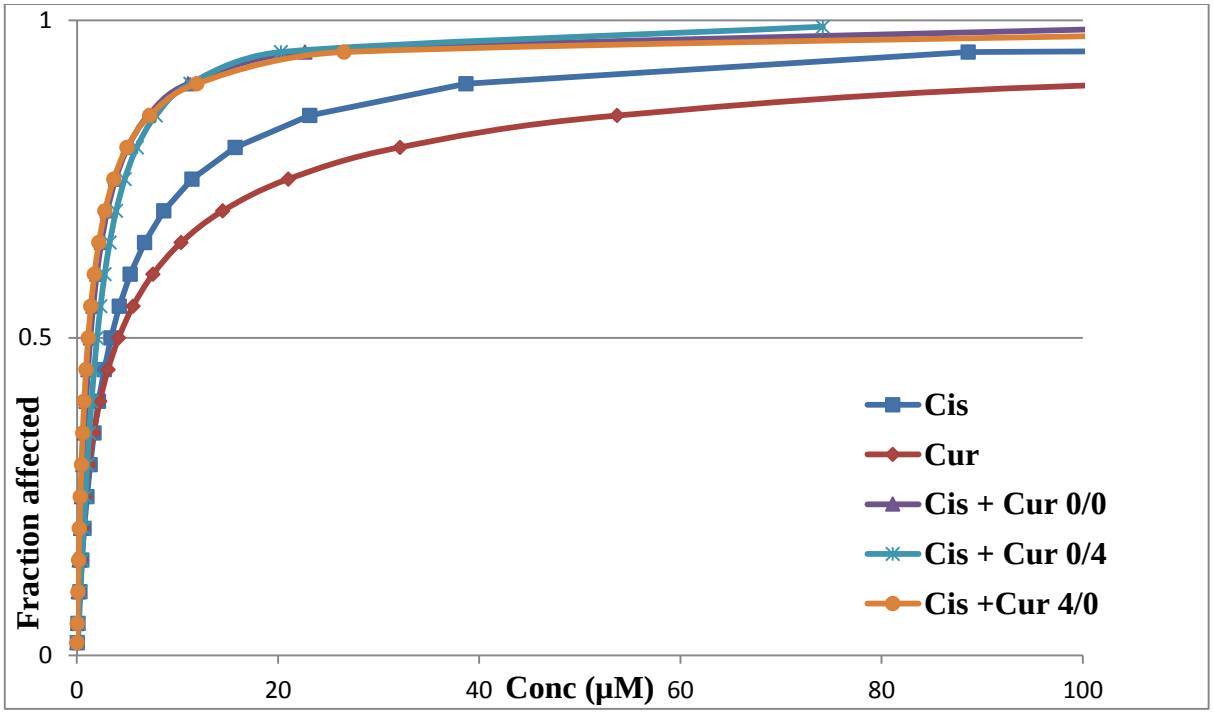

Figure 3.6 : Dose response curves obtained from combination of Cis with Cur as employed to HT-29 cell line

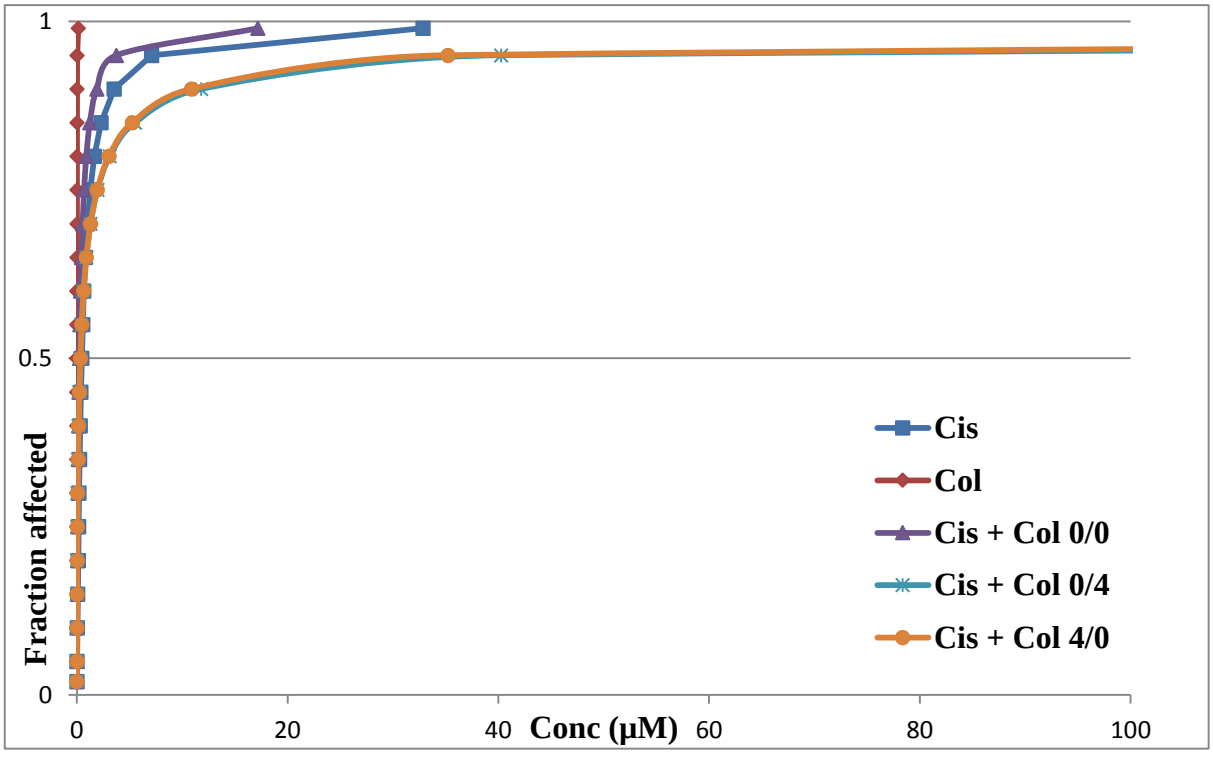

Figure 3.7 : Dose response curves obtained from combination of Cis with Col as employed to HT-29 cell line

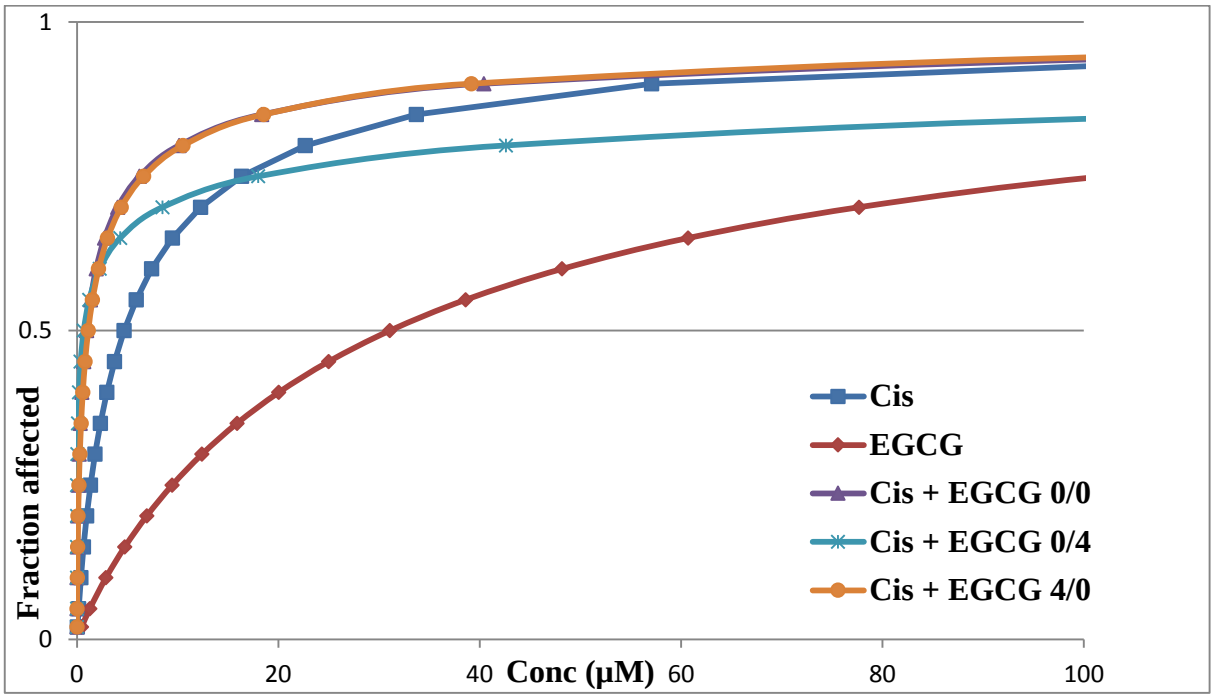

Figure 3.8 : Dose response curves obtained from combination of Cis with EGCG as employed to HT-29 cell line

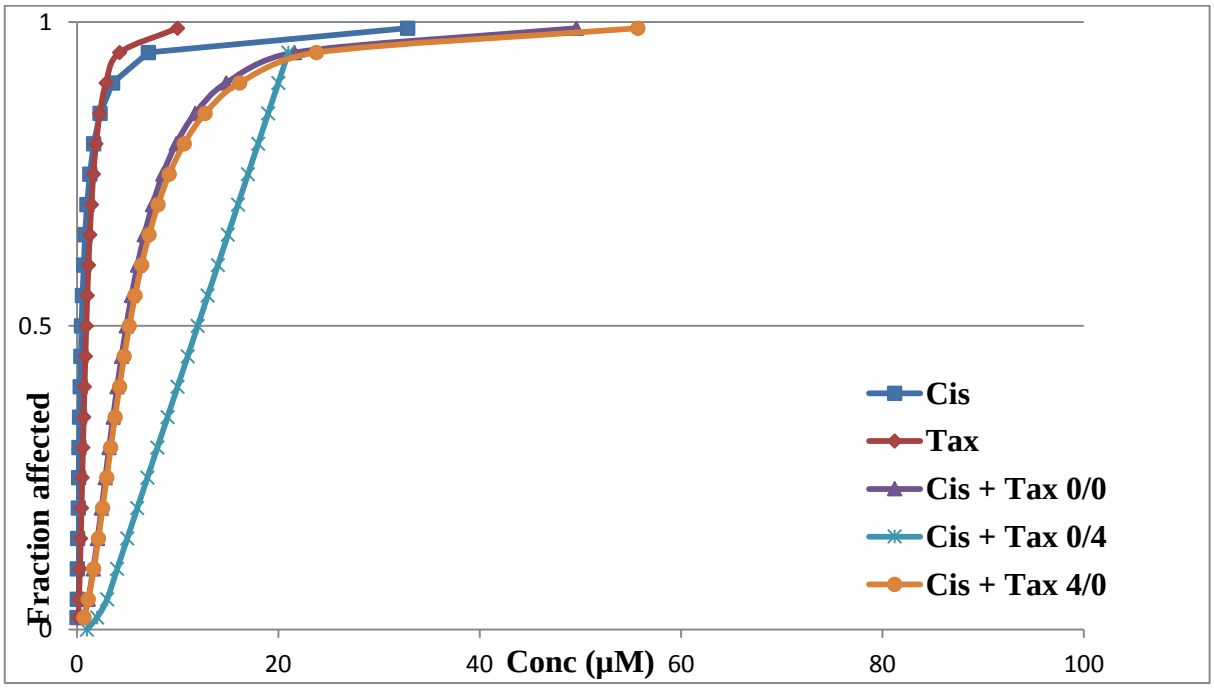

Figure 3.9 : Dose response curves obtained from combination of Cis with Tax as employed to HT-29 cell line

Table 3.3 gives the dose effect values (affected cell fractions) at three different concentrations of Ox and phytochemicals added alone and in combination according to three different sequences of administration (Ox/Phytochemical h): (0/0 h), (0/4 h), and (4/0 h) to HT-29 cell line. Figures 3.10 -3.13 represent the corresponding dose response curves.

From the dose response curve (Figure 3.10), it can be said that 4/0 addition of Ox with Cur against HT-29 cell line produced greater cell kill whereas 0/4 addition of the same was the least effective. Bolus addition of Ox with Col displayed highest cytotoxicity against HT-29 cell line while 0/4 addition did the lowest in the same cells (Figure 3.11). When Ox was combined with EGCG, bolus addition caused greater cell kill whereas 0/4 sequence of addition was the least effective (Figure 3.12). In contrast, when Ox was combined with Tax, 4/0 sequenced addition produced greater cell kill whereas bolus addition was the least effective against HT-29 cell line (Figure 3.13).

Table 3.3: Cell fractions affected by drug treatments (Ox and phytochemicals) alone and in combination against HT-29 cell line

Effects observed at different concentrations (µM) of drugs administered alone				
Ox (µM)	**Effect**			
0.04	0.001 ± 0.00			
0.38	0.44 ± 0.04			
3.76	0.75 ± 0.01			
Cur (µM)	**Effect**	**Col (µM)**	**Effect**	
1.38	0.11 ± 0.05	0.001	0.21 ± 0.03	
13.8	0.61 ± 0.02	0.01	0.49 ± 0.01	
137.98	0.90 ± 0.02	0.07	0.71 ± 0.04	
EGCG (µM)	**Effect**	**Tax (µM)**	**Effect**	
1.92	0.08 ± 0.01	0.04	0.001 ± 0.12	
19.2	0.33 ± 0.06	0.4	0.51 ± 0.05	
192	0.86 ± 0.03	4	0.88 ± 0.02	
Effects observed at different concentrations (µM) of drugs administered in combination				
Concentration		**Sequence and drug effect**		
		(0/0 h)	(0/4 h)	(4/0 h)
Ox	**Cur**	**Effect**	**Effect**	**Effect**
0.02	0.69	0.02 ± 0.00	0.01 ± 0.01	0.15 ± 0.00
0.19	6.9	0.38 ± 0.03	0.30 ± 0.03	0.56 ± 0.05
1.88	68.99	0.92 ± 0.01	0.91 ± 0.08	0.92 ± 0.09
Ox	**Col**			
0.2	0.0005	0.09 ± 0.01	0.01 ± 0.01	0.03 ± 0.02
2.0	0.0047	0.55 ± 0.03	0.28 ± 0.04	0.48 ± 0.03
20.0	0.047	0.78 ± 0.07	0.76 ± 0.05	0.77 ± 0.02
Ox	**EGCG**			
0.2	0.96	0.15 ± 0.01	0.02 ± 0.03	0.23 ± 0.01
2.0	9.6	0.71 ± 0.06	0.61 ± 0.02	0.67 ± 0.06
20.0	96	0.86 ± 0.11	0.82 ± 0.07	0.84 ± 0.05
Ox	**Tax**			
0.2	0.02	0.001 ± 0.01	0.001 ± 0.00	0.001 ± 0.07
2.0	0.2	0.25 ± 0.03	0.3 ± 0.06	0.28 ± 0.04
20.0	2	0.67 ± 0.07	0.64 ± 0.01	0.67 ± 0.06

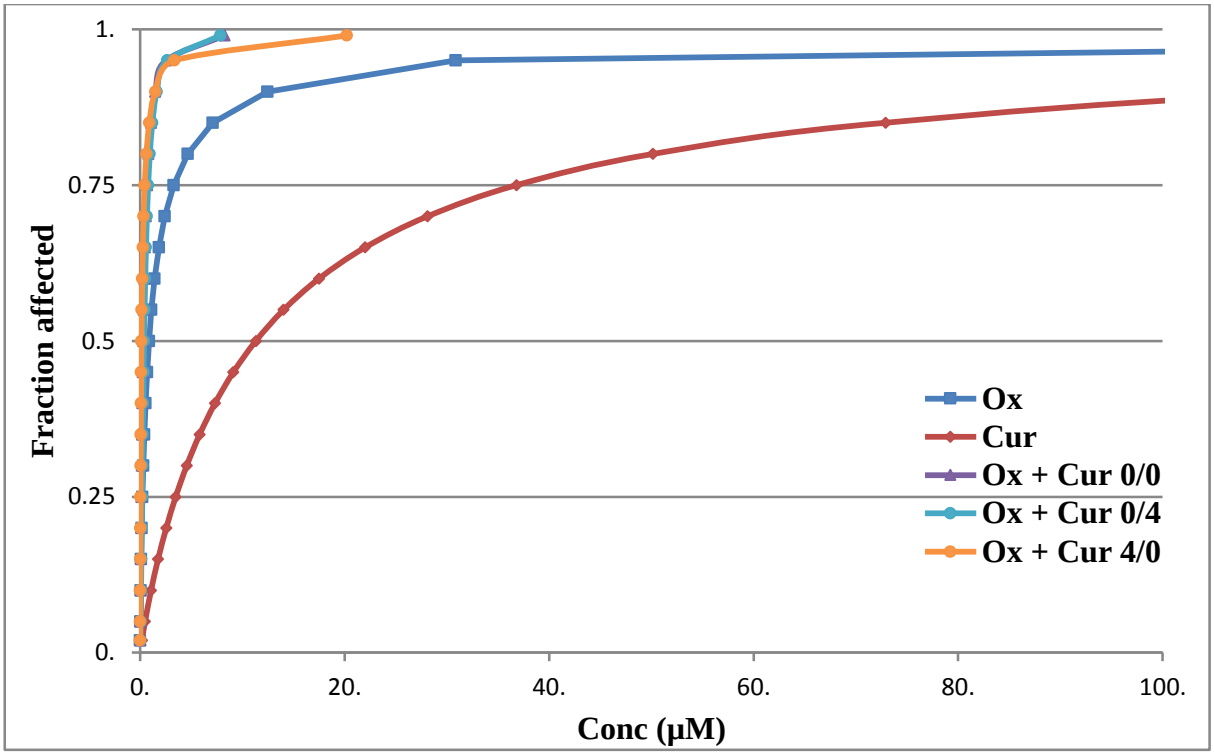

Figure 3.10 : Dose response curves obtained from combination of Ox with Cur as employed to HT-29 cell line

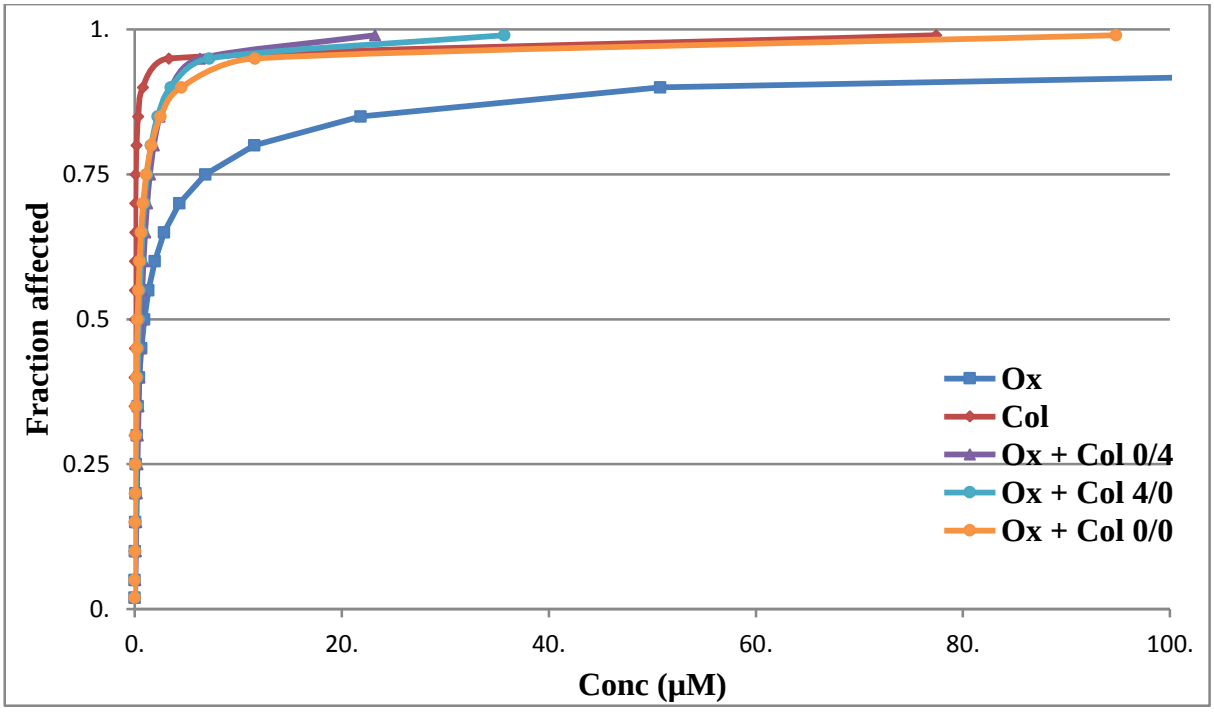

Figure 3.11 : Dose response curves obtained from combination of Ox with Col as employed to HT-29 cell line

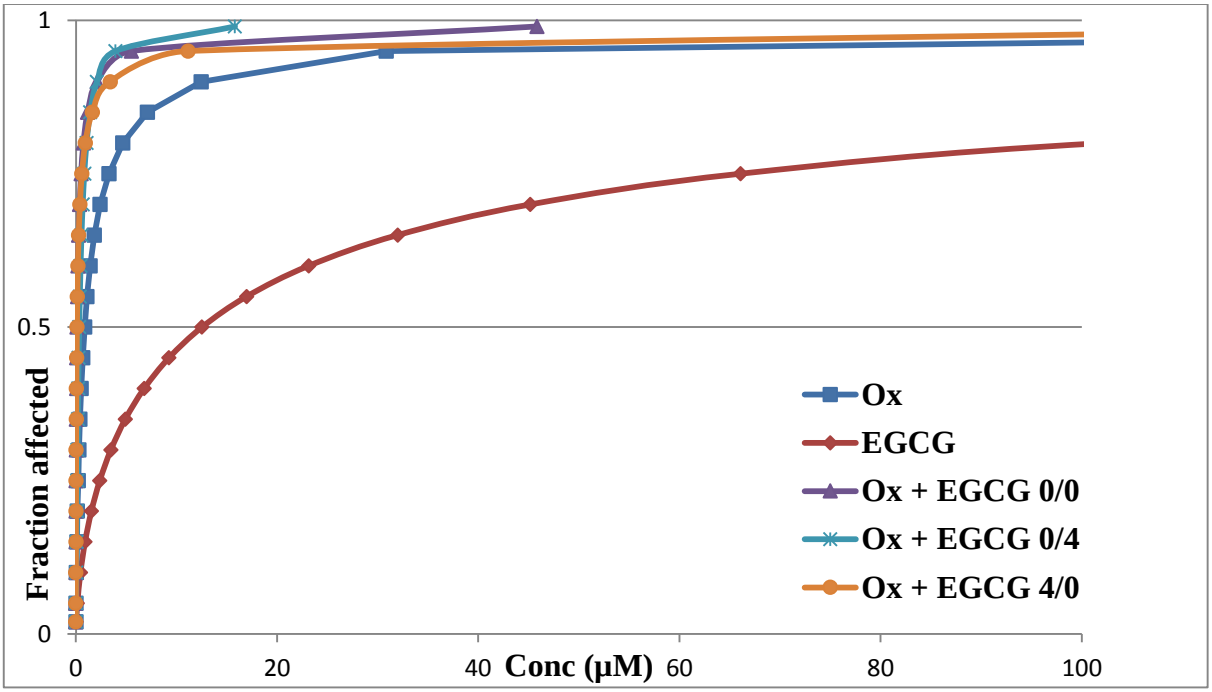

Figure 3.12 : Dose response curves obtained from combination of Ox with EGCG as employed to HT-29 cell line

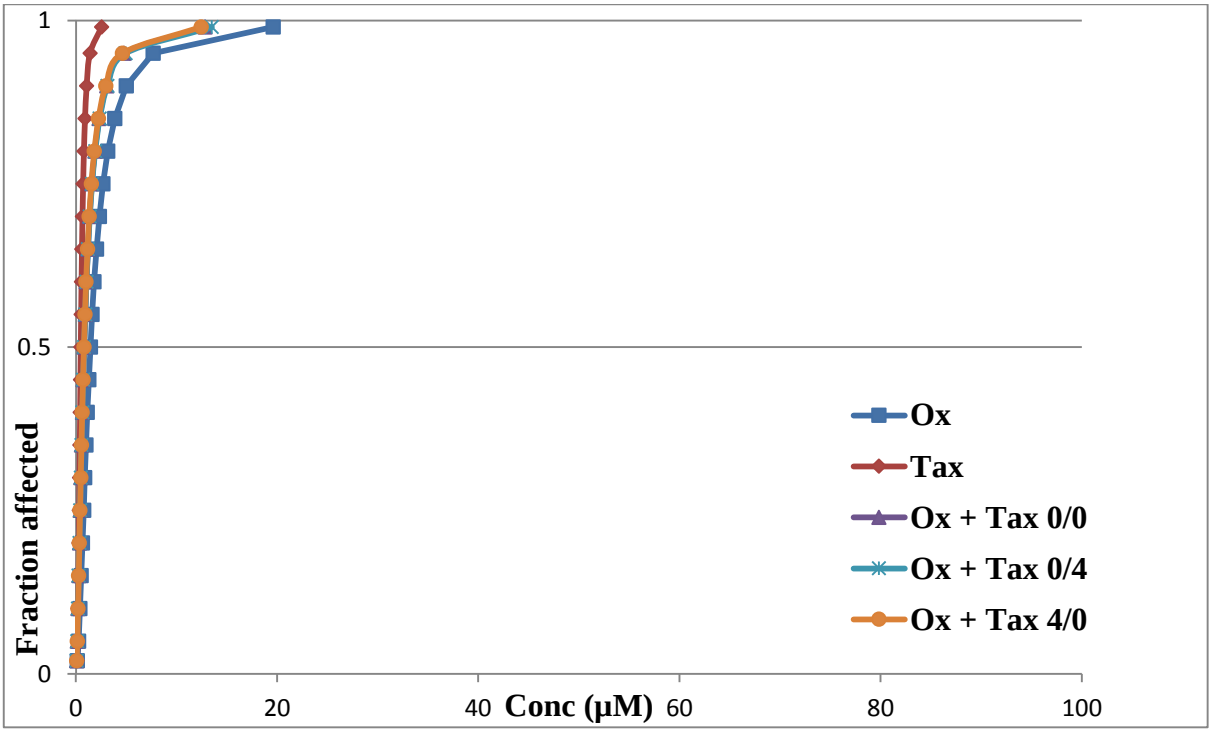

Figure 3.13: Dose response curves obtained from combination of Ox with Tax as employed to HT-29 cell line

3.2.1.2 Combinations between platinum drugs and phytochemicals in CACO-2 cell line

Table 3.4 gives the dose effect values (affected cell fractions) at three different concentrations of Cis and phytochemicals added alone and in combination according to three different sequences of administration (Cis/Phytochemical h): (0/0 h), (0/4 h), and (4/0 h) to CACO-2 cell line. Figures 3.14 -3.17 represent the corresponding dose response curves.

From the dose response curve (Figure 3.14), it can be said that bolus addition of Cis with Cur against CACO-2 cell line produced greater cell kill whereas 0/4 addition of the same was the least effective. 4/0 sequence of addition of Cis with Col displayed highest cytotoxicity against CACO-2 cell line while bolus addition did the lowest in the same cells (Figure 3.15). When Cis was combined with EGCG, 0/4 sequence of addition caused greater cell kill whereas 4/0 sequence of addition was the least effective (Figure 3.16). In contrast, when Cis was combined with Tax, bolus addition produced greater cell kill whereas 0/4 sequence of addition was the least effective against CACO-2 cell line (Figure 3.17).

Table 3.4: Cell fractions affected by drug treatments (Cis and phytochemicals) alone and in combination against CACO-2 cell line

Effects observed at different concentrations (µM) of drugs administered alone				
Cis (µM)	**Effect**			
4.1632	0.25 ± 0.10			
20.816	0.71 ± 0.02			
104.08	0.87 ± 0.01			
Cur (µM)	**Effect**	**Col (µM)**	**Effect**	
1.7	0.1 ± 0.03	0.02	0.35 ± 0.06	
16.96	0.43 ± 0.02	0.15	0.47 ± 0.03	
169.56	0.88 ± 0.05	1.5	0.60 ± 0.01	
EGCG (µM)	**Effect**	**Tax (µM)**	**Effect**	
4.9	0.15 ± 0.02	0.12	0.001 ± 0.04	
49.04	0.32 ± 0.05	1.2	0.09 ± 0.01	
490.4	0.83 ± 0.08	12	0.48 ± 0.02	
Effects observed at different concentrations (µM) of drugs administered in combination				
Concentration		**Sequence and drug effect**		
		(0/0 h)	(0/4 h)	(4/0 h)
Cis	**Cur**	**Effect**	**Effect**	**Effect**
2.0816	0.085	0.21 ± 0.02	0.15 ± 0.01	0.2 ± 0.02
10.408	8.488	0.65 ± 0.06	0.55 ± 0.05	0.63 ± 0.05
52.04	84.78	0.89 ± 0.06	0.87 ± 0.08	0.89 ± 0.09
Cis	**Col**			
2.0816	0.01	0.001 ± 0.10	0.41 ± 0.04	0.35 ± 0.03
10.408	0.075	0.81 ± 0.05	0.78 ± 0.07	0.84 ± 0.06
52.04	0.75	0.92 ± 0.07	0.92 ± 0.06	0.91 ± 0.02
Cis	**EGCG**			
2.0816	2.45	0.17 ± 0.02	0.15 ± 0.01	0.17 ± 0.01
10.408	24.52	0.78 ± 0.06	0.77 ± 0.03	0.76 ± 0.07
52.04	245.2	0.85 ± 0.01	0.86 ± 0.07	0.83 ± 0.05
Cis	**Tax**			
2.0816	0.06	0.15 ± 0.01	0.17 ± 0.02	0.17 ± 0.02
10.408	0.6	0.77 ± 0.10	0.76 ± 0.07	0.78 ± 0.11
52.04	6	0.86 ± 0.13	0.83 ± 0.08	0.85 ± 0.07

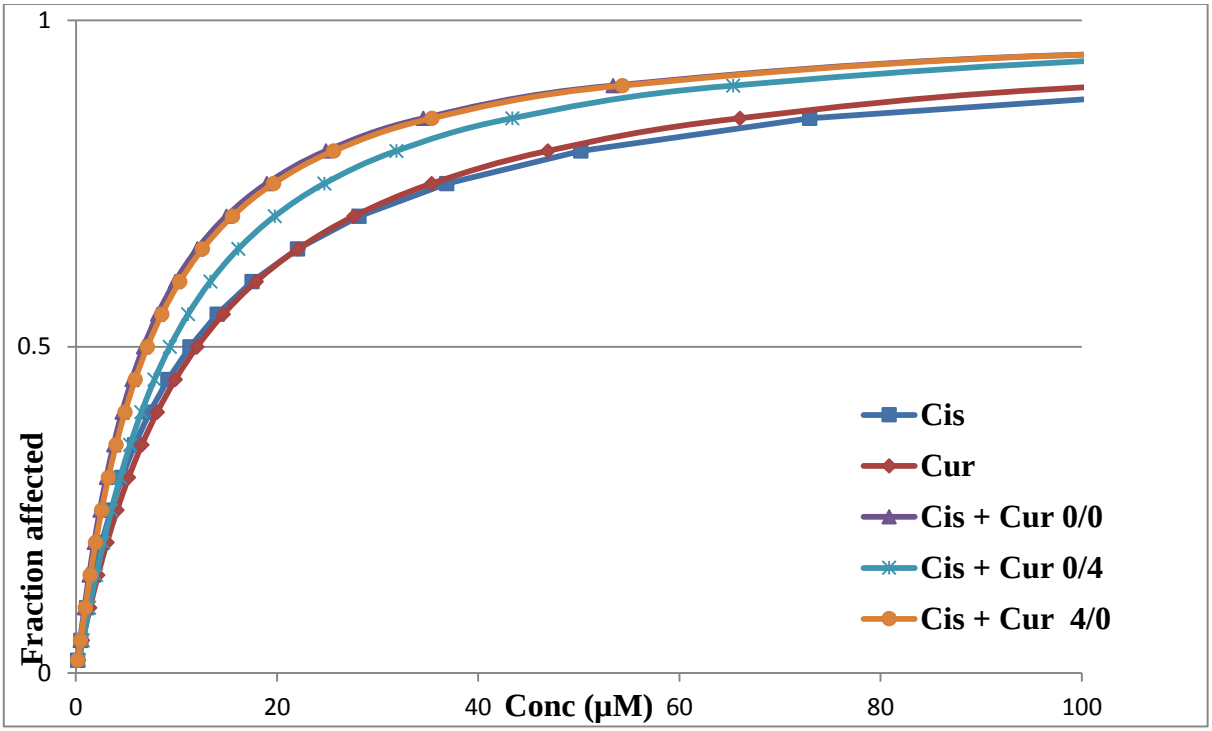

Figure 3.14 : Dose response curves obtained from combination of Cis with Cur as employed to CACO-2 cell line

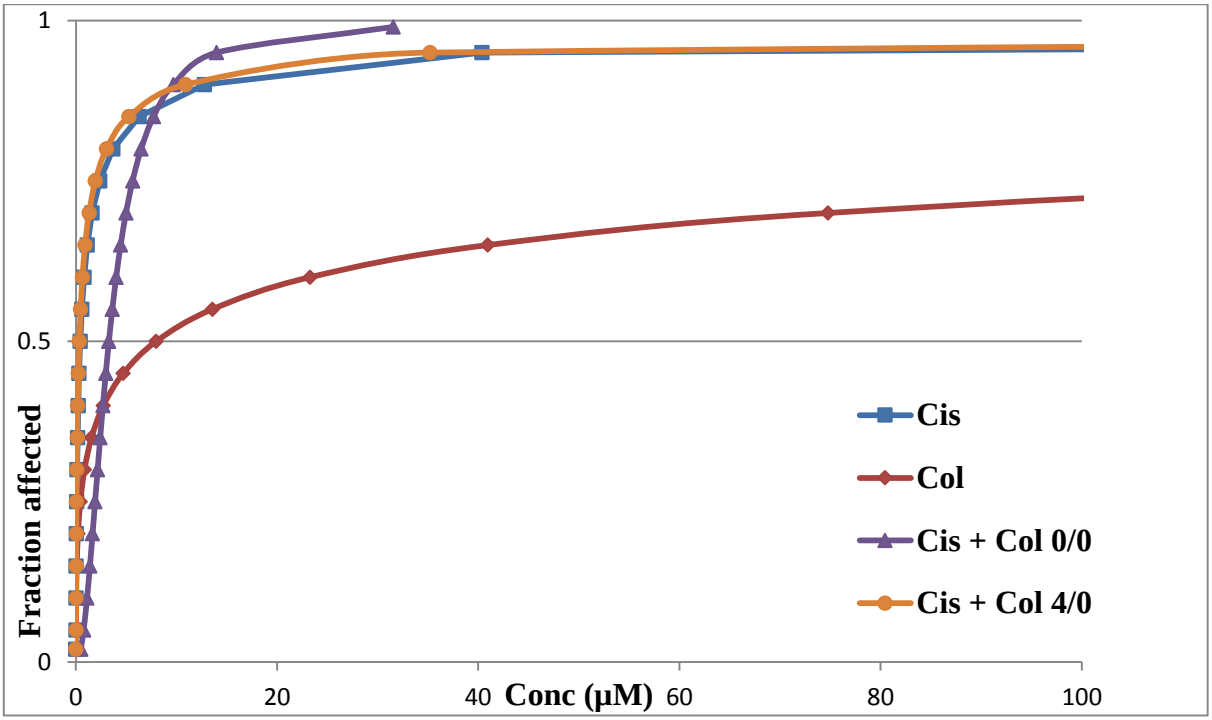

Figure 3.15: Dose response curves obtained from combination of Cis with Col as employed to CACO-2 cell line

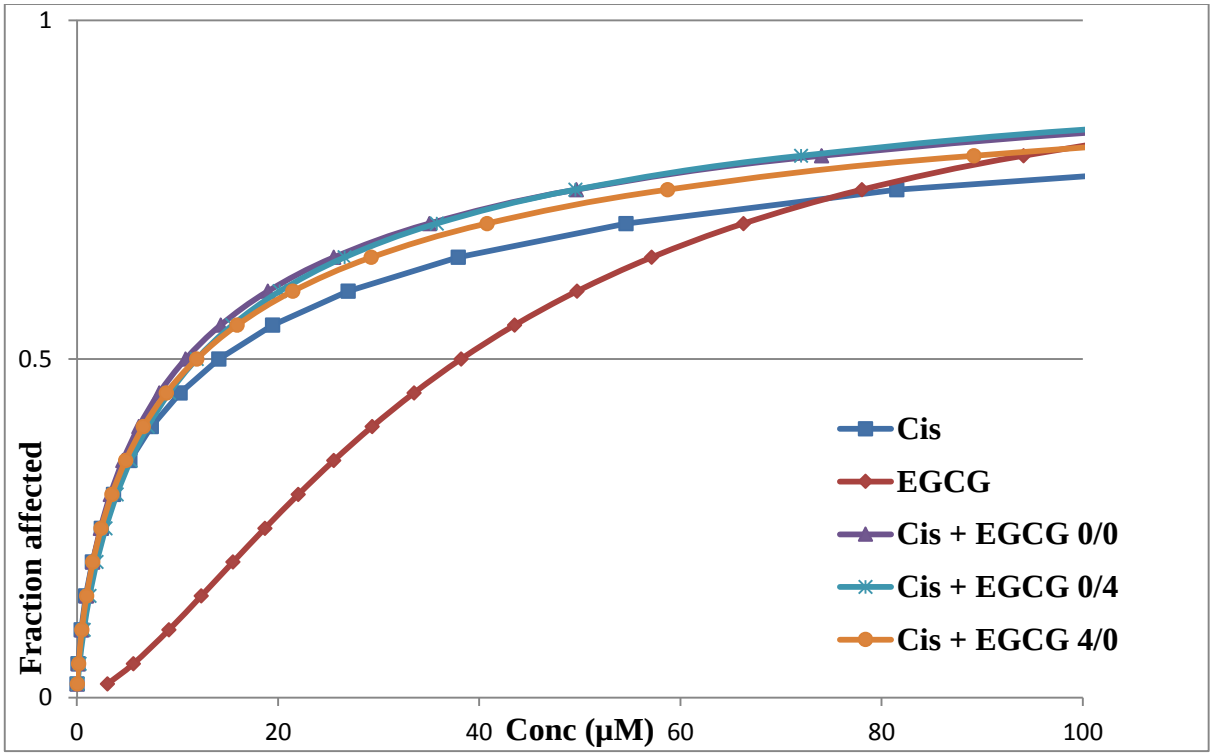

Figure 3.16: Dose response curves obtained from combination of Cis with EGCG as employed to CACO-2 cell line

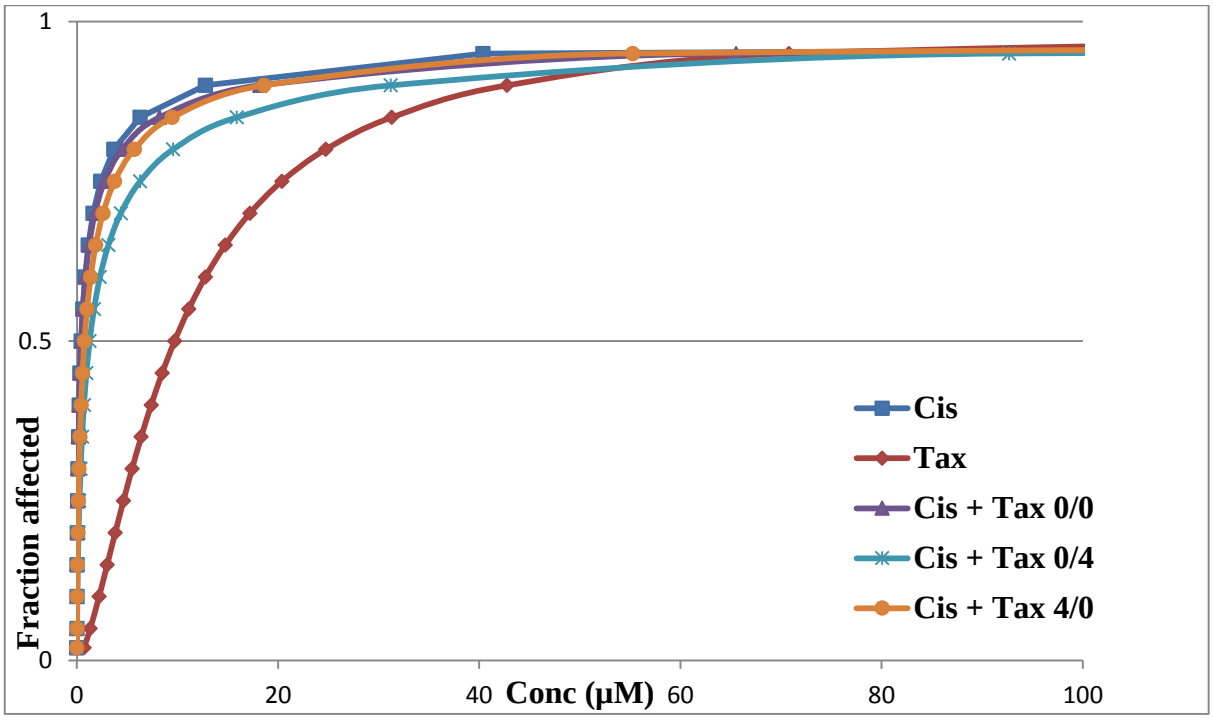

Figure 3.17: Dose response curves obtained from combination of Cis with Tax as employed to CACO-2 cell line

Table 3.5 gives the dose effect values (affected cell fractions) at three different concentrations of Ox and phytochemicals added alone and in combination according to three different sequences of administration (Ox/Phytochemical h): (0/0 h), (0/4 h), and (4/0 h) to CACO-2 cell line. Figures 3.18 -3.21 represent the corresponding dose response curves.

From the dose response curve (Figure 3.18), it can be said that bolus addition of Ox with Cur against CACO-2 cell line produced greater cell kill whereas 4/0 addition of the same was the least effective. Bolus addition of Ox with Col displayed highest cytotoxicity against CACO-2 cell line while 0/4 sequence of addition did the lowest in the same cells (Figure 3.19). When Ox was combined with EGCG, bolus addition caused greater cell kill whereas 0/4 sequence of addition was the least effective (Figure 3.20). In contrast, when Ox was combined with Tax, 4/0 sequence of addition produced greater cell kill whereas 0/4 sequence of addition was the least effective against CACO-2 cell line (Figure 3.21).

Table 3.5: Cell fractions affected by drug treatments (Ox and phytochemicals) alone and in combination against CACO-2 cell line

Effects observed at different concentrations (µM) of drugs administered alone				
Ox (µM)	**Effect**			
0.22	0.26 ± 0.00			
2.18	0.47 ± 0.04			
21.76	0.73 ± 0.01			
Cur (µM)	**Effect**	**Col (µM)**	**Effect**	
1.7	0.10 ± 0.01	0.02	0.35 ± 0.11	
16.96	0.43 ± 0.08	0.15	0.47 ± 0.05	
169.56	0.88 ± 0.03	1.5	0.60 ± 0.02	
EGCG (µM)	**Effect**	**Tax (µM)**	**Effect**	
4.9	0.15 ± 0.01	0.12	0.001 ± 0.02	
49.04	0.32 ± 0.06	1.2	0.09 ± 0.07	
490.4	0.83 ± 0.01	12	0.48 ± 0.04	
Effects observed at different concentrations (µM) of drugs administered in combination				
Concentration		**Sequence and drug effect**		
		(0/0 h)	(0/4 h)	(4/0 h)
Ox	**Cur**	**Effect**	**Effect**	**Effect**
0.11	0.085	0.2 ± 0.02	0.14 ± 0.01	0.16 ± 0.01
1.09	8.488	0.44 ± 0.04	0.37 ± 0.03	0.46 ± 0.04
10.88	84.78	0.9 ± 0.06	0.89 ± 0.08	0.85 ± 0.07
Ox	**Col**			
0.11	0.01	0.09 ± 0.01	0.08 ± 0.01	0.16 ± 0.01
1.09	0.075	0.47 ± 0.03	0.15 ± 0.01	0.54 ± 0.04
10.88	0.75	0.7 ± 0.06	0.66 ± 0.04	0.68 ± 0.02
Ox	**EGCG**			
0.11	2.45	0.25 ± 0.02	0.11 ± 0.01	0.28 ± 0.02
1.09	24.52	0.50 ± 0.04	0.42 ± 0.02	0.52 ± 0.03
10.88	245.2	0.85 ± 0.11	0.80 ± 0.07	0.82 ± 0.05
Ox	**Tax**			
0.11	0.06	0.001 ± 0.06	0.15 ± 0.07	0.13 ± 0.08
1.09	0.6	0.32 ± 0.04	0.57 ± 0.05	0.57 ± 0.06
10.88	6	0.72 ± 0.01	0.65 ± 0.01	0.75 ± 0.01

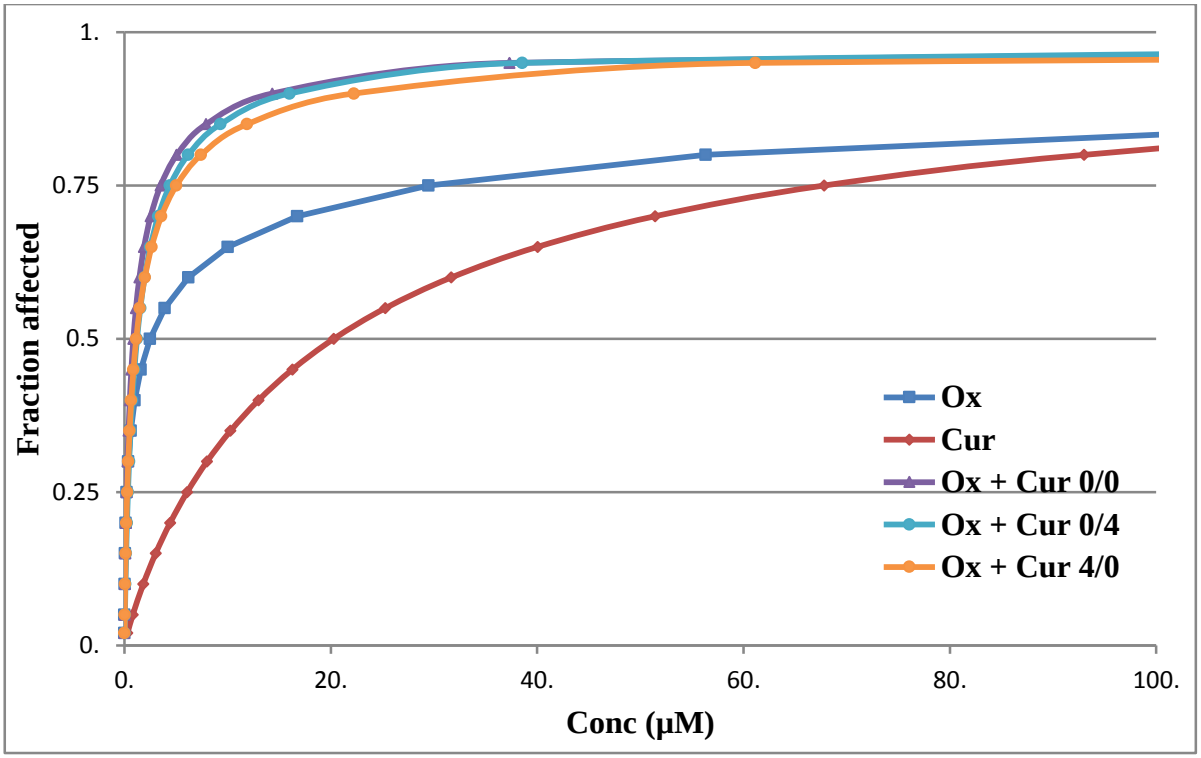

Figure 3.18 : Dose response curves obtained from combination of Ox with Cur as employed to CACO-2 cell line

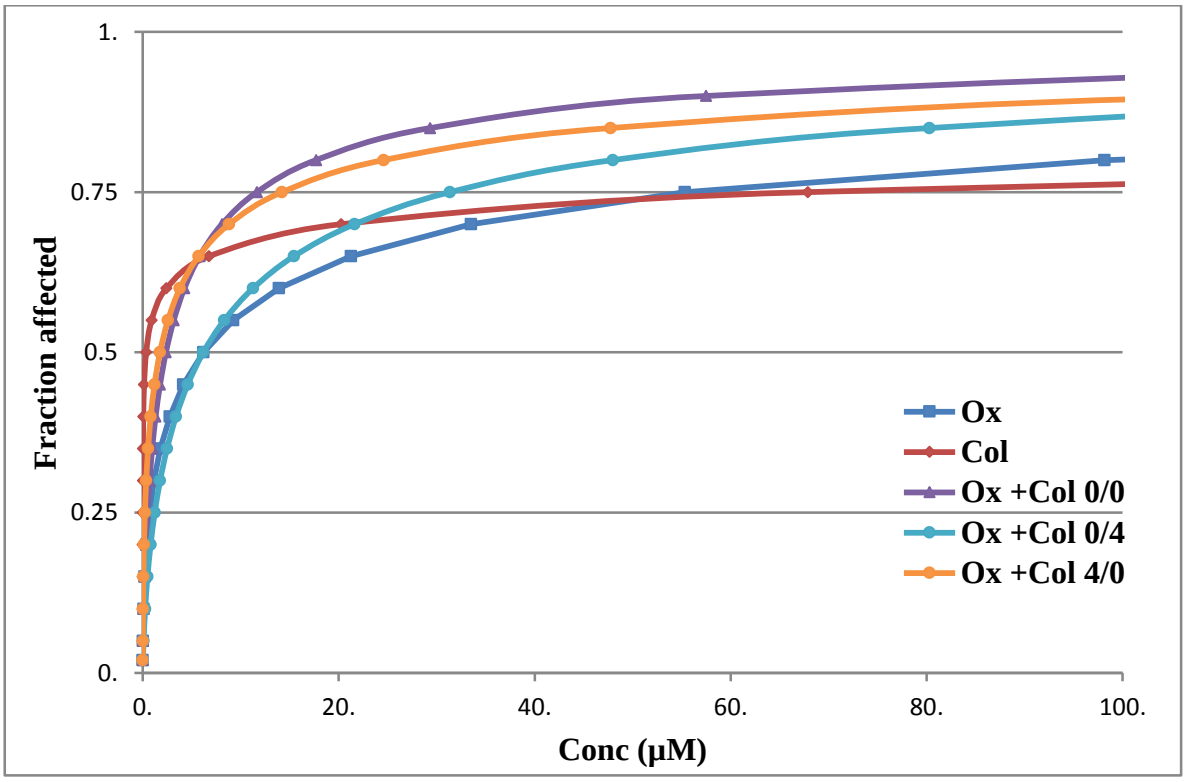

Figure 3.19 : Dose response curves obtained from combination of Ox with Col as employed to CACO-2 cell line

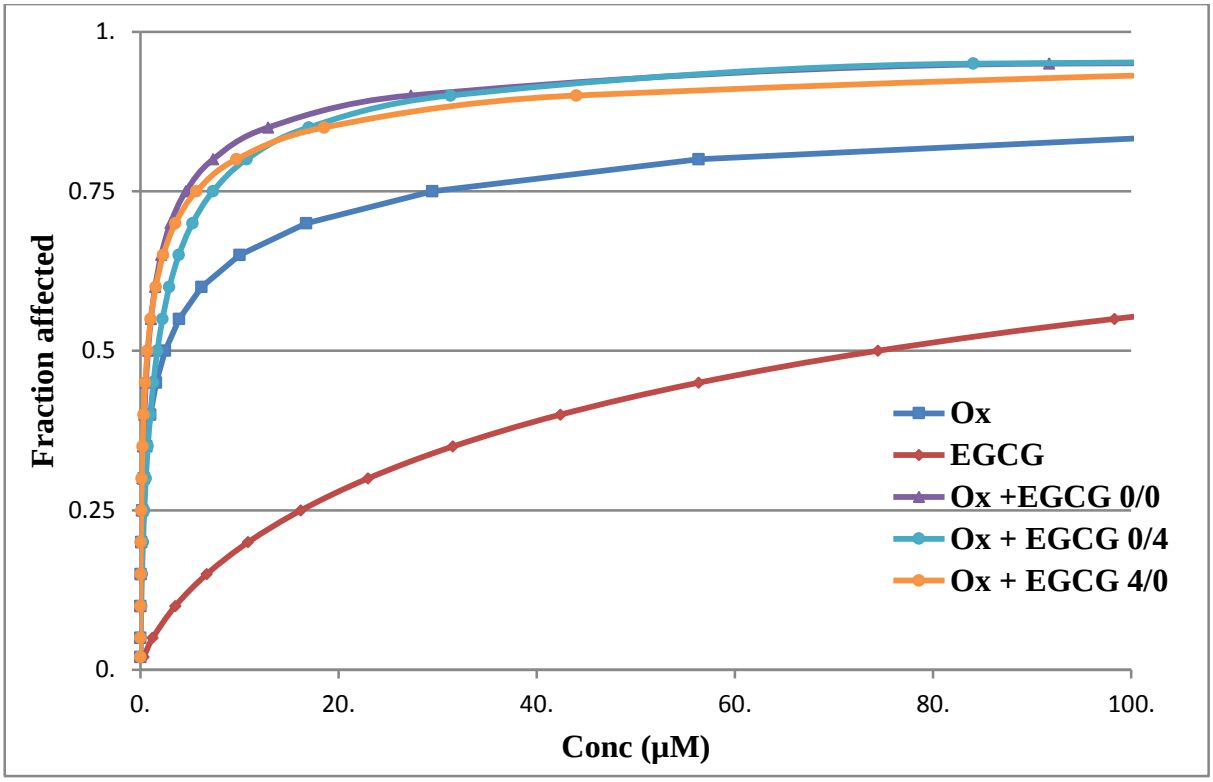

Figure 3.20 : Dose response curves obtained from combination of Ox with EGCG as employed to CACO-2 cell line

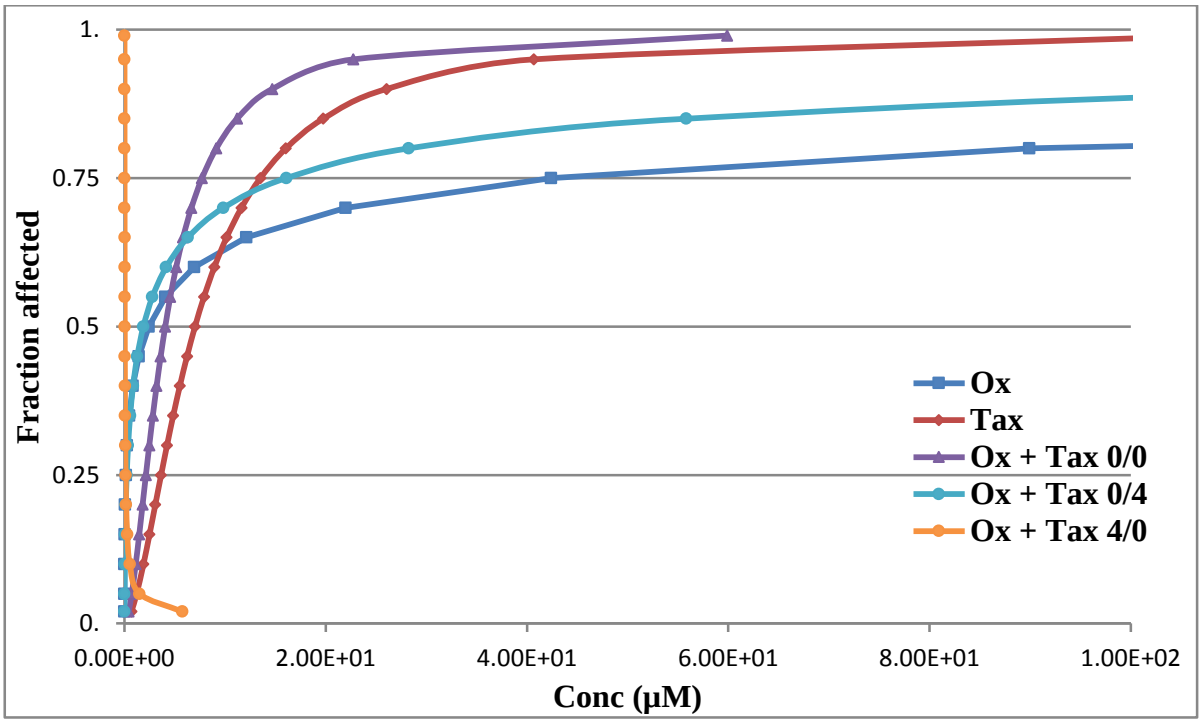

Figure 3.21 : Dose response curves obtained from combination of Ox with Tax as employed to CACO-2 cell line

3.2.1.3 Combinations between platinum drugs and phytochemicals in LIM-1215 cell line

Table 3.6 gives the dose effect values (affected cell fractions) at three different concentrations of Cis and phytochemicals added alone and in combination according to three different sequences of administration (Cis/Phytochemical h): (0/0 h), (0/4 h), and (4/0 h) to LIM-1215 cell line. Figures 3.22 -3.25 represent the corresponding dose response curves.

From the dose response curve (Figure 3.22), it can be said that combination of Cis with Cur 4/0 sequence of addition caused greater cell kill at lower concentration but 0/4 sequence of addition produced greater cell kill at higher concentration against LIM-1215 cell line. 0/4 sequence of addition of Cis with Col displayed highest cytotoxicity against LIM-1215 cell line while bolus addition did the lowest in the same cells (Figure 3.23). When Cis was combined with EGCG, bolus addition caused greater cell kill whereas 4/0 sequence of addition was the least effective (Figure 3.24). In contrast, when Cis was combined with Tax, 4/0 sequence of addition produced greater cell kill whereas 0/4 sequence of addition was the least effective against LIM-1215 cell line (Figure 3.25).

Table 3.6: Cell fractions affected by drug treatments (Cis and phytochemicals) alone and in combination against LIM-1215 cell line

Effects observed at different concentrations (µM) of drugs administered alone				
Cis (µM)	**Effect**			
0.5992	0.001 ± 0.04			
5.992	0.172 ± 0.02			
59.92	0.8009 ± 0.01			
Cur (µM)	**Effect**	**Col (µM)**	**Effect**	
1.33	0.001 ± 0.05	0.001	0.19 ± 0.12	
13.33	0.5562 ± 0.03	0.02	0.22 ± 0.04	
133.28	0.8204 ± 0.02	0.18	0.83 ± 0.03	
EGCG (µM)	**Effect**	**Tax (µM)**	**Effect**	
1.17	0.1682 ± 0.01	0.04	0.19 ± 0.03	
11.68	0.3341 ± 0.01	0.4	0.25 ± 0.02	
116.8	0.7637 ± 0.04	4	0.60 ± 0.02	
Effects observed at different concentrations (µM) of drugs administered in combination				
Concentration		**Sequence and drug effect**		
		(0/0 h)	(0/4 h)	(4/0 h)
Cis	**Cur**	**Effect**	**Effect**	**Effect**
0.2995	0.665	0.31 ± 0.03	0.40 ± 0.03	0.28 ± 0.04
2.996	6.665	0.55 ± 0.05	0.59 ± 0.06	0.53 ± 0.02
29.96	66.64	0.87 ± 0.06	0.89 ± 0.08	0.87 ± 0.08
Cis	**Col**			
0.2995	0.0005	0.07 ± 0.14	0.001 ± 0.01	0.001 ± 0.08
2.996	0.01	0.32 ± 0.04	0.31 ± 0.03	0.23 ± 0.07
29.96	0.09	0.78 ± 0.02	0.79 ± 0.04	0.74 ± 0.02
Cis	**EGCG**			
0.2995	0.585	0.19 ± 0.01	0.10 ± 0.01	0.015 ± 0.01
2.996	5.84	0.32 ± 0.02	0.22 ± 0.01	0.27 ± 0.04
29.96	58.4	0.80 ± 0.04	0.81 ± 0.07	0.78 ± 0.02
Cis	**Tax**			
0.2995	0.02	0.18 ± 0.11	0.17 ± 0.03	0.001 ± 0.01
2.996	0.20	0.31 ± 0.04	0.32 ± 0.02	0.26 ± 0.04
29.96	2	0.72 ± 0.01	0.54 ± 0.05	0.67 ± 0.06

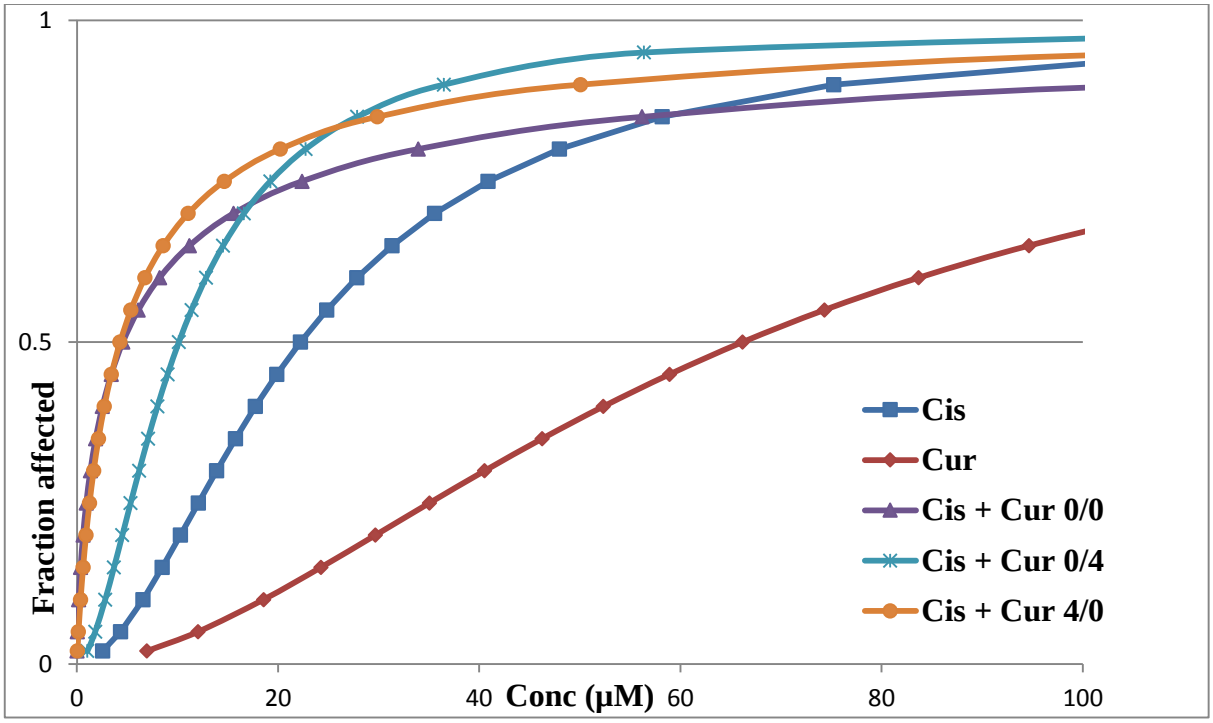

Figure 3.22 : Dose response curves obtained from combination of Cis with Cur as employed to LIM-1215 cell line

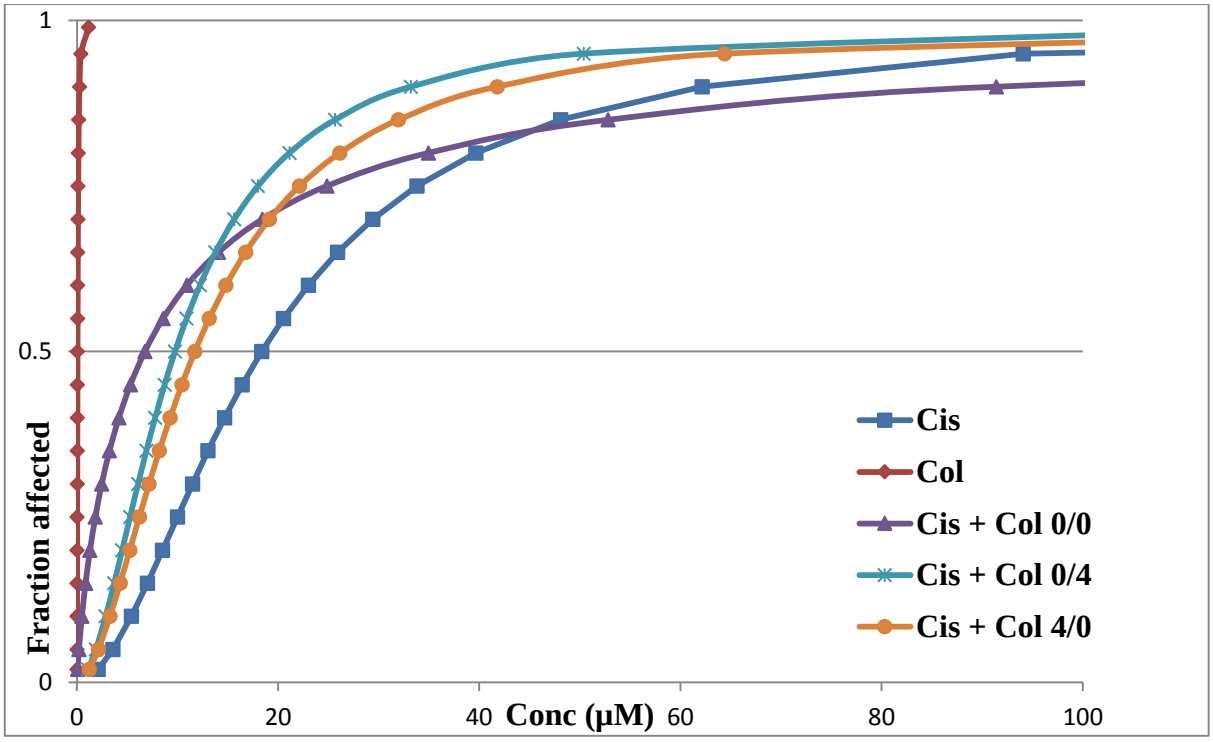

Figure 3.23 : Dose response curves obtained from combination of Cis with Col as employed to LIM-1215 cell line

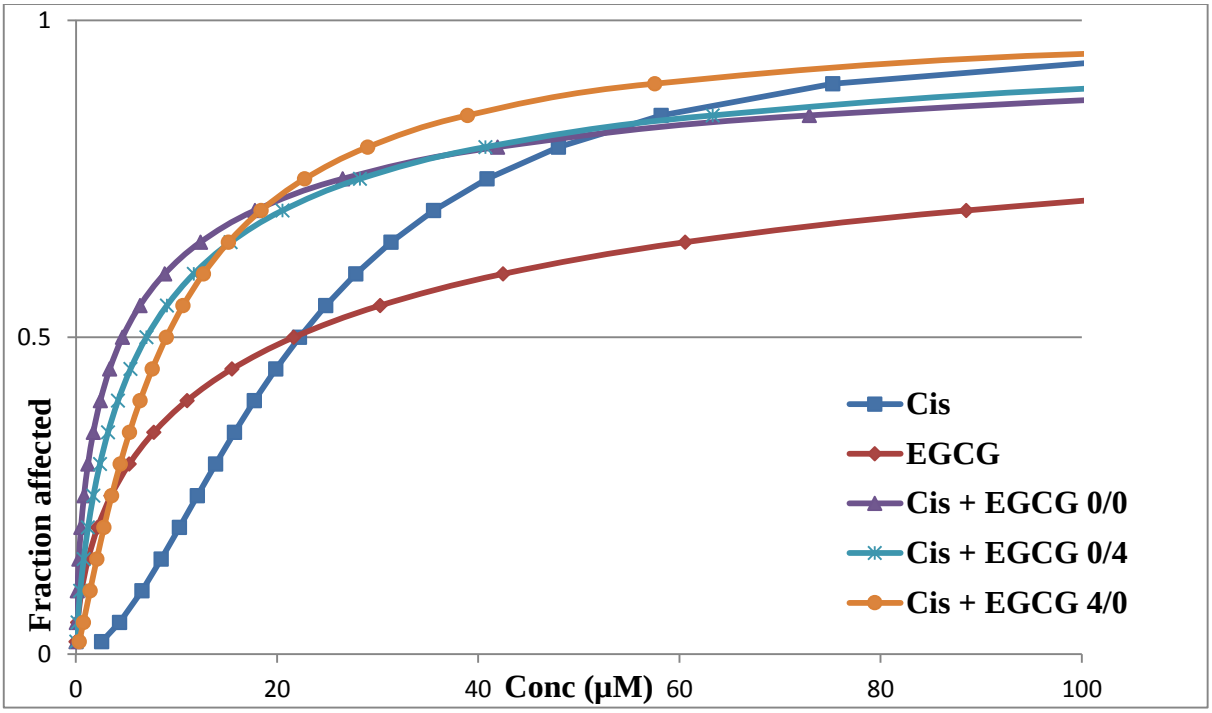

Figure 3.24 : Dose response curves obtained from combination of Cis with EGCG as employed to LIM-1215 cell line

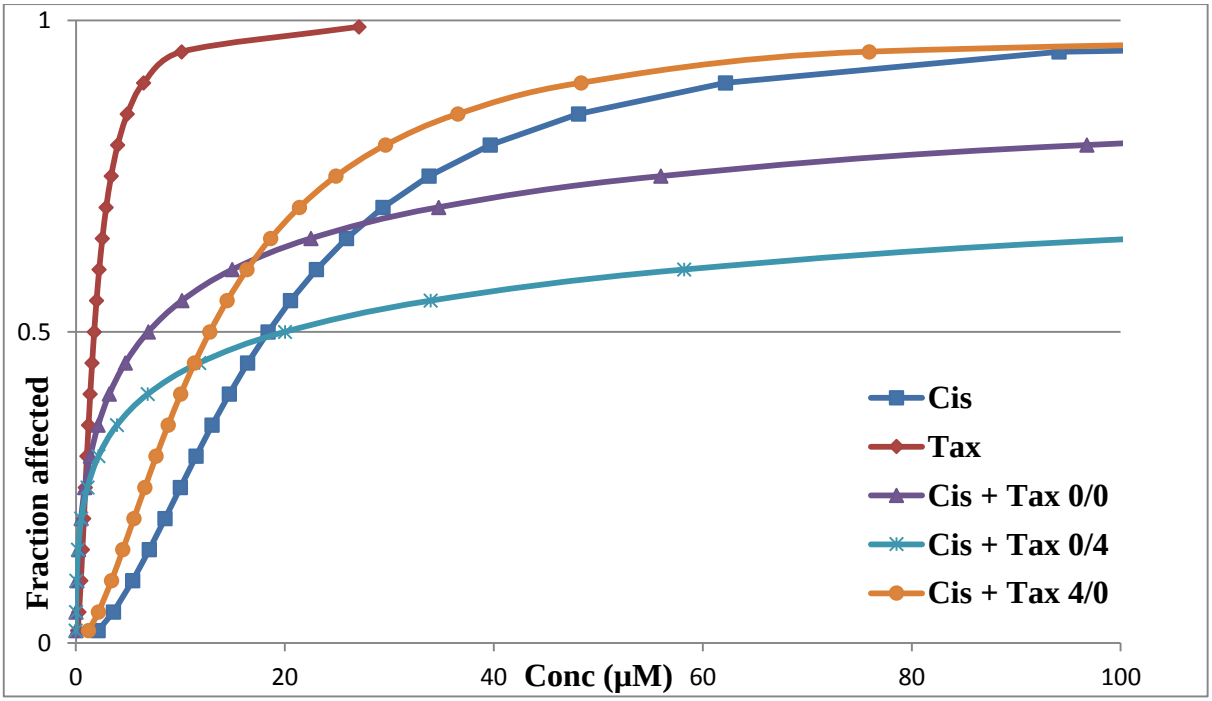

Figure 3.25 : Dose response curves obtained from combination of Cis with Tax as employed to LIM-1215 cell line

Table 3.7 gives the dose effect values (affected cell fractions) at three different concentrations of Ox and phytochemicals added alone and in combination according to three different sequences of administration (Ox/Phytochemical h): (0/0 h), (0/4 h), and (4/0 h) to LIM-1215 cell line. Figures 3.26 -3.29 represent the corresponding dose response curves.

From the dose response curve (Figure 3.26), it can be said that combination of Ox with Cur bolus addition caused greater cell kill at lower concentration but 4/0 sequence of addition produced greater cell kill at higher concentration against LIM-1215 cell line. Bolus addition of Ox with Col displayed highest cytotoxicity against LIM-1215 cell line while 4/0 sequence of addition did the lowest in the same cells (Figure 3.27). When Ox was combined with EGCG, 4/0 sequence of addition caused greater cell kill whereas bolus addition was the least effective (Figure 3.28). In contrast, when Ox was combined with Tax, bolus addition produced greater cell kill whereas 4/0 sequence of addition was the least effective against LIM-1215 cell line (Figure 3.29).

Table 3.7: Cell fractions affected by drug treatments (Ox and phytochemicals) alone and in combination against LIM-1215 cell line

Effects observed at different concentrations (µM) of drugs administered alone				
Ox (µM)	**Effect**			
0.1	0.12 ± 0.10			
1	0.11 ± 0.02			
10	0.64 ± 0.01			
Cur (µM)	**Effect**	**Col (µM)**	**Effect**	
1.33	0.001 ± 0.04	0.001	0.19 ± 0.07	
13.33	0.56 ± 0.01	0.02	0.22 ± 0.05	
133.28	0.82 ± 0.03	0.18	0.83 ± 0.08	
EGCG (µM)	**Effect**	**Tax (µM)**	**Effect**	
1.17	0.17 ± 0.01	0.04	0.19 ± 0.09	
11.68	0.33 ± 0.01	0.4	0.25 ± 0.02	
116.8	0.76 ± 0.04	4	0.60 ± 0.05	
Effects observed at different concentrations (µM) of drugs administered in combination				
Concentration		**Sequence and drug effect**		
		(0/0 h)	(0/4 h)	(4/0 h)
Ox	**Cur**	**Effect**	**Effect**	**Effect**
0.05	0.665	0.11 ± 0.01	0.001 ± 0.01	0.001 ± 0.01
0.5	6.665	0.27 ± 0.02	0.20 ± 0.02	0.36 ± 0.03
5	66.64	0.88 ± 0.06	0.89 ± 0.08	0.88 ± 0.05
Ox	**Col**			
0.05	0.0005	0.11 ± 0.01	0.03 ± 0.01	0.09 ± 0.01
0.5	0.01	0.13 ± 0.01	0.14 ± 0.02	0.17 ± 0.01
5	0.09	0.82 ± 0.07	0.75 ± 0.05	0.72 ± 0.03
Ox	**EGCG**			
0.05	0.585	0.11 ± 0.01	0.03 ± 0.01	0.09 ± 0.04
0.5	5.84	0.13 ± 0.04	0.14 ± 0.01	0.17 ± 0.02
5	58.4	0.82 ± 0.11	0.75 ± 0.06	0.72 ± 0.03
Ox	**Tax**			
0.05	0.02	0.07 ± 0.01	0.13 ± 0.02	0.16 ± 0.05
0.5	0.20	0.18 ± 0.02	0.19 ± 0.04	0.26 ± 0.03
5	2	0.68 ± 0.06	0.68 ± 0.01	0.58 ± 0.04

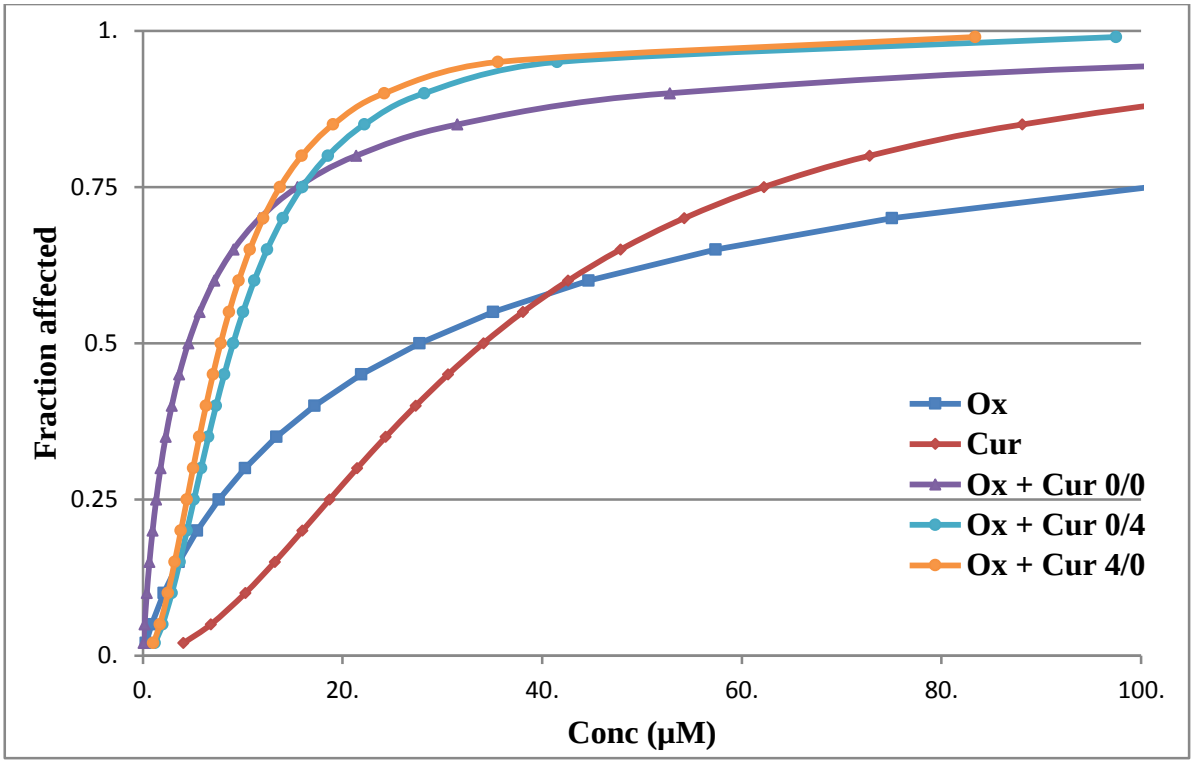

Figure 3.26 : Dose response curves obtained from combination of Ox with Cur as employed to LIM-1215 cell line

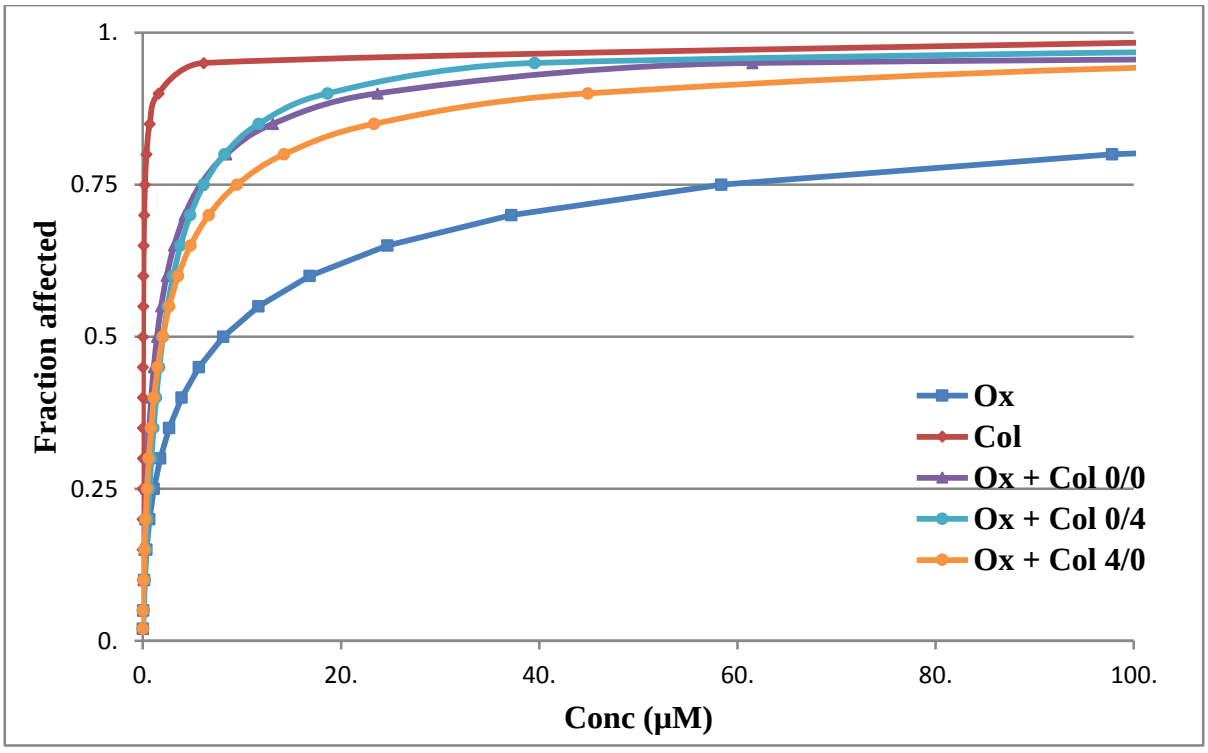

Figure 3.27 : Dose response curves obtained from combination of Ox with Col as employed to LIM-1215 cell line

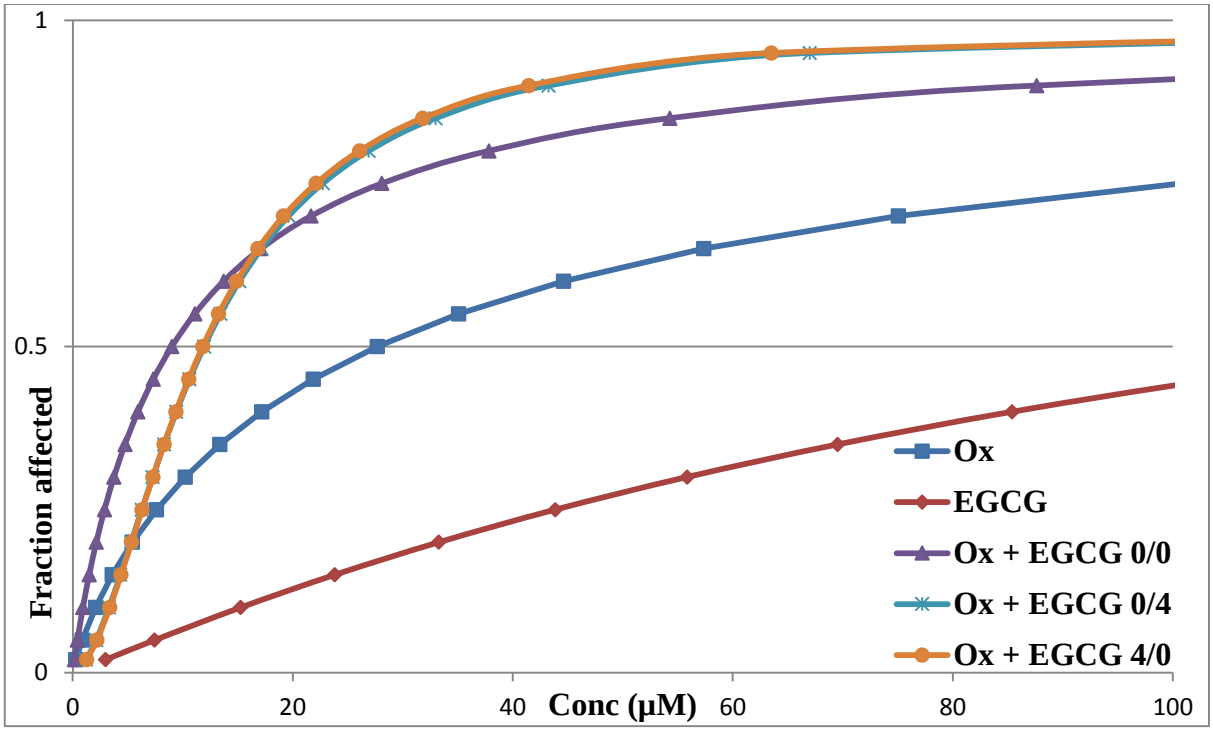

Figure 3.28 : Dose response curves obtained from combination of Ox with EGCG as employed to LIM-1215 cell line

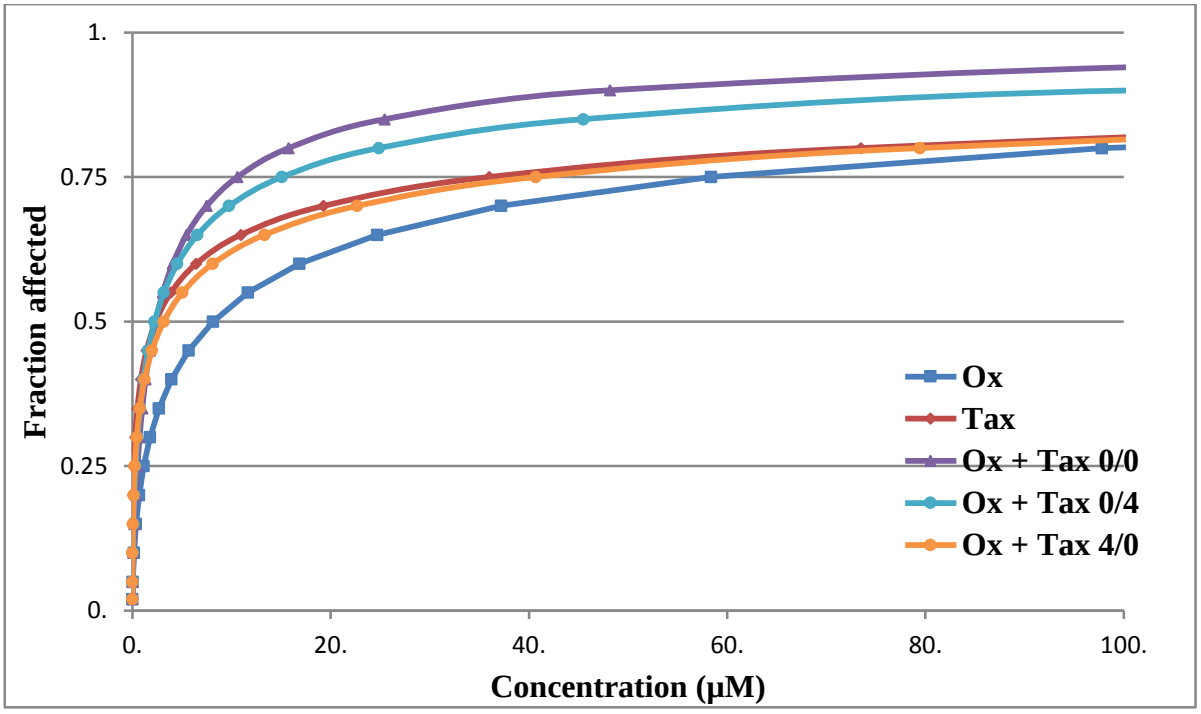

Figure 3.29 : Dose response curves obtained from combination of Ox with Tax as employed to LIM-1215 cell line

3.2.1.4 Combinations between platinum drugs and phytochemicals in LIM-2405 cell line

Table 3.8 gives the dose effect values (affected cell fractions) at three different concentrations of Cis and phytochemicals added alone and in combination according to three different sequences of administration (Cis/Phytochemical h): (0/0 h), (0/4 h), and (4/0 h) to LIM-2405 cell line. Figures 3.30 -3.33 represent the corresponding dose response curves.

From the dose response curve (Figure 3.30), it can be said that 0/4 sequence of addition of Cis with Cur against LIM-2405 cell line produced greater cell kill whereas bolus addition of the same was the least effective. 0/4 sequence of addition of Cis with Col displayed highest cytotoxicity against LIM-2405 cell line while 4/0 sequence of addition did the lowest in the same cells (Figure 3.31). When Cis was combined with EGCG, bolus addition caused greater cell kill whereas 4/0 sequence of addition was the least effective (Figure 3.32). Similarly, when Cis was combined with Tax, bolus addition produced greater cell kill whereas 4/0 sequence of addition was the least effective against LIM-2405 cell line (Figure 3.33).

Table 3.8: Cell fractions affected by drug treatments (Cis and phytochemicals) alone and in combination against LIM-2405 cell line

Effects observed at different concentrations (µM) of drugs administered alone				
Cis (µM)	**Effect**			
0.4	0.15 ± 0.01			
3.98	0.52 ± 0.10			
39.84	0.97 ± 0.06			
Cur (µM)	**Effect**	**Col (µM)**	**Effect**	
0.67	0.07 ± 0.02	0.001	0.06 ± 0.07	
6.66	0.11 ± 0.05	0.01	0.16 ± 0.02	
66.64	0.88 ± 0.02	0.09	0.74 ± 0.03	
EGCG (µM)	**Effect**	**Tax (µM)**	**Effect**	
2.96	0.08 ± 0.03	0.12	0.03 ± 0.02	
29.6	0.11 ± 0.01	1.2	0.07 ± 0.01	
296	0.86 ± 0.01	12	0.74 ± 0.04	
Effects observed at different concentrations (µM) of drugs administered in combination				
Concentration		**Sequence and drug effect**		
		(0/0 h)	(0/4 h)	(4/0 h)
Cis	**Cur**	**Effect**	**Effect**	**Effect**
0.2	0.33	0.21 ± 0.02	0.15 ± 0.01	0.2 ± 0.03
1.99	3.33	0.65 ± 0.06	0.55 ± 0.04	0.63 ± 0.01
19.92	33.32	0.89 ± 0.05	0.87 ± 0.02	0.89 ± 0.01
Cis	**Col**			
0.2	0.0005	0.16 ± 0.02	0.12 ± 0.01	0.02 ± 0.01
1.99	0.005	0.22 ± 0.01	0.31 ± 0.06	0.39 ± 0.03
19.92	0.045	0.94 ± 0.02	0.94 ± 0.03	0.59 ± 0.01
Cis	**EGCG**			
0.2	1.48	0.11 ± 0.01	0.0001 ± 0.07	0.13 ± 0.02
1.99	14.8	0.29 ± 0.04	0.32 ± 0.01	0.39 ± 0.01
19.92	148	0.90 ± 0.02	0.78 ± 0.03	0.70 ± 0.04
Cis	**Tax**			
0.2	0.06	0.16 ± 0.13	0.001 ± 0.03	0.14 ± 0.08
1.99	0.60	0.28 ± 0.01	0.29 ± 0.01	0.05 ± 0.02
19.92	6	0.90 ± 0.04	0.49 ± 0.05	0.87 ± 0.01

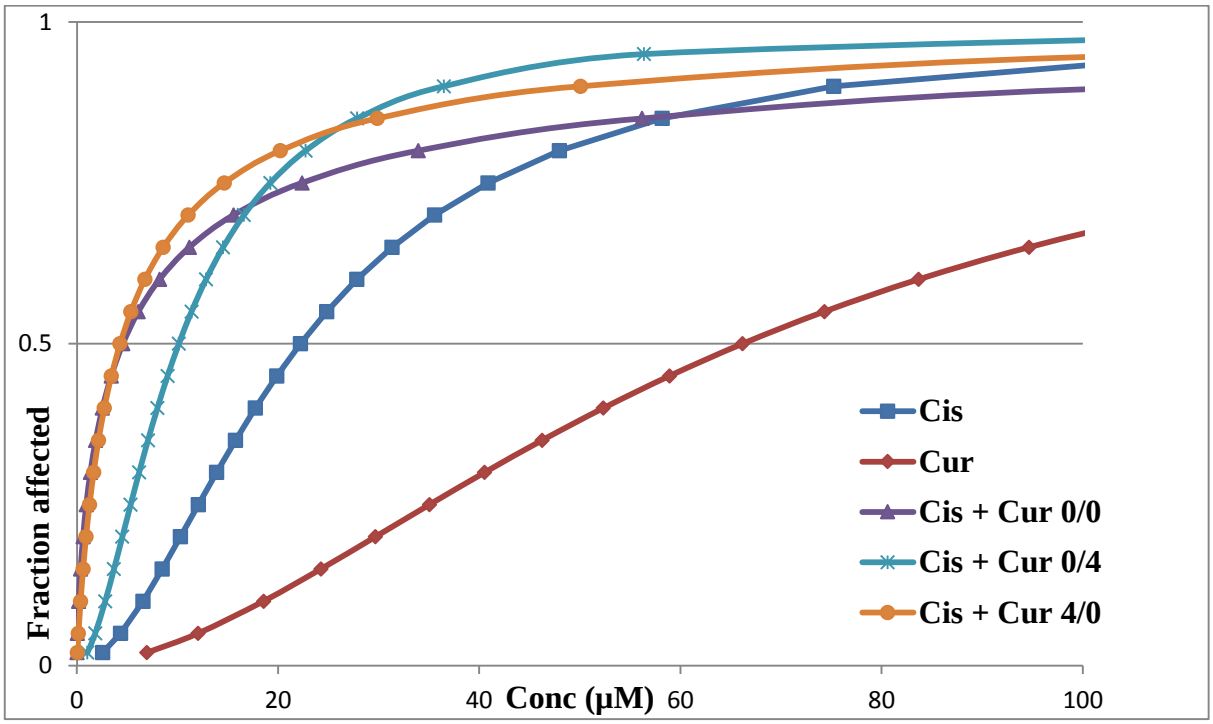

Figure 3.30 : Dose response curves obtained from combination of Cis with Cur as employed to LIM-2405 cell line

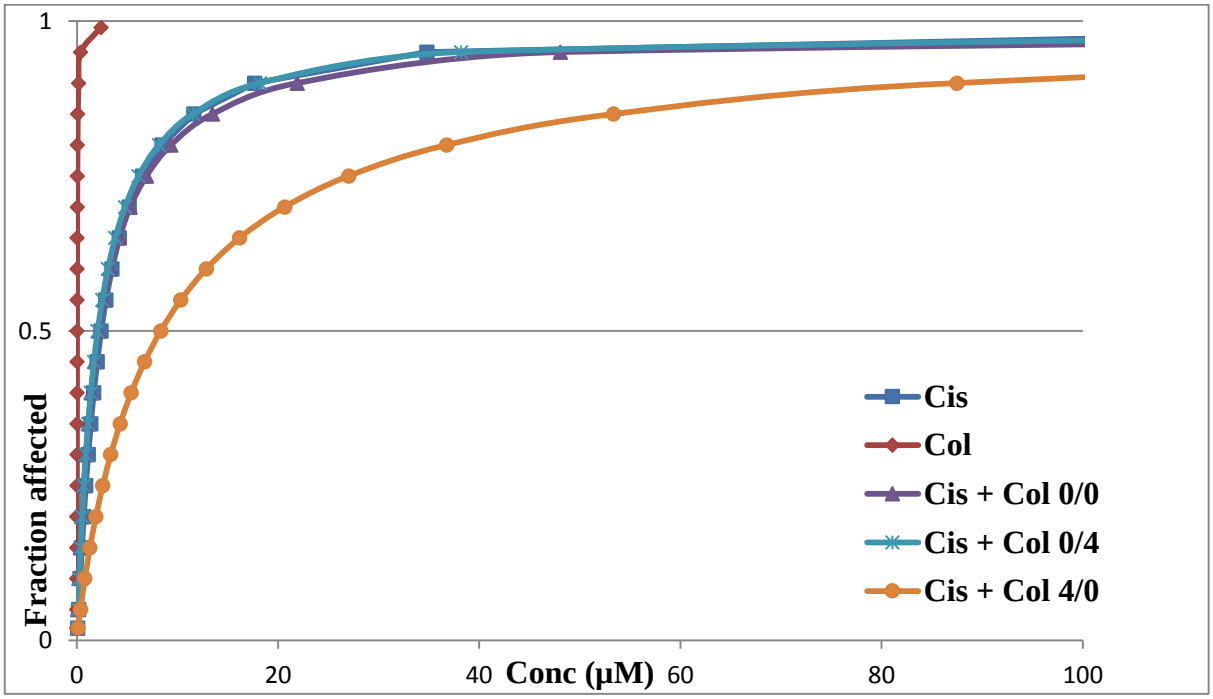

Figure 3.31 : Dose response curves obtained from combination of Cis with Col as employed to LIM-2405 cell line

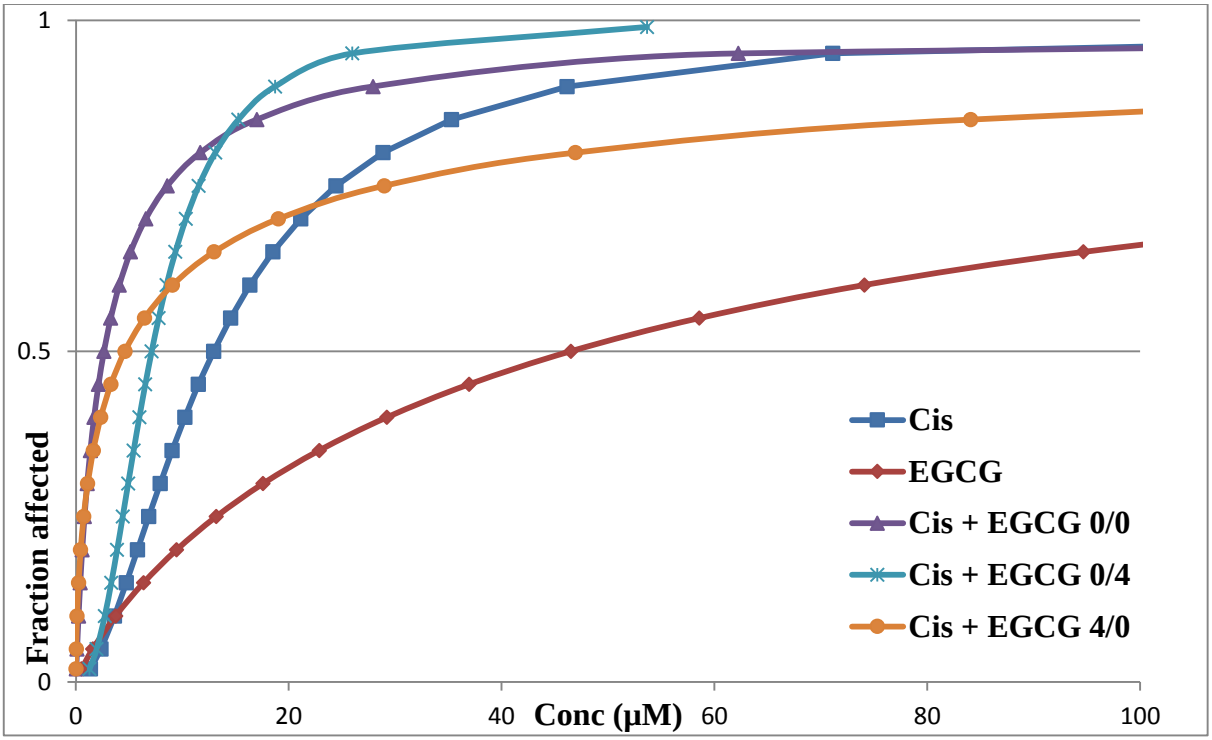

Figure 3.32 : Dose response curves obtained from combination of Cis with EGCG as employed to LIM-2405 cell line

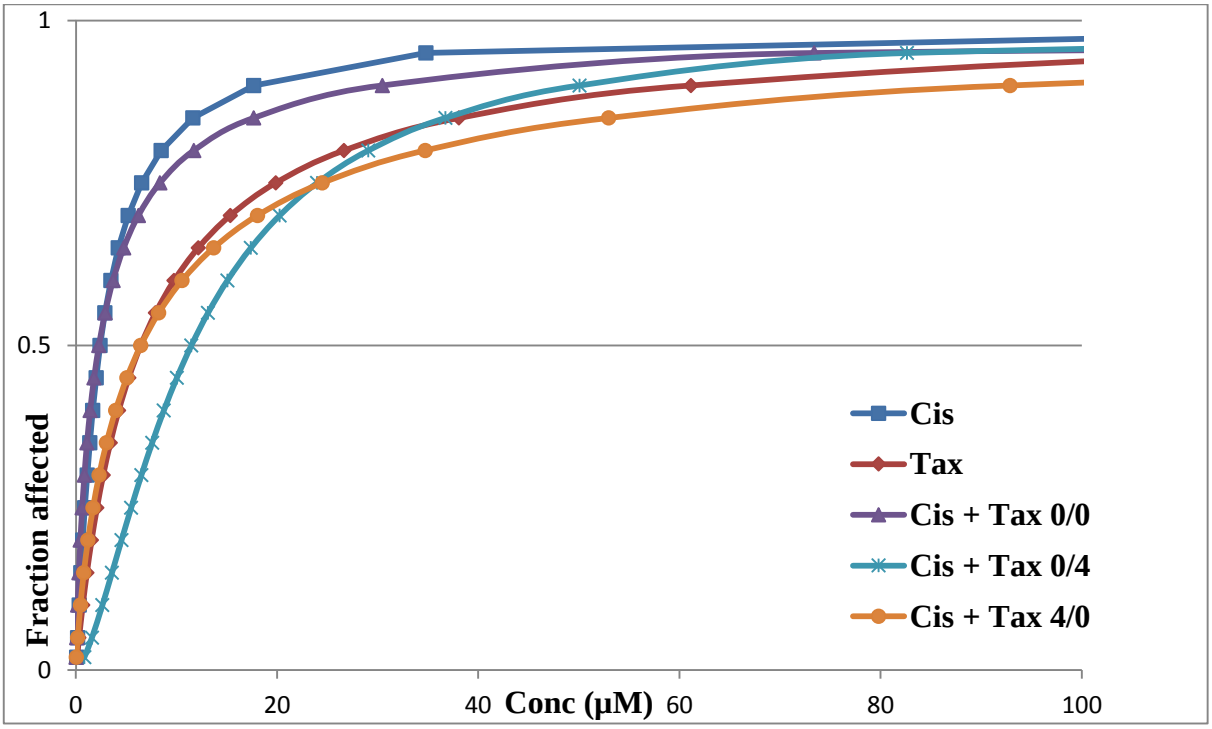

Figure 3.33 : Dose response curves obtained from combination of Cis with Tax as employed to LIM-2405 cell line

Table 3.9 gives the dose effect values (affected cell fractions) at three different concentrations of Ox and phytochemicals added alone and in combination according to three different sequences of administration (Ox/Phytochemical h): (0/0 h), (0/4 h), and (4/0 h) to LIM-2405 cell line. Figures 3.34 -3.37 represent the corresponding dose response curves.

From the dose response curve (Figure 3.34), it can be said that bolus addition of Ox with Cur against LIM-2405 cell line produced greater cell kill whereas 4/0 sequence of addition of the same was the least effective. 4/0 sequence of addition of Ox with Col displayed highest cytotoxicity against LIM-2405 cell line while 0/4 sequence of addition did the lowest in the same cells (Figure 3.27). When Ox was combined with EGCG, 4/0 sequence of addition caused greater cell kill whereas bolus addition was the least effective (Figure 3.28). In contrast, when Ox was combined with Tax, 0/4 sequence of addition produced greater cell kill whereas bolus addition was the least effective against LIM-2405 cell line (Figure 3.29).

Table 3.9: Cell fractions affected by drug treatments (Ox and phytochemicals) alone and in combination against LIM-2405 cell line

Effects observed at different concentrations (µM) of drugs administered alone				
Ox (µM)	Effect			
0.61	0.09 ± 0.01			
6.08	0.41 ± 0.03			
60.8	0.71 ± 0.03			
Cur (µM)	Effect	Col (µM)	Effect	
0.67	0.07 ± 0.01	0.001	0.06 ± 0.06	
6.66	0.114 ± 0.02	0.01	0.16 ± 0.03	
66.64	0.879 ± 0.01	0.09	0.74 ± 0.02	
EGCG (µM)	Effect	Tax (µM)	Effect	
2.96	0.08 ± 0.02	0.12	0.03 ± 0.01	
29.6	0.11 ± 0.01	1.2	0.07 ± 0.04	
296	0.86 ± 0.03	12	0.74 ± 0.02	
Effects observed at different concentrations (µM) of drugs administered in combination				
Concentration		Sequence and drug effect		
		(0/0 h)	(0/4 h)	(4/0 h)
Ox	Cur	Effect	Effect	Effect
0.305	0.33	0.06 ± 0.01	0.01 ± 0.02	0.01 ± 0.02
3.04	3.33	0.15 ± 0.01	0.09 ± 0.01	0.05 ± 0.03
30.4	33.32	0.87 ± 0.04	0.86 ± 0.03	0.87 ± 0.08
Ox	Col			
0.305	0.0005	0.09 ± 0.01	0.11 ± 0.02	0.02 ± 0.01
3.04	0.005	0.33 ± 0.02	0.22 ± 0.04	0.25 ± 0.02
30.4	0.045	0.72 ± 0.06	0.62 ± 0.03	0.77 ± 0.02
Ox	EGCG			
0.305	1.48	0.04 ± 0.01	0.01 ± 0.01	0.01 ± 0.01
3.04	14.8	0.13 ± 0.03	0.10 ± 0.07	0.06 ± 0.01
30.4	148	0.79 ± 0.01	0.80 ± 0.02	0.84 ± 0.04
Ox	Tax			
0.305	0.06	0.04 ± 0.01	0.01 ± 0.06	0.09 ± 0.07
3.04	0.60	0.23 ± 0.04	0.20 ± 0.03	0.30 ± 0.04
30.4	6	0.62 ± 0.05	0.64 ± 0.02	0.69 ± 0.01

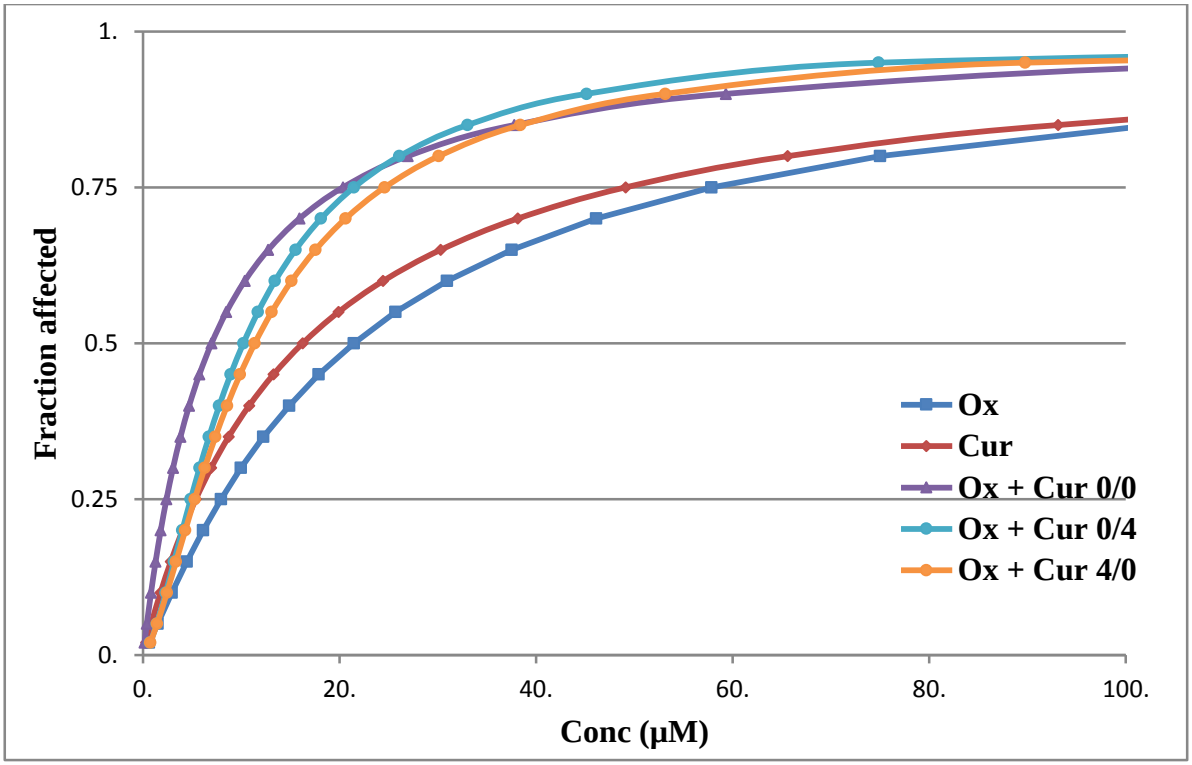

Figure 3.34 : Dose response curves obtained from combination of Ox with Cur as employed to LIM-2405 cell line

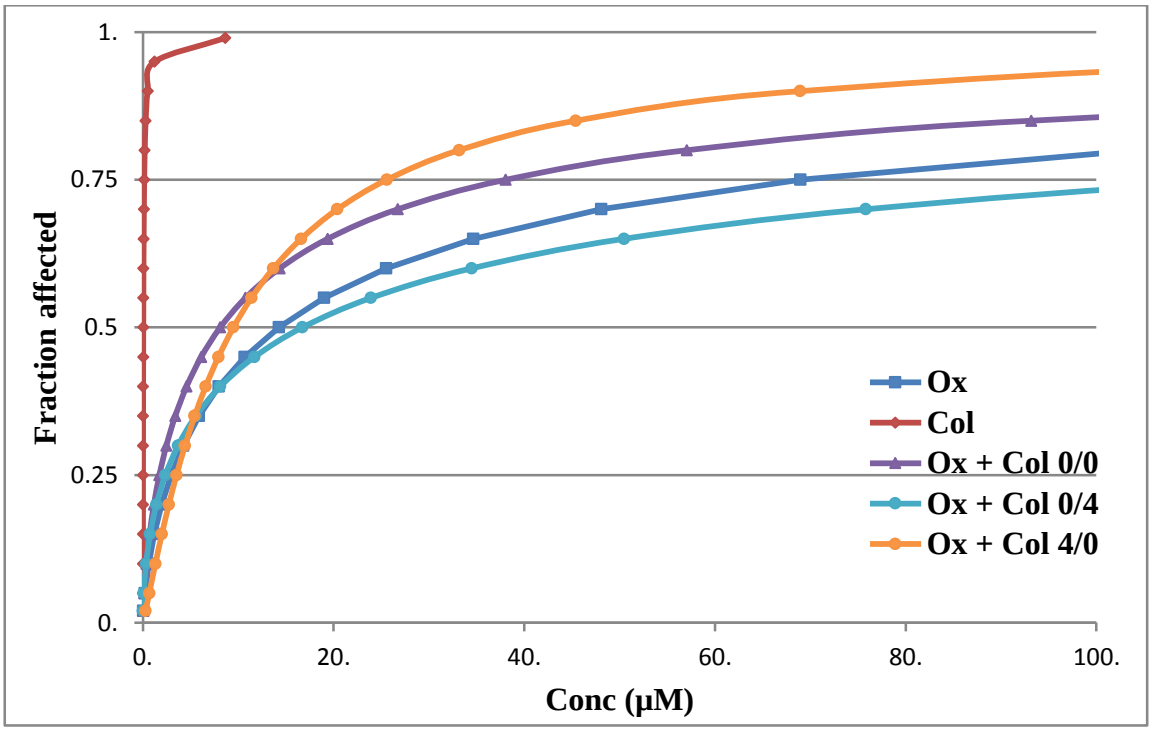

Figure 3.35 : Dose response curves obtained from combination of Ox with Col as employed to LIM-2405 cell line

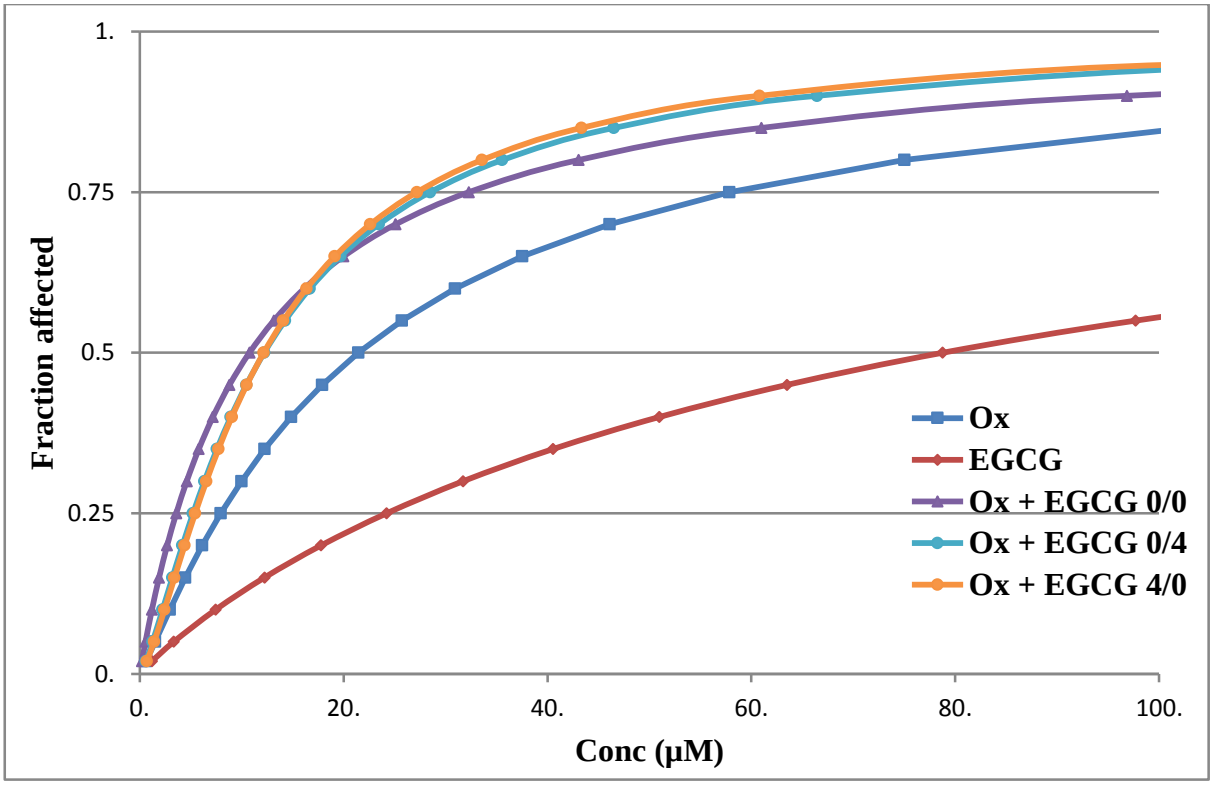

Figure 3.36 : Dose response curves obtained from combination of Ox with EGCG as employed to LIM-2405 cell line

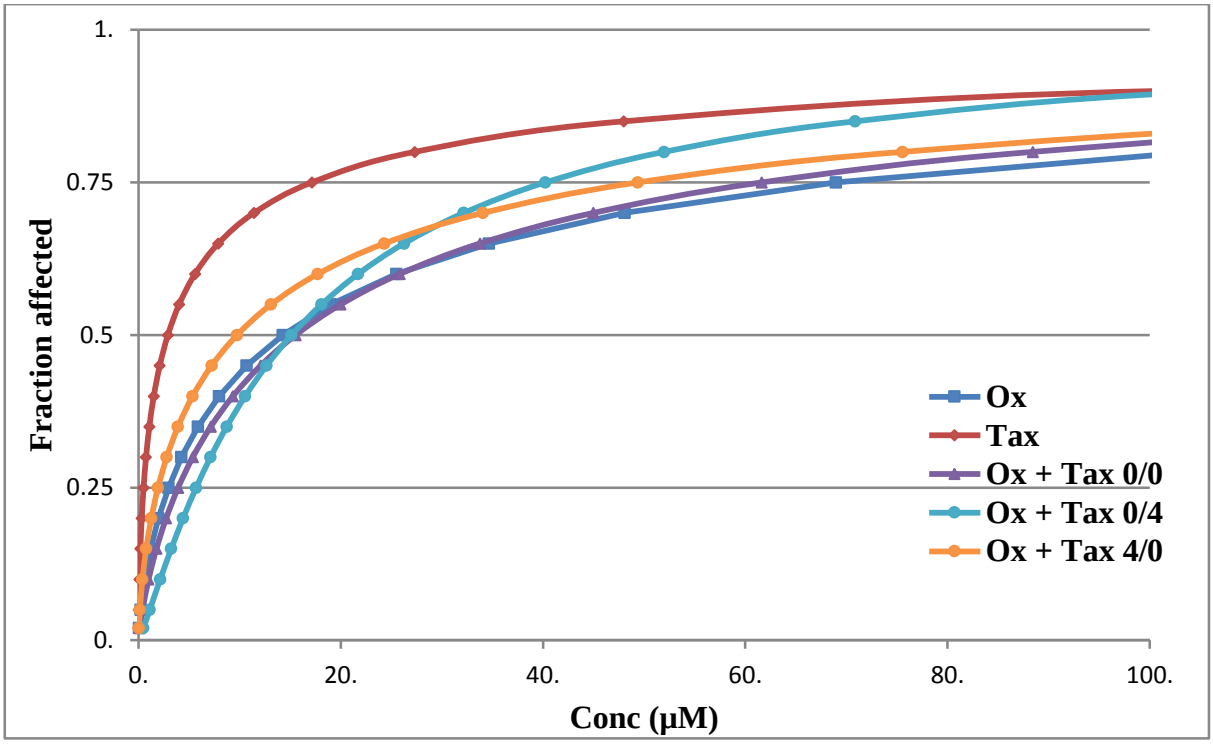

Figure 3.37 : Dose response curves obtained from combination of Ox with Tax as employed to LIM-2405 cell line

3.3 Combination Index (CI) values

CI provides the quantitative measure of combined drug action which is more reliable and accurate than dose effect curves. If the potency of the combined drugs differ greatly, interpretation of results from dose effect curves may mislead towards wrong findings. In this study, Calcusyn software was used to determine the CI values. CI<1 refers to synergism; CI>1 refers to antagonism and CI=1 refers to additiveness.

3.3.1 Combinations from Cis and phytochemicals against HT-29 cell line

Table 3.10 describes the list of CI values obtained from the combinations of Cis with Cur, Col, EGCG and Tax at three different sequences of additions and concentrations. It is evident from Table 3.10 that, among all combinations only Cis with Col produced synergism at all different concentrations and sequences of additions. Highest synergism was shown by Cis with EGCG at ED_{50} level with all sequences of additions. Cis in combination with Cur showed antagonism at ED_{50} level. Cis in combination with Tax displayed antagonism irrespective of sequences and added concentrations. Figure 3.38 shows pictorial presentation of CI as a function of added sequences and concentrations at ED_{50} level for all combinations of selected phytochemicals with Cis against HT-29 cell line.

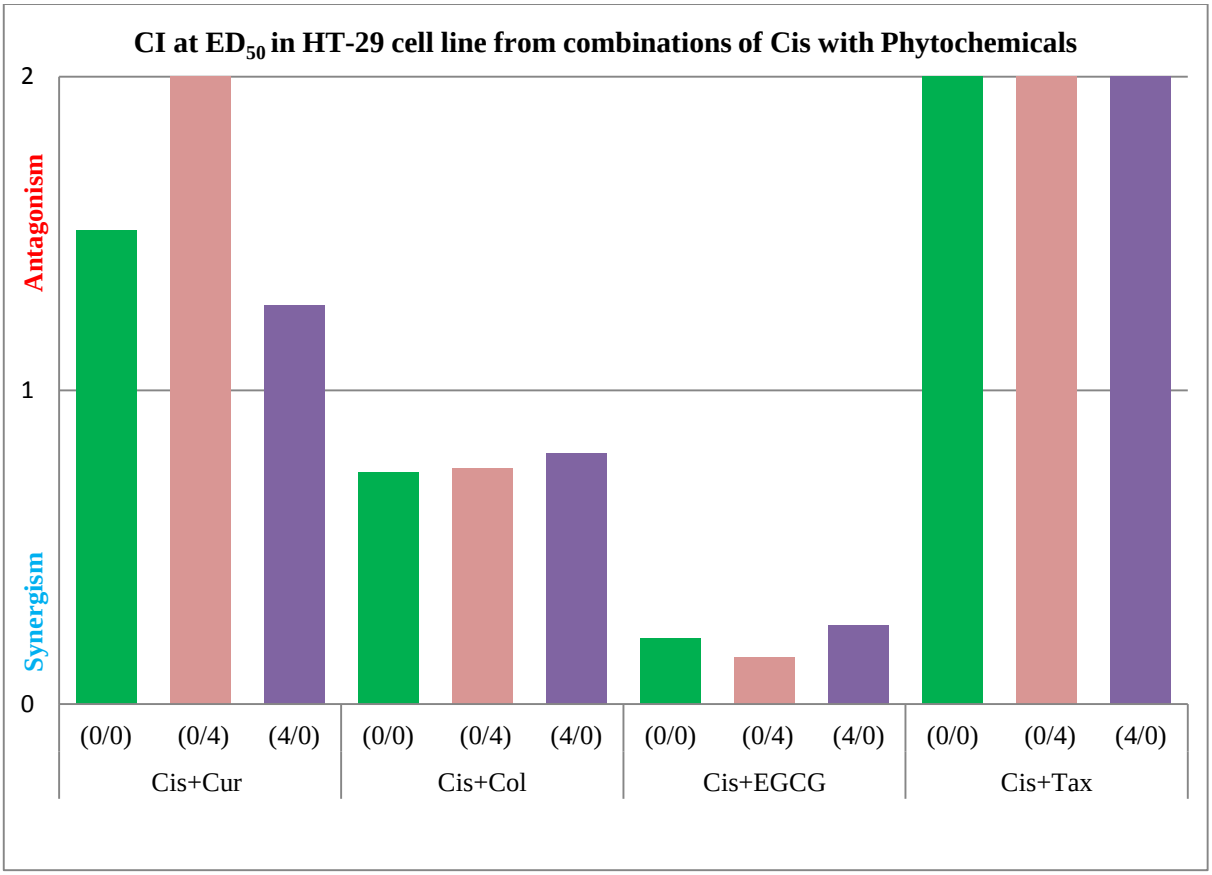

Figure 3.38 : Combination indices at ED_{50} in HT-29 cell line (Cis with Phytochemicals)

Table 3.10: Combination indices (CIs) at ED_{50}, ED_{75} and ED_{90}, applying to binary combinations of cisplatin and phytochemicals (Cur, Col, EGCG and Tax) for the three modes of addition: (0/0 h), (0/4 h), and (4/0 h), in the colorectal cancer cell line HT-29. (D_m is the medium effect dose, m is the exponent defining shape of the dose effect curve and r is the reliability coefficient)

Drug	**Combination Index Values at**					
	ED_{50}	ED_{75}	ED_{90}	D_m	m	R
Cis	NA	NA	NA	3.38	0.90	0.9947
Cur	NA	NA	NA	4.15	0.67	0.96
Cis + Cur 0/0	1.51	0.97	0.65	1.33	1.04	0.98
Cis + Cur 0/4	2.26	1.20	0.665	2.00	1.27	0.99
Cis +Cur 4/0	1.27	0.92	0.69	1.12	0.93	0.98
Col	N/A	N/A	N/A	0.002	1.11	0.99
Cis +Col 0/0	0.74	0.74	0.74	0.24	1.08	0.99
Cis +Col 0/4	0.75	0.83	0.92	0.32	0.60	0.99
Cis +Col 4/0	0.80	0.83	0.85	0.34	0.63	0.95
EGCG	N/A	N/A	N/A	31.0	0.92	0.99
Cis +EGCG 0/0	0.21	0.39	0.73	0.95	0.58	0.99
Cis +EGCG 0/4	0.15	1.14	8.75	0.67	0.33	1.00
Cis +EGCG 4/0	0.25	0.42	0.71	1.11	0.61	0.99
Tax	NA	NA	NA	0.92	1.93	0.95
Cis +Tax 0/0	11.17	7.20	4.70	4.90	1.98	0.98
Cis +Tax 0/4	10.97	7.09	4.65	4.81	1.97	0.97
Cis +Tax 4/0	11.87	7.75	5.12	5.21	1.93	0.98

3.3.2 Combinations from Ox and phytochemicals against HT-29 cell line

Table 3.11 describes the list of CI values obtained from the combinations of Ox with Cur, Col, EGCG and Tax at three different sequences of additions and concentrations. It is evident from Table 3.11 that, among all combinations Ox with EGCG and Ox with Cur produced synergism at all different concentrations and sequences of additions. Highest synergism was shown by Ox with Cur at all added concentrations with 4/0 sequence of addition. Ox in combination with Col showed strong synergism at ED_{90} level. Ox in combination with Tax displayed antagonism irrespective of sequences and added concentrations. Figure 3.39 shows pictorial presentation of CI as a function of added sequences and concentrations at ED_{50} level for all combinations of selected phytochemicals with Ox against HT-29 cell line.

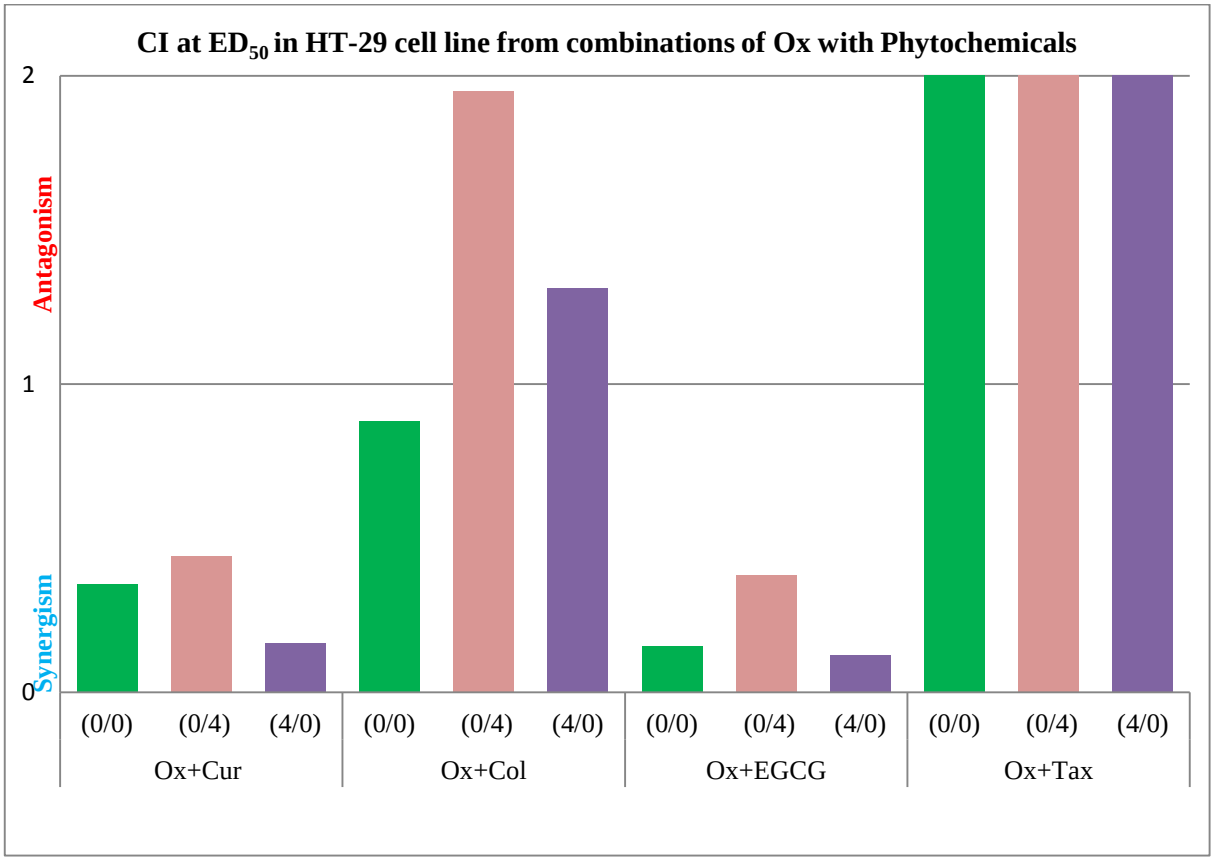

Figure 3.39 : Combination indices at ED_{50} in HT-29 cell line (Ox with Phytochemicals)

Table 3.11 Combination indices (CIs) at ED_{50}, ED_{75} and ED_{90}, applying to binary combinations of oxaliplatin and phytochemicals (Cur, Col, EGCG and Tax) for the three modes of addition: (0/0 h), (0/4 h), and (4/0 h), in the colorectal cancer cell line HT-29. (D_m is the medium effect dose, m is the exponent defining shape of the dose effect curve and r is the reliability coefficient)

Drug	**Combination Index Values at**					
	ED_{50}	ED_{75}	ED_{90}	D_m	m	r
Ox	NA	NA	NA	0.86	0.82	0.98
Cur	NA	NA	NA	0.31	1.39	1.00
Ox + Cur 0/0	0.35	0.21	0.12	0.31	1.39	1.00
Ox + Cur 0/4	0.44	0.24	0.13	0.38	1.52	1.00
Cis +Cur 4/0	0.16	0.14	0.12	0.14	0.92	1.00
Col	N/A	N/A	N/A	0.01	0.52	1.00
Ox +Col 0/0	0.88	0.45	0.23	0.28	0.79	0.97
Ox +Col 0/4	1.95	0.59	0.18	0.61	1.26	0.99
Ox +Col 4/0	1.31	0.48	0.18	0.41	1.03	0.97
EGCG	N/A	N/A	N/A	12.54	0.66	0.86
OX +EGCG 0/0	0.15	0.16	0.17	0.13	0.78	0.96
Ox +EGCG 0/4	0.38	0.25	0.17	0.33	1.19	0.94
Ox +EGCG 4/0	0.12	0.18	0.27	0.10	0.63	0.98
Tax	N/A	N/A	N/A	0.48	2.77	1.00
Ox +Tax 0/0	2.66	3.30	1.67	0.82	0.96	2.17
Ox +Tax 0/4	2.17	2.70	3.38	0.83	1.64	0.94
Ox +Tax 4/0	2.10	2.58	3.20	0.80	1.67	0.95

3.3.3 Combinations from Cis and phytochemicals against CACO-2 cell line

Table 3.12 describes the list of CI values obtained from the combinations of Cis with Cur, Col, EGCG and Tax at three different sequences of additions and concentrations. It is evident from Table 3.12 that, no combination produced synergism at all different concentrations and sequences of additions. Greater synergism was shown by Cis with Col at sequenced additions (0/4 and 4/0) than all other combinations. Cis with EGCG and Cis with Cur showed additiveness towards antagonism at different concentrations and sequence of additions. Cis in combination with Tax displayed antagonism irrespective of sequences and added concentrations. Figure 3.40 shows pictorial presentation of CI as a function of added sequences and concentrations at ED_{50} level for all combinations of selected phytochemicals with Cis against CACO-2 cell line.

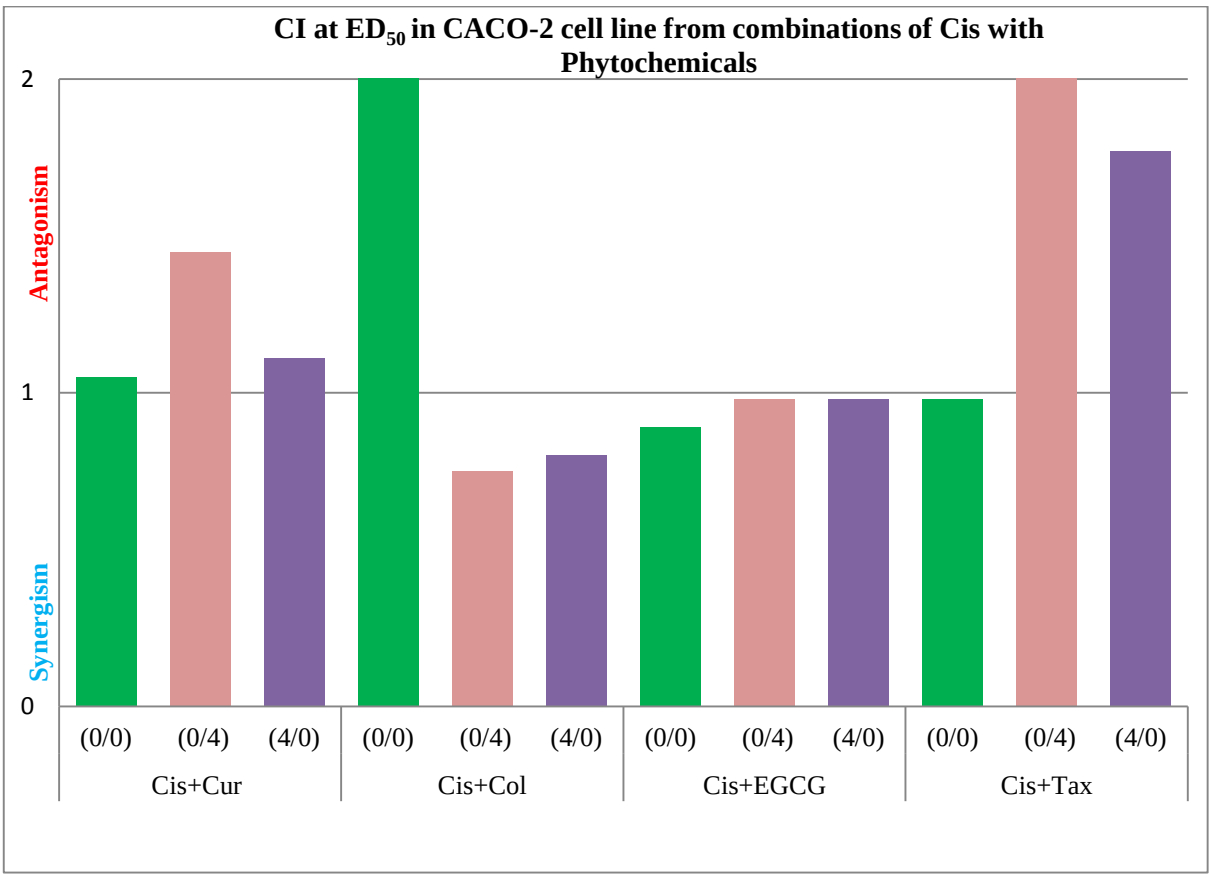

Figure 3.40 : Combination indices at ED_{50} in CACO-2 cell line (Cis with Phytochemicals)

Table 3.12: Combination indices (CIs) at ED_{50}, ED_{75} and ED_{90}, applying to binary combinations of cisplatin and phytochemicals (Cur, Col, EGCG and Tax) for the three modes of addition: (0/0 h), (0/4 h), and (4/0 h), in the colorectal cancer cell line CACO-2. (D_m is the medium effect dose, m is the exponent defining shape of the dose effect curve and r is the reliability coefficient)

Drug	**Combination Index Values at**					
	ED_{50}	ED_{75}	ED_{90}	D_m	m	r
Cis	N/A	N/A	N/A	11.34	0.93	0.98
Cur	N/A	N/A	N/A	12.05	1.02	0.99
Cis + Cur 0/0	1.05	0.95	0.86	6.74	1.06	1.00
Cis + Cur 0/4	1.45	1.24	1.06	9.34	1.13	1.00
Cis +Cur 4/0	1.11	0.99	0.88	7.10	1.08	1.00
Col	N/A	N/A	N/A	7.99	0.38	0.87
Cis +Col 0/0	7.62	2.40	0.76	3.28	2.03	0.91
Cis +Col 0/4	0.75	0.83	0.92	0.32	0.61	1.00
Cis +Col 4/0	0.80	0.83	0.85	0.35	0.64	0.95
EGCG	N/A	N/A	N/A	38.20	1.54	1.00
Cis +EGCG 0/0	0.89	0.88	1.09	10.82	0.72	0.92
Cis +EGCG 0/4	0.98	0.88	0.99	11.92	0.77	0.93
Cis +EGCG 4/0	0.98	1.04	1.39	11.91	0.69	0.92
Tax	N/A	N/A	N/A	9.71	1.48	0.98
Cis +Tax 0/0	0.98	1.21	1.55	0.42	0.58	0.97
Cis +Tax 0/4	2.96	2.76	2.66	1.27	0.69	0.91
Cis +Tax 4/0	1.77	1.65	1.59	0.76	0.69	1.00

3.3.4 Combinations from Ox and phytochemicals against CACO-2 cell line

Table 3.13 describes the list of CI values obtained from the combinations of Ox with Cur, Col, EGCG and Tax at three different sequences of additions and concentrations. It is evident from Table 3.13 that, among all combinations Ox with EGCG and Ox with Cur produced synergism at all different concentrations and sequences of additions. Strongest synergism was shown by Ox with Cur at all added sequences at ED_{90} level. Ox in combination with Col showed strong synergism at ED_{90} level. Ox in combination with Tax displayed mixed outcome with synergism and antagonism depending on sequences and added concentrations. Figure 3.41 shows pictorial presentation of CI as a function of added sequences and concentrations at ED_{50} level for all combinations of selected phytochemicals with Ox against CACO-2 cell line.

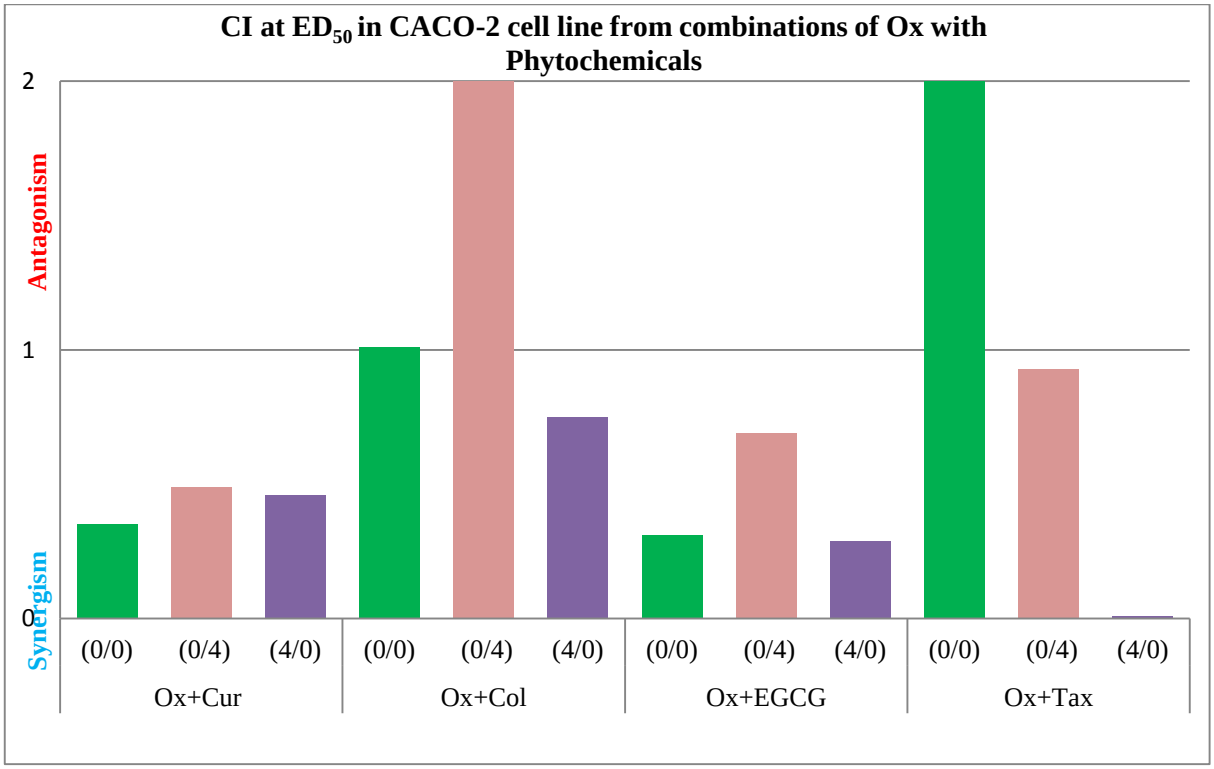

Figure 3.41 : Combination indices at ED_{50} in CACO-2 cell line (Ox with Phytochemicals)

Table 3.13: Combination indices (CIs) at ED_{50}, ED_{75} and ED_{90}, applying to binary combinations of oxaliplatin and phytochemicals (Cur, Col, EGCG and Tax) for the three modes of addition: (0/0 h), (0/4 h), and (4/0 h), in the colorectal cancer cell line CACO-2. (D_m is the medium effect dose, m is the exponent defining shape of the dose effect curve and r is the reliability coefficient)

Drug	**Combination Index Values at**					
	ED_{50}	ED_{75}	ED_{90}	D_m	m	R
Ox	N/A	N/A	N/A	2.49	0.44	1.00
Cur	N/A	N/A	N/A	20.28	0.91	1.00
Ox + Cur 0/0	0.35	0.13	0.05	0.86	0.78	0.98
Ox + Cur 0/4	0.49	0.16	0.05	1.21	0.85	0.98
Cis +Cur 4/0	0.46	0.18	0.08	1.13	0.74	1.00
Col	N/A	N/A	N/A	0.34	0.21	0.99
Ox +Col 0/0	1.01	0.23	0.12	2.36	0.69	0.98
Ox +Col 0/4	2.65	0.61	0.32	6.18	0.68	0.95
Ox +Col 4/0	0.75	0.28	0.23	1.75	0.52	0.96
EGCG	N/A	N/A	N/A	74.43	0.72	0.97
OX +EGCG 0/0	0.31	0.16	0.08	0.77	0.62	0.99
Ox +EGCG 0/4	0.69	0.25	0.09	1.72	0.76	1.00
Ox +EGCG 4/0	0.29	0.19	0.13	0.73	0.54	1.00
Tax	N/A	N/A	N/A	7.01	1.67	1.00
Ox +Tax 0/0	2.00	0.50	0.33	4.04	1.70	0.95
Ox +Tax 0/4	0.93	1.04	3.10	1.87	0.51	0.92
Ox +Tax 4/0	0.01	0.00	0.00	0.02	-0.71	0.41

3.3.5 Combinations from Cis and phytochemicals against LIM-1215 cell line

Table 3.14 describes the list of CI values obtained from the combinations of Cis with Cur, Col, EGCG and Tax at three different sequences of additions and concentrations. It is evident from Table 3.14 that, among all combinations Cis with Cur produced synergism at all different concentrations and sequences of additions except for ED_{90} at bolus addition. Greater synergism was shown by Cis with Cur at ED_{50} level of all added sequences of administration. Combination of Cis with Col displayed synergism with all added sequences and concentrations except for bolus addition which showed antagonism. Cis with EGCG showed mainly additiveness whereas Cis with Tax displayed antagonism. Figure 3.42 shows pictorial presentation of CI as a function of added sequences and concentrations at ED_{50} level for all combinations of selected phytochemicals with Cis against LIM-1215 cell line.

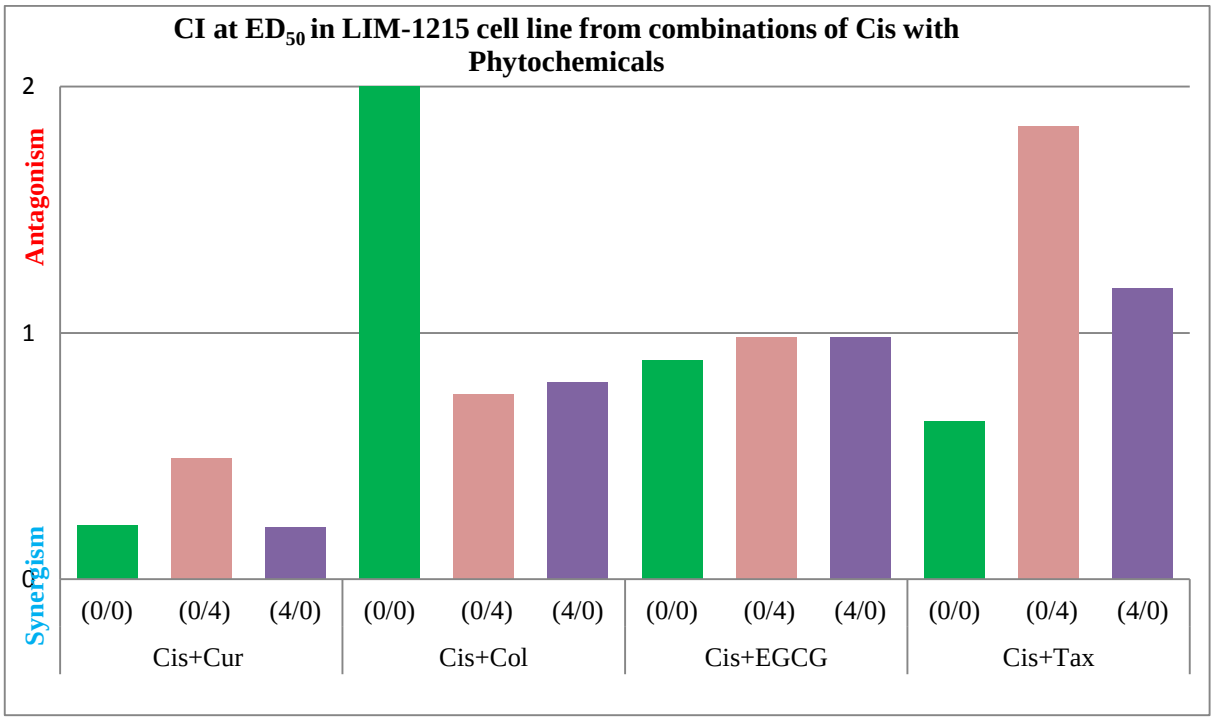

Figure 3.42 : Combination indices at ED_{50} in Lim-1215 cell line (Cis with Phytochemicals)

Table 3.14: Combination indices (CIs) at ED_{50}, ED_{75} and ED_{90}, applying to binary combinations of cisplatin and phytochemicals (Cur, Col, EGCG and Tax) for the three modes of addition: (0/0 h), (0/4 h), and (4/0 h), in the colorectal cancer cell line LIM-1215. (D_m is the medium effect dose, m is the exponent defining shape of the dose effect curve and r is the reliability coefficient)

Drug	**Combination Index Values at**					
	ED_{50}	ED_{75}	ED_{90}	D_m	m	R
Cis	N/A	N/A	N/A	22.23	1.80	0.99
Cur	N/A	N/A	N/A	66.17	1.73	0.93
Cis + Cur 0/0	0.22	0.59	1.57	4.57	0.69	0.95
Cis + Cur 0/4	0.49	0.51	0.52	10.14	1.72	0.99
Cis +Cur 4/0	0.21	0.39	0.72	4.30	0.89	1.00
Col	N/A	N/A	N/A	7.99	0.38	0.87
Cis +Col 0/0	7.62	2.40	0.76	3.28	2.03	0.91
Cis +Col 0/4	0.75	0.83	0.92	0.32	0.61	1.00
Cis +Col 4/0	0.80	0.83	0.85	0.35	0.64	0.95
EGCG	N/A	N/A	N/A	38.20	1.54	1.00
Cis +EGCG 0/0	0.89	0.88	1.09	10.82	0.72	0.92
Cis +EGCG 0/4	0.98	0.88	0.99	11.92	0.77	0.93
Cis +EGCG 4/0	0.98	1.04	1.39	11.91	0.69	0.92
Tax	N/A	N/A	N/A	1.75	1.68	0.97
Cis +Tax 0/0	0.64	2.75	11.87	6.93	0.53	0.97
Cis +Tax 0/4	1.84	17.73	170.57	20.03	0.38	1.00
Cis +Tax 4/0	1.18	1.22	1.27	12.83	1.66	0.95

3.3.6 Combinations from Ox and phytochemicals against LIM-1215 cell line

Table 3.15 describes the list of CI values obtained from the combinations of Ox with Cur, Col, EGCG and Tax at three different sequences of additions and concentrations. It is evident from Table 3.15 that, all combinations from Ox with selected phytochemicals demonstrated significant synergism at all added concentrations and sequence of additions except for very few instances. For example Ox with Cur and Ox with EGCG at ED_{90} with bolus addition, Ox with Tax at higher concentrations from 4/0 addition exhibited additiveness. Figure 3.43 shows pictorial presentation of CI as a function of added sequences and concentrations at ED_{50} level for all combinations of selected phytochemicals with Ox against LIM-1215 cell line.

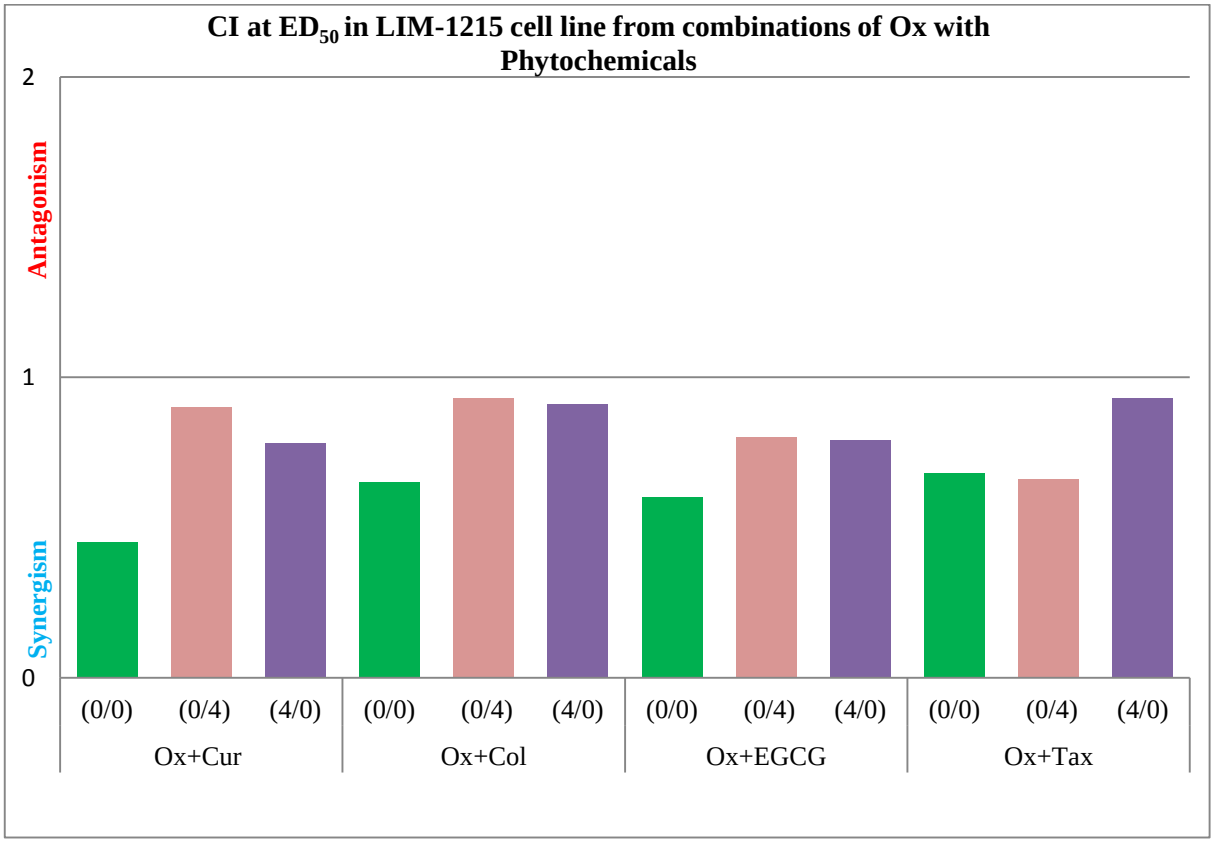

Figure 3.43 : Combination indices at ED_{50} in Lim-1215 cell line (Ox with Phytochemicals)

Table 3.15: Combination indices (CIs) at ED_{50}, ED_{75} and ED_{90}, applying to binary combinations of oxaliplatin and phytochemicals (Cur, Col, EGCG and Tax) for the three modes of addition: (0/0 h), (0/4 h), and (4/0 h), in the colorectal cancer cell line LIM-1215. (D_m is the medium effect dose, m is the exponent defining shape of the dose effect curve and r is the reliability coefficient)

Drug	**Combination Index Values at**					
	ED_{50}	ED_{75}	ED_{90}	D_m	m	R
Ox	N/A	N/A	N/A	27.70	0.85	0.92
Cur	N/A	N/A	N/A	34.12	1.83	0.93
Ox + Cur 0/0	0.45	0.70	1.16	4.55	0.90	0.96
Ox + Cur 0/4	0.90	0.72	0.62	9.04	1.93	0.99
Cis +Cur 4/0	0.78	0.62	0.53	7.79	1.94	0.97
Col	N/A	N/A	N/A	0.03	0.55	0.85
Ox +Col 0/0	0.65	0.36	0.20	1.43	0.78	0.89
Ox +Col 0/4	0.93	0.39	0.16	2.04	0.99	0.99
Ox +Col 4/0	0.91	0.60	0.39	2.01	0.71	0.95
EGCG	N/A	N/A	N/A	314.59	1.86	0.98
OX +EGCG 0/0	0.60	0.76	1.07	9.02	0.97	1.00
Ox +EGCG 0/4	0.80	0.61	0.53	11.95	1.71	0.96
Ox +EGCG 4/0	0.79	0.60	0.51	11.82	1.75	0.98
Tax	N/A	N/A	N/A	2.36	0.40	0.94
Ox +Tax 0/0	0.68	0.30	0.15	2.33	0.73	0.98
Ox +Tax 0/4	0.66	0.43	0.32	2.24	0.58	0.93
Ox +Tax 4/0	0.93	1.15	1.63	3.17	0.43	0.98

3.3.7 Combinations from Cis and phytochemicals against LIM-2405 cell line

Table 3.16 describes the list of CI values obtained from the combinations of Cis with Cur, Col, EGCG and Tax at three different sequences of additions and concentrations. It is evident from Table 3.16 that, Cis with Cur produced synergism at all different concentrations and sequences of additions except for ED_{75} and ED_{90} at bolus addition. Cis in combination with EGCG also exhibited synergism at all added concentrations and sequences, but for higher concentrations with 4/0 additions. Combination of Cis with Col and Cis with Tax displayed antagonism irrespective of sequences and concentrations. Figure 3.44 shows pictorial presentation of CI as a function of added sequences and concentrations at ED_{50} level for all combinations of selected phytochemicals with Cis against LIM-2405 cell line.

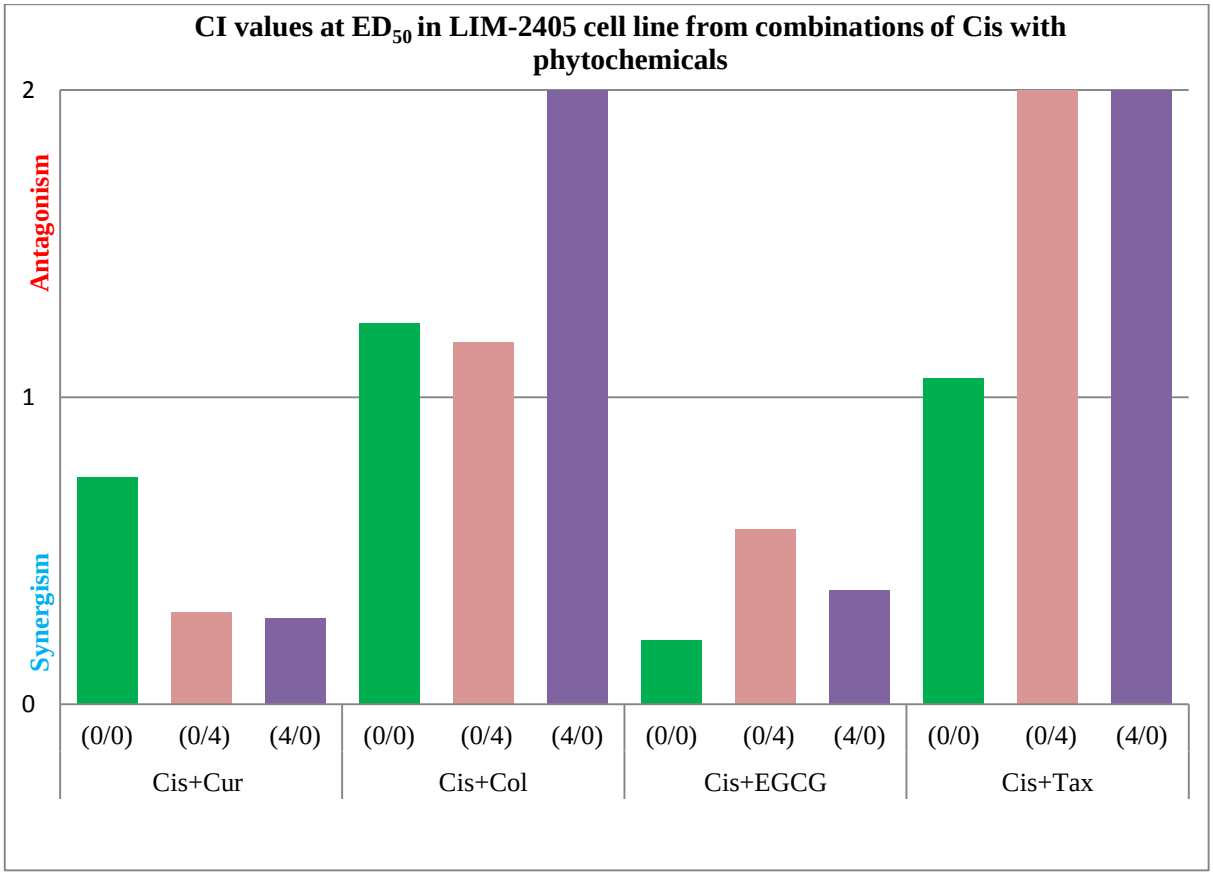

Figure 3.44 : Combination indices at ED_{50} in Lim-2405 cell line (Cis with Phytochemicals)

Table 3.16: Combination indices (CIs) at ED_{50}, ED_{75} and ED_{90}, applying to binary combinations of cisplatin and phytochemicals (Cur, Col, EGCG and Tax) for the three modes of addition: (0/0 h), (0/4 h), and (4/0 h), in the colorectal cancer cell line LIM-2405. (D_m is the medium effect dose, m is the exponent defining shape of the dose effect curve and r is the reliability coefficient)

Drug	**Combination Index Values at**					
	ED_{50}	ED_{75}	ED_{90}	D_m	m	R
Cis	N/A	N/A	N/A	12.94	1.73	0.93
Cur	N/A	N/A	N/A	29.32	0.69	0.96
Cis + Cur 0/0	0.74	1.66	4.00	7.62	0.70	0.97
Cis + Cur 0/4	0.30	0.38	0.51	3.08	1.10	0.98
Cis +Cur 4/0	0.28	0.41	0.65	2.89	0.96	0.98
Col	N/A	N/A	N/A	0.01	0.89	0.95
Cis +Col 0/0	1.24	1.38	1.53	2.18	0.95	0.91
Cis +Col 0/4	1.18	1.22	1.28	2.07	1.01	0.96
Cis +Col 4/0	4.77	5.38	6.12	8.35	0.94	0.94
EGCG	N/A	N/A	N/A	46.52	0.87	0.98
Cis +EGCG 0/0	0.21	0.36	0.61	2.64	0.93	0.97
Cis +EGCG 0/4	0.57	0.48	0.41	7.13	2.28	0.94
Cis +EGCG 4/0	0.37	1.21	4.00	4.61	0.60	1.00
Tax	N/A	N/A	N/A	6.45	0.98	0.94
Cis +Tax 0/0	1.06	1.41	1.87	2.29	0.85	0.94
Cis +Tax 0/4	5.30	4.04	3.08	11.49	1.49	0.92
Cis +Tax 4/0	2.98	4.12	5.71	6.46	0.82	0.73

3.3.8 Combinations from Ox and phytochemicals against LIM-2405 cell line

Table 3.17 describes the list of CI values obtained from the combinations of Ox with Cur, Col, EGCG and Tax at three different sequences of additions and concentrations. It is evident from Table 3.17 that, among all combinations only Ox with EGCG demonstrated synergism at all added concentrations and sequence of additions. Combination of Ox with Cur also displayed synergism in all added concentrations and sequences but for ED_{50} level with 0/4 and 4/0 sequence of additions. Ox with Col and Ox with Tax exhibited predominantly antagonism. Figure 3.45 shows pictorial presentation of CI as a function of added sequences and concentrations at ED_{50} level for all combinations of selected phytochemicals with Ox against LIM-2405 cell line.

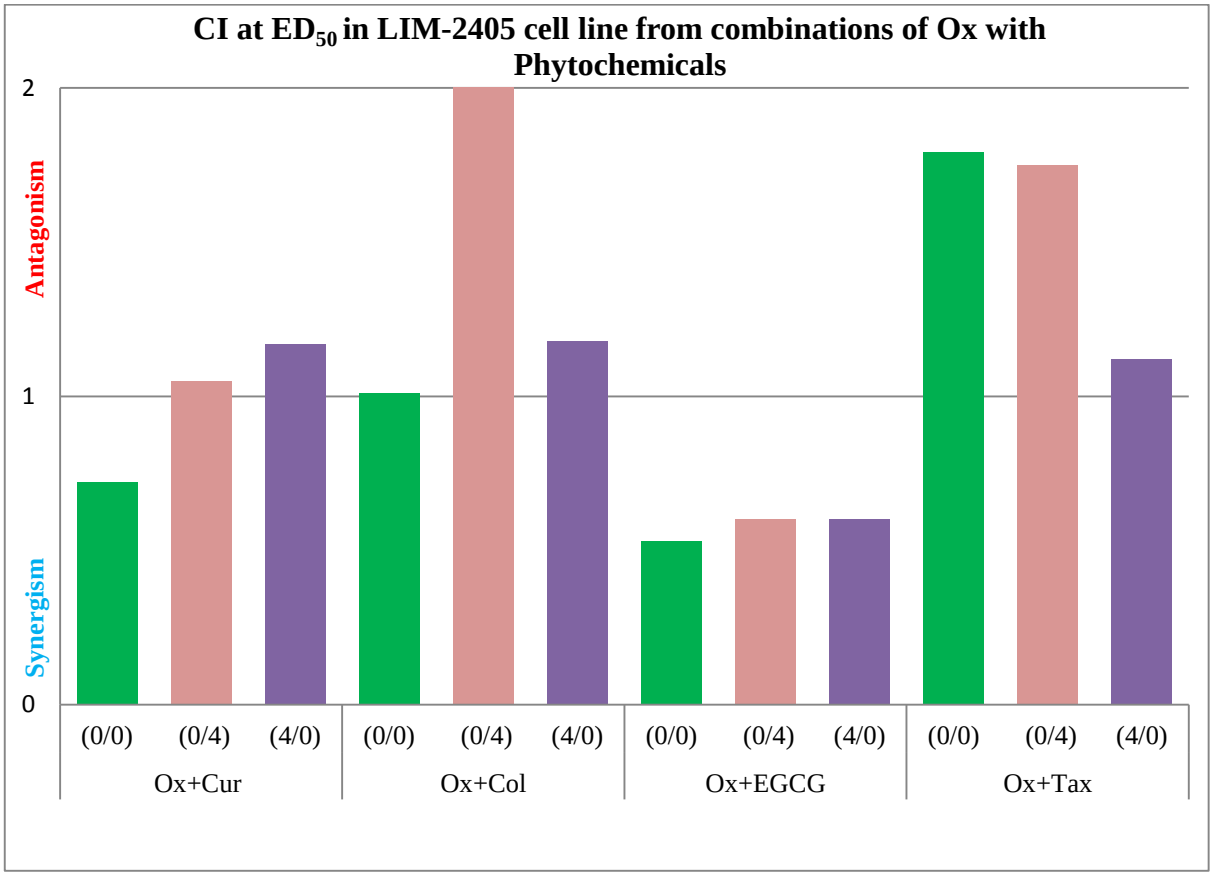

Figure 3.45 : Combination indices at ED_{50} in Lim-2405 cell line (Ox with Phytochemicals)

Table 3.17 Combination indices (CIs) at ED_{50}, ED_{75} and ED_{90}, applying to binary combinations of oxaliplatin and phytochemicals (Cur, Col, EGCG and Tax) for the three modes of addition: (0/0 h), (0/4 h), and (4/0 h), in the colorectal cancer cell line LIM-2405. (D_m is the medium effect dose, m is the exponent defining shape of the dose effect curve and r is the reliability coefficient)

Drug	**Combination Index Values at**					
	ED_{50}	ED_{75}	ED_{90}	D_m	m	R
Ox	N/A	N/A	N/A	21.45	1.11	0.95
Cur	N/A	N/A	N/A	16.26	0.99	0.92
Ox + Cur 0/0	0.72	0.73	0.74	6.98	1.03	0.95
Ox + Cur 0/4	1.05	0.77	0.57	10.22	1.48	0.99
Cis +Cur 4/0	1.17	0.88	0.67	11.38	1.43	0.96
Col	N/A	N/A	N/A	0.04	0.84	0.97
Ox +Col 0/0	1.01	1.11	1.25	8.11	0.71	1.00
Ox +Col 0/4	2.09	3.48	5.90	16.73	0.56	0.98
Ox +Col 4/0	1.18	0.75	0.48	9.49	1.11	1.00
EGCG	N/A	N/A	N/A	78.77	0.93	0.90
OX +EGCG 0/0	0.53	0.58	0.64	10.77	1.00	0.97
Ox +EGCG 0/4	0.60	0.52	0.44	12.21	1.30	0.99
Ox +EGCG 4/0	0.60	0.49	0.40	12.16	1.37	0.97
Tax	N/A	N/A	N/A	2.89	0.62	0.99
Ox +Tax 0/0	1.79	1.36	1.05	15.53	0.80	1.00
Ox +Tax 0/4	1.75	0.89	0.46	15.13	1.12	0.99
Ox +Tax 4/0	1.12	1.09	1.07	9.74	0.68	1.00

3.4 Cellular Accumulation and DNA Binding

Cellular accumulations of platinum and platinum-DNA binding study was conducted for platinum drugs (cisplatin and oxaliplatin) alone and few selected combinations with Col, Cur, EGCG and Tax as applied to the cell lines HT-29 and CACO-2. The aim of this study was to determine whether there was any correlation between cellular accumulation of platinum drugs and Pt–DNA binding levels with the combined drug action. Based on the dose response curves and combination indices; few synergistic, antagonistic and additive combinations were selected for this study to obtain the mechanistic insight of combined drug action.

3.4.1 Cellular accumulation study

3.4.1.1 HT-29 cell line

Table 3.18 gives the results of cellular accumulation of platinum expressed as nmol Pt per $5x10^6$ cells in HT-29 cell line for cisplatin and oxaliplatin administered alone and its selected combinations with the phytochemicals. Figure 3.46 (a) and Figure 3.46 (b) shows the visual presentation of the same.

Table 3.18: Cellular accumulations of platinum in HT-29 cell line

Sample	**Combined Effect at ED_{50}**	**Pt (nmol/5x10^6cell)**	**Standard deviation**
Cis (alone)	Not applicable	4.27	0.04
Cis with Cur (4/0)	Additive	4.90	0.26
Cis with EGCG (0/0)	Synergistic	9.10	0.23
Ox (alone)	Not applicable	0.09	0.28
Ox with Cur (0/0)	Synergistic	0.08	0.01
Ox with Cur (4/0)	Synergistic	0.09	0.22
Ox with EGCG(0/0)	Synergistic	0.11	0.02
Ox with Col (0/4)	Additive	0.03	0.12
Ox with Tax (4/0)	Antagonistic	0.07	0.14

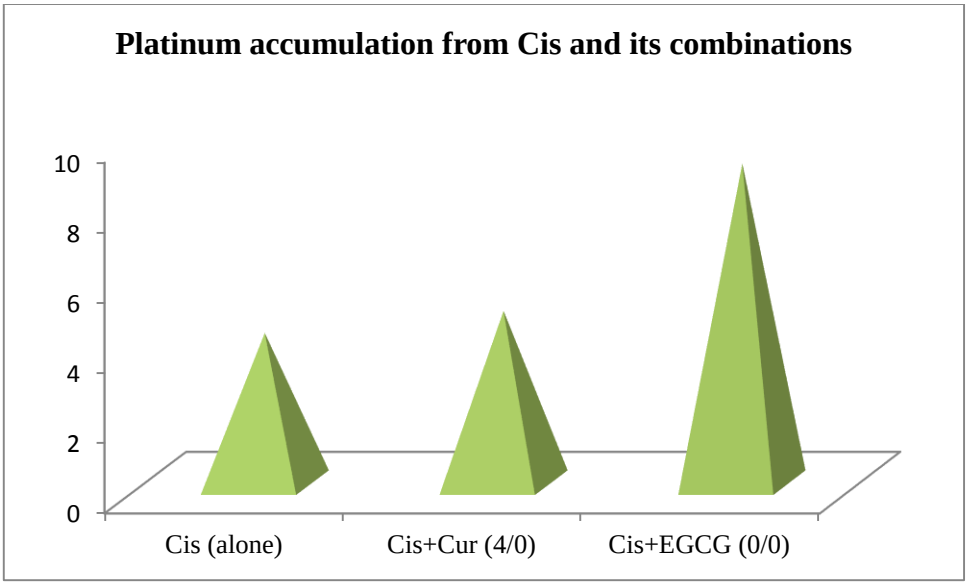

(a) Accumulation of Pt from Cis and its combinations

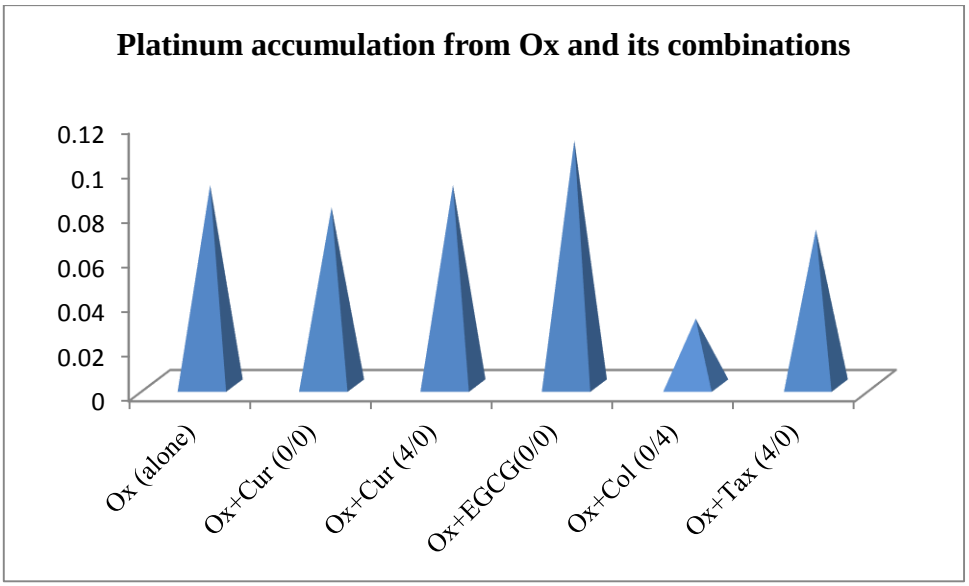

(b) Accumulation of Pt from Ox and its combinations

Figure 3.46 : Cellular accumulation of platinum in HT-29 cell line

From the above results it can be seen than, synergistic combination of Cis with EGCG (bolus) manifests higher platinum accumulation into HT-29 cells than Cis alone and additive treatment of Cis with Cur (4/0). In contrary, synergistic combined treatments from combinations of Ox did not show increase in platinum accumulation except for Ox with EGCG (bolus). However, antagonistic and additive combinations cause reduction in platinum accumulation compared to Ox alone and synergistic treatments.

3.4.1.2 CACO-2 cell line

Table 3.19 gives the results of cellular accumulation of platinum expressed as nmol Pt per $5x10^6$ cells in CACO-2 cell line for cisplatin and oxaliplatin administered alone and its selected combinations with the phytochemicals. Figure 3.47 (a) and Figure 3.47 (b) shows the visual presentation of the same.

Table 3.19: Cellular accumulations of platinum in CACO-2 cell line

Sample	Combined Effect at ED_{50}	Pt (nmol/$5x10^6$cell)	Standard deviation
Cis (alone)	Not applicable	2.02	0.03
Cis with Cur (4/0)	Additive	3.52	0.03
Cis with EGCG (0/0)	Synergistic	5.48	0.22
Ox (alone)	Not applicable	0.27	0.30
Ox with Cur (0/0)	Synergistic	0.09	0.19
Ox with EGCG(0/0)	Synergistic	0.17	0.12
Ox with Col (0/4)	Antagonistic	0.12	0.05
Ox with Tax (4/0)	Antagonistic	0.10	0.03

It is evident from the results that, additive combination from Cis with Cur (4/0) and synergistic combination from Cis with EGCG (0/0) caused greater platinum accumulation than Cis alone treatment. Similar to HT-29 cell line, synergistic combined treatments from Ox and phytochemicals did not cause greater cellular accumulation of platinum than Ox alone treatment. But Antagonistic treatment of Ox with Tax (4/0) showed lower platinum accumulation than synergistic treatments and Ox alone treatment.

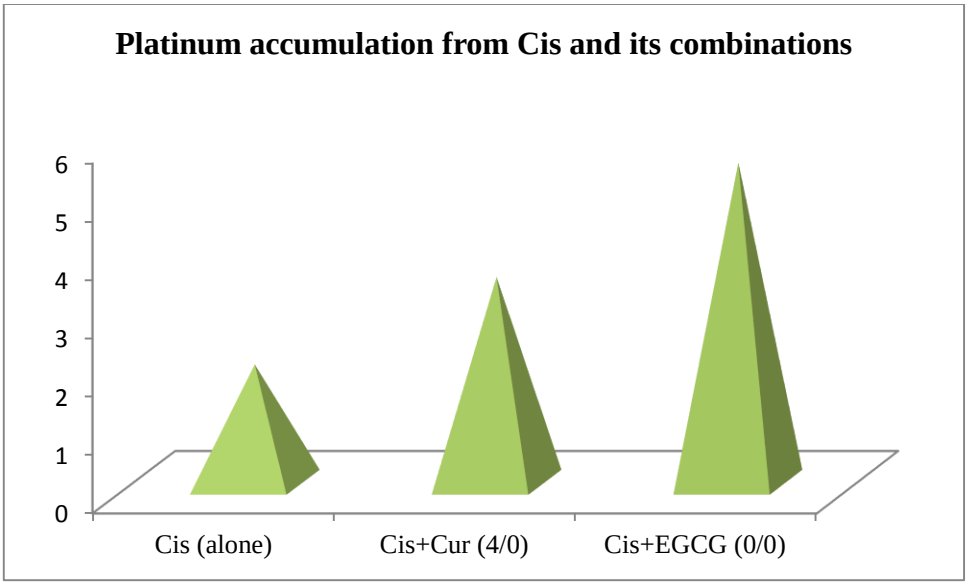

(a) Accumulation of Pt from Cis and its combinations

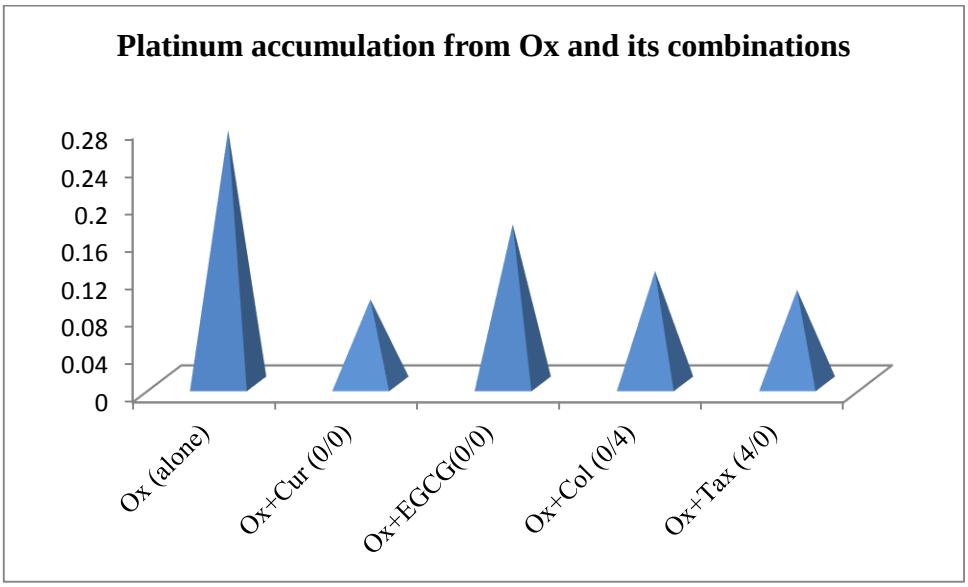

(b) Accumulation of Pt from Ox and its combinations

Figure 3.47 : Cellular accumulation of platinum in CACO-2 cell line

3.4.2 Platinum–DNA binding study

3.4.2.1 HT-29 cell line

Table 3.20 gives the results of Pt–DNA binding levels, expressed as nmol Pt per mg of DNA in HT-29 cell line for cisplatin and oxaliplatin administered alone and its selected combinations with the phytochemicals. Figure 3.48 (a) and Figure 3.48 (b) shows the visual presentation of the same.

Table 3.20: Platinum–DNA binding in HT-29 cell line

Sample	Combined Effect at ED_{50}	Pt (nmol)/DNA(mg)	Standard deviation
Cis (alone)	Not applicable	1.00	0.08
Cis with Cur (4/0)	Additive	0.93	0.15
Cis with EGCG (0/0)	Synergistic	11.30	0.12
Ox (alone)	Not applicable	0.20	0.03
Ox with Cur (0/0)	Synergistic	0.26	0.15
Ox with Cur (4/0)	Synergistic	0.24	0.04
Ox with EGCG(0/0)	Synergistic	0.14	0.14
Ox with Col (0/4)	Additive	0.15	0.14
Ox with Tax (4/0)	Antagonistic	0.11	0.01

It is observed from the study that synergistic combination of Cis with EGCG (bolus) showed greater extent of binding of DNA with platinum than Cis alone and additive combined treatment Cis with Cur (4/0). The same trend was also evident from study with Ox and its combinations: synergistic combined treatments displayed higher degree of Pt–DNA binding than Ox alone treatment. Antagonistic and additive treatments manifested lower degree of Pt–DNA binding compared to Ox alone treatment in HT-29 cell line.

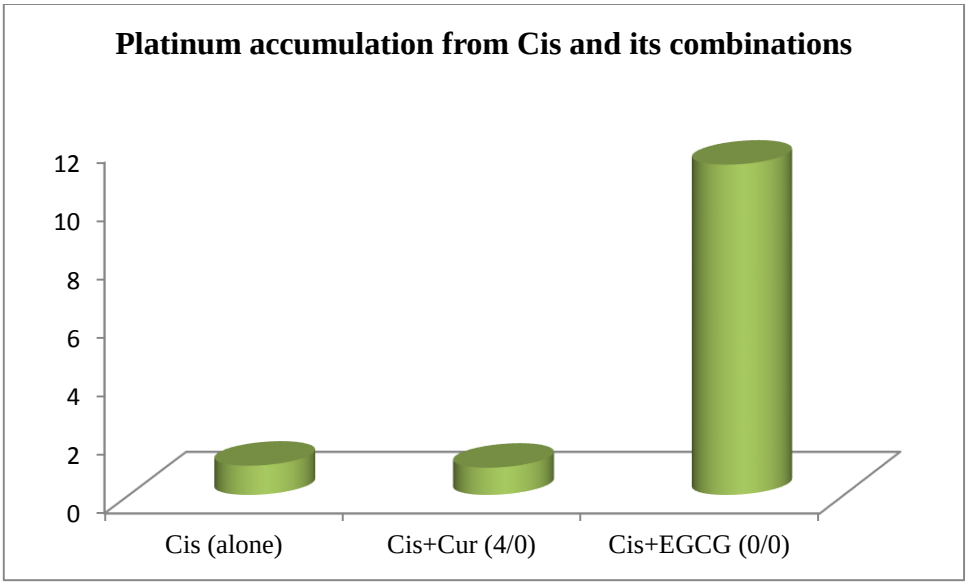

(a) Extent of Pt–DNA binding from Cis and its combinations

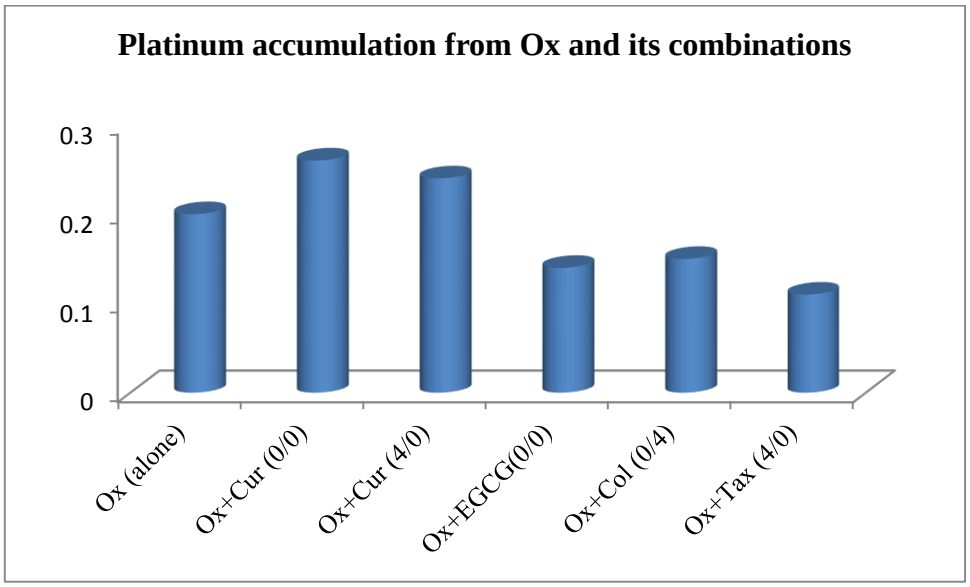

(b) Extent of Pt–DNA binding from Ox and its combinations

Figure 3.48 : Magnitude of Pt–DNA binding in HT-29 cell line

3.4.2.2 CACO-2 cell line

Table 3.21 gives the results of Pt–DNA binding levels, expressed as nmol Pt per mg of DNA in CACO-2 cell line for cisplatin and oxaliplatin administered alone and its selected combinations with the phytochemicals. Figure 3.49 (a) and Figure 3.49 (b) shows the visual presentation of the same.

Table 3.21: Platinum–DNA binding in CACO-2 cell line

Sample	Combined Effect at ED_{50}	Pt (nmol)/DNA(mg)	Standard deviation
Cis (alone)	Not applicable	1.28	0.14
Cis with Cur (4/0)	Additive	1.55	0.27
Cis with EGCG (0/0)	Synergistic	0.79	0.33
Ox (alone)	Not applicable	0.19	0.50
Ox with Cur (0/0)	Synergistic	0.17	0.12
Ox with EGCG(0/0)	Synergistic	0.21	0.17
Ox with Col (0/4)	Antagonistic	0.12	0.12
Ox with Tax (4/0)	Antagonistic	0.11	0.02

It can be said from the above results that, combined treatments of Cis with phytochemicals did not follow any specific trend in regards to the extent of platinum–DNA binding in CACO-2 cell line. Synergistic combined treatment of Ox with EGCG (0/0) increased the magnitude of platinum–DNA binding. Antagonistic and additive combined treatments decrease the Pt-DNA binding level in CACO-2 cell line.

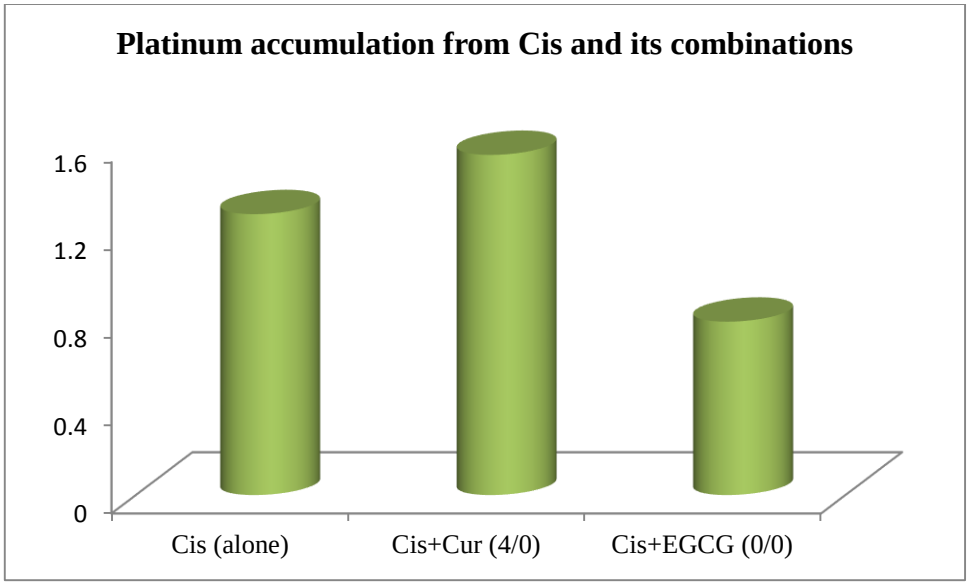

(a) Extent of Pt–DNA binding from Cis and its combinations

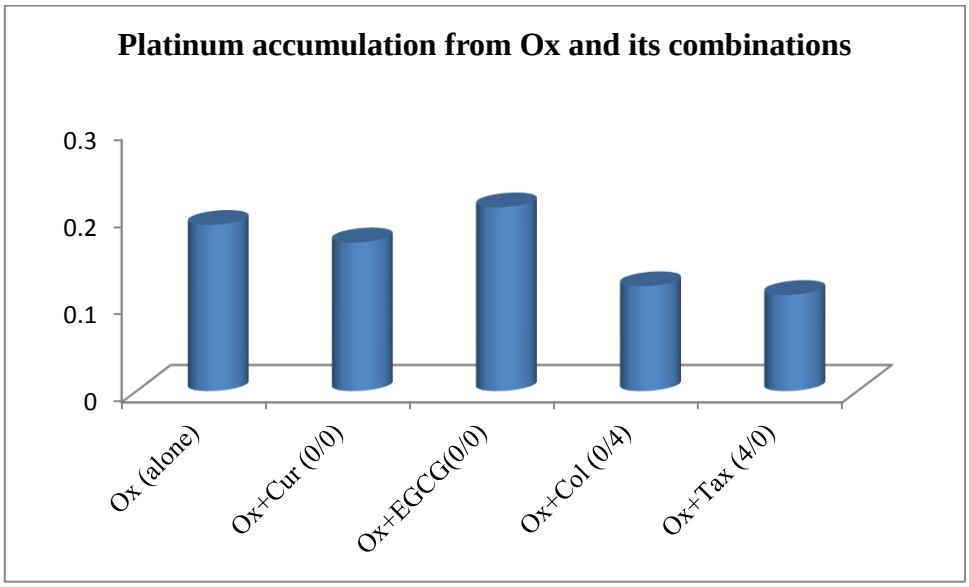

(b) Extent of Pt–DNA binding from Cis and its combinations

Figure 3.49 : Magnitude of Pt–DNA binding in CACO-2 cell line

3.5 Interactions with DNA

One of the modes of action of anticancer drugs is targeting of the DNA of cancer cells. In this study, agar gel electrophoresis was conducted to gather qualitative information on conformational changes in DNA and DNA damage due to interaction with platinum drugs and phytochemicals while administered alone and in combinations.

3.5.1 HT-29 cell line

Table 3.22 provides the mobility and fluorescence of DNA obtained from HT-29 cell line after different drug treatments and control. Figure 3.50, figure 3.51 and figure 3.52 represents the electrophoretograms, mobility and net intensity of DNA bands respectively.

Table 3.22: Mobility and fluorescence of DNA bands in HT-29 cell line

Bands	Sample	Mobility (mm)	Net Intensity
1 & 14	HT-Blank	3.96	49801.49
2	HT-Cis	3.7	45927.49
3	HT-Cis + Cur (4/0)	3.79	39748.15
4	HT-Cis + EGCG(0/0)	4.04	6477.8
5	HT-Col	3.62	31469.5
6	HT-Tax	3.79	35536.18
7	HT-Ox	3.79	32815.53
8	HT-Ox + Cur (4/0)	4.13	6273.96
9	HT-Ox + EGCG(0/0)	4.46	19459.7
10	HT-Ox + Col (0/4)	4.29	28103.68
11	HT-Ox + Tax (4/0)	3.96	66926.4
12	HT-Cur	4.46	10979.88
13	HT-EGCG	4.38	28408.44

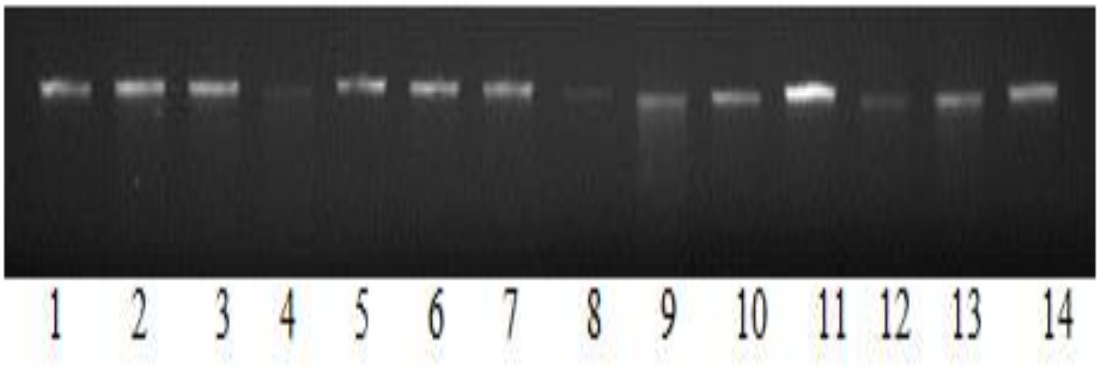

Figure 3.50 : Electrophoretograms of HT-DNA

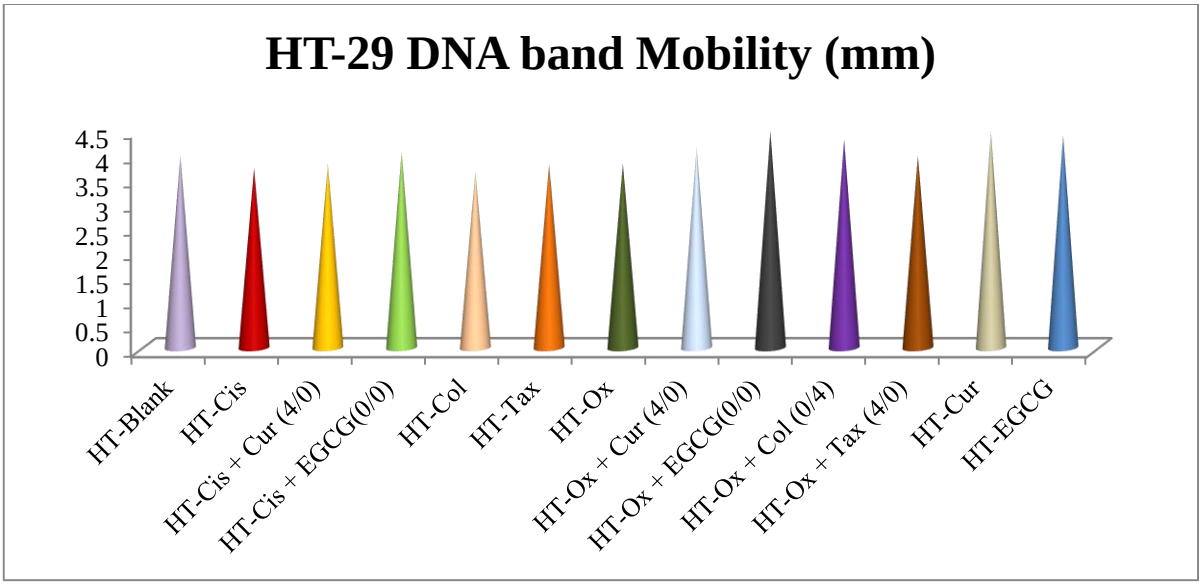

Figure 3.51 : Mobility of DNA obtained from HT-29 cells

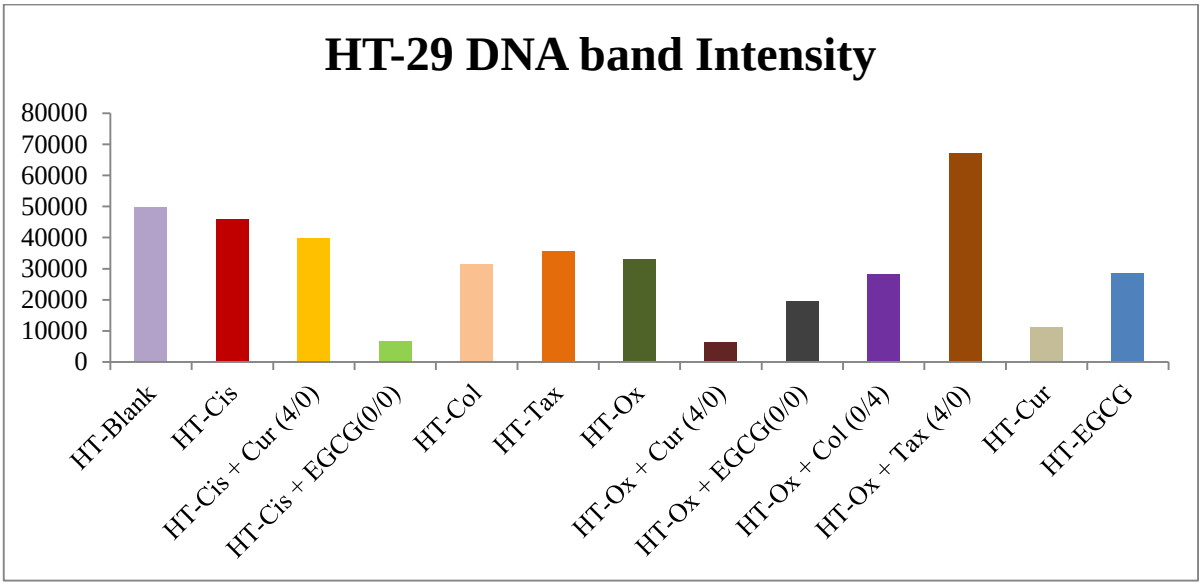

Figure 3.52 : Fluorescence of DNA obtained from HT-29 cells

It has been observed from the above study that, combination of Ox with Cur (4/0) caused the highest DNA damage in HT-29 cell line followed by Cis with EGCG (bolus). Combination of Ox with Tax (4/0) was found to be least damaging towards DNA. The detailed discussion of the results is given in next chapter.

3.5.2 CACO-2 cell line

Table 3.23 provides the mobility and fluorescence of DNA obtained from CACO-2 cell line after different drug treatments and control. Figure 3.53, figure 3.54 and figure 3.55 represents the electrophoretograms, mobility and net intensity of DNA bands respectively.

Table 3.23: Mobility and fluorescence of DNA bands in CACO-2 cell line

Bands	Sample	Mobility (mm)	Net Intensity
1	CA-Blank	5.8	16623
2	CA-Cis	5.21	13041.2
3	CA-Cis + Cur (4/0)	5.29	9644
4	CA-Cis + EGCG(0/0)	5.13	22608.2
5	CA-Ox	5.04	23210.5
6	CA-Ox + Cur (4/0)	5.13	11958.9
7	CA-Ox + EGCG(0/0)	5.04	13045.7
8	CA-Ox + Col (0/4)	5.13	21688.8
9	CA-Ox + Tax (4/0)	4.87	24323
10	CA- Cur	5.13	16467.5
11	CA-EGCG	5.04	17917.2
12	CA-Col	4.71	25248.1
13	CA-Tax	4.45	32933.3

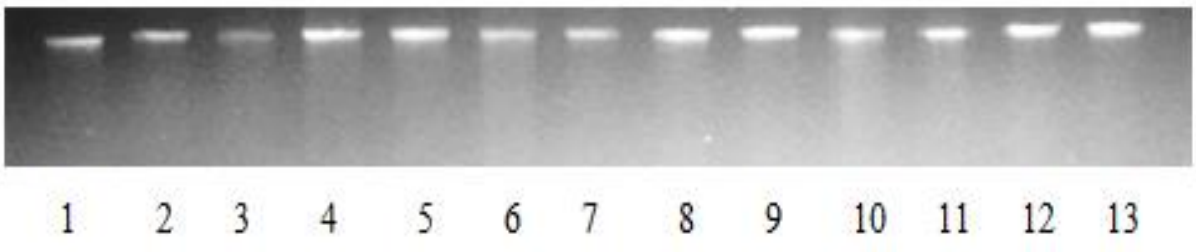

Figure 3.53 : Electrophoretograms of CACO-2 DNA

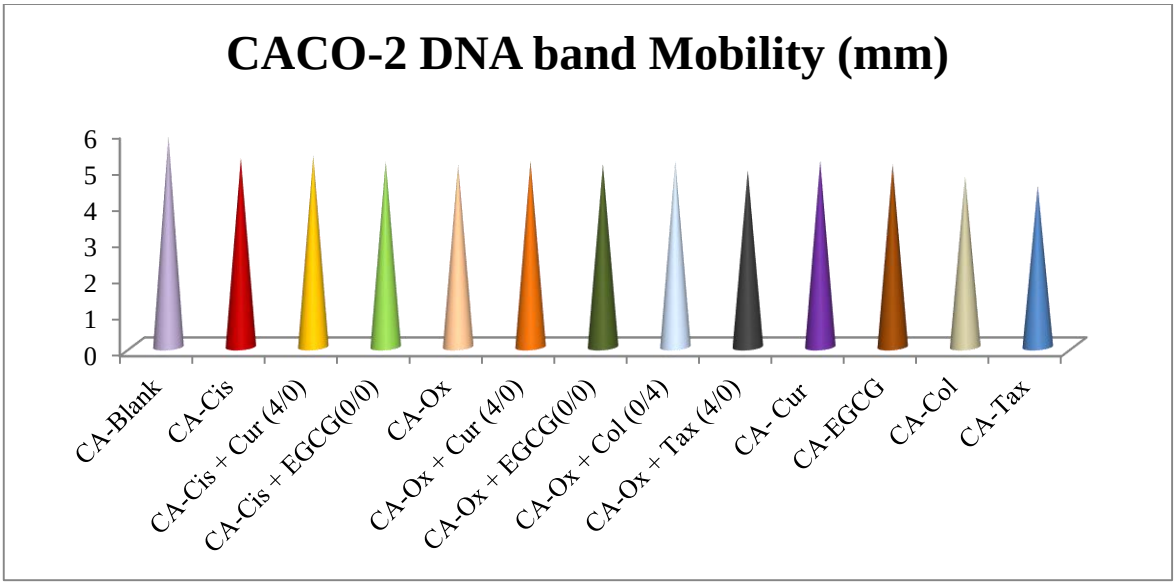

Figure 3.54 : Mobility of DNA obtained from HT-29 cells

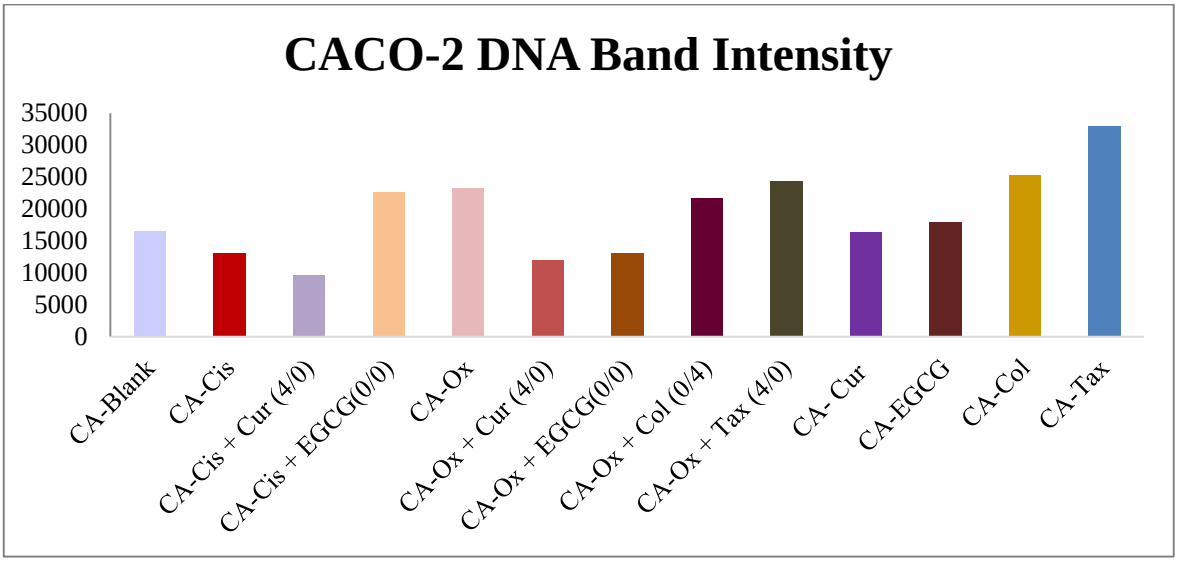

Figure 3.55 : Fluorescence of DNA obtained from CACO-2 cells

It is evident from the above results that among all treated drugs whether alone or in combination in CACO-2 cell line; the most damaging is the combination of Cis with Cur (4/0 h), followed by Ox with Cur (4/0 h). Among the combinations, the least damaging was Ox with Tax (4/0 h).

3.6 Proteomic study

The study was carried out with the aim of identifying proteins which are responsible for the drug actions alone or in combinations. Two dimensional gel electrophoresis study was conducted using IEF and SDS-PAGE gel. Ox, Col, Cur, EGCG alone and their selected combinations were chosen for this study.

For analysis of results ten matched groups were created for all of the images of gels through Melanie Software and then combined into two classes. First class was named as HT-29 gels which included untreated control, Ox alone, Col alone, EGCG alone, Ox with Col (0/4) and Ox with EGCG (bolus). Another class was named as CACO-2 gels which was consisted untreated control, Ox alone, Cur alone and Ox with Cur (bolus). According to the software, 153 protein spots were identified from HT-29 untreated gel and 195 from CACO-2 untreated gel. All of the proteins identified as spots were given common match ID throughout the groups. Expression of each protein spot in the treated gels was then compared with the expression of the same in untreated gels. The difference in expression of a protein spot 1.5 or greater was considered as significant.

3.6.1 Expression of protein in HT-29 gels

Among 153 spots identified in untreated HT-29 gels, 60 spots underwent significant alteration in expression in Col alone treated gel. However the number of spots experienced significant changes in expression with EGCG alone and Ox alone treatments were 42 and 44 respectively. Interestingly the same number of spots (42 and 44) underwent significant altered expression with the treatments of Col (0/4) and Ox with EGCG (bolus) respectively, but the match ID of the spots were different. The spots were selected for excision based on the criteria that showed significant changes in

expression commonly with most of the treatments. However many of the spots were not able to cut due to very low intensity in untreated reference gel, unsuitable position of the spot and other factors. At last only 7 spots were chosen for excision from HT-29 gels, followed by characterization of the protein using matrix-assisted laser desorption/ionization (MALDI) mass spectrometry combined with Swiss-Prot Database. But spot 2 and spot 134 both appeared to be same protein after characterization as Glutathione S transferase P1. Figure 3.56 give the images of untreated and treated HT-29 gels showing the spots. Figure 3.57 represents the annotated untreated HT-29 gel. The protein spots underwent significant changes in expression commonly in the treated gels and selected for further characterization are listed in Table 3.24.

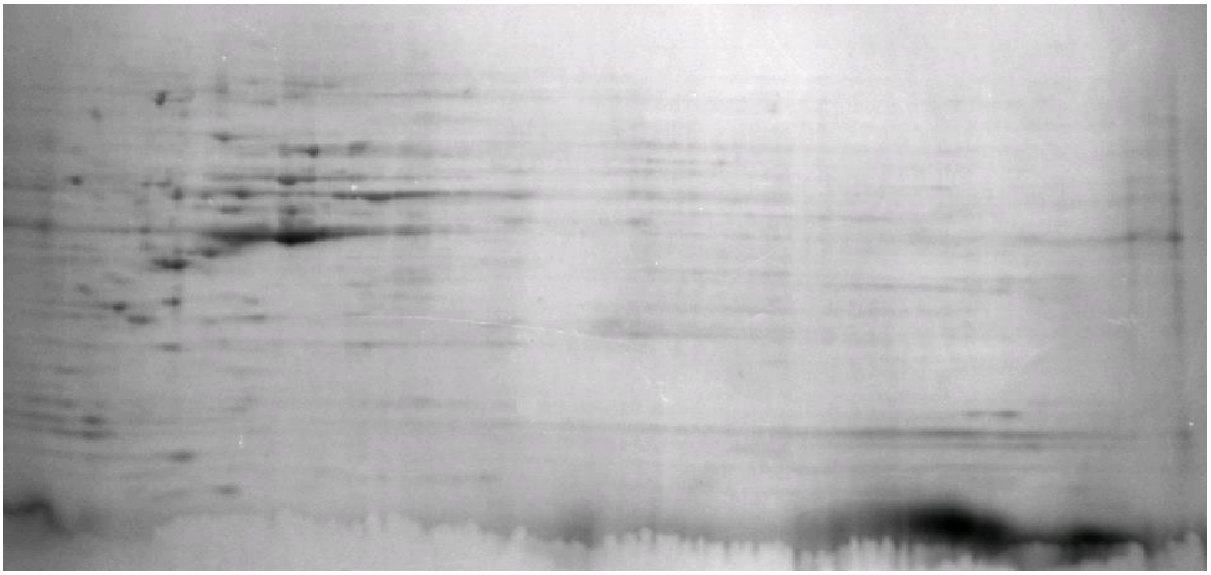

(a) HT-29 reference gel (not treated with drug, blank)

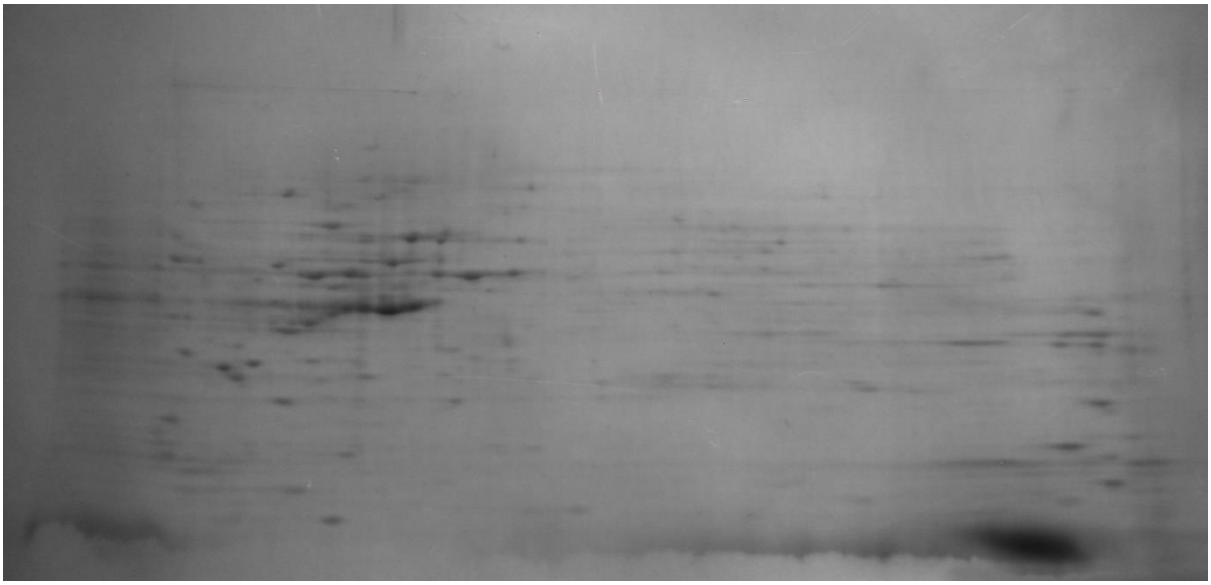

(b) Ox alone treated HT-29 gel

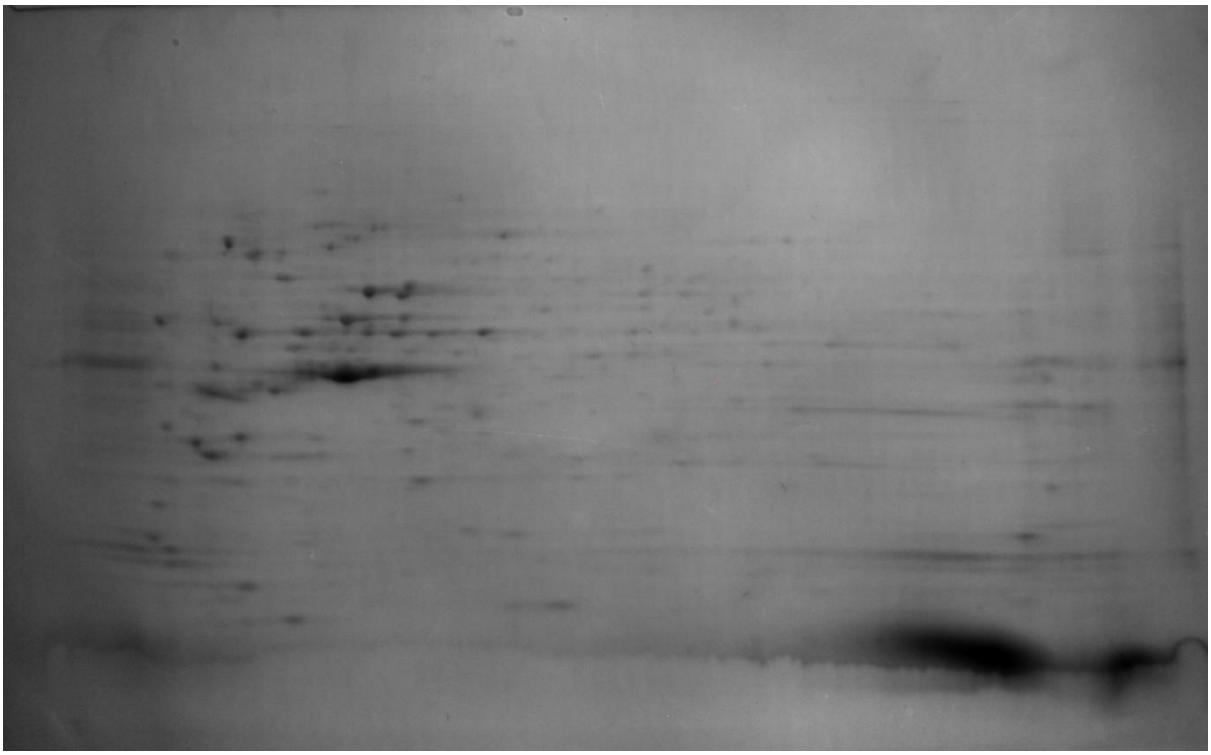

(c) Col alone treated HT-29 gel

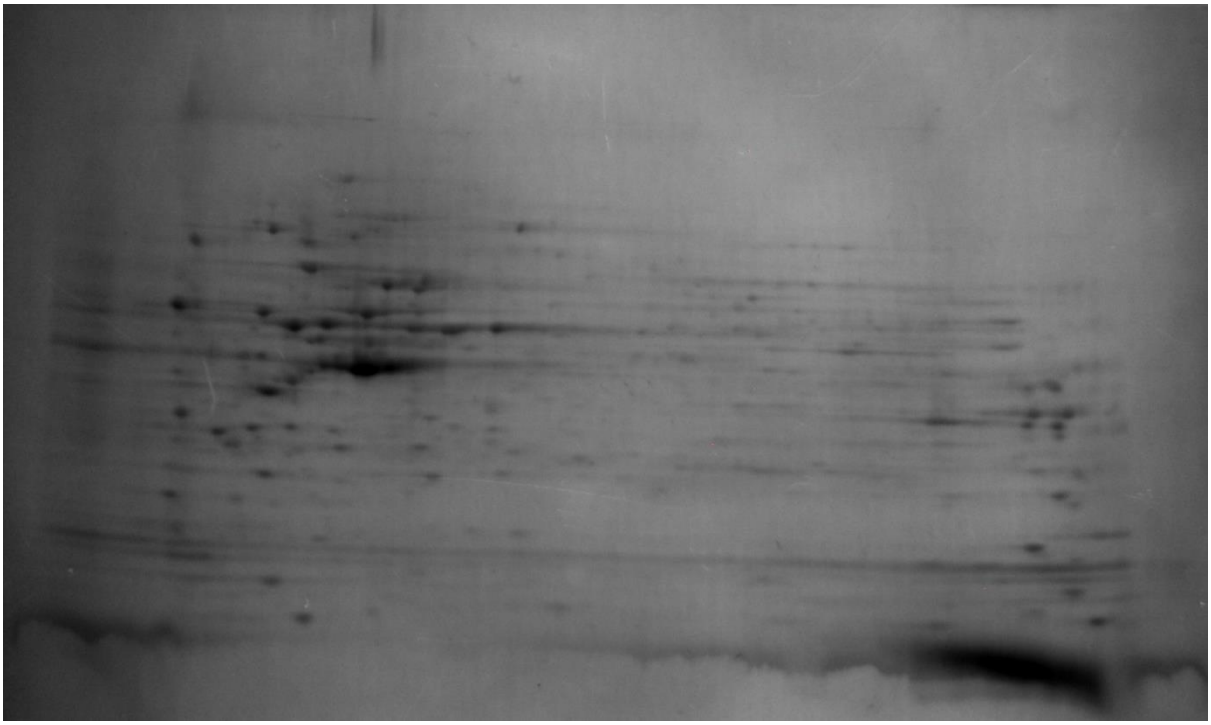

(c) EGCG alone treated HT-29 gel

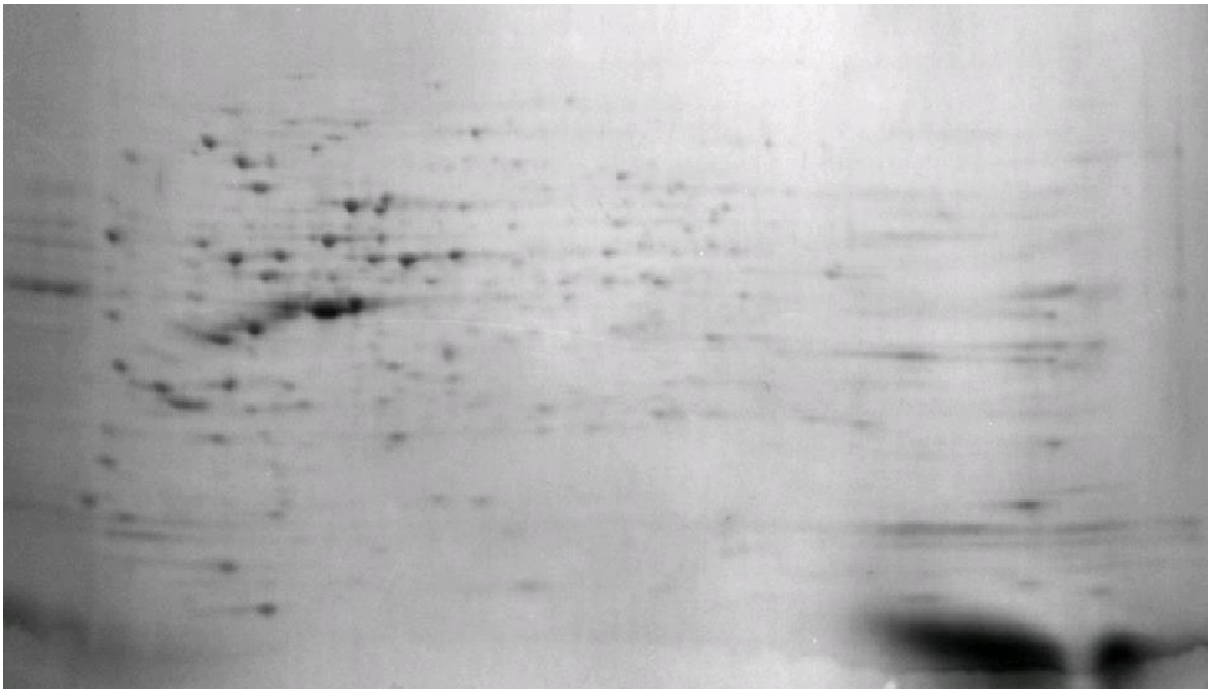

(d) Ox with Col (0/4) treated HT-29 gel

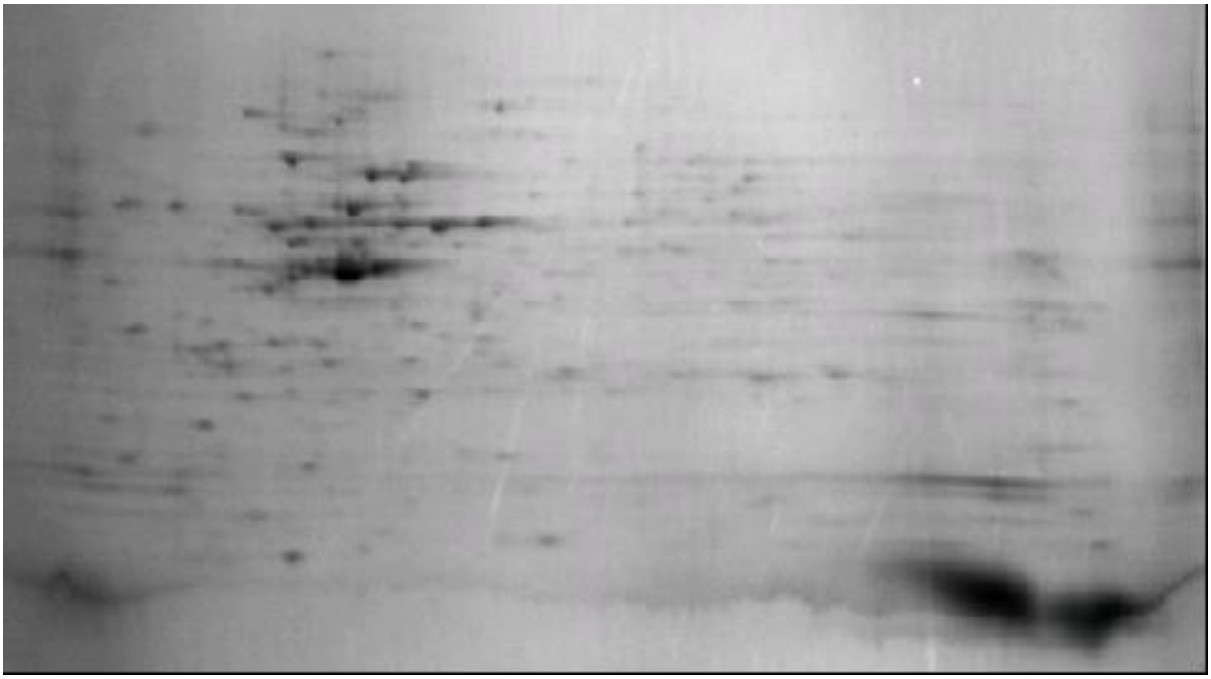

(e) Ox with EGCG (bolus) treated HT-29 gel

Figure 3.56: Two dimensional gel images (a-e) of HT-29 gels

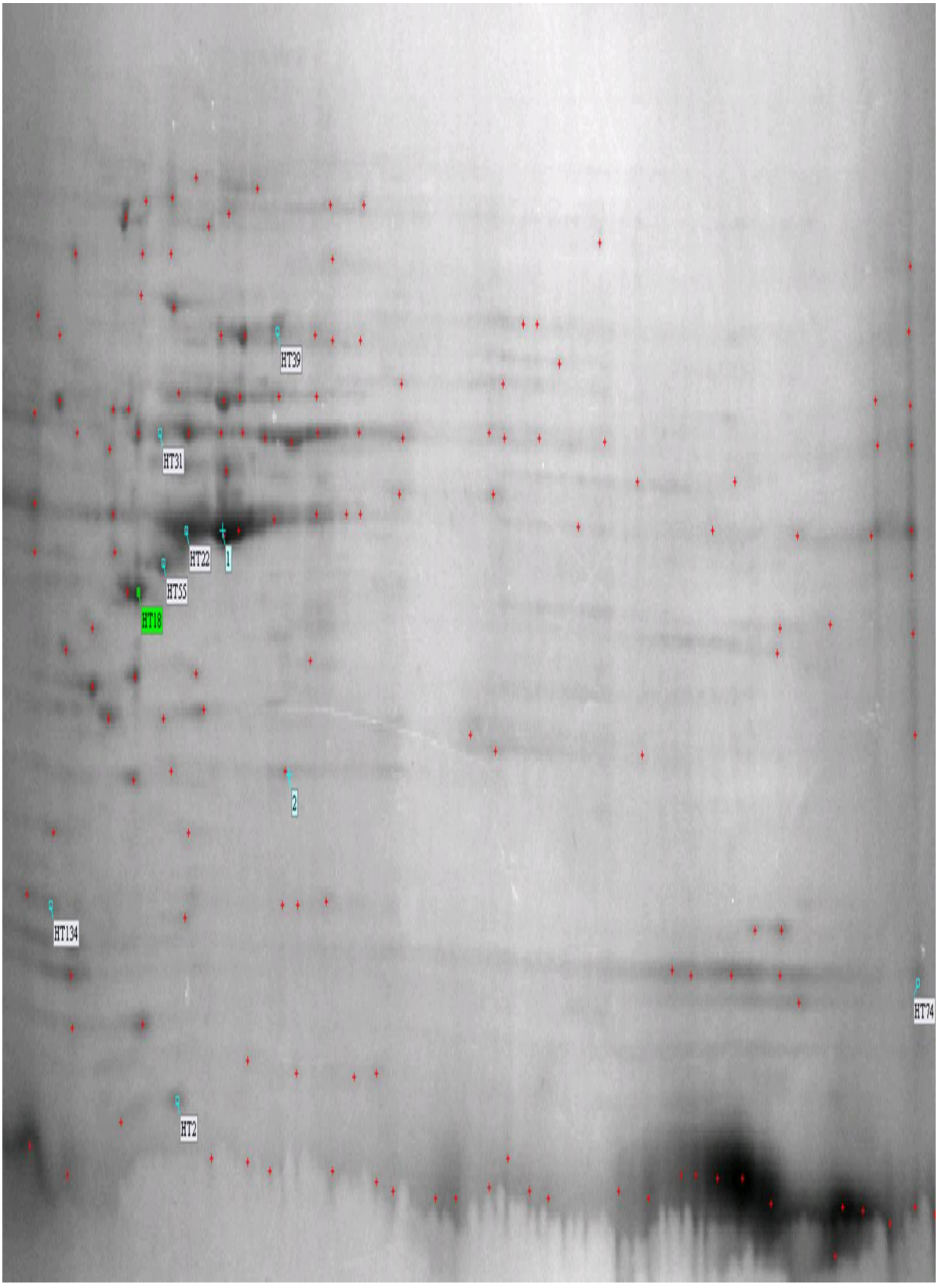

Figure 3.57 : Annotated HT-29 reference gel (showing the noted spot number)

Table 3.24: Selected spots of the proteins displayed alteration in expression in HT-29 gel

Match ID	Ox alone	Col alone	EGCG alone	Ox + Col (0/4)	Ox + EGCG (0/0)
HT18	Up-regulated	Not detected	Down-regulated	Not changed	Not detected
HT22	Down-regulated	Down-regulated	Down-regulated	Down-regulated	SDR
HT31	Up-regulated	Down-regulated	Up-regulated	Not detected	Down-regulated
HT39	Not changed	Up-regulated	Up-regulated	Not changed	Up-regulated
HT55	Up-regulated	Up-regulated	SDR	Up-regulated	Down-regulated
HT134	Not changed	Up-regulated	Up-regulated	Not changed	Down-regulated

SDR denotes slight downregulation

The summary of the characterized proteins is given in Table 3.25 and the further details are provided in Appendix II.

Table 3.25: Proteins characterized from HT-29 cell lines (MALDI-MASS analysis)

Match ID	Short name	Full Nmae	Mass (Da)/pI	Mascot score and Sequence coverage (%)
HT18	NPM	Nucleolar phosphoprotein B23	32555/4.64	65 and 14
HT22	ACTB	Actin cytoplasmic 1 protein	41710/5.29	220 and 15
HT31	TBB5	Tubulin beta chain	49639/4.78	130 and 18
HT39	HSP7C	Heat shock cognate 71 kDa protein	70854/5.37	80 and 18
HT55	K2CB	Keratin, type II cytoskeletal 8	53671/4.95	348 and 12
HT134	GSTP1	Glutathione S transferase P 1	23341/5.43	343 and 27

3.6.2 Expression of protein in CACO-2 gels

Among 195 protein spots identified in reference (untreated) CACO-2 gels, 80 spots underwent significant alteration in expression in Cur alone treated gel. However the number of spots experienced significant changes in expression with Ox alone treatments were 148. After treatment with Ox with Cur (bolus) 86 protein spots underwent significant altered expression. The criteria for selection of the spots to be cut for further characterization were the same as described in section 3.5.1. Finally 24 spots were chosen for excision from CACO-2 gels but only seven proteins were successfully characterized. Figure 3.58 give the images of untreated and treated CACO-2 gels showing the spots. Figure 3.59 represents the annotated untreated CACO-2 gel. The protein spots underwent significant changes in expression commonly in the treated gels and selected for further characterization are listed in Table 3.26. The summary of the characterized proteins is listed in Table 3.27 and further details are given in Appendix III.

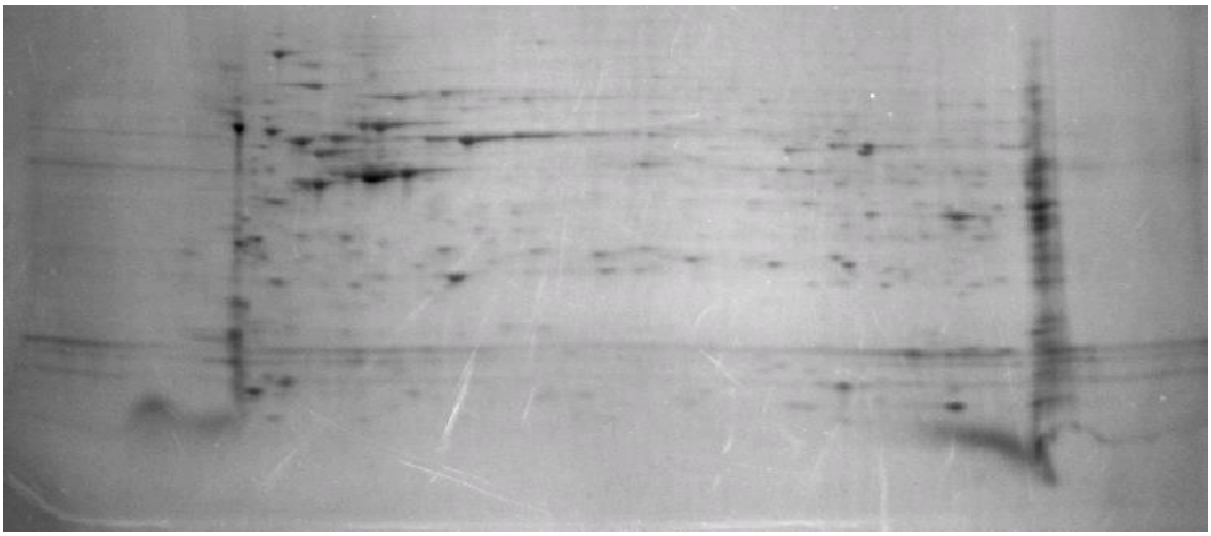

(a) CACO-2 reference gel (not treated with drug, blank)

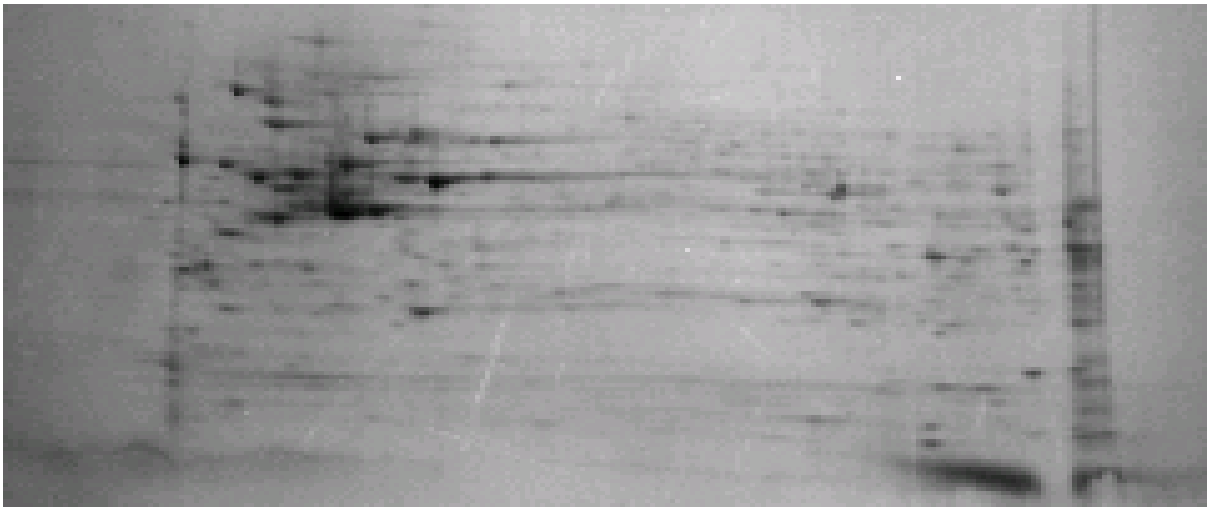

(b) Ox alone treated CACO-2 gel

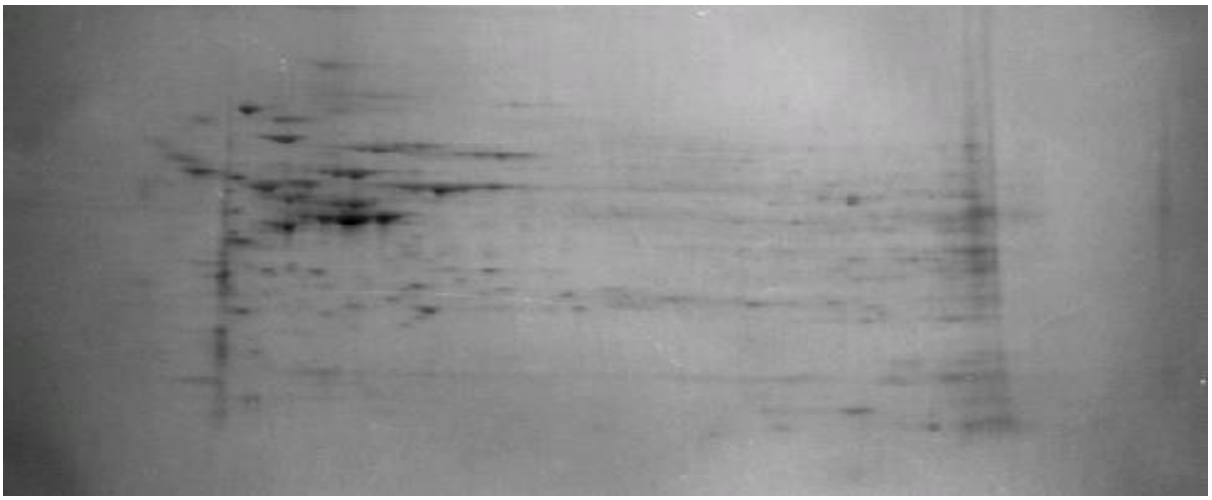

(c) Cur alone treated CACO-2 gel

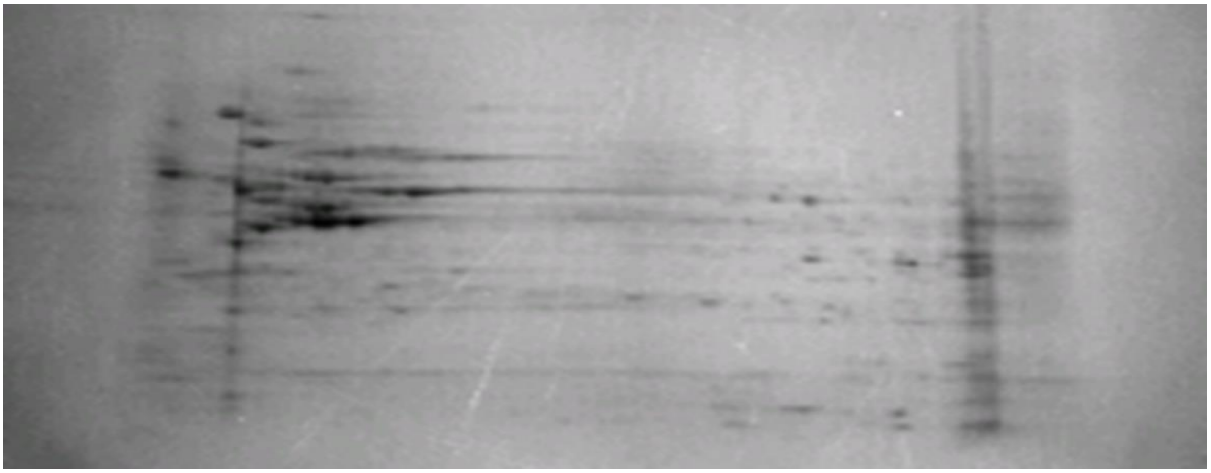

(d) Ox with Cur (bolus) treated CACO-2 gel

Figure 3.58: Two dimensional gel images (a-d) of CACO-2 gels

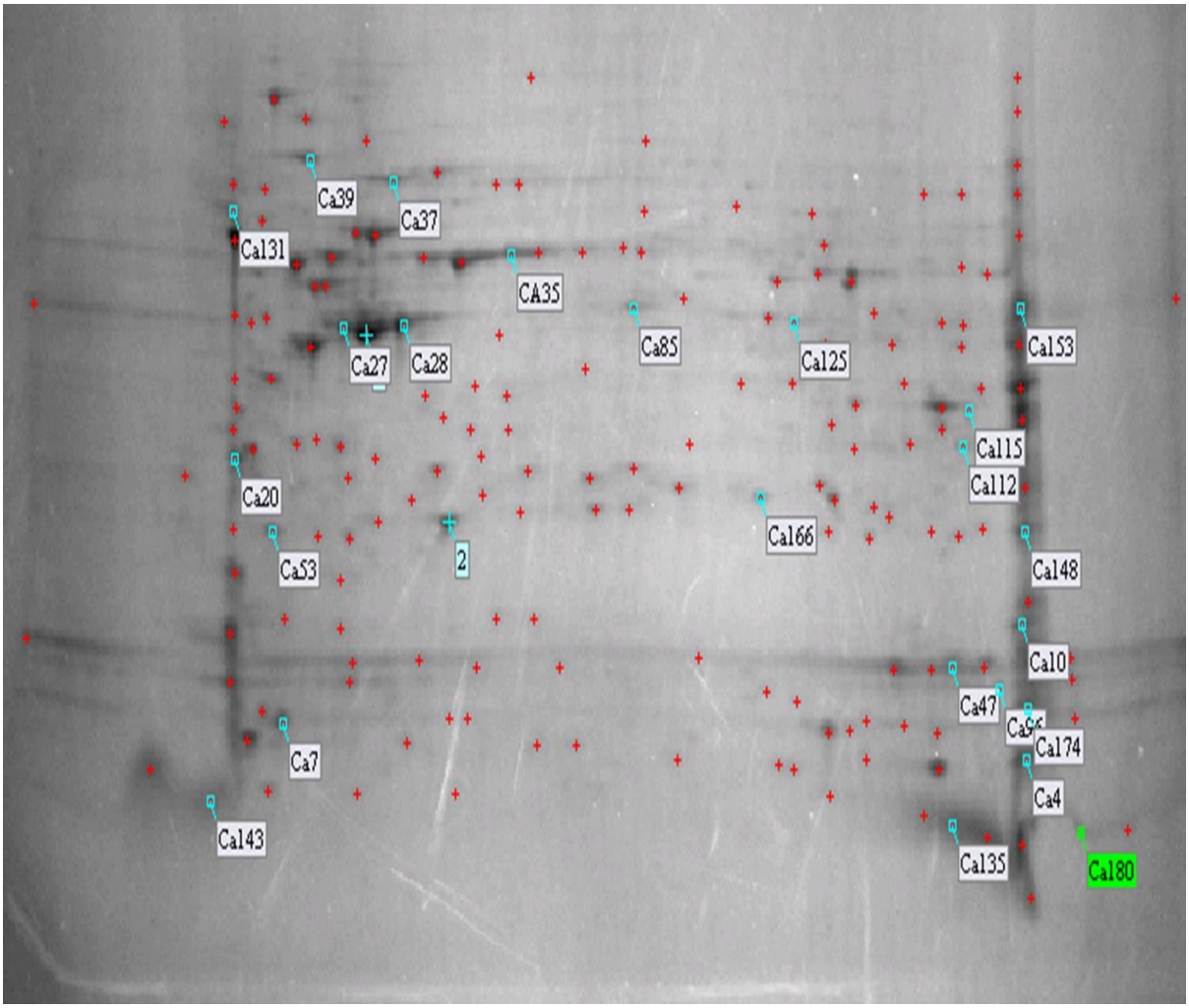

Figure 3.59 : Annotated CACO-2 reference gel (showing the noted spot number)

Table 3.26: Selected spots of the proteins displayed alteration in expression in CACO-2 gel

Match ID	Ox alone	Cur alone	Ox with Cur (0/0)
Ca35	SDR	Up-regulated	Up-regulated
Ca37	SUR	Up-regulated	Up-regulated
Ca39	Up-regulated	Up-regulated	Up-regulated
Ca53	Down-regulated	Up-regulated	Not changed
Ca85	SUR	Down-regulated	Up-regulated
Ca125	Up-regulated	SUR	Up-regulated
Ca166	SUR	Up-regulated	Up-regulated

SDR denotes slightly downregulated and SUR denotes slightly upregulated

Table 3.27: Proteins characterized from CACO-2 cell lines (MALDI-MASS analysis)

Match ID	Short name	Full Nmae	Mass (Da)/pI	Mascot score and Sequence coverage (%)
Ca35	K2CB	Keratin, type II cytoskeletal 8	53671/4.95	256 and 19
Ca37	HSP7C	Heat shock cognate 71 kDa protein	70854/5.37	536 and 24
Ca39	GRP78	78 kDa glucose-regulated protein	72288/5.07	588 and 27
Ca53	PSB6	Proteasome subunit beta type-6	25341/4.80	62 and 10
Ca85	COF1	Cofilin-1	18491/8.22	138 and 31
Ca125	IDHC	Isocitrate dehydrogenase [NADP] cytoplasmic	46630/6.53	130 and 16
Ca166	K1C18	Keratin, type I cytoskeletal 18	48029/6.36	345 and 4

3.6.3 MALDI-Mass spectral analysis of the identified proteins

Among seven excised protein spots from HT-29 gels, two were identical of GSTP1. Although no such coincidence observed among the seven protein spots cut from CACO-2 gels. However, two proteins namely K2CB and HSP7C were found to be characterized from both HT-29 and CACO-2 gels. That is why total number of proteins characterized and found to contribute substantially in anticancer action of the drugs studied ultimately reduced to eleven.

3.6.3.1 Nucleolar phosphoprotein B23 (NPM)

The protein was appeared as spot number HT18 in HT-29 gel which was downregulated followed by most of drug treatments except for Ox alone treatment where upregulation was evidenced. Molecular mass of the protein was 32.55 kDa with isoelectric point (pI) of 4.64. The peptides found from this study matched with 14% of entire sequence of the protein NPM, showing mascot score of 65. Base peak in the mass spectrum was found at m/z of 842.56. The sequence of matched peptides for the protein NPM (spot HT18) obtained from UniprotKB database; masses of peptides from MALDI-MS scan and mascot score histogram are shown in Figure 3.60.

```
  1 MEDSMDMDMS PLRPQNYLFG CELKADKDYH FKVDNDENEH QLSLRTVSLG
 51 AGAKDELHIV EAEAMNYEGS PIKVTLATLK MSVQPTVSLG GFEITPPVVL
101 RLKCGSGPVH ISGQHLVAVE EDAESEDEEE EDVKLLSISG KRSAPGGGSK
151 VPQKKVKLAA DEDDDDDDEE DDDEDDDDDD FDDEEAEEKA PVKKSIRDTP
201 AKNAQKSNQN GKDSKPSSTP RSKGQESFKK QEKTPKTPKG PSSVEDIKAK
251 MQASIEKGGS LPKVEAKFIN YVKNCFRMTD QEAIQDLWQW RKSL
```

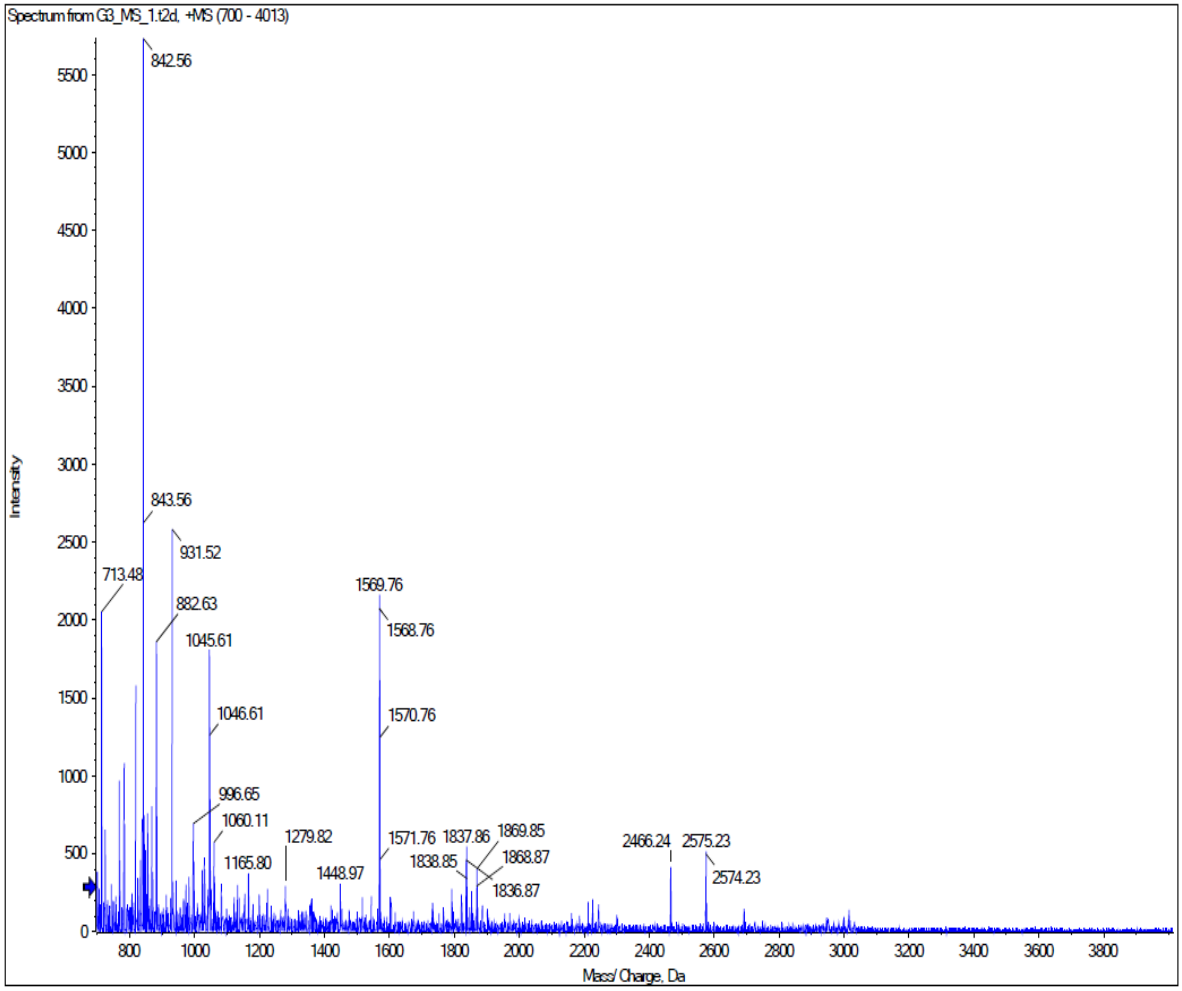

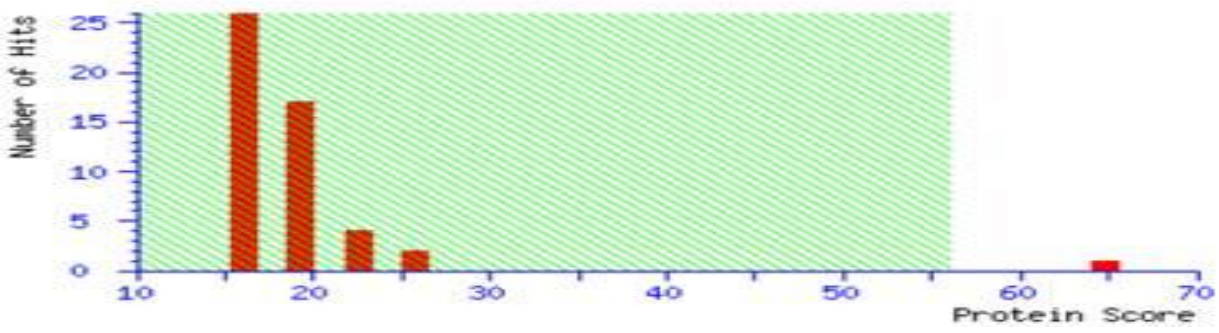

Figure 3.60: Matched peptides, mass spectrum and mascot score histogram for NPM

3.6.3.2 Actin Cytoplasmic 1 protein (ACTB)

The protein was appeared as spot number HT22 in HT-29 gel which was downregulated followed by all of the drug treatments. Molecular mass of the protein was 41.71 kDa with isoelectric point (pI) of 5.29. The peptides found from this study matched with 15% of entire sequence of the protein ACTB, showing mascot score of 220. Base peak in the mass spectrum was found at m/z of 1516.77. The sequence of matched peptides for the protein ACTB (spot HT22) obtained from UniprotKB database; masses of peptides from MALDI-MS scan and mascot score histogram are shown in Figure 3.61.

```
  1 MDDDIAALVV DNGSGMCKAG FAGDDAPRAV FPSIVGRPRH QGVMVGMGQK
 51 DSYVGDEAQS KRGILTLKYP IEHGIVTNWD DMEKIWHHTF YNELRVAPEE
101 HPVLLTEAPL NPKANREKMT QIMFETFNTP AMYVAIQAVL SLYASGRTTG
151 IVMDSGDGVT HTVPIYEGYA LPHAILRLDL AGRDLTDYLM KILTERGYSF
201 TTTAEREIVR DIKEKLCYVA LDFEQEMATA ASSSSLEKSY ELPDGQVITI
251 GNERFRCPEA LFQPSFLGME SCGIHETTFN SIMKCDVDIR KDLYANTVLS
301 GGTTMYPGIA DRMQKEITAL APSTMKIKII APPERKYSVW IGGSILASLS
351 TFQQMWISKQ EYDESGPSIV HRKCF
```

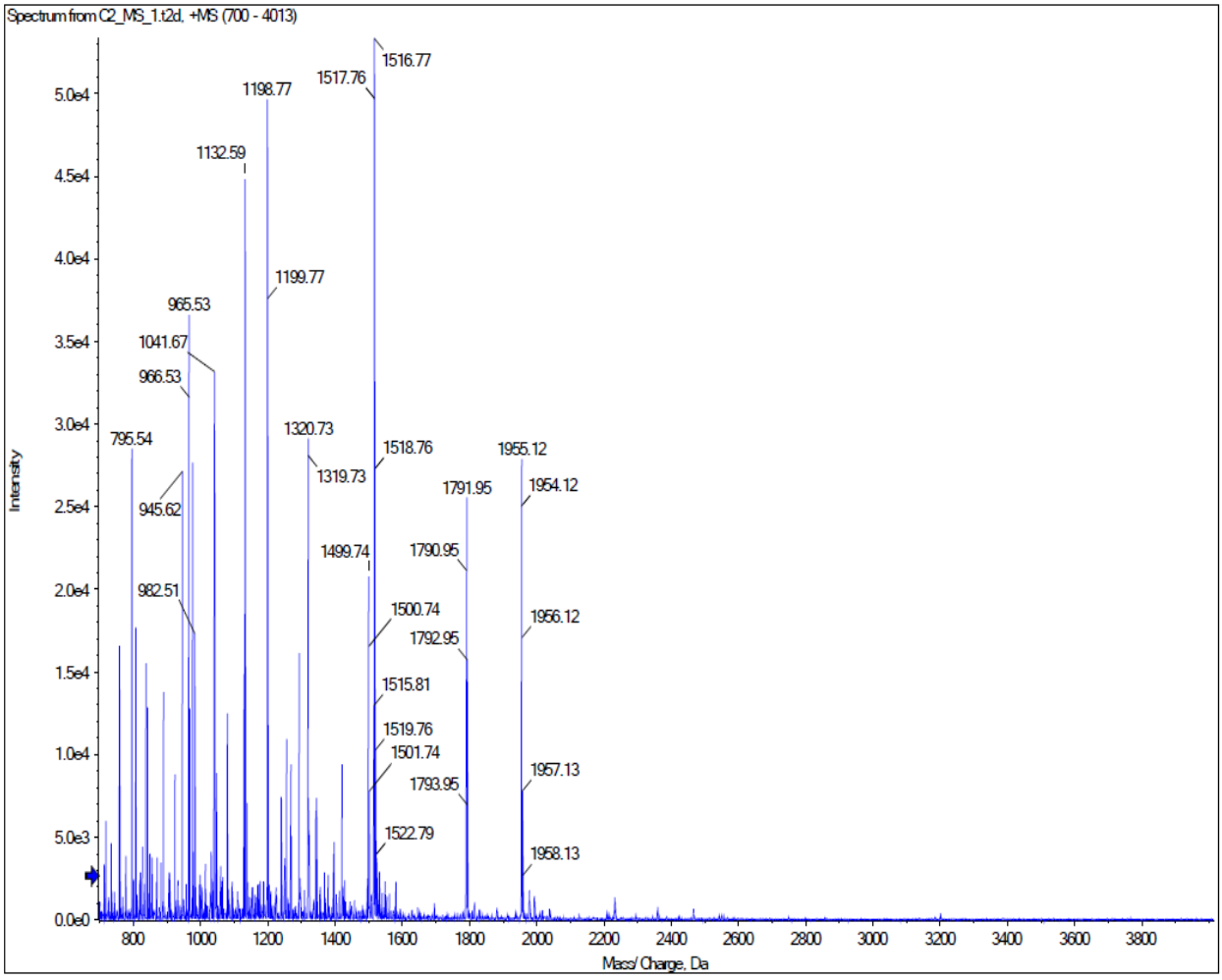

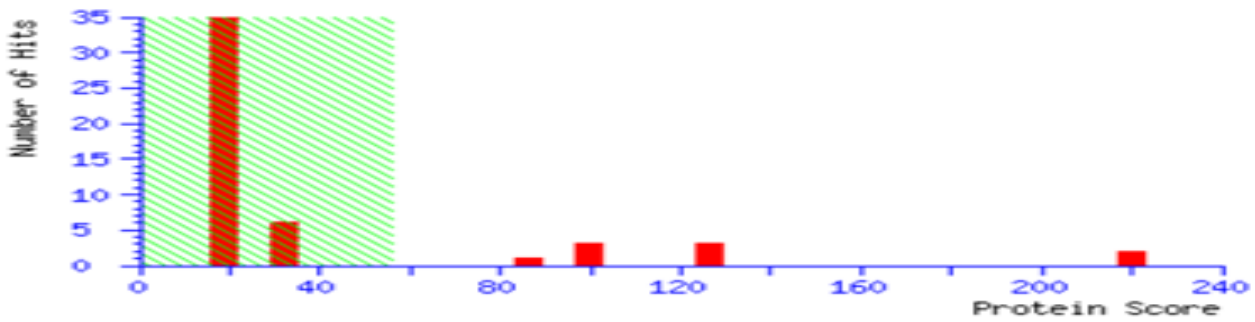

Figure 3.61: Matched peptides, mass spectrum and mascot score histogram for ACTB

3.6.3.3 Tubulin beta chain (TBB5)

The protein was appeared as spot number HT31 in HT-29 gel which was upregulated after treatments with Ox alone and EGCG alone. However the same protein was downregulated followed by the rest of the drug treatments. Molecular mass of the protein was 49.63 kDa with isoelectric point (pI) of 4.78. The peptides found from this study matched with 18% of entire sequence of the protein TBB5, showing mascot score of 130. Base peak in the mass spectrum was found at m/z of 842.53.The sequence of matched peptides for the protein TBB5 (spot HT31) obtained from UniprotKB database; masses of peptides from MALDI-MS scan and mascot score histogram are shown in Figure 3.62.

```
  1 MREIVHIQAG QCGNQIGAKF WEVISDEHGI DPTGTYHGDS DLQLDRISVY
 51 YNEATGGKYV PRAILVDLEP GTMDSVRSGP FGQIFRPDNF VFGQSGAGNN
101 WAKGHYTEGA ELVDSVLDVV RKEAESCDCL QGFQLTHSLG GGTGSGMGTL
151 LISKIREEYP DRIMNTFSVV PSPKVSDTVV EPYNATLSVH QLVENTDETY
201 CIDNEALYDI CFRTLKLTTP TYGDLNHLVS ATMSGVTTCL RFPGQLNADL
251 RKLAVNMVPF PRLHFFMPGF APLTSRGSQQ YRALTVPELT QQVFDAKNMM
301 AACDPRHGRY LTVAAVFRGR MSMKEVDEQM LNVQNKNSSY FVEWIPNNVK
351 TAVCDIPPRG LKMAVTFIGN STAIQELFKR ISEQFTAMFR RKAFLHWYTG
401 EGMDEMEFTE AESNMNDLVS EYQQYQDATA EEEEDFGEEA EEEA
```

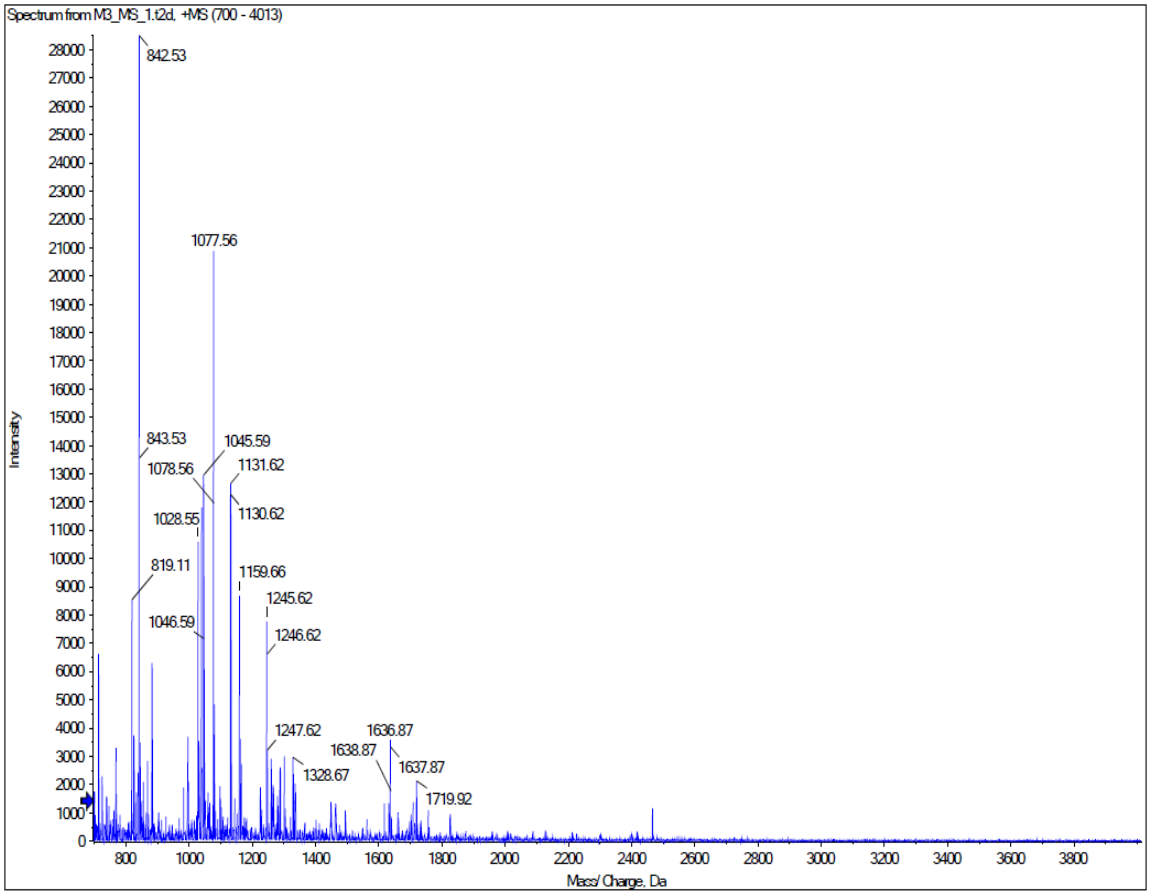

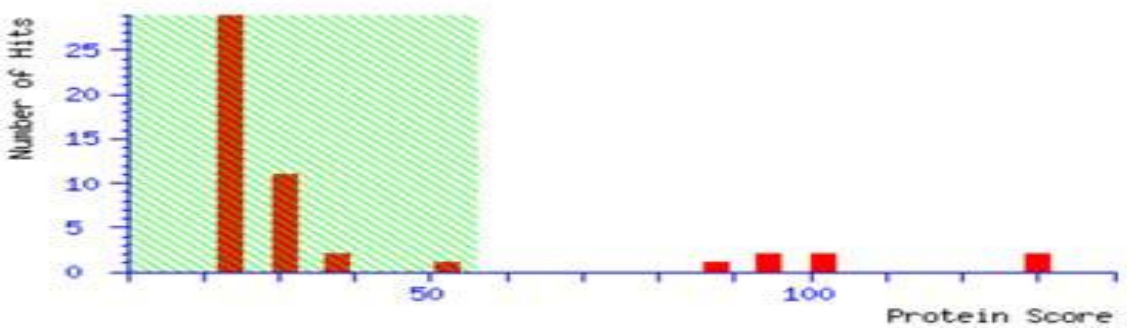

Figure 3.62 : Matched peptides, mass spectrum and mascot score histogram for TBB5

3.6.3.4 Heat shock cognate 71 kDa (HSP7C)

The protein was appeared as spot number HT39 in HT-29 gel and spot number Ca37 in CACO-2 gel. HSP7C was upregulated after most of treatments in both cell lines. Mascot was higher in the protein obtained from CACO-2 (536) cell line compared to HT-29 (80) cell line. Similarly matched peptide sequence was also greater in case of CACO-2 gel excised protein (24%) than the one excised from HT-29 gel (18%). The sequence of matched peptides for the protein HSP7C (spot HT39) obtained from UniprotKB database; masses of peptides from MALDI-MS scan and mascot score histogram are shown in Figure 3.63. Although the protein was identified from both HT-29 and CACO-2 gels, data images of only one spot of HT-29 is shown here as a representative. Molecular mass of the protein was 70.85 kDa with isoelectric point (pI) of 5.37. The base peak in the mass spectrum was observed at m/z of 819.12 and 1487.76.

```
  1 MSKGPAVGID LGTTYSCVGV FQHGKVEIIA NDQGNRTTPS YVAFTDTERL
 51 IGDAAKNQVA MNPTNTVFDA KRLIGRRFDD AVVQSDMKHW PFMVVNDAGR
101 PKVQVEYKGE TKSFYPEEVS SMVLTKMKEI AEAYLGKTVT NAVVTVPAYF
151 NDSQRQATKD AGTIAGLNVL RIINEPTAAA IAYGLDKKVG AERNVLIFDL
201 GGGTFDVSIL TIEDGIFEVK STAGDTHLGG EDFDNRMVNH FIAEFKRKHK
251 KDISENKRAV RRLRTACERA KRTLSSSTQA SIEIDSLYEG IDFYTSITRA
301 RFEELNADLF RGTLDPVEKA LRDAKLDKSQ IHDIVLVGGS TRIPKIQKLL
351 QDFFNGKELN KSINPDEAVA YGAAVQAAIL SGDKSENVQD LLLLDVTPLS
401 LGIETAGGVM TVLIKRNTTI PTKQTQTFTT YSDNQPGVLI QVYEGERAMT
451 KDNNLLGKFE LTGIPPAPRG VPQIEVTFDI DANGILNVSA VDKSTGKENK
501 ITITNDKGRL SKEDIERMVQ EAEKYKAEDE KQRDKVSSKN SLESYAFNMK
551 ATVEDEKLQG KINDEDKQKI LDKCNEIINW LDKNQTAEKE EFEHQQKELE
601 KVCNPIITKL YQSAGGMPGG MPGGFPGGGA PPSGGASSGP TIEEVD
```

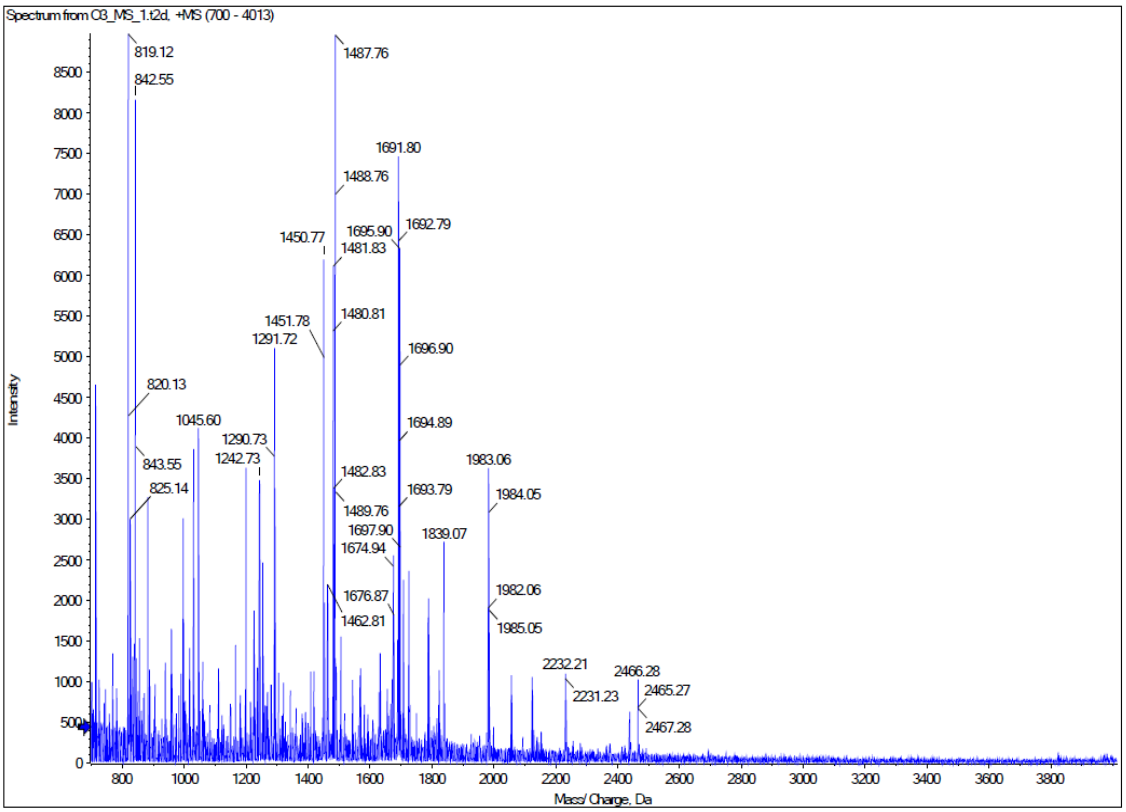

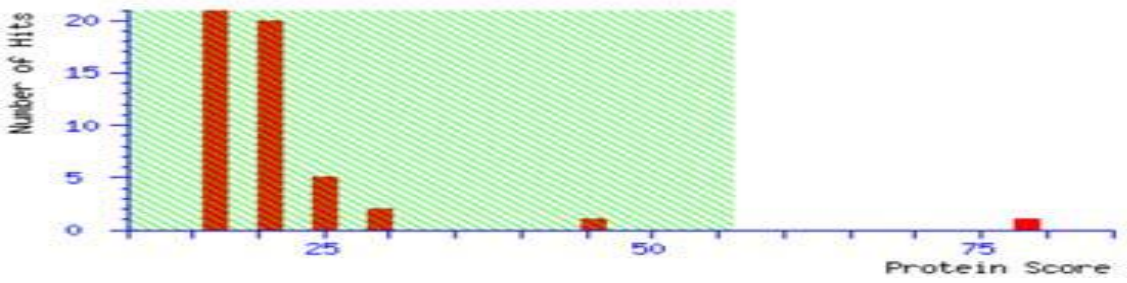

Figure 3.63: Matched peptides, mass spectrum and mascot score histogram for HSP7C

3.6.3.5 Keratin, type II cytoskeletal 8 (K2CB)

The protein was appeared as spot number HT55 in HT-29 gel and spot number Ca35 in CACO-2 gel. K2CB was upregulated after most of treatments in both cell lines. Mascot was higher in the protein obtained from HT-29 (348) cell line compared to CACO-2 (256) cell line. But matched peptide sequence was greater in case of CACO-2 gel excised protein (19%) than the one excised from HT-29 gel (12%). The sequence of matched peptides for the protein K2CB (spot HT55) obtained from UniprotKB database; masses of peptides from MALDI-MS scan and mascot score histogram are shown in Figure 3.64. Although the protein was identified from both HT-29 and CACO-2 gels, data images of only one spot of HT-29 is shown here as a representative. Molecular mass of the protein was 53.67 kDa with isoelectric point (pI) of 4.95. The base peak in the mass spectrum was observed at m/z of 1082.60.

```
  1 MASNVTNKTD PRSMNSRVFI GNLNTLVVKK SDVEAIFSKY GKIVGCSVHK
 51 GFAFVQYVNE RNARAAVAGE DGRMIAGQVL DINLAAEPKV NRGKAGVKRS
101 AAEMYGSVTE HPSPSPLLSS SFDLDYDFQR DYYDRMYSYP ARVPPPPPIA
151 RAVVPSKRQR VSGNTSRRGK SGFNSKSGQR GSSKSGKLKG DDLQAIKKEL
201 TQIKQKVDSL LENLEKIEKE QSKQAVEMKN DKSEEEQSSS SVKKDETNVK
251 MESEGGADDS AEEGDLLDDD DNEDRGDDQL ELIKDDEKEA EEGEDDRDSA
301 NGEDDS
```

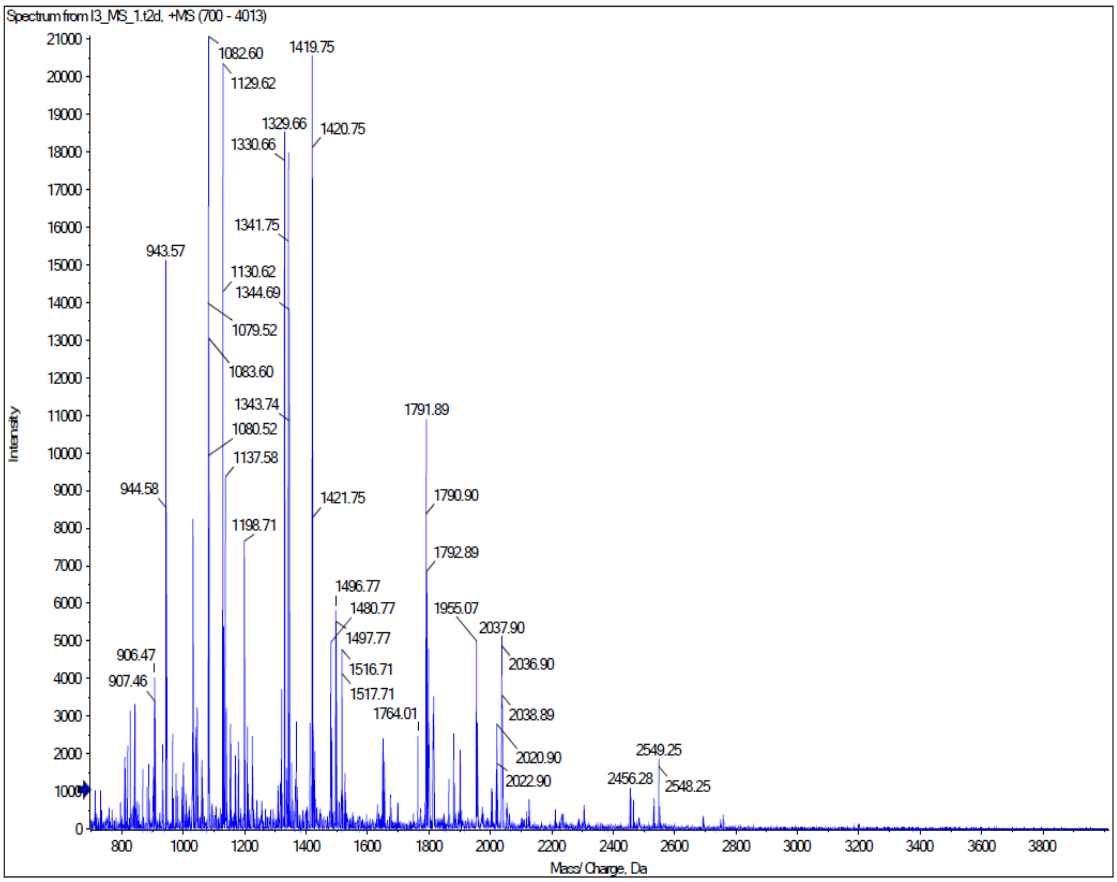

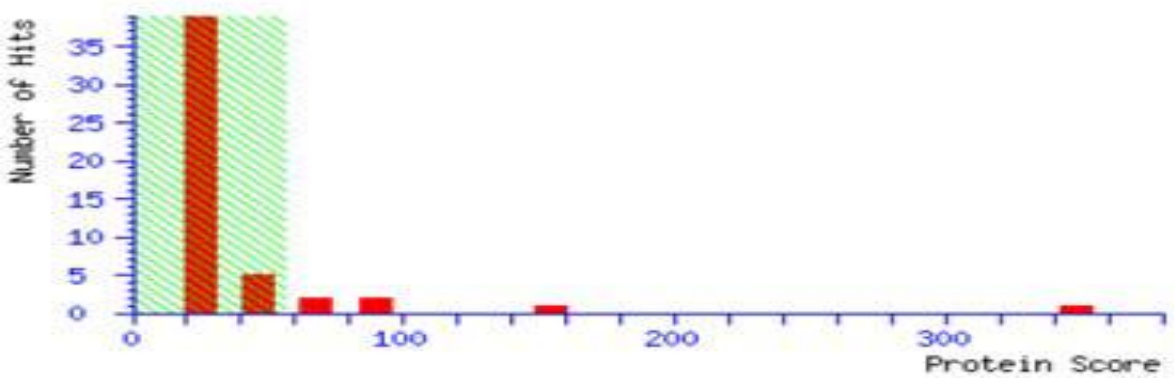

Figure 3.64: Matched peptides, mass spectrum and mascot score histogram for K2CB

3.6.3.6 Glutathione S transferase P1 (GSTP1)

The protein was appeared as spot number HT134 in HT-29 gel which was upregulated after treatments with Col alone and EGCG alone. However the same protein was downregulated followed by combined treatment of Ox with EGCG (bolus). Molecular mass of the protein was 23.34 kDa with isoelectric point (pI) of 5.43. The peptides found from this study matched with 27% of entire sequence of the protein GSTP1, showing mascot score of 343. Base peak in the mass spectrum was found at m/z of 1060.07.The sequence of matched peptides for the protein GSTP1 (spot HT134) obtained from UniprotKB database; masses of peptides from MALDI-MS scan and mascot score histogram are shown in Figure 3.65.

```
  1 MPPYTVVYFP VRGRCAALRM LLADQGQSWK EEVVTVETWQ EGSLKASCLY
 51 GQLPKFQDGD LTLYQSNTIL RHLGRTLGLY GKDQQEAALV DMVNDGVEDL
101 RCKYISLIYT NYEAGKDDYV KALPGQLKPF ETLLSQNQGG KTFIVGDQIS
151 FADYNLLDLL LIHEVLAPGC LDAFPLLSAY VGRLSARPKL KAFLASPEYV
201 NLPINGNGKQ
```

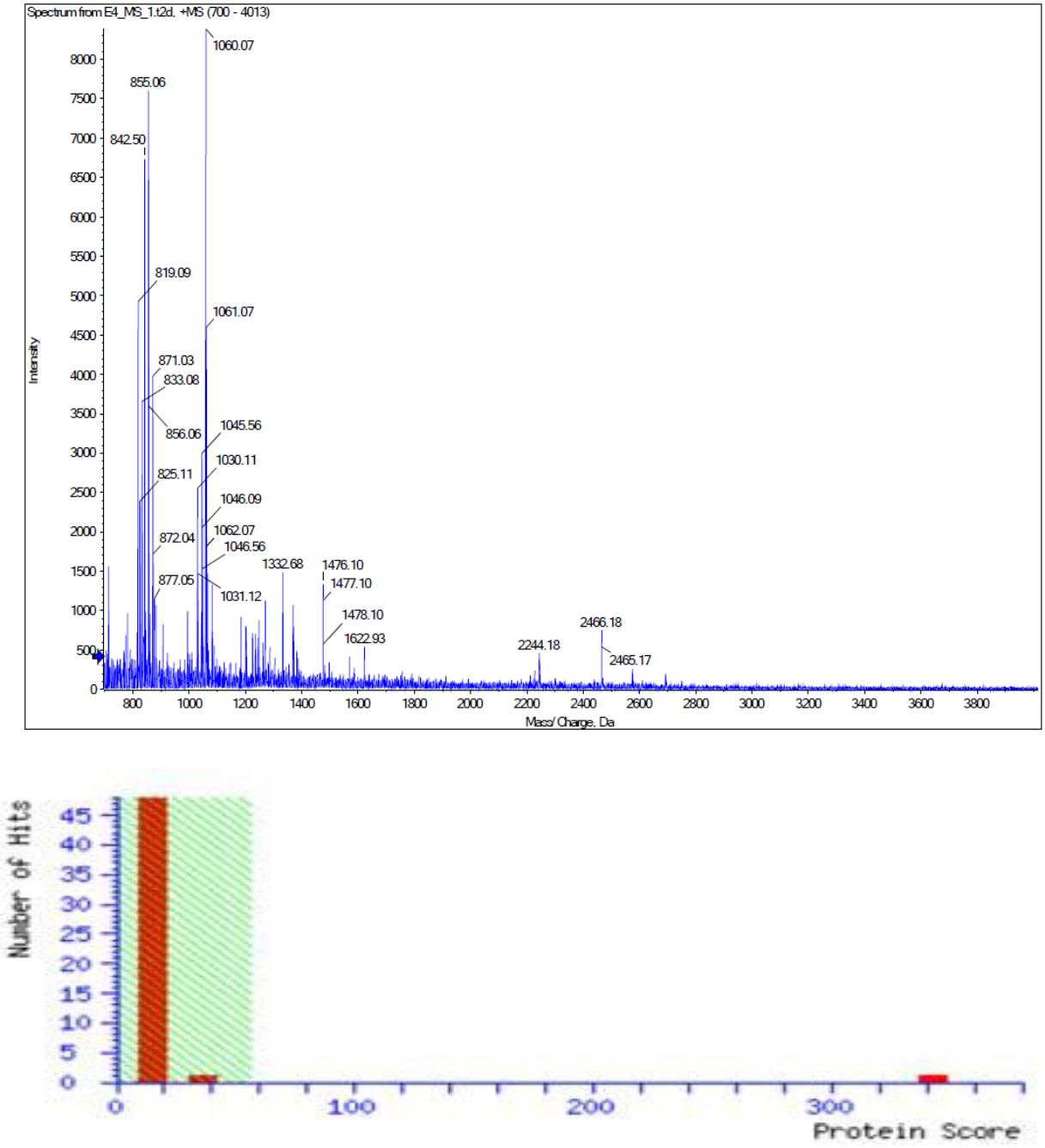

Figure 3.65 : Matched peptides, mass spectrum and mascot score histogram for GSTP1

3.6.3.7 78 kDa glucose regulated protein (GRP78)

The protein was appeared as spot number Ca39 in CACO-2 gel which was upregulated following all the treatments. Molecular mass of the protein was 72.28 kDa with isoelectric point (pI) of 5.07. The peptides found from this study matched with 27% of entire sequence of the protein GRP78, showing mascot score of 588. Base peak in the mass spectrum was found at m/z of 1566.81.The sequence of matched peptides for the protein GRP78 (spot Ca39) obtained from UniprotKB database; masses of peptides from MALDI-MS scan and mascot score histogram are shown in Figure 3.66.

```
  1 MKLSLVAAML LLLSAARAEE EDKKEDVGTV VGIDLGTTYS CVGVFKNGRV
 51 EIIANDQGNR ITPSYVAFTP EGERLIGDAA KNQLTSNPEN TVFDAKRLIG
101 RTWNDPSVQQ DIKFLPFKVV EKKTKPYIQV DIGGGQTKTF APEEISAMVL
151 TKMKETAEAY LGKKVTHAVV TVPAYFNDAQ RQATKDAGTI AGLNVMRIIN
201 EPTAAAIAYG LDKREGEKNI LVFDLGGGTF DVSLLTIDNG VFEVVATNGD
251 THLGGEDFDQ RVMEHFIKLY KKKTGKDVRK DNRAVQKLRR EVEKAKRALS
301 SQHQARIEIE SFYEGEDFSE TLTRAKFEEL NMDLFRSTMK PVQKVLEDSD
351 LKKSDIDEIV LVGGSTRIPK IQQLVKEFFN GKEPSRGINP DEAVAYGAAV
401 QAGVLSGDQD TGDLVLLDVC PLTLGIETVG GVMTKLIPRN TVVPTKKSQI
451 FSTASDNQPT VTIKVYEGER PLTKDNHLLG TFDLTGIPPA PRGVPQIEVT
501 FEIDVNGILR VTAEDKGTGN KNKITITNDQ NRLTPEEIER MVNDAEKFAE
551 EDKKLKERID TRNELESYAY SLKNQIGDKE KLGGKLSSED KETMEKAVEE
601 KIEWLESHQD ADIEDFKAKK KELEEIVQPI ISKLYGSAGP PPTGEEDTAE
651 KDEL
```

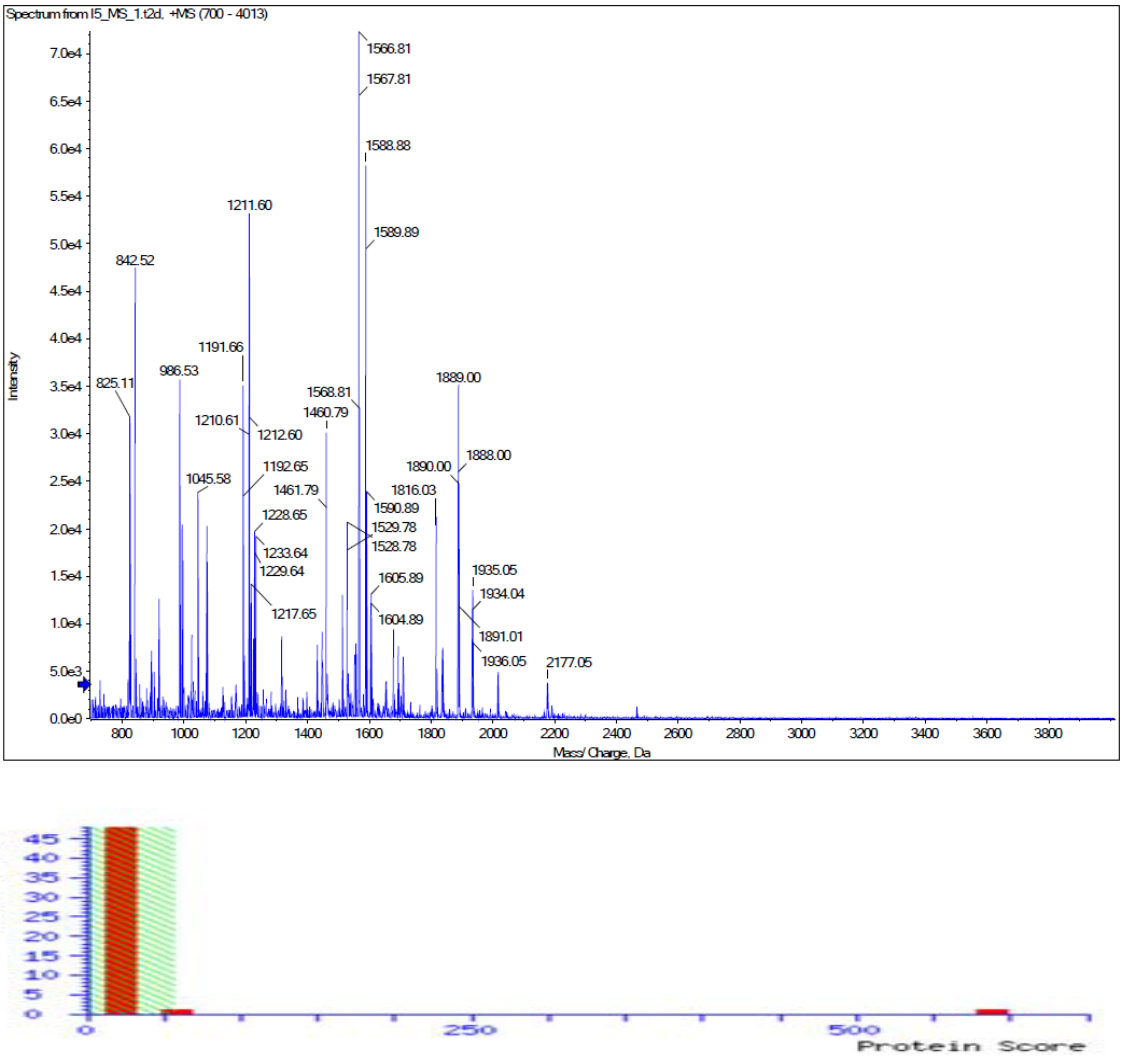

Figure 3.66 : Matched peptides, mass spectrum and mascot score histogram for GRP78

3.6.3.8 Proteasome subunit beta type-6 (PSB6)

The protein was appeared as spot number Ca53 in CACO-2 gel which was upregulated following Cur alone treatment but downregulation of the same protein was observed following Ox alone treatment. Molecular mass of the protein was 25.34 kDa with isoelectric point (pI) of 4.80. The peptides found from this study matched with 10% of entire sequence of the protein PSB6, showing mascot score of 62. Base peak in the mass spectrum was found at m/z of 842.51.The sequence of matched peptides for the protein PSB6 (spot Ca53) obtained from UniprotKB database; masses of peptides from MALDI-MS scan and mascot score histogram are shown in Figure 3.67.

```
  1 MAATLLAARG AGPAPAWGPE AFTPDWESRE VSTGTTIMAV QFDGGVVLGA
 51 DSRTTTGSYI ANRVTDKLTP IHDRIFCCRS GSAADTQAVA DAVTYQLGFH
101 SIELNEPPLV HTAASLFKEM CYRYREDLMA GIIIAGWDPQ EGGQVYSVPM
151 GGMMVRQSFA IGGSGSSYIY GYVDATYREG MTKEECLQFT ANALALAMER
201 DGSSGGVIRL AAIAESGVER QVLLGDQIPK FAVATLPPA
```

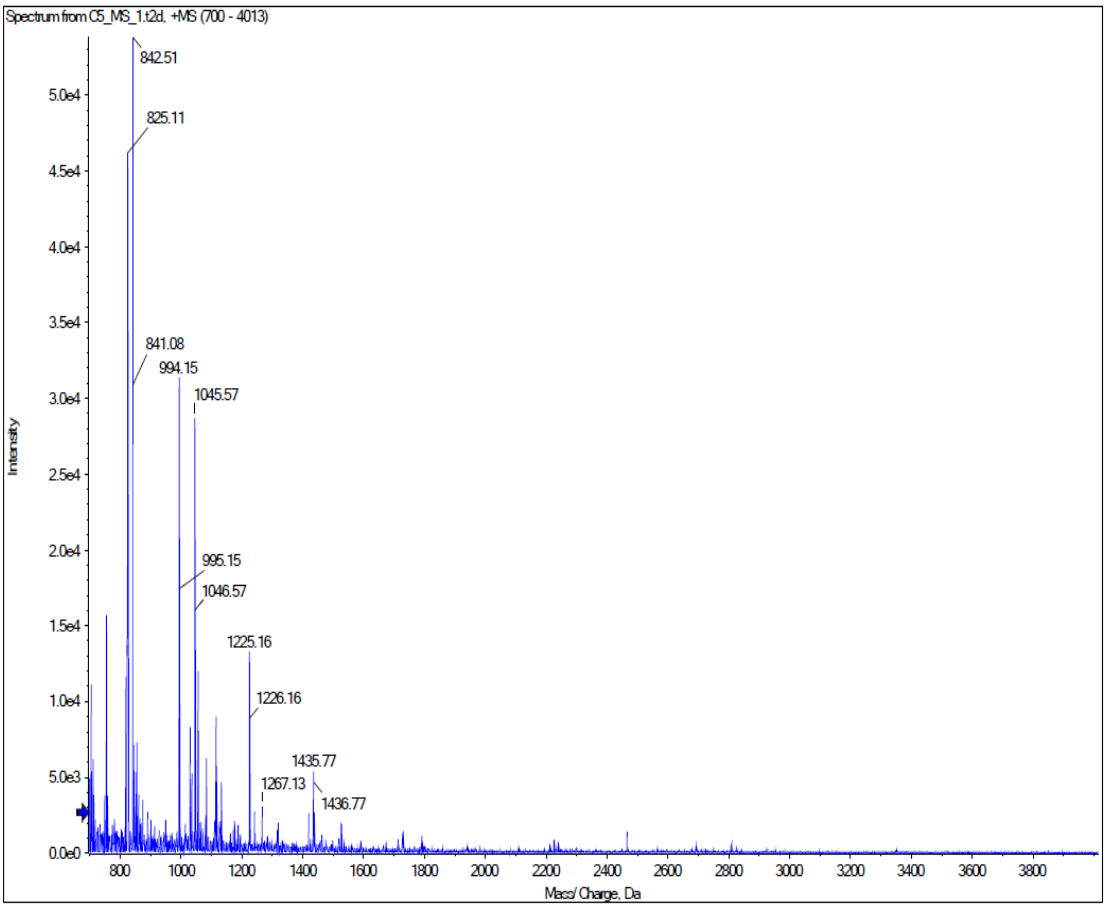

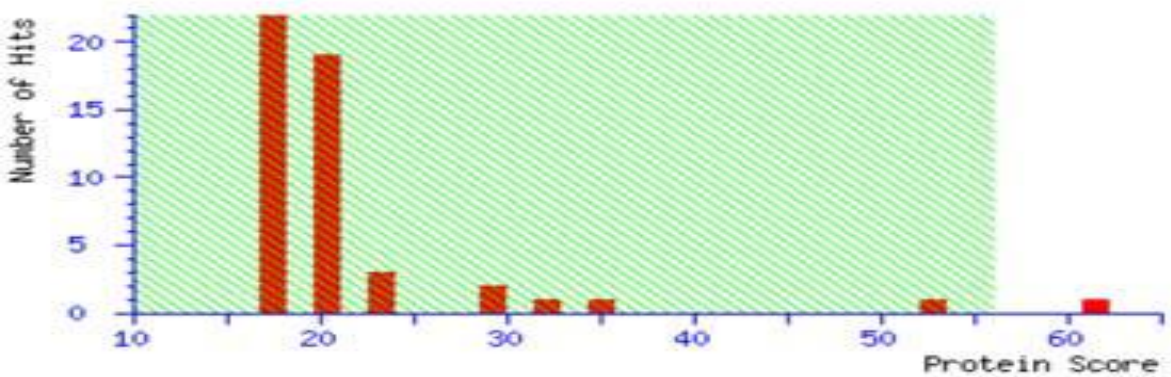

Figure 3.67 : Matched peptides, mass spectrum and mascot score histogram for PSB6

3.6.3.9 Cofilin1 (COF1)

The protein was appeared as spot number Ca85 in CACO-2 gel which was downregulated following Cur alone but upregulation of the same protein was found following combined treatment of Ox with Cur (bolus) treatment. Molecular mass of the protein was 18.49 kDa with isoelectric point (pI) of 8.22. The peptides found from this study matched with 31% of entire sequence of the protein COF1, showing mascot score of 138. Base peak in the mass spectrum was found at m/z of 842.51.The sequence of matched peptides for the protein COF1 (spot Ca85) obtained from UniprotKB database; masses of peptides from MALDI-MS scan and mascot score histogram are shown in Figure 3.68.

```
  1 MASGVAVSDG VIKVFNDMKV RKSSTPEEVK KRKKAVLFCL SEDKKNIILE
 51 EGKEILVGDV GQTVDDPYAT FVKMLPDKDC RYALYDATYE TKESKKEDLV
101 FIFWAPESAP LKSKMIYASS KDAIKKKLTG IKHELQANCY EEVKDRCTLA
151 EKLGGSAVIS LEGKPL
```

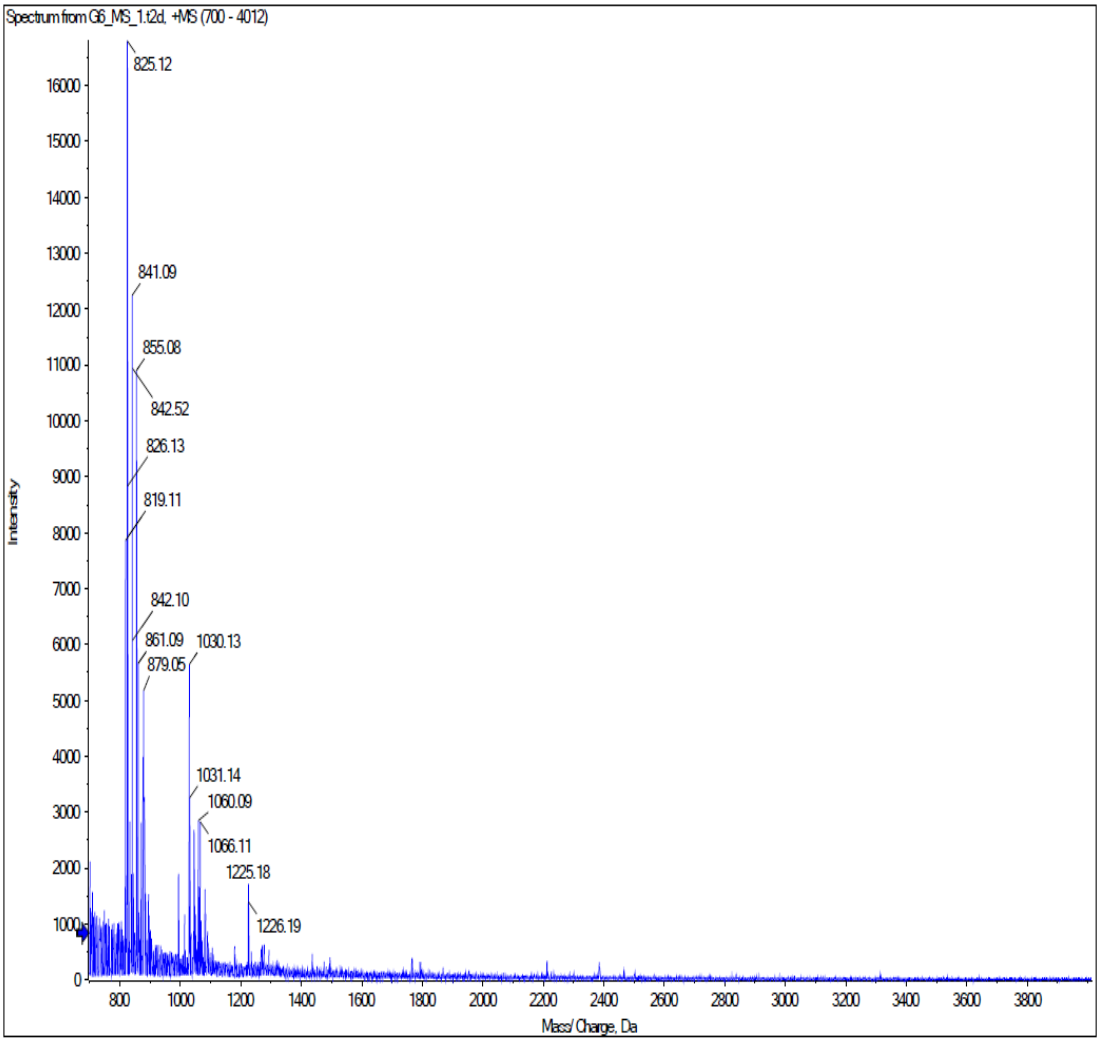

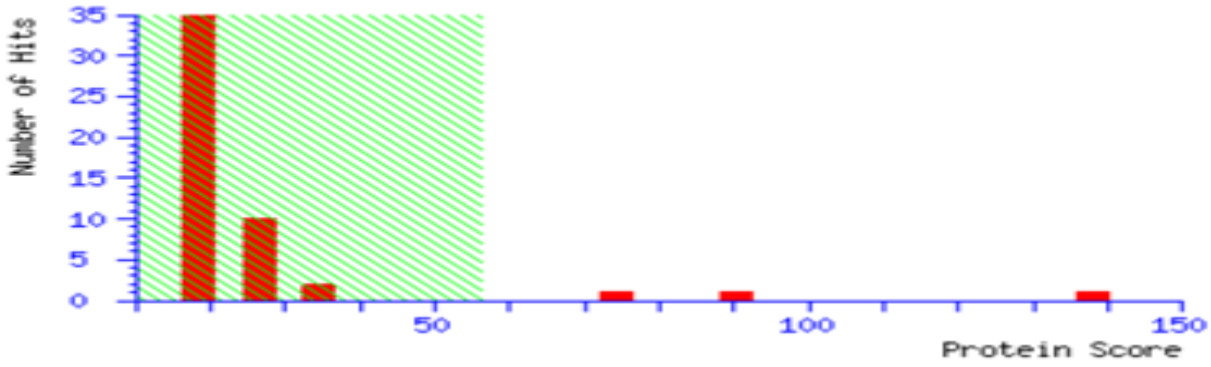

Figure 3.68 : Matched peptides, mass spectrum and mascot score histogram for COF1

3.6.3.10 Isocitrate dehydrogenase [NADP] cytoplasmic (IDHC)

The protein was appeared as spot number Ca125 in CACO-2 gel which was upregulated following all the drug treatments. Molecular mass of the protein was 46.63 kDa with isoelectric point (pI) of 6.53. The peptides found from this study matched with 16% of entire sequence of the protein IDHC, showing mascot score of 130. Base peak in the mass spectrum was found at m/z of 903.45.The sequence of matched peptides for the protein IDHC (spot Ca125) obtained from UniprotKB database; masses of peptides from MALDI-MS scan and mascot score histogram are shown in Figure 3.69.

```
  1 MSKKISGGSV VEMQGDEMTR IIWELIKEKL IFPYVELDLH SYDLGIENRD
 51 ATNDQVTKDA AEAIKKHNVG VKCATITPDE KRVEEFKLKQ MWKSPNGTIR
101 NILGGTVFRE AIICKNIPRL VSGWVKPIII GRHAYGDQYR ATDFVVPGPG
151 KVEITYTPSD GTQKVTYLVH NFEEGGGVAM GMYNQDKSIE DFAHSSFQMA
201 LSKGWPLYLS TKNTILKKYD GRFKDIFQEI YDKQYKSQFE AQKIWYEHRL
251 IDDMVAQAMK SEGGFIWACK NYDGDVQSDS VAQGYGSLGM MTSVLVCPDG
301 KTVEAEAAHG TVTRHYRMYQ KGQETSTNPI ASIFAWTRGL AHRAKLDNNK
351 ELAFFANALE EVSIETIEAG FMTKDLAACI KGLPNVQRSD YLNTFEFMDK
401 LGENLKIKLA QAKL
```

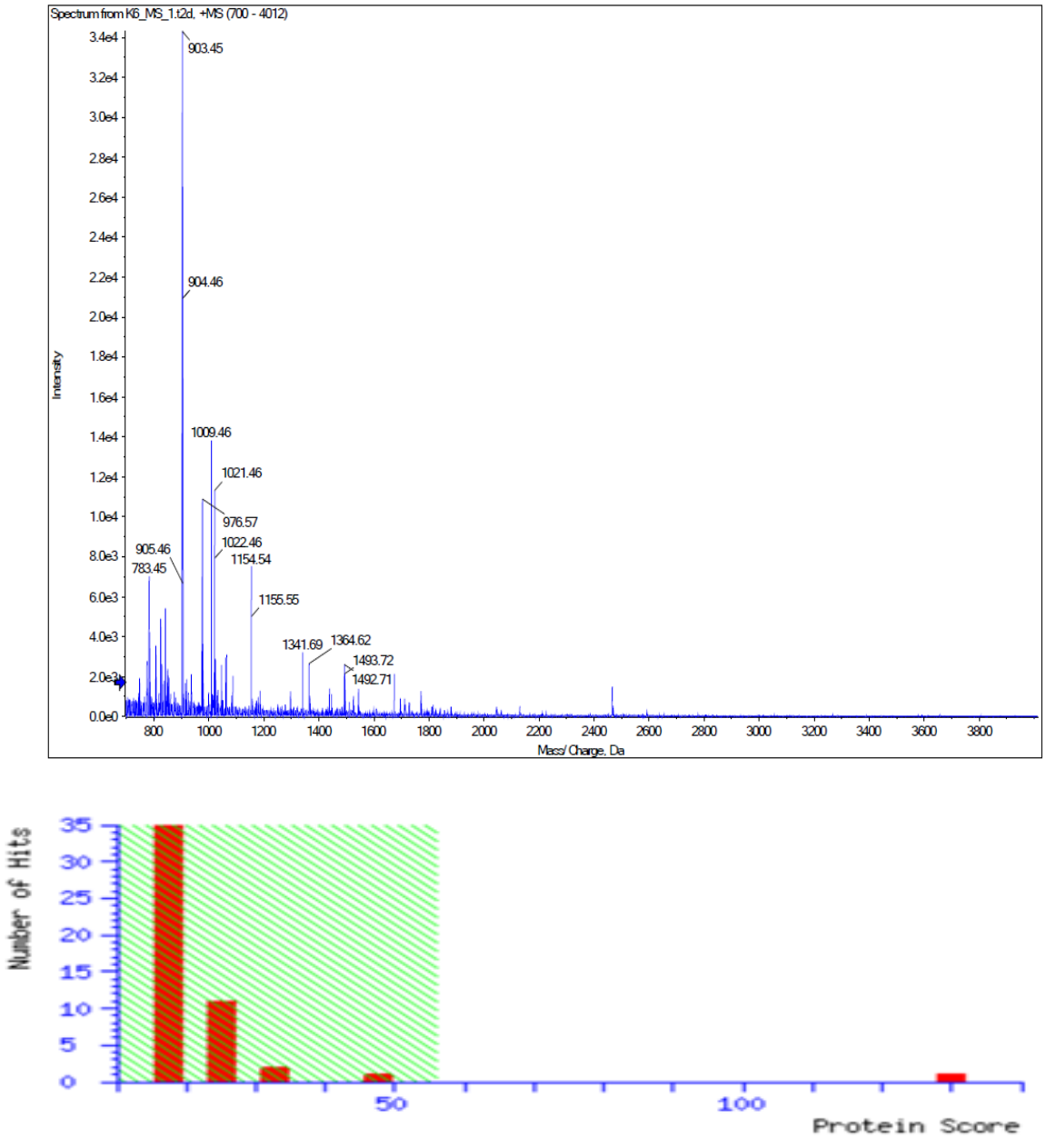

Figure 3.69: Matched peptides, mass spectrum and mascot score histogram for IDHC

3.6.3.11 Keratin, type I cytoskeletal 18 (K1C18)

The protein was appeared as spot number Ca166 in CACO-2 gel which was upregulated following all the drug treatments. Molecular mass of the protein was 48.02 kDa with isoelectric point (pI) of 6.36. The peptides found from this study matched with 4% of entire sequence of the protein K1C18, showing mascot score of 345. Base peak in the mass spectrum was found at m/z of 1041.62.The sequence of matched peptides for the protein K1C18 (spot Ca166) obtained from UniprotKB database; masses of peptides from MALDI-MS scan and mascot score histogram are shown in Figure 3.69.

```
  1 MRVVVIGAGV IGLSTALCIH ERYHSVLQPL DIKVYADRFT PLTTTDVAAG
 51 LWQPYLSDPN NPQEADWSQQ TFDYLLSHVH SPNAENLGLF LISGYNLFHE
101 AIPDPSWKDT VLGFRKLTPR ELDMFPDYGY GWFHTSLILE GKNYLQWLTE
151 RLTERGVKFF QRKVESFEEV AREGADVIVN CTGVWAGALQ RDPLLQPGRG
201 QIMKVDAPWM KHFILTHDPE RGIYNSPYII PGTQTVTLGG IFQLGNWSEL
251 NNIQDHNTIW EGCCRLEPTL KNARIIGERT GFRPVRPQIR LEREQLRTGP
301 SNTEVIHNYG HGGYGLTIHW GCALEAAKLF GRILEEKKLS RMPPSHL
```

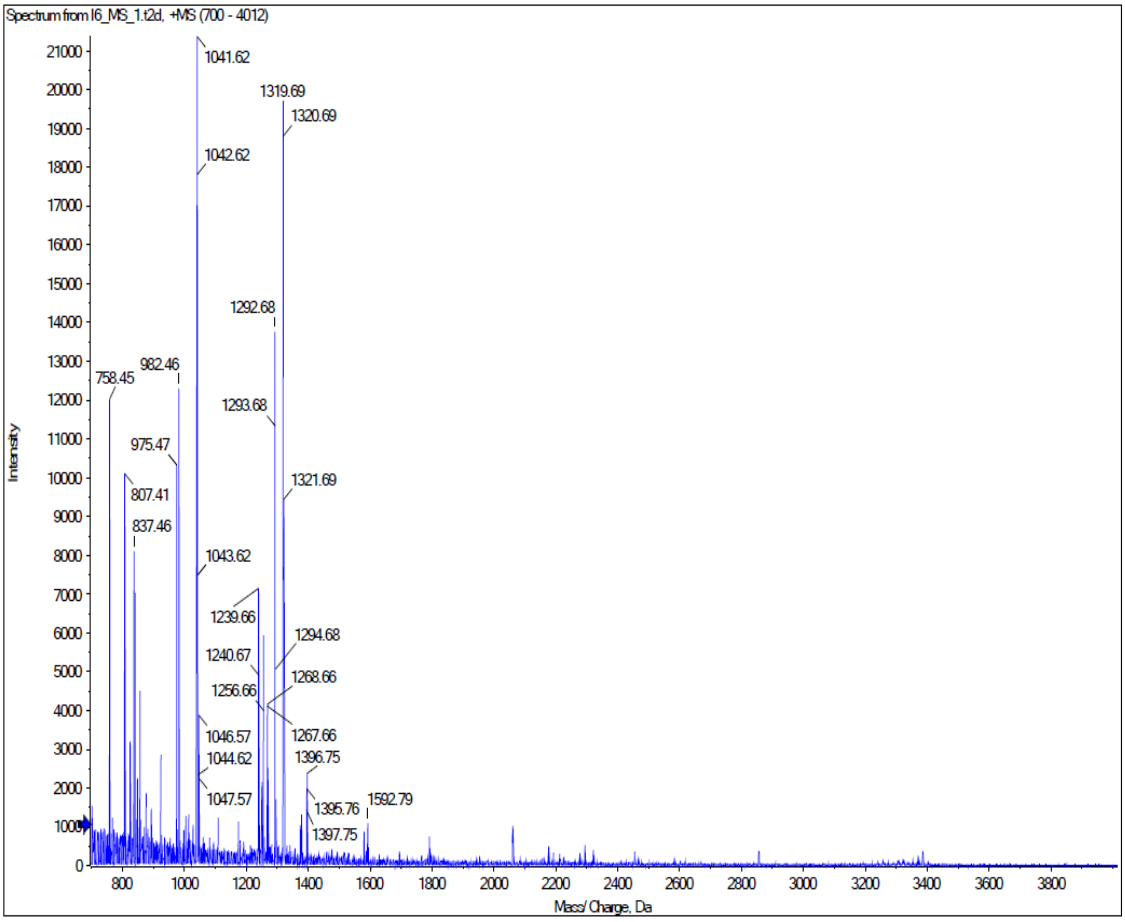

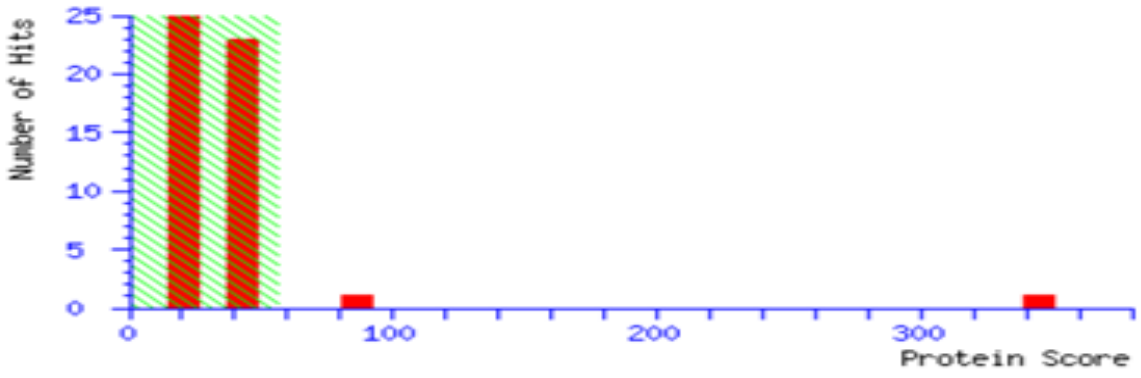

Figure 3.70: Matched peptides, mass spectrum and mascot score histogram for K1C18

4 DISCUSSION

Preamble

Cancer remains a major health concern all over the world with colorectal cancer being the 2nd most common cancer in Australia and 3rd (1.23 million) worldwide, treated with different methods and drugs according to the disease stage. For advanced stages of CRC chemotherapy in combination with surgery and radiotherapy is the front-line treatment strategy. The primary goal of this study was to determine the drug effects from the combinations of platinum based chemotherapeutics and phytochemicals in terms of synergism, additiveness or antagonism against CRC. This chapter provides the detail discussion of the results mentioned in chapter three. Mechanistic insights of the combined drug actions obtained from DNA-damage study, cellular accumulation and Pt-DNA binding study is also discussed. Finally the proteins identified from proteomic study which ultimately determines the drug actions alone or in combination are also discussed.

4.1 Cytotoxicity of the compounds alone

Anticancer activity of the compounds against four colorectal cancer cell lines has been given in Table 3.1. It is evident from the result that Col has demonstrated highest antitumour activity against all tested cell lines, having the lowest IC_{50} value of the order of 10 nM against HT-29 and LIM-2405 cell line. IC_{50} values of Col were found about 20 nM and 190 nM against LIM-1215 and CACO-2 cell lines respectively. Compared to clinical standard Ox, Col showed 14 to 760 times greater cytotoxicity against the tested cell lines. The activity was 136 to 500 and 13 to 150 times higher when compared with other clinical drugs Cis and Tax respectively. Although high anticancer activity of

Col has been noted before, studies against CRC is very limited (Sivakumar 2013). IC_{50} values of Col at nanomolar levels also have been reported against parent and resistant A2780 ovarian cancer models (Alamro 2015). In an *in vivo* mice model study it has been found that Col significantly reduced the progression of advanced level cancer (Baguley, Holdaway et al. 1991). Activity of colchicine has been attributed to its capacity to bind with tubulin and microtubules (Ahmed, Peters et al. 2006). However the major limitation of Col for development as an anticancer agent, is its toxicity against normal cells (Balasubramanian and Gajendran 2013). One possible way to overcome the toxicity of Col is to combine with other chemotherapeutics producing synergism which would further reduce the dose required to kill cancer cells and eventually reduce the side effects.

Second most active drug against the selected colorectal tumour models found from this study was Tax, the most successful phytochemical for treatment against cancer. In this study, Tax displayed superiority over all other studied compounds except colchicine. The drug is being clinically used against lung, breast and ovarian cancer but very few reports available in literature regarding the effect of Tax against CRC (Kennedy, Harrison et al. 2000). Antitumour activity of Tax also has been associated with the binding with tubulin and microtubules. Tax is considered to be the first drug that targets tubulin and named as microtubule stabilizing agents (Orr, Verdier-Pinard et al. 2003). Moreover it can block the cell cycles as well (Hamel 2008). However, Tax suffers from drug resistance and toxicity at high doses. Interestingly, it has been observed from this study that both Col and Tax were most potent towards HT-29 cell line and least towards CACO-2 cell line. This is might be due to their similarity in mechanism of action.

Platinum compound Ox is proved as third most active compound among all the tested compounds against the four colorectal cancer cell lines. The order of activity from highest to lowest among different cell lines was:

HT-29>LIM-1215>CACO-2>LIM2405.

Another platinum compound Cis showed the order oactivity as the following:

LIM2405≈HT-29>LIM1215>CACO-2.

Cis had lower activity compared to Ox against all cell lines except for LIM-2405. Ox and Cis displayed similar cytotoxicity profile in other tumour models as well (Nessa, Beale et al. 2012). Greater activity of Ox than Cis has been implicated with the presence of bulky ligand (1,2-diaminocyclohexane) in the structure of Ox (Nessa, Beale et al. 2012).

Among three common phytochemicals used daily in the kitchen, curcumin showed greater antitumour activity than EGCG and 6-gingerol against all cell lines except for EGCG in LIM-1215. Cur manifested greatest sensitivity against LIM-2405, followed by HT-29 and CACO-2, the least against LIM-1215 cell lines. In contrast, EGCG showed the highest sensitivity against 1215, followed by HT-29 and LIM-2405, the least against CACO-2 cell lines. The IC_{50} values for Cur and EGCG found in this study were higher than those found against ovarian tumour models, indicating lower cytotoxicity of the phytochemicals in CRC (Mazumder, Beale et al. 2012, Nessa, Beale et al. 2012, Alamro 2015).

Mechanism of anticancer action of curcumin in colorectal cancer has been reviewed by Johnson and Mukhtar. The authors mentioned that curcumin can cause tumour cell death by inducing apoptosis and cell cycle arrest using multiple signalling pathways including: inhibition of PKC (serine/threonine kinases – protein kinase C) and JNK (c-jun N-terminal kinase); inhibition of AP-1 (Activator protein-1); inhibition of NF-κB

(Nuclear factor-kappa B); reduction of early growth response (Egr-1) gene products and inhibition of Cycloxygenase-2 (COX-2) (Johnson and Mukhtar 2007). Moreover, curcumin showed the capacity to inhibit metastasis through blocking MMPs (Matrix metalloproteinase) (Hong, Ahn et al. 2006).

Anticancer action of EGCG against CRC has been associated with inhibition of AMPK signalling pathway (Hwang, Ha et al. 2007); inhibition of insulin like growth factor receptor-1 (Shimizu, Deguchi et al. 2005); inhibition of the expression of HER3 and COX-2 (Shimizu, Deguchi et al. 2005); regulation of Notch signalling (Jin, Gong et al. 2013) and inhibition of VEGF (Shimizu, Shirakami et al. 2010). EGCG also has been reported to induce autophagic cell death (Hu, Wei et al. 2015).

Table 3.1 shows that, the least active compound was 6-gin among all compounds studied against colorectal cancer models. The low activity of 6-gin against colorectal cancer models (SW480, HT-29, LoVo, and Caco-2) is also supported by previous report (Lee, Cekanova et al. 2008). Due to the large range of IC_{50} values displayed by 6-gin against all colorectal cancer cell lines, the compound was not selected for combination and mechanistic studies.

4.2 Drugs in combination

The major hurdle in cancer treatment is probably drug resistance, when treatment does not respond. Drug resistance can be of two types: intrinsic (cancer cells show insensitivity against the drug at the very beginning of exposure) or acquired (cancer cells develop resistance gradually after long term exposure of the drug and cause relapse of the disease) (Holohan, Van Schaeybroeck et al. 2013). One of the proposed methods of combating multidrug resistant cancers is to administer two or more drugs simultaneously which act differently against cancer cells (Al-Lazikani, Banerji et al.

2012). Combination therapy can provide benefits over monotherapy by improving the efficacy and reducing the side effects. However, most of the combination therapy currently being used (e.g. chemotherapy with monoclonal antibody, chemotherapy with mRNA, two or more chemotherapeutics) suffers with the increase of treatment cost (Lu, Lu et al. 2013). Combining phytochemicals having anticancer potential with chemotherapeutic drug might provide cost-effective solution of drug resistance in cancer. Of note, sequence of administered chemotherapeutic drugs has been implicated to determine the combined drug actions (Levis, Pham et al. 2004). In this study binary combination of platinum drugs and four phytochemicals have been investigated using three different sequences of administration and concentrations against colorectal cancer models.

4.2.1 Combination of platinums with curcumin

When Cis was combined with Cur against the colorectal tumour models, strong synergism was found in LIM-1215 cell line and LIM-2405 cell lines depending on concentrations and sequence of administrations. In LIM-1215 cell line, stronger synergism was observed at lower concentrations than at higher concentrations. But only 0/4 and 4/0 sequences showed synergism against LIM-2405 cell line, with greater synergism being observed at lower concentrations. In contrary, antagonism was predominant in HT-29 and CACO-2 cell lines except for ED_{90} level in HT-29 model where moderate synergism was evident.

When Ox was combined with Cur, synergism was found against all tested colorectal tumour models at all added concentrations and sequences of administrations. A general trend of increasing synergistic effect was evidenced with the increase in added concentration for all sequences of administrations against the colorectal cancer models.

Stronger synergism was demonstrated against CACO-2 tumour model compared to other cell lines.

It can be concluded from the above discussion that combination of Ox with Cur is better in cell kill than that of Cis with Cur against studied CRC models. Higher concentrations showed greater synergism in the combination of Ox with Cur but the effect is converse in case of Cis with Cur. Previous studies from our group against ovarian cancer models (including cisplatin and picoplatin resistant A2780 cell lines) also revealed synergism from the combination of cisplatin and curcumin (Yunos, Beale et al. 2011, Nessa, Beale et al. 2012). Younos *et al.* also reported that the observed synergism from the combination of cisplatin and curcumin is stronger at ED_{50} levels compared to that of ED_{75} and ED_{90} levels. Similarly, oxaliplatin in combination with curcumin also produced sequenced dependent synergism against ovarian tumour models. Sequenced addition of curcumin first and platinum drugs 2 h later was found to show more pronounced synergistic effect against three ovarian cancer cells (Nessa, Beale et al. 2012). Another group also noticed significant synergism from combination of curcumin with cisplatin and oxaliplatin against 2008 and C13 ovarian cancer cell lines (Montopoli, Ragazzi et al. 2009). Moreover, curcumin and carboplatin in combination synergistically inhibited apoptosis and metastasis against lung cancer (Kang, Kang et al. 2015).

A number of studies against CRC models also demonstrated synergism from the combinations of curcumin with platinum drugs. Oxaliplatin in combination with liposomal curcumin showed significant synergism during *in vitro* and *in vivo* xenograft model study using Lovo and Colo-205 colorectal cancer cells (Li, Ahmed et al. 2007). Another *in vitro* and *in vivo* model study using HCT-116 cell lines reported that curcumin in combination with oxaliplatin reduces the chemoresistance towards

oxaliplatin (Howells, Sale et al. 2011). Curcumin in combination with camptothecin also exhibited strong synergism against a colorectal cancer model (Xiao, Si et al. 2015). In an animal model study using FOLFOX resistant HT-29 and HCT-116 cancer cells, curcumin in combination with dasatinib showed inhibition of tumour growth, metastasis and colonosphere formation. The combined therapy significantly decreased the number of cancer stem cells by reducing CD133, CD44, CD166 and ALDH (Nautiyal, Kanwar et al. 2011). The mechanism behind the synergistic effects from combination of curcumin with platinum drugs was reported to be associated with the down regulation of matrix metalloproteinases (MMP-2 and MMP-9), BCL-2, NF-κB as well as upregulation of caspases (caspase-3 and caspase-9) and p53 (Kang, Kang et al. 2015). The mechanisms behind the combined drug actions of curcumin with different drugs have been reviewed by Troselj *et al* (Gall Troselj and Novak Kujundzic 2014). The proposed mechanisms of synergistic actions of Curcumin with platinum drugs are summarised in Figure 4.1.

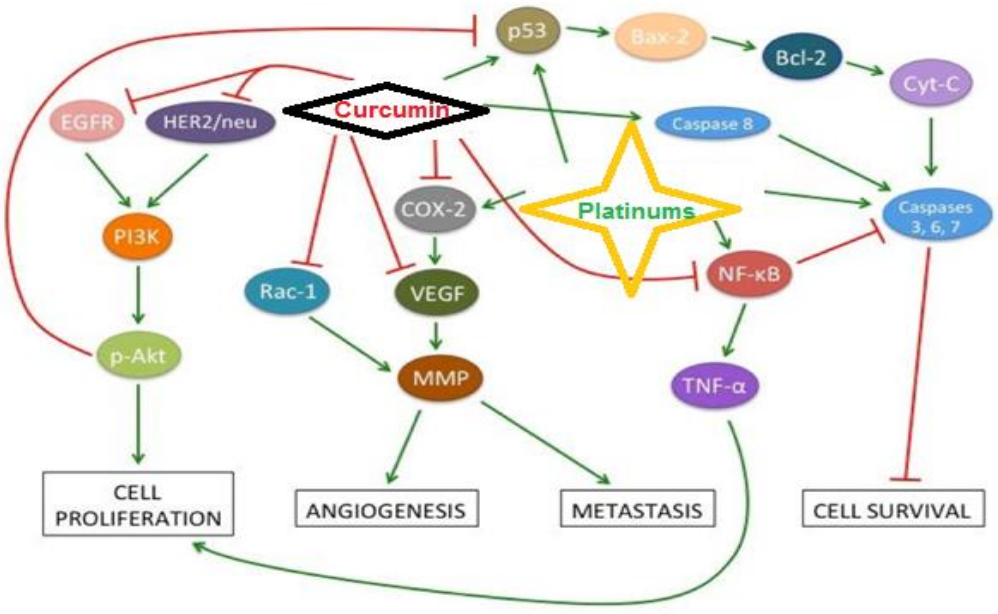

Figure 4.1: Mechanisms of synergistic action from curcumin with platinums

4.2.2 Combination of platinums with colchicine

When Cis was combined with Col against the colorectal tumour models, moderate synergism was found in HT-29 cell line at all added concentrations and sequence of administrations. In CACO-2 and LIM-1215 cell line, synergism was observed only with 0/4 and 4/0 sequences of administration but antagonism was found with bolus administration. The degree of synergism was higher at lower added concentration than higher concentrations in all of the above mentioned three cell lines. In contrast, antagonism was evidenced in LIM-2405 cell lines irrespective of sequences of administration and concentrations.

When Ox was combined with Col, synergism was found in LIM-1215 cell line at all added concentrations and sequence of administrations. But the observed synergism was increased with the increase of added concentrations. In HT-29 and CACO-2 cell lines synergism was found only at ED_{75} and ED_{90} levels, but antagonism at ED_{50} level. In contrast to the observed synergism in these cell lines, antagonism was predominant in LIM-2405 cell line.

It is obvious from the above discussion that combination of cisplatin with colchicine is better in synergistic outcome at lower concentration than higher added concentrations and the converse is true for the combination of oxaliplatin with colchicine. Combination of both of the platinums with colchicine is mostly synergistic against HT29, CACO-2 and LIM-1215 colorectal cancer models, but antagonistic against LIM-2405 cell line. In an earlier study from the host laboratory, it has been reported that 4/0 sequence of addition of cisplatin with colchicine at ED_{50} level produced strongest synergism against ovarian cancer models (Yunos, Beale et al. 2010). Similarly oxaliplatin in combination with colchicine exhibited the greatest synergism while oxaliplatin was administered 4 h after the administration of colchicine against parent and cisplatin resistant A2780

ovarian cancer cell lines (Yunos, Beale et al. 2011). Moreover colchicine in combination with curcumin, EGCG and resveratrol displayed sequence and dose dependent synergism against three ovarian cancer models (Alamro 2015). Since antitumour activity of colchicine has been solely attributed to its ability to disrupt the assembly of microtubule, colchicine might provide synergistic actions in combinations with other platinums by killing cancer cells using a different mechanism of actions. Although colchicine has not been considered as a single agent therapy against cancer due to its toxicity, it could be further investigated as a combination therapy for safety and efficacy in a suitable animal model.

4.2.3 Combination of platinums with EGCG

When Cis was combined with EGCG against the colorectal tumour models, additive to moderate synergism was generally found in the four studied cell lines. In very few instances depending on concentration or sequence of administration antagonism was manifested. Strongest synergism was shown at ED_{50} level with all the sequences of administration in HT-29 cell line. Generally, lower added concentrations displayed greater synergism than higher added concentrations.

When Ox was combined with EGCG, synergism was found against all tested colorectal tumour models at all added concentrations and sequence of administrations (except for at ED_{90} level with bolus administration in LIM-1215). A general trend of increasing synergistic effect was evidenced with the increase of added concentration for all sequences of administration against the colorectal cancer models. Stronger synergism was demonstrated against HT-29 and CACO-2 tumour models compared to other cell lines.

It is obvious from the above discussion that combination of Ox with EGCG is better than that of Cis with EGCG against tested CRC models. Higher added concentrations showed more synergism in the combination of Ox with Cur but the converse was true for Cis with Cur. Article published from our group reported that cisplatin in combination with EGCG showed sequence and concentration dependent synergism against four ovarian tumour models, where more synergism was observed at lower added concentrations (Yunos, Beale et al. 2011, Mazumder, Beale et al. 2012). Many other research groups also reported synergistic action of EGCG in combination with platinum drugs and other chemotherapeutic and chemopreventive agents against a variety of cancer models. In a study against colorectal cancer cell lines (DLD-1 and HT-29), EGCG acted synergistically with cisplatin and oxaliplatin through inducing

autophagic cell death. Autophagy was confirmed by elevated levels of LC3-II protein, acidic vesicular organelles, and development of autophagosome (Hu, Wei et al. 2015). Another study in lung cancer models revealed that combination of cisplatin with EGCG enhanced the sensitivity against resistant cells through upregulation of copper transporter-1 CTR1 which caused increased uptake of cisplatin into the cells (Jiang, Wu et al. 2016). EGCG in combination with N-(4-hydroxyphenyl) retinamide was also reported to provide synergistic effect against neuroblastoma via modulating oncogenic mRNAs (Chakrabarti, Khandkar et al. 2012). Sulforaphane in combination with EGCG displayed synergism against paclitaxel resistant ovarian cancer cells by down regulating BCL-2 and telomerase regulatory subunit hTERT (Chen, Landen et al. 2013). The detail mechanisms for the synergistic effects obtained from 42 *in vitro* and 13 animal model studies from the combination of EGCG with NSAIDs, phytochemicals, and anticancer drugs have been portrayed in a published review (Fujiki, Sueoka et al. 2015). Co-administration of EGCG with other chemotherapeutic drugs has not only demonstrated increased cancer cell death but also reduce side effects mediated by chemotherapy (Lecumberri, Dupertuis et al. 2013). A proposed mechanism has been given in figure 4.2 showing how EGCG reduce nephrotoxicity produced by cisplatin (Pan, Chen et al. 2015).

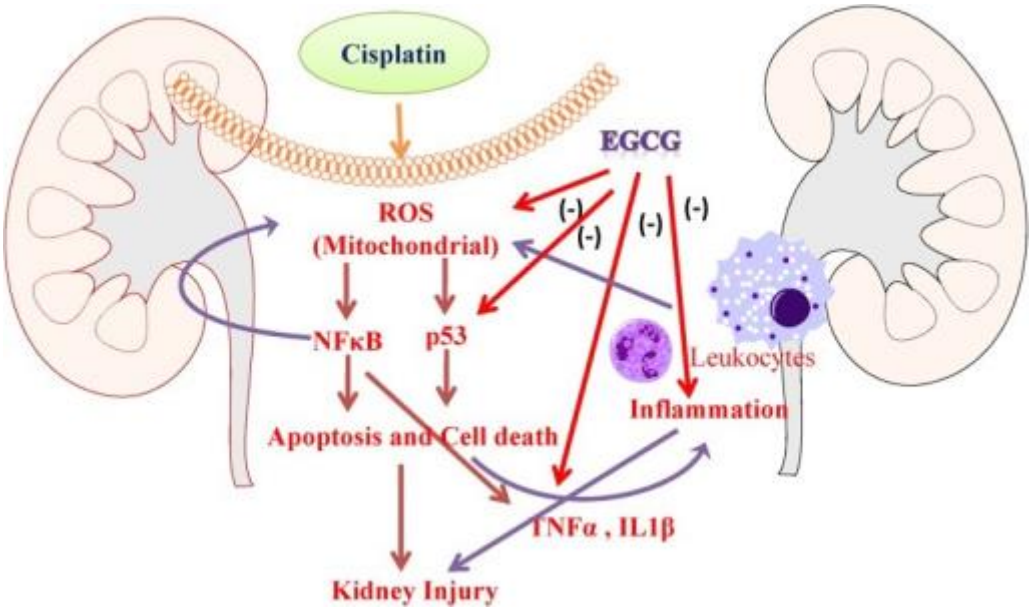

Figure 4.2: Role of EGCG in preventing nephrotoxicity mediated by cisplatin [Adapted from (Pan, Chen et al. 2015)]

It can be suggested that EGCG can be investigated further in clinical settings with conventional chemotherapies (platinum drugs) in colorectal and other cancers.

4.2.4 Combination of platinums with taxol

When Cis was combined with Tax against the colorectal tumour models, strong antagonism was found against all cell lines studied. However, Ox in combination with Tax gave synergism in CACO-2 and LIM-1215 cell lines. Strongest synergism was evident with 4/0 administration at all added concentrations in CACO-2 cell line. Bolus administration also displayed synergism but only at higher concentrations in the same cell line. 0/4 addition proved to be additive at ED_{50} level but antagonistic at ED_{75} and ED_{90} levels in CACO-2 cell line. In contrast, bolus and 0/4 sequences of administration produced synergism in LIM-1215 cell line, more so at higher added concentrations. 4/0 sequence of administration exhibited additiveness at lower concentrations but antagonism at higher concentrations against LIM-1215 cell line. Against HT-29 and

LIM-2405 cell line combination of Ox with Tax showed antagonism with all added sequences of administration and concentrations.

Although the combined effect is antagonistic for cisplatin with taxol against four colorectal tumour models as found in the present study, synergism was reported earlier from the same combination against ovarian tumour models (Yunos, Beale et al. 2010). Another study from our group also described sequence and dose dependent synergism from the combination of taxol with cisplatin and oxaliplatin against three ovarian cancer cell lines (Nessa 2013). Taxol is being used in the clinic to treat ovarian cancer in combination with carboplatin. Moreover, taxol has also been gone through clinical trials in combination with oxaliplatin against lung cancer (Liu, Kraut et al. 2002, Winegarden, Mauer et al. 2004). However combination study with taxol and platinums against colorectal tumour models is very scarce in literature. One study reported that sequenced administration of taxol followed by oxaliplatin produced synergism but oxaliplatin followed by taxol displayed antagonism (Fujie, Yamamoto et al. 2005). Figure 4.3 depicts the mechanism through which taxol give anticancer actions (Kampan, Madondo et al. 2015). Since multiple signalling pathways are modulated by the administration of taxol, it is conceivable that Tax can kill cancer cells using the pathways different than Ox and thus aid the synergistic effects. However it could not be understood from this study why Tax exhibited antagonism in combination with Cis against all cell lines, and also with Ox against HT-29 and Lim-2405 cell lines.

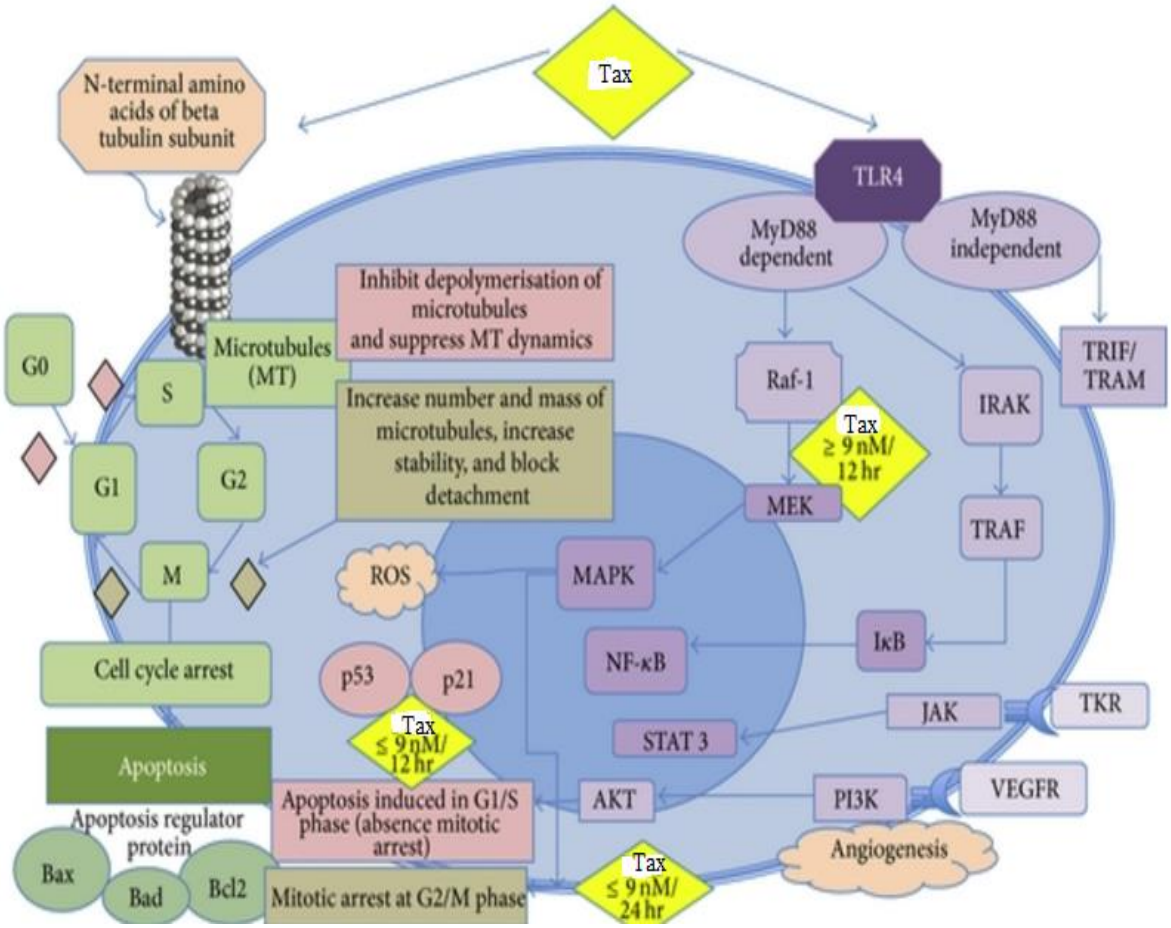

Figure 4.3: Signalling pathways modulated by Tax administration [Adapted from Kampan, Madondo et al. 2015)]

4.3 Cellular accumulation of platinums from alone and combined treatments

To reach into the targets to give antitumour activity, drugs must have to enter into the cell. Moreover, one of the key mechanisms for the development of resistance towards platinum based anticancer drugs is to decrease the influx of the drugs into the cell. Another important mechanism is to increase the efflux of platinums from the cell (Zhu, Shanbhag et al. 2017). In both of the cases, ultimate result is reduced accumulation of platinums to reach into the target DNA to show its antitumour activity (Yu, Yang et al. 2015). Cellular accumulation study was conducted with the idea that: synergistic and

additive treatments would cause increased cellular accumulation of platinum or at least would not reduce the accumulation; and antagonistic treatment might cause lower cellular accumulation of platinum.

It is apparent from Table 3.18 that synergistic (Cis with EGCG using bolus administration) and additive (Cis with Cur using 4/0 sequence of administration) combined treatments from Cis and phytochemicals caused significant increase in the accumulation of platinum into HT-29 cells compared to Cis alone treatment. Cellular accumulation of platinum was increased by 2.13 folds with synergistic combined treatment. However the increase in platinum accumulation with additive treatment was not substantial, which suggests that synergism from combination of Cis with phytochemicals might be due to increased cellular accumulation. When the study was conducted with the combinations from Ox with phytochemicals in HT-29 cell line, it was also observed that synergistic combined treatment of Ox with EGCG using bolus administration produced 1.22 times greater platinum accumulation than Ox alone treatment. However synergistic combined treatments of Ox with Cur using bolus and 4/0 administration did not cause significant increase in accumulation of platinum, rather displayed almost the same amount of accumulation when compared with Ox alone treatment. But additive and antagonistic combined treatments of Ox with Col using 0/4 sequence of administration and Ox with Tax using 4/0 sequence of administration reduced the platinum accumulation in HT-29 cell by 3.33 and 1.27. This study also supports the concept that, antagonistic effect in HT-29 cell line from combination of Ox with phytochemical is due to either decreased uptake of platinum into the cell or increased efflux of platinum from the cell. The findings are corroborated with earlier reports where synergistic combinations displayed increased accumulation of platinum in many instances (Mazumder 2013, Arzuman 2014).

When the study was further extended in CACO-2 cell line to find out the relationship with the combined drug action and cellular uptake levels, the results (Table 3.19) reinforced the outcome obtained from the study in HT-29 cell line. Synergistic combined treatment of Cis with EGCG using bolus administration caused 2.5 times greater platinum accumulation in CACO-2 cell line than Cis administered alone. Additive combined treatment of Cis with Cur using 4/0 sequence of administration also increased the platinum accumulation. In contrast, no combined treatment produced greater cellular accumulation of platinum in CACO-2 cell line than Ox alone treatment. However, synergistic combined treatment of Ox with EGCG using bolus administration showed significantly greater accumulation of platinum into the cell than antagonistic treatments. All told, it can be proposed from this study that synergism obtained from this study was correlated with the increased accumulation of platinums inside the cell and antagonism is the consequence of vice versa.

4.4 Platinum–DNA binding from alone and combined treatments

Platinum drugs are believed to kill cancer cells through forming covalent bonds with DNA. That is why it was assumed that synergistic combined drug action from platinums and phytochemicals might be the result of increased platinum–DNA binding and antagonism is the converse. It is noticeable from Table 3.20 that, synergistic combined treatment of Cis with EGCG using bolus administration displayed 11.3 times greater extent of platinum–DNA binding than Cis alone and additive (Cis with Cur, 4/0) treatments in HT-29 cell line. Synergistic combined treatments of Ox with Cur using bolus and 4/0 administration demonstrated 1.2 to1.3 times greater extent of platinum–DNA binding than Ox alone treatment in the same cell line. In contrast,

antagonistic combined treatment of Ox with Tax using 4/0 sequence of administration reduced the extent of platinum–DNA binding by half compared to Ox alone treatment in HT-29 cell line. The above discussed results obtained from platinum–DNA binding study in HT-29 cell line suggest that synergism attained from the combination of platinums and phytochemicals in this study is directly proportional to the extent of platinum–DNA binding.

The study was further extended in CACO-2 cell line but no significant correlation was perceived between the observed combined drug action and the extent of platinum–DNA binding from the combination of Cis and phytochemicals. However, combinations from Ox with phytochemicals revealed that synergistic combined effect might be the outcome of greater extent of platinum–DNA binding and antagonistic effect was due to reduced extent of platinum–DNA binding (Table 3.21) in CACO-2 cell line. Altogether, it can be perceived from this study that combined drug actions of platinums and phytochemicals are associated with the extent of platinum–DNA binding in colorectal cancer models where synergism is evidenced from greater binding and antagonism with lesser binding.

4.5 Study on interactions of DNA

DNA damage study was conducted to get the relationship between damage towards DNA and combined drug action. The results of DNA damage study has been presented in Table 3.22 (HT-29 cell line) and Table 3.23 (CACO-2 cell line). Synergistic combinations (Cis with EGCG, bolus; Ox with Cur, 4/0 and Ox with EGCG, bolus), antagonistic combinations (Ox with Col, 0/4 and Ox with Tax, 4/0) and additive combination (Cis with Cur, 4/0) were selected for this study along with the single treatments of Cis, Ox, Cur, Col, EGCG and Tax. It has been noticed from Table 3.22

that synergistic combinations caused more damage towards DNA compared to antagonistic and additive treatments in HT-29 cell line. Highest damage was displayed by band 4 (Figure 3.50) which represented synergistic combination of Cis with EGCG at bolus administration followed by band 8 (Figure 3.50) representing synergistic combination of Ox with Cur at 4/0 sequence of administration. The lowest DNA damage was seen for band 11 (Figure 3.50) applying to antagonistic combination of Ox with Tax at 4/0 sequence of administration. The increase in intensity was observed in band 11 compared to band 1 and band 14 (untreated HT-29, control) which indicates the DNA protection effect from combined treatment of Ox and Tax at 4/0 sequence of administration. The combination index value at ED_{50} level of Ox with Tax, 4/0 indicated strong antagonism which proved that co-administration of Tax inhibited the cytotoxic effect of Ox which is perceived due to the protection effect on DNA. When the phytochemicals were interacted with DNA as a single compound, it was found that Tax caused least damage towards DNA which further validates that how DNA damage is linked with the antagonism revealed from the combination of Ox with Tax at 4/0 sequence of administration in HT-29 cell line. However, the antitumour activity of the compounds alone and their DNA damage property could not be correlated in HT-29 cell line.

When the study was conducted in CACO-2 cell line synergistic combinations (Cis with EGCG, bolus; Ox with Cur, 4/0 and Ox with EGCG bolus), antagonistic combinations (Ox with Col, 0/4 and Ox with Tax, 4/0) and additive combination (Cis with Cur, 4/0) were selected along with the single treatments of Cis, Ox, Cur, Col, EGCG and Tax.

Highest damage was displayed by band 3 (Figure 3.51) which represented additive combination of Cis with cur at 4/0 sequence of administration followed by band 6

(Figure 3.51) applying to synergistic combination of Ox with Cur at 4/0 sequence of administration.

The lowest DNA damage was seen for band 9 (Figure 3.51) applying to antagonistic combination of Ox with Tax at 4/0 sequence of administration. This was indicated by lowest mobility and increased intensity. Similar to the findings in HT-29 cell line, no correlation was observed between the antitumour activity of the compounds alone and their DNA damaging attributes in CACO-2 cell line.

Finally, it can be concluded from the above discussion that synergistic combinations exhibited greater DNA damage and antagonistic combinations did the least damage. But DNA damage is not the only determinant of the antitumour activity of compound, rather the binding nature and extent of binding with DNA has more impact on recognition of the downstream proteins which are involved in the signalling mechanisms associated with cell survival or cell death (Abdullah, Huq et al. 2006, Mazumder 2013). That is why Cur and EGCG apparently caused greater DNA damage than Cis, Ox and Tax in both HT-29 and CACO-2 cell lines although less active.

4.6 Proteomic study

Proteomics involve the study of vibrant proteins present in the genome as well as the interactions of protein derivatives which connects the gap between genome sequence and cellular activities (Dove 1999). Two dimensional gel electrophoresis study followed by MALDI-MASS characterization of proteins have been conducted in the present study to identify the proteins associated with the combined drug actions. Among 153 proteins identified from HT-29 cell line only seven proteins matched the selection criteria (mentioned in chapter three) whereas seven were chosen from 195 spots of CACO-2 cell line. However only eleven individual proteins were identified from the

two cell lines which underwent significant changes in expression following all different treatments. Based on the molecular functions the identified proteins fell into four classes namely:

- Cytoskeleton organization proteins: Actin Cytoplasmic 1 protein , Tubulin beta chain , Keratin, type II cytoskeletal 8 , Keratin, type I cytoskeletal 18 and Cofilin1
- Molecular chaperones: Nucleolar phosphoprotein B23 , Heat shock cognate 71 kDa and 78 kDa glucose regulated protein
- Metabolic enzymes: Glutathione S transferase P1 and Isocitrate dehydrogenase [NADP] cytoplasmic
- Proteasome associated protein: Proteasome subunit beta type-6

Functional classification of the identified proteins is given in Figure 4.4. It is evident from the figure that most of the proteins belonged to cytoskeleton organization group comprising 46% of totality. Stress regulation proteins were the second most abundant group encompassing 27% of all identified proteins. 18% of the characterized proteins from this study categorized as enzymes and the rest 9% considered being proteasome associated protein.

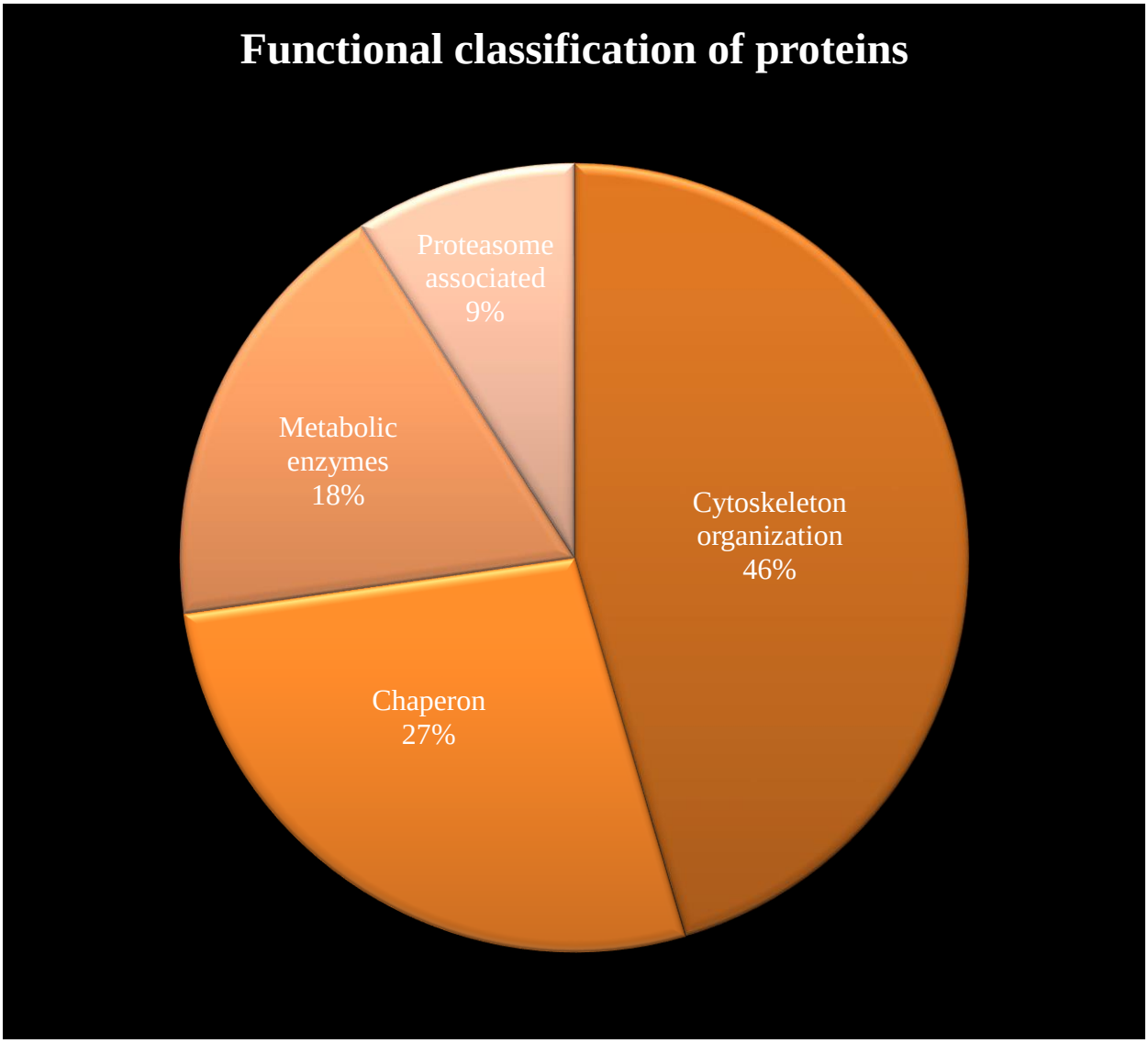

Figure 4.4: Functional classification of identified proteins based on functions

4.6.1 Cytoskeleton organization proteins

The network of filaments that gives support to plasma membrane, contributes to provide the cell an overall shape, appropriate placing of organelles, tracking the movement of vesicles as well as regulate cell motility is called cytoskeleton. There are mainly three types of protein fibers which constructs the cytoskeleton in eukaryotes: actin microfilaments with a diameter of 6 nm, intermediate filaments with a diameter around

10 nm and microtubules with a diameter of 23-25 nm (Rufino-Palomares, Reyes-Zurita et al. 2013). In a normal cell cytoskeletal proteins regulate growth and stiffness, maintains polarity, and patterns the extracellular matrix. Thus cytoskeletal proteins subsequently impact on development and tissue differentiation (Bezanilla, Gladfelter et al. 2015). In cancer cytoskeleton are involved by modulating cell cycle events, morphogenesis and cellular migration or metastasis (Hall 2009). The proteins which belonged to this class and found to exhibit significantly changes in expression in this study are discussed here.

4.6.1.1 Actin Cytoplasmic 1 protein

Actin is a highly conservative protein which appears in vertebrates in multiple isoforms. Two isoforms are found in striated muscles e.g. α-skeletal muscle actin and α-cardiac muscle actin. Whereas two isoforms are avaiale in smooth muscles e.g. α-smooth muscle actin and γ-smooth muscle actin. Another two isoforms is abundant in cytoplasm also known as non-muscle variants: β-cytoplasmic actin and γ-cytoplasmic actin (Popow, Nowak et al. 2006). Actin cytoplasmic 1 protein (beta actin) is the non muscle variant of actin, highly abundant in humans and other eukaryotes which serves in cell motility, mitosis, foetal development, healing process of wounds and gene expression (Bunnell, Burbach et al. 2011). The protein constitutes the meshwork actin which is primary found in the area of dynamic cytoplasm and appear at the tips of protrusive structures. That is how it functionally differs from another cytoplasmic actin (G-actin) which is predominant in the stress fibers and regulates cell shape as well as provide mechanical resistance (Herman 1993, Nowak and Malicka-Błaszkiewicz 1999, Popow, Nowak et al. 2006, Dominguez and Holmes 2011). Structurally, beta actin differs from gamma actin by only four similar amino acid acid residues (Bunnell, Burbach et al. 2011). In an animal model study it has been proved that beta actin is

essential for in vivo survival while G-actin is not like so. Knock out of beta actin results with deficiency in migration and cell growth (Bunnell, Burbach et al. 2011).

Although corresponding gene of beta actin ACTB has been considered as a reference gene for many cancers (Majidzadeh-A, Esmaeili et al. 2011), now such use has been challenged (Jung, Ramankulov et al. 2007, Guo, Liu et al. 2013). Deregulation of ACTB has been evidenced in various malignancies e.g. hepatoma, melanoma, renal carcinoma, colon carcinoma, gastrocarcinoma, pancreatic carcinoma, breast adenocarcinoma, ovarian carcinoma, liquid blood cancer and solid lymphoma (Guo, Liu et al. 2013). In most of the above mentioned cancers, elevated expression of ACTB was found. However, four folds downregulation of ACTB was observed in a colorectal tumour model of DLD-1 cell compared to non cancerous cells (Kwon, Oh et al. 2009). Several other studies also showed altered expression of ACTB in colorectal cancer (Andersen, Jensen et al. 2004, Dydensborg, Herring et al. 2006, Kheirelseid, Chang et al. 2010).

In the present study, beta actin was downregulated following all the treatments in HT-29 cell line. Col alone treatment caused the highest downregulation of the protein by the factor of 7.38. The extent of downregulation caused by Ox alone, EGCG alone and antagonistic combined treatment of Ox with Col using 0/4 sequence of administration were found to be almost equal by the factor of 2. However, synergistic combined treatment of Ox with EGCG using bolus administration did not produce significant downregulation (1.2 fold change was obseved). It could be assumed from this study that beta actin might act as an antiapoptotic protein in HT-29 cell line, which was upregulated in cancerous cell line and downregulated by the effect of drug treatments. However, it remained unclear why anatgonistic combined treatment (Ox with Col, 0/4) caused downregulation of beta actin.

4.6.1.2 Tubulin beta chain

Tubulins are the structural subunits of microtubules and composed of primarily with two subunits namely: alpha and beta. Tubulin monomers are bound with guanosine triphosphate (GTP) molecules which can be exchanged when it is attached with beta subunit. Alpha and beta tubulin shares forty percent of same amino acid sequences and differ in the rest sixty percent. Each subunit is composed of two beta-sheets encircled by alpha-helices and thus form a central core. Both alpha and beta subunits have multiple isoforms. Tubulin beta chain is one of the isoforms of beta subunit and responsible for intracellular transport and mitosis in all eukaryotes (Nogales, Wolf et al. 1998). Abnormalities in the expression of tubulin beta chain is evident is many solid cancers and recognized as potential cause for chemotherapy resistance (Fan, Gao et al. 2013). The protein has been considered as sepecific antigen for esophageal, gastric, pancreatic and colon cancer with sensitivity of 20% to 40% and sepecificity of 96% (Fan, Li et al. 2013). Beta tubulin was found to be upregulated in CRC (Fan, Kang et al. 2014), breast cancer (Cortesi, Barchetti et al. 2009) and esophageal cancer (Qi, Chiu et al. 2005).

In the present study, the protein was uprgulated following the treatments of Ox alone and EGCG alone in HT-29 cell line. However, it was downregulated after the treatment of Col alone and synergistic combined treatment of Ox with EGCG using bolus administration in the same cell line. The protein was not able to be detected following antagonistic combined treatment of Ox with Col using 0/4 sequence of administration in HT-29 cell line. The disapperance of the protein after drug treatment was thought to be due to extreme downregulation. However, it was difficult to decide about the nature of the protein from this study due to variation of response with different treatments.

4.6.1.3 Cofilin1

Cofilin1 is an actin binding protein belong to the family of actin depolymerizing factor (ADF)/cofilin family. This superfamily comprises of 39 similar members, all of them have same backbone (ADF-homology domains) of six stranded mixed beta sheets composed of 150 amino acid residues (Lappalainen, Kessels et al. 1998). Cofilin1 (non muscle isoform) is one of the traditional cofilins along with cofilin2 (muscle isoform-skeletal or cardiac) and destrins (available various tissues) (Bernstein and Bamburg 2010). Cofilin1 is responsible for actin polymerization and depolymerization through severing of filaments. The dynamics of actin filaments (assembly or deassembly) is dependent on the concentration of active cofilin1. Activity of cofilin1 relies on the upstream effectors: LIM and and TES kinases which cause phosphorylation and make cofilin1 inactive. In contrary, slingshot and chronophin phosphatases turns back the protein into active state through dephosphorylation (Yamaguchi and Condeelis 2007). At lower concentration cofilin1 favours severing of actin filaments and facilitate depolymerization, whereas at higher concentration actin nucleation and polymerization takes place (Shishkin, Eremina et al. 2016). Cofilin1 faciliates the polymerization process of actin filaments by creating free pointed ends and providing actin monomers. Thus it is considered as essential regulator of cell motility and metastasis in malignannt cells (Ghosh, Song et al. 2004). Moreover, cofilin1 plays vital role in restructuring of actin cytoskeleton when exposed towards variety of stimuli and stressed conditions. Other molecular level fuctions of cofilin1 includes: release of cytochrome C (Chua, Volbracht et al. 2003) and activation of phospholipase D1 (Han, Stope et al. 2007).

Elevated expression of cofilin1 has been found in lung (Keshamouni, Michailidis et al. 2006), pancreatic (Sinha, Hütter et al. 1999), oral (Turhani, Krapfenbauer et al. 2006), kidney (Unwin, Craven et al. 2003), colorectal (Zhao, Liu et al. 2007) and ovarian

cancer (Martoglio, Tom et al. 2000). However downregulation of cofilin1 is also evidenced in lymphoma, cervical, hepatic and colon cancer (Nebl, Meuer et al. 1996). The role of cofilin1 (COF1) in mediating cancer and the mechanism of action has been portrayed in Figure 4.5.

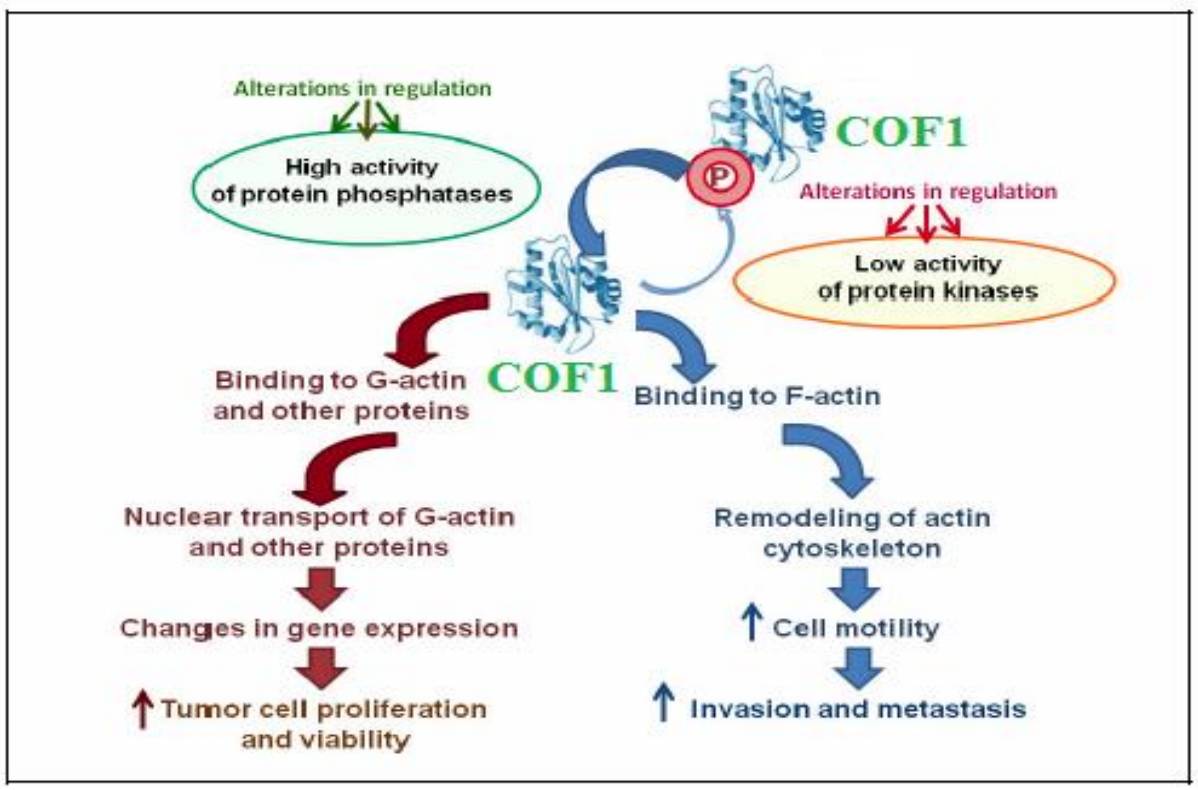

Figure 4.5: Contribution of cofilin1 (COF1) in cancer [Adapted from (Shishkin, Eremina et al. 2016)]

In the present study, the protein was slightly upregulated after treatment with Ox alone and significantly upregualted following the treatment of synergistic combination of Ox with Cur using bolus administration in CACO-2 cell line. However, the protein was downregulated after the treatment with Cur alone in the same cell line. The variation in the expression of cofilin1 following drug treatments makes it difficult to ascertain the nature of the protein. The controversial nature of cofilin1 has been reported earlier as well (Tsai, Lin et al. 2015). The authors mention that, although strong evidence on

upregulation of cofilin1 in multiple cancers is evident but overexpression of the protein may also cause suprression of cancer growth and invasion of cancer cells (Tsai, Lin et al. 2015). It was suggested that overexpression of cofilin1 cause cell cycle arrest but not induce apoptotic cell death. That is why strict control of cofilin1 expression is indispensable for normal functioning of cells (Tsai, Chiu et al. 2009).

4.6.1.4 Keratin, type II cytoskeletal 8

Keratin is one type of intermediate filaments which belong to a family of similar proteins including keratin, desmin and peripherin; contribute in maintaining cell shape and structural reorganization (Wax and Backman 2009). Keratin is relatively stable cytoskeletal structure which acts as elastic materials during mechanical stress and resist breakage by providing high stiffness at large strains (Beil, Micoulet et al. 2003). 54 different types of keratins identified which are broadly classified into two groups: type I (K9–K10, K12–K28, K31–K40) and type II (K1–K8, K71–K86). All keratins share common structural similarity among themselves by encompassing a central shaft domain of around 310 amino acids; forms alpha-helix lined by non-helical head and tail (Moll, Divo et al. 2008).

Keratin, type II cytoskeletal 8 (K2CB) is a type II cytoskeletal 8 keratin (K8) and usually coexpressed with K18 in normal epithelial cells. K2CB protein is the oldest keratin among all identified and play significant role in regulation of cell cycle (Magin, Vijayaraj et al. 2007), protecting cells from stress (Ku, Soetikno et al. 2003), injury and apoptosis (Caulin, Ware et al. 2000). Altered expression of K2CB protein is evidenced in lung (Hmmier, O'Brien et al. 2017), pancreatic, breast, renal, colorectal (Yamamoto, Kudo et al. 2016), liver (Takegoshi, Okada et al. 2016), endometrial, ovarian and gastric cancer (Moll, Divo et al. 2008). K2CB protein was reported to be upregulated in breast

cancer (Wu, Hancock et al. 2003, Hamler, Zhu et al. 2004), skin carcinoma (Larcher, Bauluz et al. 1992), bladder cancer cells (Lei, Zhao et al. 2013) compared to non cancerous counterparts. However downregulation of the protein in cisplatin resistant esophageal cell line and lung cancer has also been reported (Lai, Chan et al. 2016, Hmmier, O'Brien et al. 2017).

In the present study, K2CB protein was identified from both HT-29 and CACO-2 cell lines as spot number 55 and match ID 35 respectively. The protein was upregulated following the treatments with Ox alone, Col alone and anatgonistic combined treatment of Ox with Col using 0/4 sequence of administration. In contrast, K2CB protein was downregulated after the treatment of EGCG alone and synergsitic combined treatment of Ox with EGCG using bolus administration in HT-29 cell line. However, the same protein was upregulated following the treatments of Cur alone and synergistic combined treatment of Ox with using bolus administration but downregulated after the treatment of Ox alone. The role of the protein remained unclear from this study due to inconsistency in the expression of K2CB protein following different treatments. For exanple, following Ox alone treatment in HT-29 cell line the protein was upregulated but downregulation was found in CACO-2 cell line with the same treatment. Highly synergistic combined treatment of Ox with EGCG (bolus) caused downregulation of K2CB protein in HT-29 cell line but upregulation was revealed in CACO-2 cell line following highly synergistic combination treatment of Ox with Cur (Bolus). However, literature suggests that K2CB protein contributes significantly in promoting colorectal cancer. Natural tumour active compound sulforaphene has been reported to give anticancer activity by supressing K2CB protein; subsequently increased Fas concentration, decreased cFLIP activity and induced apoptosis (Yang, Ren et al. 2016). In a study on 25 patients of prostate cancer while receiving chemotherapy, level of K18

was monitored which is usually coexpressed with K2CB protein. It was observed that circulatory K18 level was increased or decreased following adminstration of different drugs. The authors commented that cell death induced by chemotherapy does not inevitably depend on apoptosis, rather multiple mechanisms are involved (Ueno, Toi et al. 2005). Further study is required to ascertain the role of K2CB protein in colorectal cancer.

4.6.1.5 Keratin, type I cytoskeletal 18

Five major groups of intermediate filaments are found in human among which type I, type II, type III, type IV are cytoskeletal and type V is neucleoskeletal (Helfand, Chang et al. 2004). Keratins comprise the largest portion of intermediate filaments and belong into first two groups: type I and type II. K1C18 protein is a type I cytoskeletal 18 keratin (K18) protein which is highly conserved from teleosts to mammals. In 1950s the association of keratins including K1C18 protein was reported (Björklund and Björklund 1957, Björklund 1978). Later on it was discovered that K1C18 protein is cleaved during apoptosis of normal and malignant cells at two sites into three fragments (Ueno, Toi et al. 2005).

Upregulation of K1C18 protein in ovarian carcinoma (Wang, Kachman et al. 2004), cholangiocarcinoma (Srisomsap, Sawangareetrakul et al. 2004) and breast carcinoma (Wu, Hancock et al. 2003, Vergara, Simeone et al. 2013) has been observed in different studies. On the contrary, other studies showed downregulation of K1C18 protein in several cancers including: prostate (O'Connell, Prencipe et al. 2012), cervical (Buddaseth, Göttmann et al. 2013) and colon carcinoma (Roblick, Hirschberg et al. 2004). One earlier studies suggested upregulation of K1C18 protein is the good prognostic factor in breast cancer (Schaller, Fuchs et al. 1996).

In the present study, the protein has been identified from CACO-2 cell line. K1C18 protein was upregulated following all the treatments indicating that the protein might act as apoptotic protein. The highest upregulation of the protein was caused with Cur alone treatment by a factor of 7.26. Whereas, synergistic treatment of Ox with Cur (bolus) caused 6.26 folds upregulation of K1C18 protein and Ox alone produced 2.6 times upregulation of the same protein. Similar to this study, oxaliplatin has been reported to cause upregulation of the protein in three diffirent colorectal cancer cell lines (Yao, Jia et al. 2009). Moreover, the result of the present study is in accordance with earlier findings where maslinic acid (antitumour compound) downregulated the expression of K1C18 protein significantly in HT-29 colon cancer cell line (Rufino-Palomares, Reyes-Zurita et al. 2013). Another *in vivo* study also revealed that elevated expression of the protein leads to supression of malignancy in breast cancer cell (Bühler and Schaller 2005). It can be concluded that K1C18 protein is an apoptotic protein and could be targeted to design newer anticancer drugs.

4.6.2 Molecular chaperone

Living organism has to expose different stressful conditions throughout its life cycle to survive. For most of the organisms moderate increase in temperature above the optimum cause threats to their life. To cope with the challenge of heat stress and exposure of toxic agents, cells actuate the expression of heat shock proteins (HSPs) which subsequently undergo multiple signalling mechanisms to avoid cell death (Richter, Haslbeck et al. 2010). These heat shock proteins have been classified into seven different categories such as: molecular chaperones, proteolytic system associated proteins , DNA-RNA modifying enzymes, metabolic enzymes, transcription factors and kinases, cytoskeleton sustaining proteins, transport and detoxification associated

proteins. Among the above mentioned heat shock proteins, the most predominant are molecular chaperones across the species. These molecular chaperones are recognized as the first discovered HSPs which act during new protein synthesis by controlling folding and defolding of non native polypeptide chains (Ellis, Van der Vies et al. 1989). The most distinct feature of molecular chaperones which differentiate them from traditional enzymes is the ability to work in stoichiometric ratios. Molecular chaperones could be further categorized into HSP110, HSP100s, HSP90s, HSP70s, HSP60s, and small heat shock proteins. Three proteins belong to this group have been identified in this study which are discussed in the following section.

4.6.2.1 Heat shock cognate 71 kDa protein

Heat shock cognate 71 kDa protein (HSP7C) belongs to HSP70s class of molecular chaperones. There are at least 13 different proteins identified as a member of HSP70s, all of them sharing a highly conserved domain structure (N-terminal ATPase domain of 44 kDa, substrate-binding domain of 18 kDa and C-terminal domain of 10 kDa) (Kampinga, Hageman et al. 2009, Liu, Daniels et al. 2012). HSP7C protein is also called HSC70, located mainly in cytoplasm and considered as constitutively expressed protein which is encoded by HSPA8 gene. As a member of HSP70s class, the protein HSP7C has 85% similarity in amino acid sequence. Unlike to other HSP70s, HSP7C is mildly induced in stressed conditions but exhibit more intense effect on lipid bilayers by creating greater extent of protein folding and polypeptide translocation (Ahn, Kim et al. 2005). Other than the ATPase activity of HSP7C, it serves in different biological processes including: protein homeostasis, faciliate protein maturation and translocation, targetting protein for lysosomal and proteasomal degradation, regulation of apoptotic cell death, embryogenesis and ageing (Liu, Daniels et al. 2012). However some

cofactors/co-chaperones are inevitavle to perform the complete functions of HSP7C protein. Imporatnt cofactors are J domain, BAG family, CHIP, Hop, Hip, and HSPBP1.

In an earlier study, expression of HSP7C protein was found to be higher in cancerous cell lines compared to nonmalignant cells e.g. lung, gastric, pancreatic, breast, cervical and endometrial cancer (Maeda, Ohguro et al. 2000). The level of HSP7C protein was found to be significantly increased in 95% samples collected from the patients with colon cancer compared to the control group (Kubota, Yamamoto et al. 2010). The protein has been suggested as potential biomarker in neuroblastoma (Sandoval, Hoelz et al. 2006). In the present study, HSP7C protein was identified from both HT-29 and CACO-2 cell lines as match ID 39 and match ID 37 respectively. In HT-29 cell line, the protein was significantly upregulated following the treatments of Col alone, EGCG alone and synergistic combination of Ox with EGCG using bolus administration. Highest extent of upregulation of the protein was caused by the synergistic treatment and the lowest with Col alone treatment. However Ox alone and antagonistic combination treatments did not cause significant change in the expression of HSP7C protein. In contrast in CACO-2 cell line, the protein was upregulated following all the treatments. Synergistic combined treatment of Ox with using bolus administration produced highest upregulation by a factor of 4.53, followed by Cur alone treatment by the factor of 2.

From the above discussed results, it can be assumed that observed upregulation of HSP7C protein (following the treatments) and cell death might have a positive link. In both colorectal cell lines, synergistic combined treatments caused the highest amount of cell death. It could be the role of HSP7C protein as inducer of autophagy, promoting cytotoxity by upregulating HSP7C. The protein has been reported to induced all three

forms of autophagy: chaperone mediated autophagy, macroautoghagy and microautophagy (Stricher, Macri et al. 2013).

4.6.2.2 78 kDa glucose regulated protein

Among the 13 members of HSP70s class the major five proteins are HSP70 (HSPA1), HSPA6 (HSP70B), HSC70 (HSPA8), mortalin (HSPA9 or GRP75) and GRP78 (HSPA5) (Arispe and De Maio 2000). Another alternative name of GRP78 is Bip (immunoglobulin heavy-chain binding protein) which is mainly located in endoplasmic reticulum. 78 kDa glucose regulated protein or GRP78 acts a a master regulator during endoplasmic stress. The primary respnsibilty of GRP78 protein is to translocate the proteins, controlling the folding and assembly of proteins, identification and deletion of misfolded proteins (Macias, Williamson et al. 2011). GRP78 protein has the ability to bind with PERK, IRE1, and ATF6 and keep them in an inactive form during normal physiologic conditions. However, exposure of stress caused detachment of GRP78 protein from the mentioned transmembrane sensor proteins of endoplasnic reticulum and switches on the protective mechanism to avoid cell death (Lee 2007). Since cancer cells are continually subjected towards endoplasmic reticulum stress, GRP78 protein plays an integral role in survival of cancer cells and promote carcinogenesis. Literature suggests that GRP78 protein can also mediate chemotherapy resistance and inhibit apoptosis (Wang, Wey et al. 2009).

Elevated expression of GRP78 protein has been documented in many cancers: liver (Shuda, Kondoh et al. 2003), breast (Lee, Nichols et al. 2006), lung (Fu and Lee 2006) and prostate (Miyake, Hara et al. 2000, Daneshmand, Quek et al. 2007). In the present study, the protein was upregulated following all the treatments in CACO-2 cell line. Highest upregulation was evidenced after the treatment with Cur alone by the factor of

2.2 whereas Ox alone did upregulation of the protein by 1.61 times. Synergistic combined treament of Ox with Cur using bolus administration upregulated GRP78 protein by a factor of 1.56. However, it was difficult to undeterstand the relationship between observed upregulation of GRP78 protein following drug treatments and anticancer activity.

4.6.2.3 Nucleolar phosphoprotein B23

Nucleophosmin (NPM) is a 37 kDa phosphoprotein resided in the nucleolus of a cell and acts as a continous shuttle between nucleus and cytoplasm (Borer, Lehner et al. 1989). It is highly abundant and conserved protein, crucial for maintaining cellular homeostasis. Two isoforms of NPM is available in human namely: NPM1 and NPM1.2 which contain same sequences in their 5´ regions and almost identical in their coding region. However, they differ in 35 amino acids in C-terminal chain (Lim and Wang 2006). NPM serves as a multifunctional protein by transferring preribosomal particles for biogenesis of ribosome; maintaining stability of genome; regulating DNA transcription and molecular chaperoning activity (Grisendi, Mecucci et al. 2006). NPM protein does chaperone like activity for both proteins and nucleic acids and thus classified as nuclear chaperone (nucleoplasmin).

A large body of evidence suggest that NPM plays a key role in cancer pathogenesis. It modulates cell proliferation (Okuda, Horn et al. 2000, Colombo, Marine et al. 2002) and stimulates survival of cancer cells after damage to the DNA (Wu, Chang et al. 2002, Wu, Chang et al. 2002). However, delocalization of tumour suppressor protein p53 and ARF in absence of NPM has also been reported (Itahana, Bhat et al. 2003, Colombo, Bonetti et al. 2005). The dominancy of prooncogenic or antioncogenic activity depends on the level of expression and dosage of NPM. Overexpression of NPM has been

revealed in many types of malignancies e.g. colorectal (NOZAWA, VAN BELZEN et al. 1996), ovarian (Shields, Gerçel-Taylor et al. 1997), prostate (Subong, Shue et al. 1999) and gastric carcinoma (Tanaka, Sasaki et al. 1992). The potential mechanism through which NPM increases cell proliferation and inhibit apoptosis is given in Figure 4.6 ['a' indicates normal cell where complete balance in NPM; 'b' indicates cancer cell where NPM is overexpressed and cell proliferation is predominant; 'c' indicates the molecular mechanisms how cell proliferation is enhanced in tumour cell due to upregulation of NPM; and 'd' indicates the molecular mechanisms how cell death is inhibited in cancer cells due to elevated expression of NPM] (Grisendi, Mecucci et al. 2006).

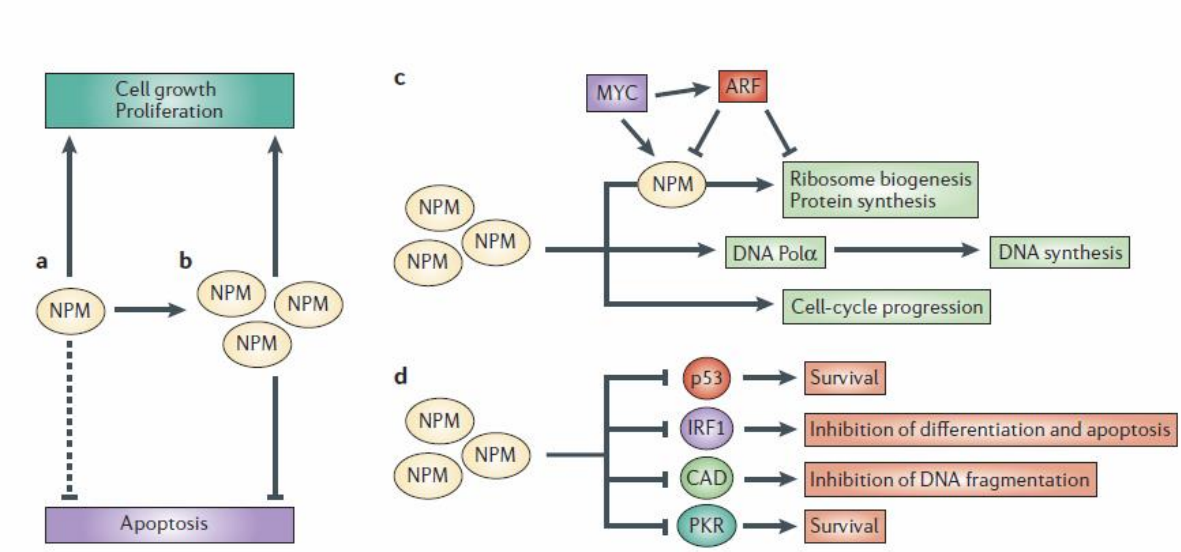

Figure 4.6: Promotion of tumorigenesis due to over expression of NPM [Adapted from Grisendi, Mecucci et al. 2006)]

In the present study, NPM protein was identified from HT-29 cell line and found to be downregulated following all the treatments except for Ox alone. The protein was extremely downregulated after the treatments with Col alone and synergistic combination of Ox with EGCG using bolus administration. In fact, the protein was

disappaered following both of the treatments. Following treatment with EGCG alone NPM protein was downregulated by the factor of 1.65 whereas antagonistic combination of Ox with Col using 0/4 sequence of administration did not cause significant changes in the expression of the protein. However, Ox alone treatment cause upregulation of the protein. It can be suggested from this study that NPM act as antiapoptic protein and can be targeted further to develop new anticancer agents. An earlier study also proposed that downregulation of NPM protein caused increased sensitivity of doxorubicin against lymphoma (Hsu, Zhao et al. 2007).

4.6.3 Metabolic enzymes

These are the proteins which are essential for cellular survival and homeostasis, serve diverse range of functions: digestion, respiration, preservation of energy, proteolysis and transcription. A variety of proteins have been included in this group such as: oxidases, peroxidases, oxygenases, reductases, hydrogenases, dehydrogenases, carboxylases, lipooxygenases, transferases and lyases etc. Two proteins were identified from this study which fell into the class of metabolic enzymes namely: GSTP1 and IDHC.

4.6.3.1 Glutathione S transferase P1

GSTP1 or Glutathione S transferase P1 belongs to the family of transferases which comprises of around 450 enzymes and functions for transferring functional groups from one compound to another. Glutathione S transferases (GSTs) catalyze nucleophilic attack of reduced glutathione (GSH) on another compounds having an electrophilic C, N, or S atom (Hayes, Flanagan et al. 2005). GSTs are categorized into three major classes namely: mitochondrial, cytosolic and microsomal. Mitochondrial and cytosolic GSTs share some structural similarities but no resemblance with microsomal type

(Holm, Morgenstern et al. 2002, Ladner, Parsons et al. 2004). Cytosolic GSTs have been futher classified into alpha (A), mu (M), pi (P), sigma (S), theta (T), zeta (Z) and omega (O) type (McIlwain, Townsend et al. 2006). GSTP1 is one of the subtypes of pi (P) class of GST, acts as a phase II drug-metabolising enzyme by conjugating glutathione with many toxic and electrophilic xenobiotics to convert into polar derivatives ready for excretion (Sawers, Ferguson et al. 2014). Highest expression of GSTP1 protein has been reported to be in brain followed by lung, placenta, kidney and pancrea. But expression of the protein in liver is negligible (Singh 2015). Structurally, GSTP1 protein is composed of domain 1 (N terminal end), linker and domain 2 (C terminal end). Amino domain adopts the resemblance of thioredoxin topology and contains 1-80 amino acid sequences (4 beta sheets flanking with 3 alpha helices). C terminal end is composed of 5 alpha helices containing residues 87-210. Domain 1 carries GSH binding site whereas domain 2 carries substrate binding site (Ålin, Jensson et al. 1985, Reinemer, Dirr et al. 1991). There are four genetic variants of GSTP1 have been discovered in human e.g. GSTP1*A, GSTP1*B, GSTP1*C and GSTP1*D (Laborde 2010).

The role of GSTP1 protein in mediating cancer has been reoprted strongly in scientific literature. Expression of GSTP1 was noticed to be associated with several transcription factors e.g. SP-1, AP-1, NF-κB and GATA1 (Moffat, McLaren et al. 1996, Duvoix, Delhalle et al. 2004). Multiple cell death pathways are also linked with GSTP1 protein such as : JNK1, ERK1/ERK2, or tumor necrosis factor receptor-associated factor 2 (TRAF2) (Ruscoe, Rosario et al. 2001, Wu, Fan et al. 2006). Figure 4.7 depicts the role of GSTP1 in tumorigenesis.

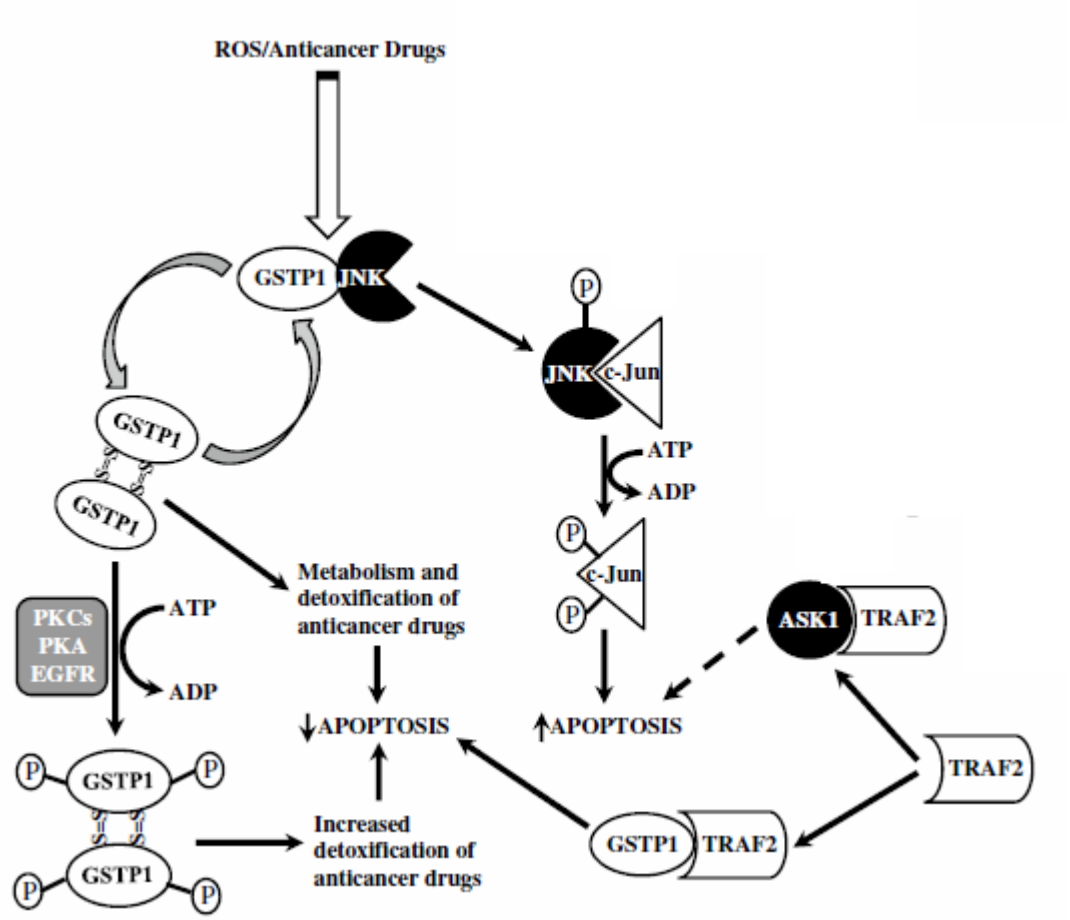

Figure 4.7: Signalling pathways linked with GSTP1 in mediating cancer

Upregulation of GSTP1 protein has been observed in many cancers including breast brain, colon, lung, oral, pancrea, bladder, rectal, testicular and pharyngeal (Schnekenburger, Karius et al. 2014, Singh 2015). In the present study, GSTP1 protein was identified from HT-29 cell line where it was upregulated following the treatments of Col alone and EGCG alone. However, the protein was downregulated following the synergistic combined treatment of Ox with EGCG using bolus administration. There was no significant changes observed after treatment with Ox alone and antagonistic combined treatment of Ox with Col using 0/4 sequence of administration. Due to variation of response in the expression of GSTP1 protein following drug treatments

alone and in combinations, the role of GSTP1 in colorectal cancer remained uncertain from this study.

4.6.3.2 Isocitrate dehydrogenase [NADP] cytoplasmic

IDHC or Isocitrate dehydrogenase [NADP] cytoplasmic is a protein belongs to oxidoreductase enzyme class. These enzymes are responsible for transfering electrons from oxidants to reductants which could be oxidases or dehydrogenases. Oxidases catalyzes the reactions when molecular oxygen acts as an acceptor of hydrogen/electrons. In contrast, dehydrogenases oxidize a substrate by transferring hydrogen to NAD^+/$NADP^+$. Isocitrate dehydrogenase (IDH) is an important enzyme required for catalyzing the conversion of isocitrate to alpha-ketoglutarate and CO_2 during Krebs cycle of aerobic glycolytic pathway (Cairns, Harris et al. 2011). Structurally IDH is a homodimer (46 kDa) consisting of of 416 residues with fourteen alpha helices and eighteen beta sheets. The α-helices are omnipresent in the protein structure, however the β-sheets are primarily located in the center of the structure. Three types of IDH have been identified in human: IDH1 or IDHC (NADP dependent, located in cytoplasm); IDH2 (NADP dependent, located in mitochondia) and IDH3 (NAD dependent, located in mitochondria) (Losman and Kaelin 2013). The key role of IDHC in normal cells is to faciliate the activity of the numerous cytoplasmic and nuclear dioxygenases that require 2-oxo-glutarate as a cosubstrate (Lee, Koh et al. 2002). Additionally, IDHC gives production of nonmitochondrial NADPH which is critical in lipid biosynthesis and protection of cells from oxidative stress and other injuries (Koh, Lee et al. 2004). Possible role of IDHC in lipogenesis and regulating redox homeostasis is given in Figure 4.8. Mutation of IDHC is evident in many cancers specially in glioma, which cause the enzyme to act in faster rate and more efficiently. However, controversy

still exists regarding the role of IDHC in cancer, whether it provides oncogenic effects or tumour suppressive effects (Reitman and Yan 2010).

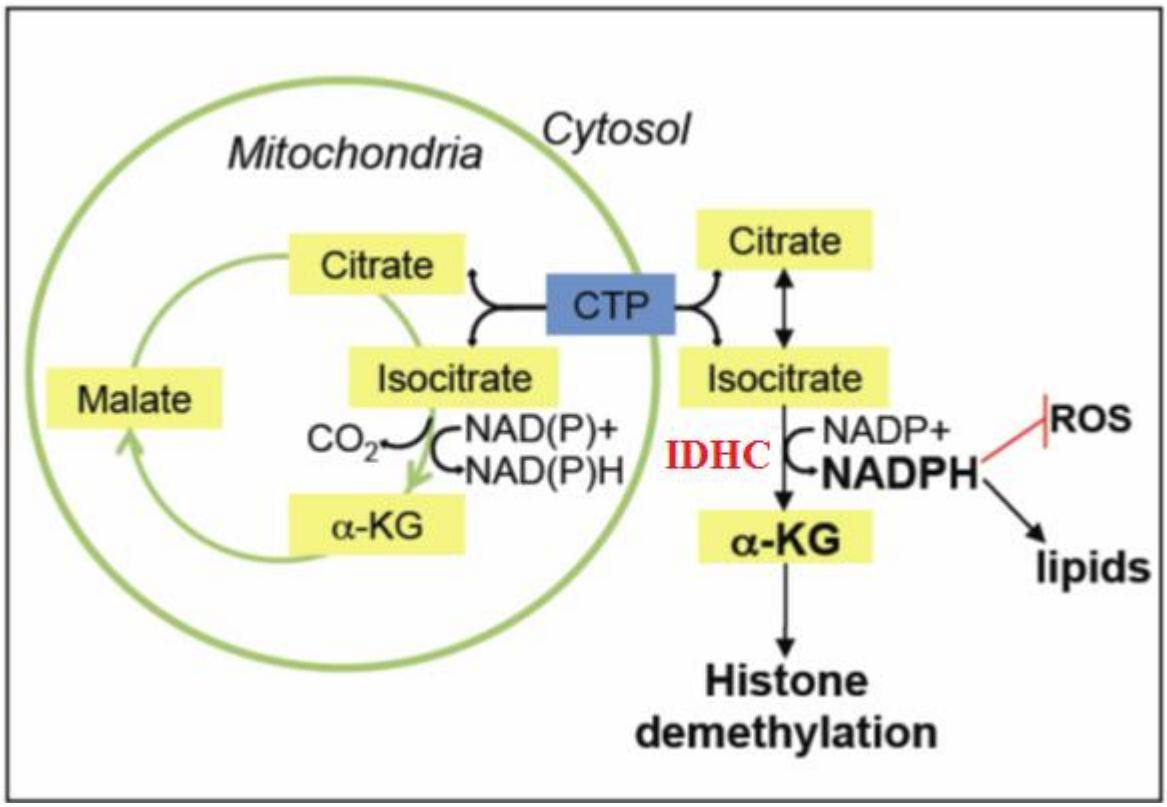

Figure 4.8: Role of IDHC in redox homeostasis and lipogenesis [Adapted from (Calvert 2017)]

In the present study, IDHC protein was identified from CACO-2 cell line. Following drug treatments either alone or in combination, the protein displayed uprgulation. Ox alone treatment caused the protein to be upregulated by 3 folds whereas Cur alone treatment did 1.8 folds upregulation. Synergistic combined treatment of Ox with Cur using bolus administration caused highest upregulation of IDHC by a factor of 5.75. It can be assumed from this study that IDHC protein might have proapoptotic action. To the best of my knowledge, this is the first report showing the changes in expression of IDHC protein in colorectal cancer cell following treatments with tumour active compounds. However, upregulation of IDHC protein has been documented in lung

(Tan, Jiang et al. 2012), breast (Russell Hilt, Wittliff et al. 1973, Xu, Yan et al. 2010) and esophageal cancer cells (Qi, Chiu et al. 2005) compared to their noncancerous counterparts. A recent study has proved that, elevated expression of IDHC protein leads towards aggravation of tumour and therapy resistance in glioblastoma. The author suggested that inhibition of IDHC protein could be a promising therapeutic strategy against glioblastoma (Calvert 2017).

4.6.4 Proteasome associated protein

Proteasome is a highly sophisticated protein complex expressed in nucleus and cytoplasm of all eukaryotes, which is responsible for selective hydrolysis of client proteins with the expenditure of metabolic energy. It works in combination with ubiquitin system exploiting cascade of enzymes categorized as E1, E2 and E3 (Adams 2003). Proteasome comprises of a 20S core subunit (catalytic core particle) which is connected with one or two 19S regulatory subunits (proteasome activator). Density-gradient centrifugation analysis of active proteasome revealed that sedimentation co-efficient value is 26S. This is why proteasome complex is sometimes referred to 26S proteasome as well (Tanaka 2009). Other than proteolysis, proteasome have been associated with wide range of functions including: tumour suppresson, regulation of cell cycle, modulation of transcription factors and anti-apoptotic proteins (Kisselev and Goldberg 2001). One protein namely PSB6, linked with proteasome has been displayed significant changes in expression in colorectal cancer model in this study.

4.6.4.1 Proteasome subunit beta type-6

PSB6 or proteasome subunit beta type-6 is part of 20S catalytic core of the proteasome. In regards to the structural conformation, 20S catalytic core looks like a cylinder which is composed of two alpha and two beta rings (Groll, Ditzel et al. 1997, Bhaumik and

Malik 2008). Each alpha and beta ring of 20S catalytic core consists of seven different components, named as alpha-1 to alpha-7 and beta-1 to beta-7 respectively. However, only three beta-components in the beta ring are catalytically active namely: chymotrypsin-like (beta-5), trypsin-like (beta-2), and caspase-like (beta-1). PSB6 protein modulates the cell cycle and many other processes through the break down of regulatory components and transcription factors (Frankland-Searby and Bhaumik 2012). Figure 4.9 protrays proteasome-ubiquitin pathway (Crawford, Walker et al. 2011). In the figure Ub refers to ubiquitin; C-L refers to caspase like; T-L refers to trypsin-like and CT-L refers to chymotrypsin-like.

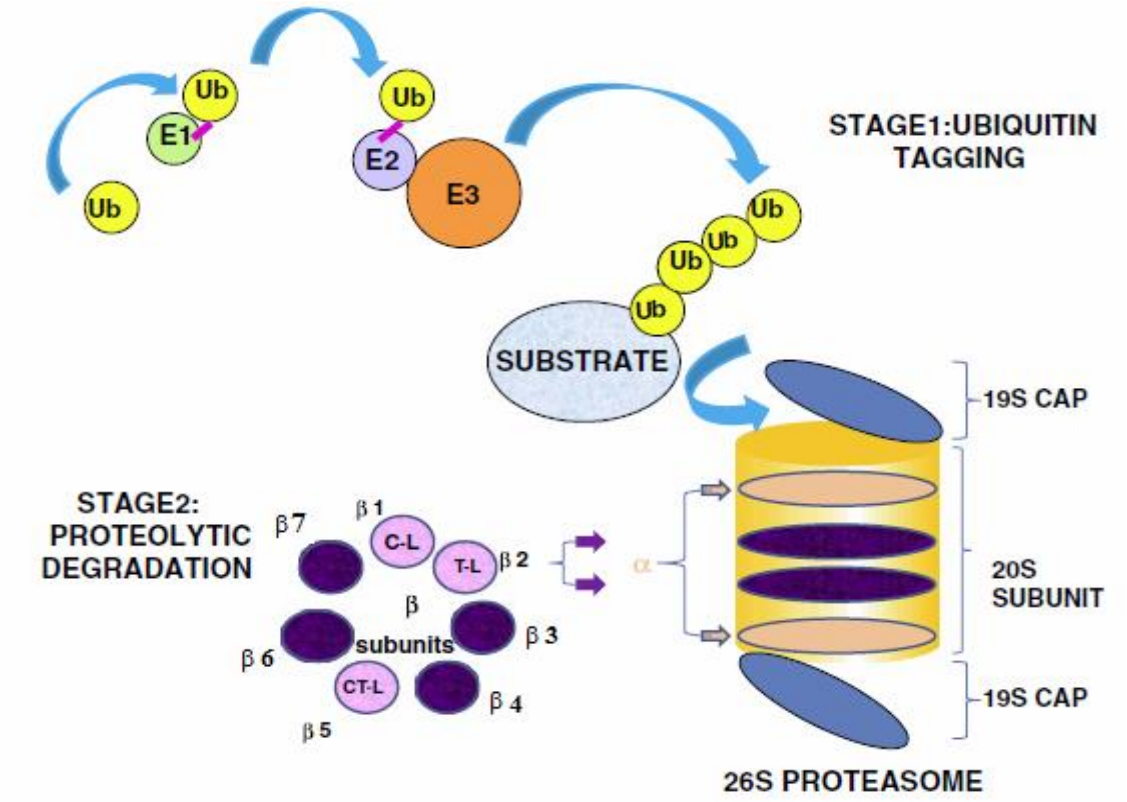

Figure 4.9: Schematic diagram representing ubiquitin-proteasome pathway [Adapted from (Crawford, Walker et al. 2011)]

Upregulation of PSB6 protein has been observed in lung cancer (Lu, Song et al. 2014), breast cancer (Canelle, Bousquet et al. 2006), thyroid cancer (Onda, Emi et al. 2004),

hypoxia (Wang, Xu et al. 2013) and prostate cancer (Davalieva, Kostovska et al. 2015). In a study of HCT-116 colon cancer cell line, elevated expression of the protein also detected. In the present study, PSB6 protein was downregulated after the treatment with Ox alone in CACO-2 cell line. In contrast, upregulation of the protein was observed following the treatment with Cur alone in the same cell line. But PSB6 protein did not show significant changes in expression following synergistic combined treatment of Ox with Cur using bolus administration in CACO-2 cell line. This might be due to counterbalancing effect between Ox and Cur. In accordance to this study, PSB6 protein reported to be upregulated following treatment with curcumin in a breast cancer model (Fang, Chen et al. 2011). Further study is warranted to target PSB6 protein as anticancer drug target.

4.6.5 Summary of proteomic study

In this study six proteins have identified to show significant changes in expression following different drug treatments in HT-29 colorectal cell line. The proteins are NPM, ACTB, TBB5, HSP7C, K2CB and GSTP1. Among these proteins, three (ACTB, TBB5 and K2CB) belong to the functional class of cytoskeletal proteins; two (NPM and HSP7C) belong to the functional class of molecular chaperone and one (GSTP1) belong to functional class of metabolic enzyme. Two proteins namely NPM and ACTB were identified as the antiapoptotic protein in this study.

Another seven proteins were identified from CACO-2 colorectal cancer cell line which displayed significant cahnges in expression following different drug treatments. The proteins are K2CB, HSP7C, GRP78, PSB6, COF1, IDHC and K1C18. Among these proteins, three (K2CB, COF1 and K1C18) were grouped in cytoplasmic protein class; two (HSP7C and GRP78) grouped into molecular chaperone class; one (IDHC) grouped

into metabolic enzyme class and one (PSB6) grouped in proteasome associated protein class. Two proteins namely K1C18 and IDHC was suggested to act as the proapoptotic protein in this study.

5 CONCLUSION

Colorectal cancer is one most common causes of death among cancer patients of both genders in developed countries. Recent trends show that the incidence of colororectal cancer is increasing more rapidly in developing countries than developed nations. Chemotherapy is the key to treat advanced level colorectal cancers when tumour cells are found to spread into other organs. Platinum drugs (cisplatin, oxaliplatin and carboplatin) constitute the frontline chemotherapeutic strategy of treating various cancers including colorectal cancer. Combination chemotherapy is now being preferred over single drug treatment due to complexity of metastasized colorectal cancer. But many such combinations increase the cost of overall treatment and side effects as well. Phytochemicals are one of the major sources of bioactive compounds having the potentiality to be used against cancer. In this study four such phytochemicals (curcumin, colchicine, EGCG and taxol) were selected for investigation in combination with platinum drugs (cisplatin and oxaliplatin) against four colororectal cancer cell lines (HT-29, CACO-2, LIM-1215 and LIM-2405). Mechanistic studies including DNA damage, cellular accumulation of platinums and platinum–DNA binding were carried out to investigate the reason behind the observed combined drug actions. Lastly, proteomic study was conducted to identify the proteins associated with the cytotoxic mechanisms of the drugs treated alone or in combination against colorectal cancer cell lines.

When the cell killing effects of the compounds were tested alone against colorectal cancer cell lines, colchicine was found to be the most active compound compared to other compounds including clinical standards. The second most active compound was taxol followed by oxaliplatin. 6-gingerol was found to be least active compound against

the tested cell lines and was not considered for combination studies. Based on the IC_{50} values obtained from MTT reduction assay, drugs were combined in binary mode at different concentrations (ED_{50}, ED_{75} and ED_{90}) and sequence of administrations (bolus, 0/4 h and 4/0 h). During combination studies against HT-29 cell line, combinations of cisplatin with colchine and cisplatin with EGCG produced synergism at ED_{50} levels at all added sequence of administrations. While other phychemicals (curcumin and taxol) in combination with cisplatin displayed antagonism at lower added concentrations irrespective of sequences of administrations against HT-29 cell lines. In contrast, oxaliplatin in combination with curcumin and EGCG showed synergism at ED_{50} levels at all added sequences of administrations in HT-29 cell line.

In CACO-2 cell line, at ED_{50} level only colchicine in combination with cisplatin produced synergism when administered using 0/4 and 4/0 sequence. No other phytochemicals in combination with cisplatin exhibited synergism in CACO-2 cell line at ED_{50} level. However, both curcumin and EGCG in combination with oxaliplatin displayed synergism irrespective of sequences in CACO-2 cell line at ED_{50} level. In LIM-1215 cell line, only curcumin in combination with cisplatin manifested synergism at all added sequnces of administrations at ED_{50} level. Intesrestingly, all phytochemicals in combination with oxaliplatin displayed synergism at all sequences of administrations in LIM-1215 cell line at ED_{50} level. Among all of these combinations treated in LIM-1215 cell line, highest degree of synergism was shown by curcumin with oxaliplatin at bolus administration. In LIM-2405 cell line, both curcumin and EGCG in combination with cisplatin displayed synergism at all sequences of administration at ED_{50} level. In contrast, only EGCG in combination with oxaliplatin exhibited synergism at all sequences of administrations at ED_{50} level in LIM-2405 cell line. All

other phytochemicals in combination with oxaliplatin showed antagonism at the same concentration and same cell line.

From cellular accumulation study in HT-29 and CACO-2 cell line, it was observed that synergistic combinations displayed greater extent of platinum accumulation than that found from cisplatin alone treatment indicating the positive correlation between synergism and platinum accumulation. However no specific trend was found from the study when phytochemicals were combined with oxaliplatin.

Platinum–DNA binding study in both HT-29 and CACO-2 cell lines proved that synergism observed from drug combinations was due to increased platinum-DNA binding. The results were confirmed from the both combined treatments: cisplatin with phytochemicals and oxaliplatin with phytochemicals. Synergistic combinations displayed higher binding and antagonistic combinations presented lower binding.

In DNA-damage study using HT-29 cell line, it was evident that Ox with Cur (4/0) was the most damaging towards DNA than any aother treated combinations. The least damaging was antagonistic combination of Ox with Tax (4/0). When the study was conducted in CACO-2 cell line, the highest damage was caused by Cis with Cur (4/0) followed by Ox with Cur (4/0 h). Among the combinations, the least damaging was again antagonistic combination of Ox with Tax (4/0 h). The study revealed that higher DNA damage might be an indication of increased cell killing but not to be necessarily true in all cases.

Eleven proteins were identified from this study which underwent significant changes in expression after different drug treatments. The proteins were NPM, ACTB, TBB5, HSP7C, K2CB, GSTP1, GRP78, PSB6, COF1, IDHC and K1C18. All of the identified proteins were found to be either directly or indirectly related to cell cycle, cell proliferation and cell death pathways. Two of those proteins namely: NPM and ACTB

were suggested to be antiapoptotic protein from this study. Another two proteins namely: IDHC and K1C18 were considered to be proapoptotic protein from this study.

Potential future directions

The instinctive way of research is continuous and ongoing journey. The more we go forward the more avenues create and instigate us to proceed further. Since this preliminary in vitro model study revelas the potentiality of phytochemicals to be used in combination with platinum drugs against colorectal cancer, it could be taken further using suitable animal model for evaluation of activity in vivo and toxicity profile. We propose that the combination of oxaliplatin with curcumin, cisplatin with colchicine and oxaliplatin with EGCG are the most suitable candidates for future animal model study. The proteomic study could also be extended to identify all proteins which showed significant changes in expression following different treatments from both HT-29 and CACO-2 cell lines. Bioinformatics analysis of the identified proteins can also be done using various pathways e.g. Ingenuity pathway, KEGG pathway and so on.

6 References

Abdullah, A., F. Huq and P. Beale (2003). "Studies on platinum (II) complexes of the forms: cis-PtL (NH." Journal of Inorganic Biochemistry **96**: 85.

Abdullah, A., F. Huq, A. Chowdhury, H. Tayyem, P. Beale and K. Fisher (2006). "Studies on the synthesis, characterization, binding with DNA and activities of two cis-planaramineplatinum (II) complexes of the form: cis-PtL (NH 3) Cl 2 where L= 3-hydroxypyridine and 2, 3-diaminopyridine." BMC chemical biology **6**(1): 3.

Adams, J. (2003). "The proteasome: structure, function, and role in the cell." Cancer Treatment Reviews **29**: 3-9.

Aebi, S., B. Kurdi-Haidar, R. Gordon, B. Cenni, H. Zheng, D. Fink, R. D. Christen, C. R. Boland, M. Koi and R. Fishel (1996). "Loss of DNA mismatch repair in acquired resistance to cisplatin." Cancer research **56**(13): 3087-3090.

Ahmed, A., N. R. Peters, M. K. Fitzgerald, J. A. Watson, F. M. Hoffmann and J. S. Thorson (2006). "Colchicine glycorandomization influences cytotoxicity and mechanism of action." Journal of the American Chemical Society **128**(44): 14224-14225.

Ahn, S.-G., S.-A. Kim, J.-H. Yoon and P. Vacratsis (2005). "Heat-shock cognate 70 is required for the activation of heat-shock factor 1 in mammalian cells." Biochemical Journal **392**(1): 145-152.

Al-Eisawi, Z., P. Beale, C. Chan, Q. Y. Jun and F. Huq (2013). "Carboplatin and oxaliplatin in sequenced combination with bortezomib in ovarian tumour models." Journal of ovarian research **6**(1): 78.

Al-Eisawi, Z., P. Beale, C. Chan, J. Q. Yu, N. Proschogo, M. Molloy and F. Huq (2016). "Changes in the in vitro activity of platinum drugs when administered in two aliquots." BMC cancer **16**(1): 688.

Al-Lazikani, B., U. Banerji and P. Workman (2012). "Combinatorial drug therapy for cancer in the post-genomic era." Nat Biotechnol **30**(7): 679-692.

Alam, M. N., M. Almoyad and F. Huq (2018). "Polyphenols in Colorectal Cancer: Current State of Knowledge including Clinical Trials and Molecular Mechanism of Action." BioMed Research International **2018**.

Alamro, A. A. S. (2015). "Studies on combination between tumour active compounds in ovarian tumour models."

Alcindor, T. and N. Beauger (2011). "Oxaliplatin: a review in the era of molecularly targeted therapy." Current Oncology **18**(1): 18-25.

Ålin, P., H. Jensson, C. Guthenberg, U. H. Danielson, M. K. Tahir and B. Mannervik (1985). "Purification of major basic glutathione transferase isoenzymes from rat liver by use of affinity chromatography and fast protein liquid chromatofocusing." Analytical biochemistry **146**(2): 313-320.

Alshehri, A., P. Beale, J. Qing Yu and F. Huq (2011). "Synergism from Combination of Cisplatin and Multicentred Platinums Coded as DH6Cl and TH1 in the Human Ovarian Tumour Models." Medicinal Chemistry **7**(6): 593-598.

Amidi, A., S. Hosseini, A. Leemans, S. R. Kesler, M. Agerbæk, L. M. Wu and R. Zachariae (2017). "Changes in brain structural networks and cognitive functions in testicular cancer patients receiving cisplatin-based chemotherapy." JNCI: Journal of the National Cancer Institute **109**(12).

Anastasiadi, M., K. Polizzi and R. J. Lambert (2018). "An improved model for the analysis of combined antimicrobials: a replacement for the Chou–Talalay combination index method." Journal of applied microbiology **124**(1): 97-107.

Andersen, C. L., J. L. Jensen and T. F. Ørntoft (2004). "Normalization of real-time quantitative reverse transcription-PCR data: a model-based variance estimation approach to identify genes suited for normalization, applied to bladder and colon cancer data sets." Cancer research **64**(15): 5245-5250.

Arango, D., A. J. Wilson, Q. Shi, G. A. Corner, M. J. Aranes, C. Nicholas, M. Lesser, J. M. Mariadason and L. H. Augenlicht (2004). "Molecular mechanisms of action and prediction of response to oxaliplatin in colorectal cancer cells." Br J Cancer **91**(11): 1931-1946.

Arispe, N. and A. De Maio (2000). "ATP and ADP Modulate a Cation Channel Formed by Hsc70 in Acidic Phospholipid Membranes." Journal of Biological Chemistry **275**(40): 30839-30843.

Arzuman, L. (2014). "Studies on newly designed monofunctional platinums as potential anticancer drugs."

Arzuman, L., P. Beale, J. Q. Yu and F. Huq (2016). "Synthesis of tris (quinoline) monochloroplatinum (II) Chloride and its Activity Alone and in Combination with Capsaicin and Curcumin in Human Ovarian Cancer Cell Lines." Anticancer research **36**(6): 2809-2818.

Ashton, J. C. (2015). "Drug Combination Studies and Their Synergy Quantification Using the Chou–Talalay Method." Cancer research **75**(11): 2400-2400.

Baguley, B. C., K. M. Holdaway, L. L. Thomsen, L. Zhuang and L. Jonathan Zwi (1991). "Inhibition of growth of colon 38 adenocarcinoma by vinblastine and colchicine: Evidence for a vascular mechanism." European Journal of Cancer **27**(4): 482-487.

Balasubramanian, E. and T. Gajendran (2013). "Comparative studies on the anticancer activity of colchicine by various controlled drug delivery modes." Int J Pharm Bio Sci **4**(1): 9-26.

Bayat Mokhtari, R., T. S. Homayouni, N. Baluch, E. Morgatskaya, S. Kumar, B. Das and H. Yeger (2017). "Combination therapy in combating cancer." Oncotarget **8**(23): 38022-38043.

Beganovic, M., M. K. Luther, L. B. Rice, C. A. Arias, M. J. Rybak and K. L. LaPlante (2018). "A Review of Combination Antimicrobial Therapy for Enterococcus Faecalis Bloodstream Infections and Infective Endocarditis." Clinical Infectious Diseases.

Beil, M., A. Micoulet, G. von Wichert, S. Paschke, P. Walther, M. B. Omary, P. P. Van Veldhoven, U. Gern, E. Wolff-Hieber and J. Eggermann (2003). "Sphingosylphosphorylcholine regulates keratin network architecture and visco-elastic properties of human cancer cells." Nature cell biology **5**(9): 803.

Bernstein, B. W. and J. R. Bamburg (2010). "ADF/cofilin: a functional node in cell biology." Trends in cell biology **20**(4): 187-195.

Bezanilla, M., A. S. Gladfelter, D. R. Kovar and W.-L. Lee (2015). "Cytoskeletal dynamics: A view from the membrane." The Journal of Cell Biology **209**(3): 329-337.

Bhattacharyya, B., D. Panda, S. Gupta and M. Banerjee (2008). "Anti-mitotic activity of colchicine and the structural basis for its interaction with tubulin." Medicinal research reviews **28**(1): 155-183.

Bhaumik, S. R. and S. Malik (2008). "Diverse regulatory mechanisms of eukaryotic transcriptional activation by the proteasome complex." Critical reviews in biochemistry and molecular biology **43**(6): 419-433.

Björklund, B. (1978). Tissue polypeptide antigen (TPA): biology, biochemistry, improved assay methodology, clinical significance in cancer and other conditions, and future outlook. Laboratory testing for cancer, Karger Publishers. **22:** 16-31.

Björklund, B. and V. Björklund (1957). "Antigenicity of pooled human malignant and normal tissues by cyto-immunological technique: presence of an insoluble, heat-labile tumor antigen." International Archives of Allergy and Immunology **10**(3): 153-184.

Blakey, D. C., F. R. Westwood, M. Walker, G. D. Hughes, P. D. Davis, S. E. Ashton and A. J. Ryan (2002). "Antitumor activity of the novel vascular targeting agent ZD6126 in a panel of tumor models." Clinical Cancer Research **8**(6): 1974-1983.

Block, K. I., A. C. Koch, M. N. Mead, P. K. Tothy, R. A. Newman and C. Gyllenhaal (2008). "Impact of antioxidant supplementation on chemotherapeutic toxicity: a systematic review of the evidence from randomized controlled trials." International Journal of Cancer **123**(6): 1227-1239.

Borer, R., C. Lehner, H. Eppenberger and E. Nigg (1989). "Major nucleolar proteins shuttle between nucleus and cytoplasm." Cell **56**(3): 379-390.

Buddaseth, S., W. Göttmann, R. Blasczyk and T. Huyton (2013). "Dysregulation of cell cycle control caused by overexpression of the oncogene pp32r1 (ANP32C) and the Tyr> His mutant pp32r1Y140H." Biochimica et Biophysica Acta (BBA)-Molecular Cell Research **1833**(5): 1212-1221.

Bühler, H. and G. Schaller (2005). "Transfection of keratin 18 gene in human breast cancer cells causes induction of adhesion proteins and dramatic regression of malignancy in vitro and in vivo." Molecular cancer research **3**(7): 365-371.

Bunnell, T. M., B. J. Burbach, Y. Shimizu and J. M. Ervasti (2011). "β-Actin specifically controls cell growth, migration, and the G-actin pool." Molecular biology of the cell **22**(21): 4047-4058.

Cairns, R. A., I. S. Harris and T. W. Mak (2011). "Regulation of cancer cell metabolism." Nature Reviews Cancer **11**(2): 85.

Calvert, A. E. (2017). Cancer-Associated Isocitrate Dehydrogenase 1 Promotes Growth and Resistance to Targeted Therapies in the Absence of Mutation, Northwestern University.

Canelle, L., J. Bousquet, C. Pionneau, J. Hardouin, G. Choquet-Kastylevsky, R. Joubert-Caron and M. Caron (2006). "A proteomic approach to investigate potential

biomarkers directed against membrane-associated breast cancer proteins." Electrophoresis **27**(8): 1609-1616.

Caulin, C., C. F. Ware, T. M. Magin and R. G. Oshima (2000). "Keratin-dependent, epithelial resistance to tumor necrosis factor-induced apoptosis." The Journal of cell biology **149**(1): 17-22.

Chakrabarti, M., M. Khandkar, N. L. Banik and S. K. Ray (2012). "Alterations in expression of specific microRNAs by combination of 4-HPR and EGCG inhibited growth of human malignant neuroblastoma cells." Brain Research **1454**: 1-13.

Chambers, A. F., A. C. Groom and I. C. MacDonald (2002). "Metastasis: dissemination and growth of cancer cells in metastatic sites." Nature Reviews Cancer **2**(8): 563.

Chen, H., C. N. Landen, Y. Li, R. D. Alvarez and T. O. Tollefsbol (2013). "Epigallocatechin gallate and sulforaphane combination treatment induce apoptosis in paclitaxel-resistant ovarian cancer cells through hTERT and Bcl-2 down-regulation." Experimental Cell Research **319**(5): 697-706.

Chong, C. R. and D. J. Sullivan Jr (2007). "New uses for old drugs." Nature **448**(7154): 645.

Chopade, V., A. Phatak, A. Upaganlawar and A. Tankar (2008). "Green tea (Camellia sinensis): Chemistry, traditional, medicinal uses and its pharmacological activities-a review." Pharmacognosy Reviews **2**(3): 157.

Chou, T.-C. and P. Talalay (1984). "Quantitative analysis of dose-effect relationships: the combined effects of multiple drugs or enzyme inhibitors." Advances in enzyme regulation **22**: 27-55.

Chua, B. T., C. Volbracht, K. O. Tan, R. Li, C. Y. Victor and P. Li (2003). "Mitochondrial translocation of cofilin is an early step in apoptosis induction." Nature cell biology **5**(12): 1083.

Colombo, E., P. Bonetti, E. L. Denchi, P. Martinelli, R. Zamponi, J.-C. Marine, K. Helin, B. Falini and P. G. Pelicci (2005). "Nucleophosmin is required for DNA integrity and p19Arf protein stability." Molecular and cellular biology **25**(20): 8874-8886.

Colombo, E., J.-C. Marine, D. Danovi, B. Falini and P. G. Pelicci (2002). "Nucleophosmin regulates the stability and transcriptional activity of p53." Nature cell biology **4**(7): 529.

Comess, K. M. and S. J. Lippard (1993). Molecular aspects of platinum-DNA interactions. Molecular aspects of anticancer drug-DNA Interactions, Springer**:** 134-168.

Cortesi, L., A. Barchetti, E. De Matteis, E. Rossi, L. Della Casa, L. Marcheselli, G. Tazzioli, M. G. Lazzaretti, G. Ficarra and M. Federico (2009). "Identification of protein clusters predictive of response to chemotherapy in breast cancer patients." Journal of proteome research **8**(11): 4916-4933.

Crawford, L. J., B. Walker and A. E. Irvine (2011). "Proteasome inhibitors in cancer therapy." Journal of cell communication and signaling **5**(2): 101-110.

Cvitkovic, E. (1998). "Ongoing and unsaid on oxaliplatin: the hope." British Journal Of Cancer **77**: 8.

Daneshmand, S., M. L. Quek, E. Lin, C. Lee, R. J. Cote, D. Hawes, J. Cai, S. Groshen, G. Lieskovsky and D. G. Skinner (2007). "Glucose-regulated protein GRP78 is up-regulated in prostate cancer and correlates with recurrence and survival." Human pathology **38**(10): 1547-1552.

Davalieva, K., I. M. Kostovska, S. Kiprijanovska, K. Markoska, K. Kubelka-Sabit, V. Filipovski, S. Stavridis, O. Stankov, S. Komina and G. Petrusevska (2015). "Proteomics analysis of malignant and benign prostate tissue by 2D DIGE/MS reveals new insights into proteins involved in prostate cancer." The Prostate **75**(14): 1586-1600.

Deogade, S. C. and S. Ghate (2015). "CURCUMIN: THERAPEUTIC APPLICATIONS IN SYSTEMIC AND ORAL HEALTH." International Journal of Biological & Pharmaceutical Research **6**(4): 281-290.

Di Francesco, A. M., A. Ruggiero and R. Riccardi (2002). "Cellular and molecular aspects of drugs of the future: oxaliplatin." Cell Mol Life Sci **59**(11): 1914-1927.

Dominguez, R. and K. C. Holmes (2011). "Actin structure and function."

Dove, A. (1999). "Proteomics: translating genomics into products?" Nature biotechnology **17**(3): 233.

Duvoix, A., S. Delhalle, R. Blasius, M. Schnekenburger, F. Morceau, M. Fougere, E. Henry, M.-M. Galteau, M. Dicato and M. Diederich (2004). "Effect of chemopreventive agents on glutathione S-transferase P1-1 gene expression mechanisms via activating protein 1 and nuclear factor kappaB inhibition." Biochemical pharmacology **68**(6): 1101-1111.

Dydensborg, A. B., E. Herring, J. Auclair, E. Tremblay and J.-F. Beaulieu (2006). "Normalizing genes for quantitative RT-PCR in differentiating human intestinal epithelial cells and adenocarcinomas of the colon." American Journal of Physiology-Gastrointestinal and Liver Physiology **290**(5): G1067-G1074.

Edwards, S. E., I. d. C. Rocha, E. M. Williamson and M. Heinrich (2015). Ginger. Phytopharmacy, John Wiley & Sons, Ltd**:** 164-167.

Ellis, R. J., S. M. Van der Vies and S. M. Hemmingsen (1989). "The molecular chaperone concept." Biochemical Society Symposia **55**: 145-153.

Evan, G. I. and K. H. Vousden (2001). "Proliferation, cell cycle and apoptosis in cancer." Nature **411**(6835): 342.

Fan, N.-J., C.-F. Gao and X.-L. Wang (2013). "Tubulin beta chain, filamin A alpha isoform 1, and cytochrome b-c1 complex subunit 1 as serological diagnostic biomarkers of esophageal squamous cell carcinoma: a proteomics study." Omics: a journal of integrative biology **17**(4): 215-223.

Fan, N.-J., R. Kang, X.-Y. Ge, M. Li, Y. Liu, H.-M. Chen and C.-F. Gao (2014). "Identification alpha-2-HS-glycoprotein precursor and tubulin beta chain as serology diagnosis biomarker of colorectal cancer." Diagnostic pathology **9**(1): 53.

Fan, N.-J., K. Li, Q.-Y. Liu, X.-L. Wang, L. Hu, J.-T. Li and C.-F. Gao (2013). "Identification of tubulin beta chain, thymosin beta-4-like protein 3, and cytochrome b–c1 complex subunit 1 as serological diagnostic biomarkers of gastric cancer." Clinical biochemistry **46**(15): 1578-1584.

Fang, H., S. Chen, D. Guo, S. Pan and Z. Yu (2011). "Proteomic identification of differentially expressed proteins in curcumin-treated MCF-7 cells." Phytomedicine **18**(8-9): 697-703.

Fearon, E. R. and B. Vogelstein (1990). "A genetic model for colorectal tumorigenesis." Cell **61**(5): 759-767.

Ferlay, J., I. Soerjomataram, M. Ervik, R. Dikshit, S. Eser, C. Mathers, M. Rebelo, D. Parkin, D. Forman and F. Bray (2015). "GLOBOCAN 2012 v1. 0, Cancer Incidence and Mortality Worldwide: IARC Cancer Base No. 11. 2014." Available from: globocan. iarc. fr.

Fischel, J. L., P. Formento, J. Ciccolini, P. Rostagno, M. C. Etienne, J. Catalin and G. Milano (2002). "Impact of the oxaliplatin-5 fluorouracil-folinic acid combination on respective intracellular determinants of drug activity." Br J Cancer **86**(7): 1162-1168.

Frankland-Searby, S. and S. R. Bhaumik (2012). "The 26S proteasome complex: an attractive target for cancer therapy." Biochimica et Biophysica Acta (BBA)-Reviews on Cancer **1825**(1): 64-76.

FREI, E., M. KARON, R. H. LEVIN, E. J. FREIREICH, R. J. TAYLOR, J. HANANIAN, O. SELAWRY, J. F. HOLLAND, B. HOOGSTRATEN and I. J. WOLMAN (1965). "The effectiveness of combinations of antileukemic agents in inducing and maintaining remission in children with acute leukemia." Blood **26**(5): 642-656.

Friboulet, L., K. A. Olaussen, J.-P. Pignon, F. A. Shepherd, M.-S. Tsao, S. Graziano, R. Kratzke, J.-Y. Douillard, L. Seymour and R. Pirker (2013). "ERCC1 isoform expression and DNA repair in non–small-cell lung cancer." New England journal of medicine **368**(12): 1101-1110.

Fu, Y. and A. S. Lee (2006). "Glucose regulated proteins in cancer progression, drug resistance and immunotherapy." Cancer biology & therapy **5**(7): 741-744.

Fujie, Y., H. Yamamoto, C. Y. Ngan, A. Takagi, T. Hayashi, R. Suzuki, K. Ezumi, I. Takemasa, M. Ikeda and M. Sekimoto (2005). "Oxaliplatin, a potent inhibitor of survivin, enhances paclitaxel-induced apoptosis and mitotic catastrophe in colon cancer cells." Japanese journal of clinical oncology **35**(8): 453-463.

Fujiki, H., E. Sueoka, T. Watanabe and M. Suganuma (2015). "Synergistic enhancement of anticancer effects on numerous human cancer cell lines treated with the combination of EGCG, other green tea catechins, and anticancer compounds." Journal of Cancer Research and Clinical Oncology **141**(9): 1511-1522.

Gall Troselj, K. and R. Novak Kujundzic (2014). "Curcumin in combined cancer therapy." Current pharmaceutical design **20**(42): 6682-6696.

Galluzzi, L., J. M. Bravo-San Pedro, O. Kepp and G. Kroemer (2016). "Regulated cell death and adaptive stress responses." Cellular and Molecular Life Sciences **73**(11): 2405-2410.

Galluzzi, L., I. Vitale, S. A. Aaronson, J. M. Abrams, D. Adam, P. Agostinis, E. S. Alnemri, L. Altucci, I. Amelio, D. W. Andrews, M. Annicchiarico-Petruzzelli, A. V. Antonov, E. Arama, E. H. Baehrecke, N. A. Barlev, N. G. Bazan, F. Bernassola, M. J. M. Bertrand, K. Bianchi, M. V. Blagosklonny, K. Blomgren, C. Borner, P. Boya, C. Brenner, M. Campanella, E. Candi, D. Carmona-Gutierrez, F. Cecconi, F. K. M. Chan,

N. S. Chandel, E. H. Cheng, J. E. Chipuk, J. A. Cidlowski, A. Ciechanover, G. M. Cohen, M. Conrad, J. R. Cubillos-Ruiz, P. E. Czabotar, V. D'Angiolella, T. M. Dawson, V. L. Dawson, V. De Laurenzi, R. De Maria, K.-M. Debatin, R. J. DeBerardinis, M. Deshmukh, N. Di Daniele, F. Di Virgilio, V. M. Dixit, S. J. Dixon, C. S. Duckett, B. D. Dynlacht, W. S. El-Deiry, J. W. Elrod, G. M. Fimia, S. Fulda, A. J. García-Sáez, A. D. Garg, C. Garrido, E. Gavathiotis, P. Golstein, E. Gottlieb, D. R. Green, L. A. Greene, H. Gronemeyer, A. Gross, G. Hajnoczky, J. M. Hardwick, I. S. Harris, M. O. Hengartner, C. Hetz, H. Ichijo, M. Jäättelä, B. Joseph, P. J. Jost, P. P. Juin, W. J. Kaiser, M. Karin, T. Kaufmann, O. Kepp, A. Kimchi, R. N. Kitsis, D. J. Klionsky, R. A. Knight, S. Kumar, S. W. Lee, J. J. Lemasters, B. Levine, A. Linkermann, S. A. Lipton, R. A. Lockshin, C. López-Otín, S. W. Lowe, T. Luedde, E. Lugli, M. MacFarlane, F. Madeo, M. Malewicz, W. Malorni, G. Manic, J.-C. Marine, S. J. Martin, J.-C. Martinou, J. P. Medema, P. Mehlen, P. Meier, S. Melino, E. A. Miao, J. D. Molkentin, U. M. Moll, C. Muñoz-Pinedo, S. Nagata, G. Nuñez, A. Oberst, M. Oren, M. Overholtzer, M. Pagano, T. Panaretakis, M. Pasparakis, J. M. Penninger, D. M. Pereira, S. Pervaiz, M. E. Peter, M. Piacentini, P. Pinton, J. H. M. Prehn, H. Puthalakath, G. A. Rabinovich, M. Rehm, R. Rizzuto, C. M. P. Rodrigues, D. C. Rubinsztein, T. Rudel, K. M. Ryan, E. Sayan, L. Scorrano, F. Shao, Y. Shi, J. Silke, H.-U. Simon, A. Sistigu, B. R. Stockwell, A. Strasser, G. Szabadkai, S. W. G. Tait, D. Tang, N. Tavernarakis, A. Thorburn, Y. Tsujimoto, B. Turk, T. Vanden Berghe, P. Vandenabeele, M. G. Vander Heiden, A. Villunger, H. W. Virgin, K. H. Vousden, D. Vucic, E. F. Wagner, H. Walczak, D. Wallach, Y. Wang, J. A. Wells, W. Wood, J. Yuan, Z. Zakeri, B. Zhivotovsky, L. Zitvogel, G. Melino and G. Kroemer (2018). "Molecular mechanisms of cell death: recommendations of the Nomenclature Committee on Cell Death 2018." Cell Death & Differentiation.

Galluzzi, L., I. Vitale, J. Michels, C. Brenner, G. Szabadkai, A. Harel-Bellan, M. Castedo and G. Kroemer (2014). "Systems biology of cisplatin resistance: past, present and future." Cell Death &Amp; Disease **5**: e1257.

Ghosh, M., X. Song, G. Mouneimne, M. Sidani, D. S. Lawrence and J. S. Condeelis (2004). "Cofilin promotes actin polymerization and defines the direction of cell motility." Science **304**(5671): 743-746.

Grisendi, S., C. Mecucci, B. Falini and P. P. Pandolfi (2006). "Nucleophosmin and cancer." Nature Reviews Cancer **6**(7): 493.

Groll, M., L. Ditzel, J. Löwe, D. Stock, M. Bochtler, H. D. Bartunik and R. Huber (1997). "Structure of 20S proteasome from yeast at 2.4 Å resolution." Nature **386**(6624): 463.

Gudzune, K. A., A. K. Monroe, R. Sharma, P. D. Ranasinghe, Y. Chelladurai and K. A. Robinson (2014). "Effectiveness of combination therapy with statin and another lipid-modifying agent compared with intensified statin monotherapy: a systematic review." Annals of internal medicine **160**(7): 468-476.

Guo, C., S. Liu, J. Wang, M.-Z. Sun and F. T. Greenaway (2013). "ACTB in cancer." Clinica Chimica Acta **417**: 39-44.

Gupta, R. K., A. K. Patel, N. Shah, A. Chaudhary, U. Jha, U. C. Yadav, P. K. Gupta and U. Pakuwal (2014). "Oxidative stress and antioxidants in disease and cancer." Asian Pac. Cancer Prev **15**: 4405-4409.

Gupta, S. C., B. Sung, J. H. Kim, S. Prasad, S. Li and B. B. Aggarwal (2013). "Multitargeting by turmeric, the golden spice: from kitchen to clinic." Molecular nutrition & food research **57**(9): 1510-1528.

Haldar, S., J. Chintapalli and C. M. Croce (1996). "Taxol induces bcl-2 phosphorylation and death of prostate cancer cells." Cancer research **56**(6): 1253-1255.

Hall, A. (2009). "The cytoskeleton and cancer." Cancer and Metastasis Reviews **28**(1): 5-14.

Hamel, E. (2008). An overview of compounds that interact with tubulin and their effects on microtubule assembly. The Role of Microtubules in Cell Biology, Neurobiology, and Oncology, Springer**:** 1-19.

Hamler, R. L., K. Zhu, N. S. Buchanan, P. Kreunin, M. T. Kachman, F. R. Miller and D. M. Lubman (2004). "A two-dimensional liquid-phase separation method coupled with mass spectrometry for proteomic studies of breast cancer and biomarker identification." Proteomics **4**(3): 562-577.

Han, L., M. B. Stope, M. L. De Jesús, P. A. O. Weernink, M. Urban, T. Wieland, D. Rosskopf, K. Mizuno, K. H. Jakobs and M. Schmidt (2007). "Direct stimulation of receptor-controlled phospholipase D1 by phospho-cofilin." The EMBO journal **26**(19): 4189-4202.

Hanahan, D. and R. A. Weinberg (2011). "Hallmarks of cancer: the next generation." cell **144**(5): 646-674.

Hayes, J. D., J. U. Flanagan and I. R. Jowsey (2005). "Glutathione transferases." Annu. Rev. Pharmacol. Toxicol. **45**: 51-88.

Helfand, B. T., L. Chang and R. D. Goldman (2004). "Intermediate filaments are dynamic and motile elements of cellular architecture." Journal of cell science **117**(2): 133-141.

Herman, I. M. (1993). "Actin isoforms." Current opinion in cell biology **5**(1): 48-55.

Hmmier, A., M. E. O'Brien, V. Lynch, M. Clynes, R. Morgan and P. Dowling (2017). "Proteomic analysis of bronchoalveolar lavage fluid (BALF) from lung cancer patients using label-free mass spectrometry." BBA clinical **7**: 97-104.

Holm, P. J., R. Morgenstern and H. Hebert (2002). "The 3-D structure of microsomal glutathione transferase 1 at 6 Å resolution as determined by electron crystallography of p22121 crystals." Biochimica et Biophysica Acta (BBA)-Protein Structure and Molecular Enzymology **1594**(2): 276-285.

Holohan, C., S. Van Schaeybroeck, D. B. Longley and P. G. Johnston (2013). "Cancer drug resistance: an evolving paradigm." Nature Reviews Cancer **13**(10): 714.

Hong, J., K. Ahn, E. Bae, S. Jeon and H. Choi (2006). "The effects of curcumin on the invasiveness of prostate cancer in vitro and in vivo." Prostate cancer and prostatic diseases **9**(2): 147.

Howells, L. M., S. Sale, S. N. Sriramareddy, G. R. Irving, D. J. Jones, C. J. Ottley, D. G. Pearson, C. D. Mann, M. M. Manson and D. P. Berry (2011). "Curcumin ameliorates oxaliplatin-induced chemoresistance in HCT116 colorectal cancer cells in vitro and in vivo." International journal of cancer **129**(2): 476-486.

Hsu, F. Y.-y., Y. Zhao, W. F. Anderson and P. B. Johnston (2007). "Downregulation of NPM-ALK by siRNA causes anaplastic large cell lymphoma cell growth inhibition and augments the anti cancer effects of chemotherapy in vitro." Cancer investigation **25**(4): 240-248.

Hu, F., F. Wei, Y. Wang, B. Wu, Y. Fang and B. Xiong (2015). "EGCG synergizes the therapeutic effect of cisplatin and oxaliplatin through autophagic pathway in human colorectal cancer cells." Journal of Pharmacological Sciences **128**(1): 27-34.

Huq, F. (2015). Synergism from combination of targeted therapy with tumor active phytochemicals in ovarian tumor models and changes in protein expression, AACR.

Huq, F., J. Q. Yu, P. Beale, C. Chan, L. Arzuman, M. U. Nessa and M. E. Mazumder (2014). "Combinations of platinums and selected phytochemicals as a means of overcoming resistance in ovarian cancer." Anticancer research **34**(1): 541-545.

Huq, F., J. Q. Yu, H. Daghriri and P. Beale (2004). "Studies on activities, cell uptake and DNA binding of four trans-planaramineplatinum (II) complexes of the form: trans-PtL (NH3) Cl2, where L= 2-hydroxypyridine, imidazole, 3-hydroxypyridine and imidazo (1, 2-α) pyridine." Journal of inorganic biochemistry **98**(8): 1261-1270.

Hwang, J.-T., J. Ha, I.-J. Park, S.-K. Lee, H. W. Baik, Y. M. Kim and O. J. Park (2007). "Apoptotic effect of EGCG in HT-29 colon cancer cells via AMPK signal pathway." Cancer letters **247**(1): 115-121.

Itahana, K., K. P. Bhat, A. Jin, Y. Itahana, D. Hawke, R. Kobayashi and Y. Zhang (2003). "Tumor suppressor ARF degrades B23, a nucleolar protein involved in ribosome biogenesis and cell proliferation." Molecular cell **12**(5): 1151-1164.

Jiang, P., X. Wu, X. Wang, W. Huang and Q. Feng (2016). "NEAT1 upregulates EGCG-induced CTR1 to enhance cisplatin sensitivity in lung cancer cells." Oncotarget **7**(28): 43337-43351.

Jin, H., W. Gong, C. Zhang and S. Wang (2013). "Epigallocatechin gallate inhibits the proliferation of colorectal cancer cells by regulating Notch signaling." OncoTargets and therapy **6**: 145.

Johnson, J. J. and H. Mukhtar (2007). "Curcumin for chemoprevention of colon cancer." Cancer Letters **255**(2): 170-181.

Jung, M., A. Ramankulov, J. Roigas, M. Johannsen, M. Ringsdorf, G. Kristiansen and K. Jung (2007). "In search of suitable reference genes for gene expression studies of human renal cell carcinoma by real-time PCR." BMC molecular biology **8**(1): 47.

K Auyeung, K. and J. K Ko (2017). "Angiogenesis and oxidative stress in metastatic tumor progression: pathogenesis and novel therapeutic approach of colon cancer." Current pharmaceutical design **23**(27): 3952-3961.

Kampan, N. C., M. T. Madondo, O. M. McNally, M. Quinn and M. Plebanski (2015). "Paclitaxel and its evolving role in the management of ovarian cancer." BioMed research international **2015**.

Kampinga, H. H., J. Hageman, M. J. Vos, H. Kubota, R. M. Tanguay, E. A. Bruford, M. E. Cheetham, B. Chen and L. E. Hightower (2009). "Guidelines for the nomenclature of the human heat shock proteins." Cell Stress and Chaperones **14**(1): 105-111.

Kang, J. H., H. S. Kang, I. K. Kim, H. Y. Lee, J. H. Ha, C. D. Yeo, H. H. Kang, H. S. Moon and S. H. Lee (2015). "Curcumin sensitizes human lung cancer cells to apoptosis and metastasis synergistically combined with carboplatin." Experimental Biology and Medicine **240**(11): 1416-1425.

Kennedy, A. S., G. H. Harrison, C. M. Mansfield, X. J. Zhou, J. F. Xu and E. K. Balcer-Kubiczek (2000). "Survival of colorectal cancer cell lines treated with paclitaxel,

radiation, and 5-FU: Effect of TP53 or hMLH1 deficiency." International journal of cancer **90**(4): 175-185.

Kensler, T. W., N. Wakabayashi and S. Biswal (2007). "Cell survival responses to environmental stresses via the Keap1-Nrf2-ARE pathway." Annu. Rev. Pharmacol. Toxicol. **47**: 89-116.

Keshamouni, V. G., G. Michailidis, C. S. Grasso, S. Anthwal, J. R. Strahler, A. Walker, D. A. Arenberg, R. C. Reddy, S. Akulapalli and V. J. Thannickal (2006). "Differential protein expression profiling by iTRAQ− 2DLC− MS/MS of lung cancer cells undergoing epithelial-mesenchymal transition reveals a migratory/invasive phenotype." Journal of proteome research **5**(5): 1143-1154.

Kheirelseid, E. A., K. H. Chang, J. Newell, M. J. Kerin and N. Miller (2010). "Identification of endogenous control genes for normalisation of real-time quantitative PCR data in colorectal cancer." BMC molecular biology **11**(1): 12.

Kim, E.-C., J.-K. Min, T.-Y. Kim, S.-J. Lee, H.-O. Yang, S. Han, Y.-M. Kim and Y.-G. Kwon (2005). "[6]-Gingerol, a pungent ingredient of ginger, inhibits angiogenesis in vitro and in vivo." Biochemical and biophysical research communications **335**(2): 300-308.

Kinzler, K. W. and B. Vogelstein (1996). "Lessons from Hereditary Colorectal Cancer." Cell **87**(2): 159-170.

Kisselev, A. F. and A. L. Goldberg (2001). "Proteasome inhibitors: from research tools to drug candidates." Chemistry & biology **8**(8): 739-758.

Kocaadam, B. and N. Şanlier (2017). "Curcumin, an active component of turmeric (Curcuma longa), and its effects on health." Critical reviews in food science and nutrition **57**(13): 2889-2895.

Koh, H.-J., S.-M. Lee, B.-G. Son, S.-H. Lee, Z. Y. Ryoo, K.-T. Chang, J.-W. Park, D.-C. Park, B. J. Song and R. L. Veech (2004). "Cytosolic NADP+-dependent isocitrate dehydrogenase plays a key role in lipid metabolism." Journal of Biological Chemistry **279**(38): 39968-39974.

Ku, N. O., R. M. Soetikno and M. B. Omary (2003). "Keratin mutation in transgenic mice predisposes to Fas but not TNF-induced apoptosis and massive liver injury." Hepatology **37**(5): 1006-1014.

Kubota, H., S. Yamamoto, E. Itoh, Y. Abe, A. Nakamura, Y. Izumi, H. Okada, M. Iida, H. Nanjo, H. Itoh and Y. Yamamoto (2010). "Increased expression of co-chaperone

HOP with HSP90 and HSC70 and complex formation in human colonic carcinoma." Cell Stress and Chaperones **15**(6): 1003-1011.

Kumar, U., D. Ghosh, S. Shaw, G. Bhaumik, R. K. Gupta, P. K. Reddy and S. B. Singh (2017). "Alterations in Carotid Body Morphology and Cellular Mechanism Under the Influence of Intermittent Hypoxia." Int J Cur Res Rev| Vol **9**(16): 49.

Kunnumakkara, A. B., D. Bordoloi, G. Padmavathi, J. Monisha, N. K. Roy, S. Prasad and B. B. Aggarwal (2017). "Curcumin, the golden nutraceutical: multitargeting for multiple chronic diseases." British journal of pharmacology **174**(11): 1325-1348.

Kwon, M. J., E. Oh, S. Lee, M. R. Roh, S. E. Kim, Y. Lee, Y.-L. Choi, Y.-H. In, T. Park and S. S. Koh (2009). "Identification of novel reference genes using multiplatform expression data and their validation for quantitative gene expression analysis." PloS one **4**(7): e6162.

Laborde, E. (2010). "Glutathione transferases as mediators of signaling pathways involved in cell proliferation and cell death." Cell death and differentiation **17**(9): 1373.

Ladner, J. E., J. F. Parsons, C. L. Rife, G. L. Gilliland and R. N. Armstrong (2004). "Parallel evolutionary pathways for glutathione transferases: structure and mechanism of the mitochondrial class kappa enzyme rGSTK1-1." Biochemistry **43**(2): 352-361.

Lai, K. K., K. T. Chan, M. Y. Choi, H. K. Wang, E. Y. Fung, H. Y. Lam, W. Tan, L. N. Tung, D. K. Tong and R. W. Sun (2016). "14-3-3σ confers cisplatin resistance in esophageal squamous cell carcinoma cells via regulating DNA repair molecules." Tumor Biology **37**(2): 2127-2136.

Lappalainen, P., M. M. Kessels, M. J. T. Cope and D. G. Drubin (1998). "The ADF homology (ADF-H) domain: a highly exploited actin-binding module." Molecular Biology of the Cell **9**(8): 1951-1959.

Larcher, F., C. Bauluz, M. Diaz-Guerra, M. Quintanilla, C. J. Conti, C. Ballestin and J. L. Jorcano (1992). "Aberrant expression of the simple epithelial type II keratin 8 by mouse skin carcinomas but not papillomas." Molecular carcinogenesis **6**(2): 112-121.

Larocque, K., P. Ovadje, S. Djurdjevic, M. Mehdi, J. Green and S. Pandey (2014). "Novel analogue of colchicine induces selective pro-death autophagy and necrosis in human cancer cells." PloS one **9**(1): e87064.

Lecumberri, E., Y. M. Dupertuis, R. Miralbell and C. Pichard (2013). "Green tea polyphenol epigallocatechin-3-gallate (EGCG) as adjuvant in cancer therapy." Clinical Nutrition **32**(6): 894-903.

Lee, A. S. (2007). "GRP78 induction in cancer: therapeutic and prognostic implications." Cancer research **67**(8): 3496-3499.

Lee, E., P. Nichols, D. Spicer, S. Groshen, C. Y. Mimi and A. S. Lee (2006). "GRP78 as a novel predictor of responsiveness to chemotherapy in breast cancer." Cancer research **66**(16): 7849-7853.

Lee, H. S., E. Y. Seo, N. E. Kang and W. K. Kim (2008). "[6]-Gingerol inhibits metastasis of MDA-MB-231 human breast cancer cells." The Journal of nutritional biochemistry **19**(5): 313-319.

Lee, S.-H., M. Cekanova and S. J. Baek (2008). "Multiple mechanisms are involved in 6-gingerol-induced cell growth arrest and apoptosis in human colorectal cancer cells." Molecular Carcinogenesis **47**(3): 197-208.

Lee, S. H., M. Cekanova and S. J. Baek (2008). "Multiple mechanisms are involved in 6-gingerol-induced cell growth arrest and apoptosis in human colorectal cancer cells." Molecular carcinogenesis **47**(3): 197-208.

Lee, S. M., H.-J. Koh, D.-C. Park, B. J. Song, T.-L. Huh and J.-W. Park (2002). "Cytosolic NADP+-dependent isocitrate dehydrogenase status modulates oxidative damage to cells." Free Radical Biology and Medicine **32**(11): 1185-1196.

Lei, T., X. Zhao, S. Jin, Q. Meng, H. Zhou and M. Zhang (2013). "Discovery of potential bladder cancer biomarkers by comparative urine proteomics and analysis." Clinical genitourinary cancer **11**(1): 56-62.

Lepre, C. and S. Lippard (1990). Interaction of platinum antitumor compounds with DNA. Nucleic Acids and Molecular Biology 4, Springer**:** 9-38.

Leung, Y. Y., L. L. Yao Hui and V. B. Kraus "Colchicine—Update on mechanisms of action and therapeutic uses." Seminars in Arthritis and Rheumatism **45**(3): 341-350.

Levis, M., R. Pham, B. D. Smith and D. Small (2004). "In vitro studies of a FLT3 inhibitor combined with chemotherapy: sequence of administration is important to achieve synergistic cytotoxic effects." Blood **104**(4): 1145-1150.

Li, L., B. Ahmed, K. Mehta and R. Kurzrock (2007). "Liposomal curcumin with and without oxaliplatin: effects on cell growth, apoptosis, and angiogenesis in colorectal cancer." Molecular cancer therapeutics **6**(4): 1276-1282.

Lim, M. J. and X. W. Wang (2006). "Nucleophosmin and human cancer." Cancer Detection and Prevention **30**(6): 481-490.

Liu, J., E. Kraut, J. Bender, R. Brooks, S. Balcerzak, M. Grever, H. Stanley, S. D'Ambrosio, R. Gibson-D'Ambrosio and K. K. Chan (2002). "Pharmacokinetics of oxaliplatin (NSC 266046) alone and in combination with paclitaxel in cancer patients." Cancer chemotherapy and pharmacology **49**(5): 367-374.

Liu, T., C. K. Daniels and S. Cao (2012). "Comprehensive review on the HSC70 functions, interactions with related molecules and involvement in clinical diseases and therapeutic potential." Pharmacology & Therapeutics **136**(3): 354-374.

Losman, J.-A. and W. G. Kaelin (2013). "What a difference a hydroxyl makes: mutant IDH,(R)-2-hydroxyglutarate, and cancer." Genes & development **27**(8): 836-852.

Lu, D., T. Lu and S. Cao (2013). "Drug combinations in cancer treatment." Clinical Experimental Pharmacology **3**(4): 134.

Lu, Z., Q. Song, J. Yang, X. Zhao, X. Zhang, P. Yang and J. Kang (2014). "Comparative proteomic analysis of anti-cancer mechanism by periplocin treatment in lung cancer cells." Cellular Physiology and Biochemistry **33**(3): 859-868.

Lynch, H. T., T. Smyrk and J. F. Lynch (1996). "Overview of natural history, pathology, molecular genetics and management of HNPCC (Lynch syndrome)." International journal of cancer **69**(1): 38-43.

Ma, P. a., H. Xiao, C. Li, Y. Dai, Z. Cheng, Z. Hou and J. Lin (2015). "Inorganic nanocarriers for platinum drug delivery." Materials Today **18**(10): 554-564.

Macias, A. T., D. S. Williamson, N. Allen, J. Borgognoni, A. Clay, Z. Daniels, P. Dokurno, M. J. Drysdale, G. L. Francis and C. J. Graham (2011). "Adenosine-derived inhibitors of 78 kDa glucose regulated protein (Grp78) ATPase: insights into isoform selectivity." Journal of medicinal chemistry **54**(12): 4034-4041.

Maeda, A., H. Ohguro, T. Maeda, I. Wada, N. Sato, Y. Kuroki and T. Nakagawa (2000). "Aberrant expression of photoreceptor-specific calcium-binding protein (recoverin) in cancer cell lines." Cancer Research **60**(7): 1914-1920.

Magin, T. M., P. Vijayaraj and R. E. Leube (2007). "Structural and regulatory functions of keratins." Experimental cell research **313**(10): 2021-2032.

Majidzadeh-A, K., R. Esmaeili and N. Abdoli (2011). "TFRC and ACTB as the best reference genes to quantify Urokinase Plasminogen Activator in breast cancer." BMC research notes **4**(1): 215.

Mandhare, A. and P. Banerjee (2016). "Therapeutic use of colchicine and its derivatives: a patent review." Expert Opinion on Therapeutic Patents **26**(10): 1157-1174.

Mao, S. and S. Huang (2014). "The signaling pathway of NADPH oxidase and its role in glomerular diseases." Journal of Receptors and Signal Transduction **34**(1): 6-11.

Martoglio, A.-M., B. Tom, M. Starkey, A. N. Corps, D. S. Charnock-Jones and S. K. Smith (2000). "Changes in tumorigenesis-and angiogenesis-related gene transcript abundance profiles in ovarian cancer detected by tailored high density cDNA arrays." Molecular Medicine **6**(9): 750.

Maruthur, N. M., E. Tseng, S. Hutfless, L. M. Wilson, C. Suarez-Cuervo, Z. Berger, Y. Chu, E. Iyoha, J. B. Segal and S. Bolen (2016). "Diabetes medications as monotherapy or metformin-based combination therapy for type 2 diabetes: a systematic review and meta-analysis." Annals of internal medicine **164**(11): 740-751.

Matsunaga, S., T. Kishi and N. Iwata (2015). "Combination therapy with cholinesterase inhibitors and memantine for Alzheimer's disease: a systematic review and meta-analysis." International Journal of Neuropsychopharmacology **18**(5).

Mattanovich, D., M. Dragosits, B. Gasser, M. Maurer and M. Sauer (2015). Production cell line, Google Patents.

Mazumder, M. E. H. (2013). Studies on New Tumour Active Palladium Complexes Targeted to Overcome Resistance in Ovarian Cancer, University of Sydney.

Mazumder, M. E. H., P. Beale, C. Chan, J. Q. Yu and F. Huq (2012). "Epigallocatechin gallate acts synergistically in combination with cisplatin and designed trans-palladiums in ovarian cancer cells." Anticancer research **32**(11): 4851-4860.

McIlwain, C., D. Townsend and K. Tew (2006). "Glutathione S-transferase polymorphisms: cancer incidence and therapy." Oncogene **25**(11): 1639.

Miyake, H., I. Hara, S. Arakawa and S. Kamidono (2000). "Stress protein GRP78 prevents apoptosis induced by calcium ionophore, ionomycin, but not by glycosylation inhibitor, tunicamycin, in human prostate cancer cells." Journal of cellular biochemistry **77**(3): 396-408.

Moffat, G. J., A. W. McLaren and C. R. Wolf (1996). "Sp1-mediated transcriptional activation of the human Pi class glutathione S-transferase promoter." Journal of Biological Chemistry **271**(2): 1054-1060.

Moll, R., M. Divo and L. Langbein (2008). "The human keratins: biology and pathology." Histochemistry and Cell Biology **129**(6): 705-733.

Moll, R., M. Divo and L. Langbein (2008). "The human keratins: biology and pathology." Histochemistry and cell biology **129**(6): 705.

Montopoli, M., E. Ragazzi, G. Froldi and L. Caparrotta (2009). "Cell-cycle inhibition and apoptosis induced by curcumin and cisplatin or oxaliplatin in human ovarian carcinoma cells." Cell proliferation **42**(2): 195-206.

Muggia, F. M., A. Bonetti, J. D. Hoeschele, M. Rozencweig and S. B. Howell (2015). "Platinum antitumor complexes: 50 years since Barnett Rosenberg's discovery." Journal of Clinical Oncology **33**(35): 4219-4226.

Nagle, D. G., D. Ferreira and Y. D. Zhou (2006). "Epigallocatechin-3-gallate (EGCG): Chemical and biomedical perspectives." Phytochemistry **67**(17): 1849-1855.

Nautiyal, J., S. S. Kanwar, Y. Yu and A. P. Majumdar (2011). "Combination of dasatinib and curcumin eliminates chemo-resistant colon cancer cells." Journal of molecular signaling **6**(1): 7.

Nebl, G., S. C. Meuer and Y. Samstag (1996). "Dephosphorylation of serine 3 regulates nuclear translocation of cofilin." Journal of Biological Chemistry **271**(42): 26276-26280.

Nessa, M. U. (2013). Studies on Combinations Between Platinum Drugs and Phytochemicals in Ovarian Tumour Models, University of Sydney.

Nessa, M. U., P. Beale, C. Chan, J. Q. Yu and F. Huq (2012). "Combinations of resveratrol, cisplatin and oxaliplatin applied to human ovarian cancer cells." Anticancer research **32**(1): 53-59.

Nessa, M. U., P. Beale, C. Chan, J. Q. Yu and F. Huq (2012). "Studies on combination of platinum drugs cisplatin and oxaliplatin with phytochemicals anethole and curcumin in ovarian tumour models." Anticancer research **32**(11): 4843-4850.

Nigam, N., K. Bhui, S. Prasad, J. George and Y. Shukla (2009). "[6]-Gingerol induces reactive oxygen species regulated mitochondrial cell death pathway in human epidermoid carcinoma A431 cells." Chemico-biological interactions **181**(1): 77-84.

Nogales, E., S. G. Wolf and K. H. Downing (1998). "Structure of the αβ tubulin dimer by electron crystallography." Nature **391**: 199.

Nosher, J. L., I. Ahmed, A. N. Patel, V. Gendel, P. G. Murillo, R. Moss and S. K. Jabbour (2015). "Non-operative therapies for colorectal liver metastases." Journal of Gastrointestinal Oncology **6**(2): 224-240.

Nowak, D. and M. Malicka-Błaszkiewicz (1999). "Actin isoforms--functional differentiation, changes in cell pathology." Postepy biochemii **45**(4): 261-269.

NOZAWA, Y., N. VAN BELZEN, M. VAN DER, C. ANGELIQUE, W. N. DINJENS and F. T. BOSMAN (1996). "Expression of nucleophosmin/B23 in normal and neoplastic colorectal mucosa." The Journal of pathology **178**(1): 48-52.

Nuki, G. (2008). "Colchicine: Its mechanism of action and efficacy in crystal-induced inflammation." Current Rheumatology Reports **10**(3): 218.

O'Connell, K., M. Prencipe, A. O'Neill, C. Corcoran, S. Rani, M. Henry, P. Dowling, P. Meleady, L. O'Driscoll and W. Watson (2012). "The use of LC-MS to identify differentially expressed proteins in docetaxel-resistant prostate cancer cell lines." Proteomics **12**(13): 2115-2126.

Obrocea, F., M. Sajin, E. C. Marinescu and D. Stoica (2011). "Colorectal cancer and the 7th revision of the TNM staging system: review of changes and suggestions for uniform pathologic reporting." Rom J Morphol Embryol **52**(2): 537-544.

Oh, S. E. and M. M. Mouradian (2017). "Cytoprotective mechanisms of DJ-1 against oxidative stress through modulating ERK1/2 and ASK1 signal transduction." Redox biology.

Okuda, M., H. F. Horn, P. Tarapore, Y. Tokuyama, A. G. Smulian, P.-K. Chan, E. S. Knudsen, I. A. Hofmann, J. D. Snyder and K. E. Bove (2000). "Nucleophosmin/B23 is a target of CDK2/cyclin E in centrosome duplication." Cell **103**(1): 127-140.

Onda, M., M. Emi, A. Yoshida, S. Miyamoto, J. Akaishi, S. Asaka, K. Mizutani, K. Shimizu, M. Nagahama and K. Ito (2004). "Comprehensive gene expression profiling of anaplastic thyroid cancers with cDNA microarray of 25 344 genes." Endocrine-related cancer **11**(4): 843-854.

Orr, G. A., P. Verdier-Pinard, H. McDaid and S. B. Horwitz (2003). "Mechanisms of Taxol resistance related to microtubules." Oncogene **22**(47): 7280.

Oyagbemi, A. A., A. B. Saba and O. I. Azeez (2010). "Molecular targets of [6]-gingerol: Its potential roles in cancer chemoprevention." Biofactors **36**(3): 169-178.

Ozols, R. F., B. N. Bundy, B. E. Greer, J. M. Fowler, D. Clarke-Pearson, R. A. Burger, R. S. Mannel, K. DeGeest, E. M. Hartenbach and R. Baergen (2003). "Phase III trial of carboplatin and paclitaxel compared with cisplatin and paclitaxel in patients with optimally resected stage III ovarian cancer: a Gynecologic Oncology Group study." Journal of Clinical Oncology **21**(17): 3194-3200.

Pan, H., J. Chen, K. Shen, X. Wang, P. Wang, G. Fu, H. Meng, Y. Wang and B. Jin (2015). "Mitochondrial modulation by Epigallocatechin 3-Gallate ameliorates cisplatin induced renal injury through decreasing oxidative/nitrative stress, inflammation and NF-kB in mice." PloS one **10**(4): e0124775.

Panahi, Y., A. Saadat, F. Beiraghdar, S. M. H. Nouzari, H. R. Jalalian and A. Sahebkar (2014). "Antioxidant effects of bioavailability-enhanced curcuminoids in patients with solid tumors: A randomized double-blind placebo-controlled trial." Journal of Functional Foods **6**: 615-622.

Park, Y. J., J. Wen, S. Bang, S. W. Park and S. Y. Song (2006). "[6]-Gingerol induces cell cycle arrest and cell death of mutant p53-expressing pancreatic cancer cells." Yonsei medical journal **47**(5): 688-697.

Pathak, S., R. Jones, J. M. Tang, C. Parmar, S. Fenwick, H. Malik and G. Poston (2011). "Ablative therapies for colorectal liver metastases: a systematic review." Colorectal Dis **13**(9): e252-265.

Patil, B. S., G. Jayaprakasha, K. Chidambara Murthy and A. Vikram (2009). "Bioactive compounds: historical perspectives, opportunities, and challenges." Journal of agricultural and food chemistry **57**(18): 8142-8160.

Perego, P. and J. Robert (2016). "Oxaliplatin in the era of personalized medicine: from mechanistic studies to clinical efficacy." Cancer Chemotherapy and Pharmacology **77**(1): 5-18.

Popow, A., D. Nowak and M. Malicka-Blaszkiewicz (2006). "ACTIN CYTOSKELETON AND ß-ACTIN EXPRESSION IN CORRELATION WITH HIGHER INVASIVENESS OF SELECTED HEPATOMA MORRIS 5123 CELLS." J. Physiol. Pharmacol **57**: 111-123.

Prasad, S., S. C. Gupta, A. K. Tyagi and B. B. Aggarwal (2014). "Curcumin, a component of golden spice: from bedside to bench and back." Biotechnology advances **32**(6): 1053-1064.

Qi, Y., J. F. Chiu, L. Wang, D. L. Kwong and Q. Y. He (2005). "Comparative proteomic analysis of esophageal squamous cell carcinoma." Proteomics **5**(11): 2960-2971.

Quinn, B. A., R. Dash, S. Sarkar, B. Azab, P. Bhoopathi, S. K. Das, L. Emdad, J. Wei, M. Pellecchia and D. Sarkar (2015). "Pancreatic cancer combination therapy using a BH3 mimetic and a synthetic tetracycline." Cancer research **75**(11): 2305-2315.

Rady, I., H. Mohamed, M. Rady, I. A. Siddiqui and H. Mukhtar (2017). "Cancer preventive and therapeutic effects of EGCG, the major polyphenol in green tea." Egyptian Journal of Basic and Applied Sciences.

Rahal, A., A. Kumar, V. Singh, B. Yadav, R. Tiwari, S. Chakraborty and K. Dhama (2014). "Oxidative stress, prooxidants, and antioxidants: the interplay." BioMed research international **2014**.

Reinemer, P., H. Dirr, R. Ladenstein, J. Schäffer, O. Gallay and R. Huber (1991). "The three-dimensional structure of class pi glutathione S-transferase in complex with glutathione sulfonate at 2.3 A resolution." The EMBO Journal **10**(8): 1997-2005.

Reitman, Z. J. and H. Yan (2010). "Isocitrate dehydrogenase 1 and 2 mutations in cancer: alterations at a crossroads of cellular metabolism." Journal of the National Cancer Institute **102**(13): 932-941.

Richter, K., M. Haslbeck and J. Buchner (2010). "The Heat Shock Response: Life on the Verge of Death." Molecular Cell **40**(2): 253-266.

Roblick, U., D. Hirschberg, J. Habermann, C. Palmberg, S. Becker, S. Krüger, M. Gustafsson, H.-P. Bruch, B. Franzen and T. Ried (2004). "Sequential proteome alterations during genesis and progression of colon cancer." Cellular and Molecular Life Sciences CMLS **61**(10): 1246-1255.

Roos, W. P., A. D. Thomas and B. Kaina (2016). "DNA damage and the balance between survival and death in cancer biology." Nature Reviews Cancer **16**(1): 20.

Ropert, S., R. Coriat, B. Verret, A. Perret, F. Lucibello, A. N. Chamseddine, J.-P. Armand, A. Paci and O. Mir (2017). "Colchicine is an active treatment for everolimus-induced oral ulcers." European Journal of Cancer **87**: 209-211.

Ross, J. S., N. E. Stagliano and M. J. Donovan (2001). "Atherosclerosis and cancer: common molecular pathways of disease development and progression." Ann N Y Acad **947**: 271-292.

Rufino-Palomares, E. E., F. J. Reyes-Zurita, L. García-Salguero, K. Mokhtari, P. P. Medina, J. A. Lupiáñez and J. Peragón (2013). "Maslinic acid, a triterpenic anti-tumoural agent, interferes with cytoskeleton protein expression in HT29 human colon-cancer cells." Journal of proteomics **83**: 15-25.

Runowicz, C. D., P. H. Wiernik, A. I. Einzig, G. L. Goldberg and S. B. Horwitz (1993). "Taxol in ovarian cancer." Cancer **71**(S4): 1591-1596.

Ruscoe, J. E., L. A. Rosario, T. Wang, L. Gaté, P. Arifoglu, C. R. Wolf, C. J. Henderson, Z. e. Ronai and K. D. Tew (2001). "Pharmacologic or Genetic Manipulation of Glutathione S-Transferase P1–1 (GSTπ) Influences Cell Proliferation Pathways." Journal of Pharmacology and Experimental Therapeutics **298**(1): 339-345.

Russell Hilt, J., W. D. R. Wittliff, D. S. Edwin, C. Thomas and R. A. Orlando (1973). "Studies on Certain Cytoplasmic Enzymes and Specific Estrogen Receptors in Human Breast Cancer and in Nonmalignant Diseases of the Breast1." CANCER RESEARCH **33**: 2054-2062.

Russo, G. L. (2007). "Ins and outs of dietary phytochemicals in cancer chemoprevention." Biochemical Pharmacology **74**(4): 533-544.

Salvato, F., M. C. Carvalho and A. L. Leite (2012). Strategies for Protein Separation. Integrative Proteomics. H.-C. E. Leung, InTech.

Sandoval, J. A., D. J. Hoelz, H. A. Woodruff, R. L. Powell, C. L. Jay, J. L. Grosfeld, R. J. HickeyD and L. H. Malkas (2006). "Novel peptides secreted from human neuroblastoma: useful clinical tools?" Journal of pediatric surgery **41**(1): 245-251.

Sawers, L., M. Ferguson, B. Ihrig, H. Young, P. Chakravarty, C. Wolf and G. Smith (2014). "Glutathione S-transferase P1 (GSTP1) directly influences platinum drug chemosensitivity in ovarian tumour cell lines." British journal of cancer **111**(6): 1150.

Schaller, G., I. Fuchs, W. Pritze, A. Ebert, H. Herbst, K. Pantel, H. Weitzel and E. Lengyel (1996). "Elevated keratin 18 protein expression indicates a favorable prognosis in patients with breast cancer." Clinical Cancer Research **2**(11): 1879-1885.

Schnekenburger, M., T. Karius and M. Diederich (2014). "Regulation of epigenetic traits of the glutathione S-transferase P1 gene: from detoxification toward cancer prevention and diagnosis." Frontiers in Pharmacology **5**(170).

Shields, L. B., Ç. Gerçel-Taylor, C. M. Yashar, T. C. Wan, W. A. Katsanis, J. A. Spinnato and D. D. Taylor (1997). "Induction of immune responses to ovarian tumor antigens by multiparity." Journal of the Society for Gynecologic Investigation **4**(6): 298-304.

Shimizu, M., A. Deguchi, Y. Hara, H. Moriwaki and I. B. Weinstein (2005). "EGCG inhibits activation of the insulin-like growth factor-1 receptor in human colon cancer cells." Biochemical and biophysical research communications **334**(3): 947-953.

Shimizu, M., A. Deguchi, A. K. Joe, J. F. McKOY, H. Moriwaki and I. B. Weinstein (2005). "EGCG inhibits activation of HER3 and expression of cyclooxygenase-2 in human colon cancer cells." Journal of experimental therapeutics & oncology **5**(1).

Shimizu, M., Y. Shirakami, H. Sakai, Y. Yasuda, M. Kubota, S. Adachi, H. Tsurumi, Y. Hara and H. Moriwaki (2010). "(−)-Epigallocatechin gallate inhibits growth and activation of the VEGF/VEGFR axis in human colorectal cancer cells." Chemico-biological interactions **185**(3): 247-252.

Shishkin, S., L. Eremina, N. Pashintseva, L. Kovalev and M. Kovaleva (2016). "Cofilin-1 and other ADF/cofilin superfamily members in human malignant cells." International journal of molecular sciences **18**(1): 10.

Shuda, M., N. Kondoh, N. Imazeki, K. Tanaka, T. Okada, K. Mori, A. Hada, M. Arai, T. Wakatsuki and O. Matsubara (2003). "Activation of the ATF6, XBP1 and grp78 genes in human hepatocellular carcinoma: a possible involvement of the ER stress pathway in hepatocarcinogenesis." Journal of hepatology **38**(5): 605-614.

Sies, H., C. Berndt and D. P. Jones (2017). "Oxidative stress." Annual review of biochemistry **86**: 715-748.

Singh, S. (2015). "Cytoprotective and regulatory functions of glutathione S-transferases in cancer cell proliferation and cell death." Cancer chemotherapy and pharmacology **75**(1): 1-15.

Singh, S., P. P. Singh, M. H. Murad, H. Singh and N. J. Samadder (2014). "Prevalence, risk factors, and outcomes of interval colorectal cancers: a systematic review and meta-analysis." The American journal of gastroenterology **109**(9): 1375.

Sinha, P., G. Hütter, E. Köttgen, M. Dietel, D. Schadendorf and H. Lage (1999). "Increased expression of epidermal fatty acid binding protein, cofilin, and 14-3-3-σ (stratifin) detected by two-dimensional gel electrophoresis, mass spectrometry and microsequencing of drug-resistant human adenocarcinoma of the pancreas." Electrophoresis **20**(14): 2952-2960.

Sitbon, O., X. Jaïs, L. Savale, V. Cottin, E. Bergot, E. A. Macari, H. Bouvaist, C. Dauphin, F. Picard and S. Bulifon (2014). "Upfront triple combination therapy in pulmonary arterial hypertension: a pilot study." European Respiratory Journal **43**(6): 1691-1697.

Sivakumar, G. (2013). "Colchicine semisynthetics: chemotherapeutics for cancer?" Current medicinal chemistry **20**(7): 892-898.

Souglakos, J., N. Androulakis, K. Syrigos, A. Polyzos, N. Ziras, A. Athanasiadis, S. Kakolyris, S. Tsousis, C. Kouroussis and L. Vamvakas (2006). "FOLFOXIRI (folinic acid, 5-fluorouracil, oxaliplatin and irinotecan) vs FOLFIRI (folinic acid, 5-fluorouracil and irinotecan) as first-line treatment in metastatic colorectal cancer (MCC): a multicentre randomised phase III trial from the Hellenic Oncology Research Group (HORG)." British journal of cancer **94**(6): 798.

Srisomsap, C., P. Sawangareetrakul, P. Subhasitanont, T. Panichakul, S. Keeratichamroen, K. Lirdprapamongkol, D. Chokchaichamnankit, S. Sirisinha and J. Svasti (2004). "Proteomic analysis of cholangiocarcinoma cell line." Proteomics **4**(4): 1135-1144.

Stewart, B. and C. P. Wild (2017). "World cancer report 2014." Health.

Stricher, F., C. Macri, M. Ruff and S. Muller (2013). "HSPA8/HSC70 chaperone protein: structure, function, and chemical targeting." Autophagy **9**(12): 1937-1954.

Subong, E. N., M. J. Shue, J. I. Epstein, J. V. Briggman, P. K. Chan and A. W. Partin (1999). "Monoclonal antibody to prostate cancer nuclear matrix protein (PRO: 4-216) recognizes nucleophosmin/B23." The Prostate **39**(4): 298-304.

Takegoshi, K., E. Okada and Q. Su (2016). "Hepatocellular carcinoma and type 2 diabets mellitus: cytokeratin 8/18 expression in hepatocellular carcinoma and glycogen-storing hepatocytes." Hepatoma Res **2**: 229-230.

Tan, F., Y. Jiang, N. Sun, Z. Chen, Y. Lv, K. Shao, N. Li, B. Qiu, Y. Gao and B. Li (2012). "Identification of isocitrate dehydrogenase 1 as a potential diagnostic and prognostic biomarker for non-small cell lung cancer by proteomic analysis." Molecular & Cellular Proteomics **11**(2): M111. 008821.

Tanaka, K. (2009). "The proteasome: Overview of structure and functions." Proceedings of the Japan Academy. Series B, Physical and Biological Sciences **85**(1): 12-36.

Tanaka, M., H. Sasaki, I. Kino, T. Sugimura and M. Terada (1992). "Genes preferentially expressed in embryo stomach are predominantly expressed in gastric cancer." Cancer research **52**(12): 3372-3377.

Tesniere, A., F. Schlemmer, V. Boige, O. Kepp, I. Martins, F. Ghiringhelli, L. Aymeric, M. Michaud, L. Apetoh, L. Barault, J. Mendiboure, J. P. Pignon, V. Jooste, P. van Endert, M. Ducreux, L. Zitvogel, F. Piard and G. Kroemer (2010). "Immunogenic death of colon cancer cells treated with oxaliplatin." Oncogene **29**(4): 482-491.

Todd, R. C. and S. J. Lippard (2009). "Inhibition of transcription by platinum antitumor compounds." Metallomics **1**(4): 280-291.

Tsai, C.-H., S.-J. Chiu, C.-C. Liu, T.-J. Sheu, C.-H. Hsieh, P. C. Keng and Y.-J. Lee (2009). "Regulated expression of cofilin and the consequent regulation of p27kip1 are essential for G1 phase progression." Cell cycle **8**(15): 2365-2374.

Tsai, C.-H., L.-T. Lin, C.-Y. Wang, Y.-W. Chiu, Y.-T. Chou, S.-J. Chiu, H.-E. Wang, R.-S. Liu, C.-Y. Wu and P.-C. Chan (2015). "Over-expression of cofilin-1 suppressed growth and invasion of cancer cells is associated with up-regulation of let-7 microRNA." Biochimica et Biophysica Acta (BBA)-Molecular Basis of Disease **1852**(5): 851-861.

Turhani, D., K. Krapfenbauer, D. Thurnher, H. Langen and M. Fountoulakis (2006). "Identification of differentially expressed, tumor-associated proteins in oral squamous cell carcinoma by proteomic analysis." Electrophoresis **27**(7): 1417-1423.

Ueno, T., M. Toi and S. Linder (2005). "Detection of epithelial cell death in the body by cytokeratin 18 measurement." Biomedicine & pharmacotherapy **59**: S359-S362.

Unwin, R. D., R. A. Craven, P. Harnden, S. Hanrahan, N. Totty, M. Knowles, I. Eardley, P. J. Selby and R. E. Banks (2003). "Proteomic changes in renal cancer and co-ordinate demonstration of both the glycolytic and mitochondrial aspects of the Warburg effect." Proteomics **3**(8): 1620-1632.

Vega, P., F. Valentín and J. Cubiella (2015). "Colorectal cancer diagnosis: Pitfalls and opportunities." World Journal of Gastrointestinal Oncology **7**(12): 422-433.

Vergara, D., P. Simeone, P. del Boccio, C. Toto, D. Pieragostino, A. Tinelli, R. Acierno, S. Alberti, M. Salzet and G. Giannelli (2013). "Comparative proteome profiling of breast tumor cell lines by gel electrophoresis and mass spectrometry reveals an epithelial mesenchymal transition associated protein signature." Molecular BioSystems **9**(6): 1127-1138.

Wang, H., M. T. Kachman, D. R. Schwartz, K. R. Cho and D. M. Lubman (2004). "Comprehensive proteome analysis of ovarian cancers using liquid phase separation, mass mapping and tandem mass spectrometry: a strategy for identification of candidate cancer biomarkers." Proteomics **4**(8): 2476-2495.

Wang, J., J. Dong, P. Johnson, G. A. Maglinte, A. Rong, B. L. Barber and J.-Y. Douillard (2015). Quality-adjusted survival in patients with RAS wild-type (WT) metastatic colorectal cancer (mCRC) receiving first-line therapy with panitumumab plus FOLFOX versus FOLFOX alone in the PRIME trial, American Society of Clinical Oncology.

Wang, J., L. Xu, X. Yun, K. Yang, D. Liao, L. Tian, H. Jiang and W. Lu (2013). "Proteomic analysis reveals that proteasome subunit beta 6 is involved in hypoxia-induced pulmonary vascular remodeling in rats." PloS one **8**(7): e67942.

Wang, M., S. Wey, Y. Zhang, R. Ye and A. S. Lee (2009). "Role of the unfolded protein response regulator GRP78/BiP in development, cancer, and neurological disorders." Antioxidants & redox signaling **11**(9): 2307-2316.

Wax, A. and V. Backman (2009). Biomedical applications of light scattering, McGraw Hill Professional.

Weaver, B. A. (2014). "How Taxol/paclitaxel kills cancer cells." Molecular biology of the cell **25**(18): 2677-2681.

Willett, W. C. and D. Trichopoulos (1996). "Nutrition and cancer: A summary of the evidence." Cancer Causes and Control **7**(1): 178-180.

Wilmes, A., C. Bielow, C. Ranninger, P. Bellwon, L. Aschauer, A. Limonciel, H. Chassaigne, T. Kristl, S. Aiche, C. G. Huber, C. Guillou, P. Hewitt, M. O. Leonard, W. Dekant, F. Bois and P. Jennings (2015). "Mechanism of cisplatin proximal tubule toxicity revealed by integrating transcriptomics, proteomics, metabolomics and biokinetics." Toxicology in Vitro **30**(1, Part A): 117-127.

Winegarden, J., A. Mauer, G. A. Otterson, C. Rudin, M. Villalona-Calero, V. Lanzotti, L. Szeto, K. Kasza, P. Hoffman and E. Vokes (2004). "A phase II study of oxaliplatin and paclitaxel in patients with advanced non-small-cell lung cancer." Annals of oncology **15**(6): 915-920.

Woynarowski, J. M., S. Faivre, M. C. Herzig, B. Arnett, W. G. Chapman, A. V. Trevino, E. Raymond, S. G. Chaney, A. Vaisman, M. Varchenko and P. E. Juniewicz (2000). "Oxaliplatin-induced damage of cellular DNA." Mol Pharmacol **58**(5): 920-927.

Wu, M. H., J. H. Chang, C. C. Chou and B. Y. Yung (2002). "Involvement of nucleophosmin/B23 in the response of HeLa cells to UV irradiation." International journal of cancer **97**(3): 297-305.

Wu, M. H., J. H. Chang and B. Y. Yung (2002). "Resistance to UV-induced cell-killing in nucleophosmin/B23 over-expressed NIH 3T3 fibroblasts: enhancement of DNA repair and up-regulation of PCNA in association with nucleophosmin/B23 over-expression." Carcinogenesis **23**(1): 93-100.

Wu, S. L., W. S. Hancock, G. G. Goodrich and S. T. Kunitake (2003). "An approach to the proteomic analysis of a breast cancer cell line (SKBR-3)." Proteomics **3**(6): 1037-1046.

Wu, Y., Y. Fan, B. Xue, L. Luo, J. Shen, S. Zhang, Y. Jiang and Z. Yin (2006). "Human glutathione S-transferase P1-1 interacts with TRAF2 and regulates TRAF2–ASK1 signals." Oncogene **25**(42): 5787.

Xiao, B., X. Si, M. K. Han, E. Viennois, M. Zhang and D. Merlin (2015). "Co-delivery of camptothecin and curcumin by cationic polymeric nanoparticles for synergistic colon cancer combination chemotherapy." Journal of Materials Chemistry B **3**(39): 7724-7733.

Xu, S.-G., P.-J. Yan and Z.-M. Shao (2010). "Differential proteomic analysis of a highly metastatic variant of human breast cancer cells using two-dimensional differential gel electrophoresis." Journal of cancer research and clinical oncology **136**(10): 1545-1556.

Yamaguchi, H. and J. Condeelis (2007). "Regulation of the actin cytoskeleton in cancer cell migration and invasion." Biochimica et Biophysica Acta (BBA)-Molecular Cell Research **1773**(5): 642-652.

Yamamoto, T., M. Kudo, W.-X. Peng, H. Takata, H. Takakura, K. Teduka, T. Fujii, K. Mitamura, A. Taga and E. Uchida (2016). "Identification of aldolase A as a potential diagnostic biomarker for colorectal cancer based on proteomic analysis using formalin-fixed paraffin-embedded tissue." Tumor Biology **37**(10): 13595-13606.

Yang, M., M. Ren, Y. Qu, W. Teng, Z. Wang, H. Li and Q. Yuan (2016). "Sulforaphene inhibits hepatocellular carcinoma through repressing keratin 8 and activating anoikis." RSC Advances **6**(74): 70326-70334.

Yao, Y., X.-Y. Jia, H.-Y. Tian, Y.-X. Jiang, G.-J. Xu, Q.-J. Qian and F.-K. Zhao (2009). "Comparative proteomic analysis of colon cancer cells in response to oxaliplatin treatment." Biochimica et Biophysica Acta (BBA)-Proteins and Proteomics **1794**(10): 1433-1440.

Ying, H., P. Dey, W. Yao, A. C. Kimmelman, G. F. Draetta, A. Maitra and R. A. DePinho (2016). "Genetics and biology of pancreatic ductal adenocarcinoma." Genes & development **30**(4): 355-385.

Yu, T., Y. Yang, J. Zhang, H. He and X. Ren (2015). "Circumvention of cisplatin resistance in ovarian cancer by combination of cyclosporin A and low-intensity ultrasound." European Journal of Pharmaceutics and Biopharmaceutics **91**: 103-110.

Yunos, N. M., P. Beale, J. Q. Yu and F. Huq (2011). "Synergism from sequenced combinations of curcumin and epigallocatechin-3-gallate with cisplatin in the killing of human ovarian cancer cells." Anticancer Research **31**(4): 1131-1140.

Yunos, N. M., P. Beale, J. Q. Yu and F. Huq (2011). "Synergism from the combination of oxaliplatin with selected phytochemicals in human ovarian cancer cell lines." Anticancer research **31**(12): 4283-4289.

Yunos, N. M., P. Beale, J. Q. Yu, D. Strain and F. Huq (2010). "Studies on combinations of platinum with paclitaxel and colchicine in ovarian cancer cell lines." Anticancer research **30**(10): 4025-4037.

Zamble, D. B. and S. J. Lippard (2006). The Response of Cellular Proteins to Cisplatin-Damaged DNA. Cisplatin, Verlag Helvetica Chimica Acta**:** 71-110.

Zeng, G.-f., S.-h. Zong, Z.-y. Zhang, S.-w. Fu, K.-k. Li, Y. Fang, L. Lu and D.-q. Xiao (2015). "The role of 6-gingerol on inhibiting amyloid β protein-induced apoptosis in PC12 Cells." Rejuvenation research **18**(5): 413-421.

Zhang, N., J.-N. Fu and T.-C. Chou (2016). "Synergistic combination of microtubule targeting anticancer fludelone with cytoprotective panaxytriol derived from panax ginseng against MX-1 cells in vitro: experimental design and data analysis using the combination index method." American journal of cancer research **6**(1): 97.

Zhao, L., L. Liu, S. Wang, Y.-f. Zhang, L. Yu and Y.-q. Ding (2007). "Differential proteomic analysis of human colorectal carcinoma cell lines metastasis-associated proteins." Journal of cancer research and clinical oncology **133**(10): 771-782.

Zhu, S., V. Shanbhag, Y. Wang, J. Lee and M. Petris (2017). "A Role for The ATP7A Copper Transporter in Tumorigenesis and Cisplatin Resistance." Journal of Cancer **8**(11): 1952.

Zwelling, L. A., T. Anderson and K. W. Kohn (1979). "DNA-protein and DNA interstrand cross-linking by cis- and trans-platinum(II) diamminedichloride in L1210 mouse leukemia cells and relation to cytotoxicity." Cancer Res **39**(2 Pt 1): 365-369.

7 APPENDIX

Appendix I: Proteomic method details

Cell lysis Buffer constituents & cell lysis method

Chemicals	Amount
8 M Urea	24.04 g
2 M Thiourea	7.61 g
4 % CHAPS	2.00 g
65 mM DTT	501 µL
mQ water up to	50 mL
Protease inhibitor (1 tablet/ 10 mL)	5 tablets

- Urea was dissolved in 10 mL of mQ water by heating it in a 45°C water bath to avoid carbamylation artifact in Isoelectric focusing (IEF)
- Other chemicals were then added and the volume was made up to 50 mL with mQ water and aliquoted into 10 mL tubes.
- 500 µL of lysis buffer was added to the cell pellets and mixed well. The cells were aspirated repeatedly using a 25-gauge needle to assure that the cells lysed.
- Then, the cells were centrifuged at 13000 rpm for 30 min at 4°C. The supernatant was transferred and aliquoted into new 1.5 mL centrifuge tubes and stored at -80°C until assayed.

Determination of protein concentration

- The lyophilized Bovine serum albumin (BSA) was reconstituted by adding 20 mL of mQ water and mixed well until dissolved. The dye reagent was prepared by diluting 1 part Dye Reagent Concentrate with 4 parts mQ, then filtered through a 0.22 µm membrane filter.
- Then four dilutions of the protein standard were prepared as following

	BSA (µg/mL)	BSA (µL)	mQ water (µL)
1	1400	50	0
2	350	12.5	37.5
3	87.5	12.5	37.5
4	21.88	12.5	37.5

- Using a 96 well plate, 10 µL of protein was pipetted into the corresponding wells then 200 µL of diluted dye reagent was added to all the wells. The plate was then mixed using a microplate mixer and incubated at room temperature for 5 min.
- The absorbance was measured at 595 nm using microplate reader BIO-RAD Model 3550. The following standard curve was used to determine the protein concentration of the samples.

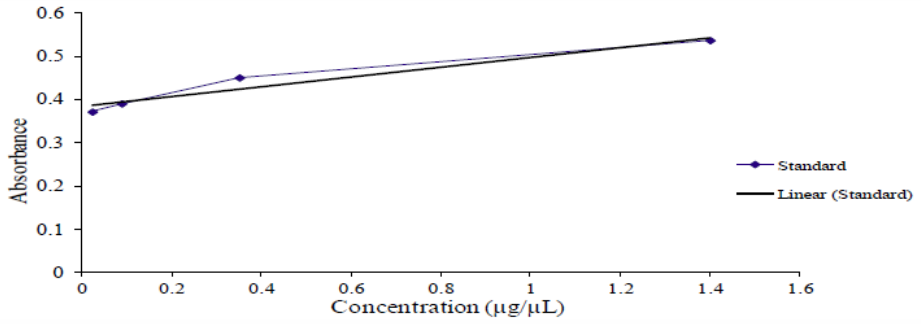

Isoelectric Focusing (IEF)

- 200µg of protein sample was mixed with the rehydration solution (prepared by following table) to a final volume of 180 µL.

Chemicals	Amount
8 M Urea	24 g
2 M Thiourea	7.6 g
60 mM DTT	0.5 g
4 % CHAPS	2 g
0.2 % Carrier ampholyte	250 µL
DeStreak	600 µL
0.0002 % Bromophenol Blue	100 µL
mQ water	to 50 mL

- The rehydration solution/protein sample was pipetted to each slot of the IPG strip rehydration tray. Then, the IPG strip was positioned in slots with the gel facing down. The rehydration tray was left on the orbital shaker overnight.
- After rehydration, dry wicks were placed within the indentation of the channels of the focusing tray and rehydrated with 5-8 µL of mQ water. The wicks were used to collect salts and other contaminants that produce high conductivity which alters the gradient and causes discontinuities in the gel.
- The IPG strip was transferred to the electrophoresis unit for first dimension-IEF with the gel side down.
- Presence of any trapped air bubbles beneath the strips was checked carefully and was removed (if any). Lid onto the tray was placed where positive "+" to the left when the inclined portion of the tray is on the right.

- Then, 2-3 mL of mineral oil was layered on the strip until the strip was completely covered to avoid evaporation of sample and carbon dioxide absorption during focusing.
- Then the focusing tray was placed into the PROTEAN IEF cell and the cover was closed. PROTEAN IEF cell was then programmed and started to initiate the electrophoresis run.
- After completion of electrophoresis run, strips were hold vertically with the forceps to let the mineral oil drain from the strip for ~5 seconds.
- A picture of the strips was then taken using ChemiDocTMMP Imaging system (BIO-RAD, Australia)

Preparation for second dimension gel electrophoresis

Prior to running the second dimension, the IPG strips were equilibrated with the anionic detergent sodium dodecyl sulfate (SDS) solution that denatured these proteins and forms negatively charged protein/SDS complex. Equilibration serves to saturate the IPG strip with the SDS buffer system required for the second-dimension separation. The amount of SDS linked into the protein is directly proportional to its weight, thus proteins that are totally coupled to SDS will migrate in polyacrylamide gel (SDS-PAGE) only due to their weight (which is the bases of the second dimension). The saturation of the IPG strip with SDS buffer was also required to maintain its pH condition in a range appropriate for electrophoresis. The equilibration buffer (EB) was prepared by mixing the required chemicals as stated below until the solution is clear.

Chemicals	**Amount**
SDS	3 g
6 M Urea	36 g
50% Glycerol	24 mL
1.5 M Tris HCl, pH 8.8	40 mL
Bromophenol blue	200 µl
mQ water	to 100 mL

The preparation of 50% Glycerol involved dissolving 50 mL of glycerol in 50 mL of water. Tris HCl (1.5 M) was prepared by adding the water to Tris. Concentrated hydrochloric acid was slowly added to the Tris solution until the pH 8.8 was reached.

The Tris solution was made up to 100 mL. The amounts of the chemicals used were listed as below:

Chemicals	Amount
Tris	18.18 g
Double distilled water	to 80 mL
4 M HCl	7.5 mL
mQ water	to 100 mL

- For the first equilibration step, 50 mL of the EB was mixed with 0.5 g Dithiothreitol (DTT) to produce EB-DTT solution. DTT ensures that disulfide bridges are broken and preserves the fully reduced state of denatured and unalkylated proteins. Each of the strips was positioned in the slot of a new set of rehydration tray. To each slot in the tray, 4 mL of EB-DTT solution was pipetted onto the gel and it was equilibrated for 15 min on a rocker.
- For the second equilibration step, 50 mL of EB was mixed with 0.5 g iodoacetamide (IAA) to produce EB-IAA solution. The IPG strip was transferred to a new slot of the tray, in which 4 mL of EB-IAA solution was pipetted onto the gel. The strip was equilibrated for 15 min on a rocker. This step helped to reduce point streaking and other artifacts in the second-dimension separation.

Running the gels for 2-D electrophoresis

The second dimension electrophoresis was performed using Criterion™ TGX™ pre-cast gels in a Criterion Dodeca™ Cell separation unit (BIO-RAD, Australia). The unit was composed of a chamber which was filled with Stock solutions of x10 time's concentrated Tris/Glycine/SDS electrophoresis running buffer (ERB) (25 mM Tris,

192 mM Glycine, 0.1% SDS, pH 8.3). The ERB was prepared by mixing all the chemicals listed below:

Chemicals	Amount
Tris base	30.25 g
Glycine	144.1 g
SDS	10 g
mQ water	to 1 L

- The individual gel cassette was removed from the packaging, washed with mQ water and laid on the bench.
- The IPG strip was washed with the electrophoresis buffer and positioned on top of the gel cassette.
- The IPG strip was inserted into the gel cassette until it touched the gel making sure no air bubbles were trapped.
- To seal the gel cassettes, agarose solution was used (BIO-RAD, Australia). Agarose sealing solution was melted using microwave oven at 800W for 1 minute.
- Finally, the gel cassette was inserted into the electrophoresis separating unit. The unit was covered and connected to the power pack. The electrophoresis was run at constant 200 V for 100 min.
- At the conclusion of the SDS-PAGE, the gel cassette was placed into a tray with mQ water, the cassette was opened and the IPG strip was removed.

Gel staining

For visualization of the proteins after separation using 2D-gel Coomasie blue staining was used. The stain was chosen due to its compatibility with protein sequencing by mass spectrometry and for its quality in protein quantitation. Hence, Coomassie blue staining was used for isolating the proteins.

- The gel was stained with 50 mL of Bio-Safe Coomassie Stain (BIO-RAD, Australia) for 60 min, in which the gel was placed on an orbital shaker for the staining period.
- The stain was then discarded, and the gel was washed with mQ for 15-30 min. The water was replaced with fresh water and the gel was left for further washing overnight.
- A picture of the gel was then taken using ChemiDoc™ MP Imaging system (BIO-RAD, Australia).

Gel preservation

In order to prolong the life of the gel, solutions of Sodium Azide (0.005%) was prepared. Sodium Azide (0.005 g) was added to 100 mL of mQ water. Then, to the gel, 100 mL of Sodium Azide solution was added and stored at room temperature for future analysis.

Protein identification

The protein spots were cut and placed in a 96-well plate. The protein gel spots were destained using 120 µL of freshly prepared (50% acetonitrile/50 mM NH_4HCO_3) solution and heated at 37°C for 30 min with mild shaking. The solution was then discarded. The gels were treated with 25 µL acetonitrile (ACN) and left to dry for 15 min. The solution was discarded then the spots were left to dry with the lid left open in the oven at 37°C for 15 min followed by cooling at 4°C. The spots were digested with 10 µL trypsin for 10 min on ice. The trypsin supernatants were placed in 96-well plate at 4°C followed by 10 µL addition of 25 mM NH_4HCO_3 for overnight digestion at 37°C. Trypsin was added to digest the proteins into smaller peptides (before proline and arginine in the amino acid sequence).

The resulting peptides were extracted with 0.1% TFA then extracted and concentrated by C18 zip-tips (Millipore, µ-C18, P10 size) on Xcise (Proteome Systems). A 1 µL aliquot was manually spotted onto a MALDI AnchorChip plate with 1 µL of matrix (CHCA, 1mg/mL in 90% v/v ACN, 0.1% TFA) and left to dry in air.

Data acquisition

Matrix Assisted Laser Desorption Ionisation mass spectrometry (MALDI-MS) was performed with 4800 plus MALDI TOF/TOF Analyser (AB Sciex). A neodymium-doped yttrium aluminum garnet (Nd:YAG) laser (355 nm) was used to irradiate the sample. Spectra were acquired in reflectron MS scan mode in the mass range of 700 to 4000 Da. The instrument was then switched to MS/MS (TOF-TOF) mode where the eight strongest peptides from the MS scan were isolated and fragmented by collision induced dissociation (CID), then re-accelerated to measure their masses and intensities. A near point calibration was applied and would give a typical mass accuracy of 50 ppm or less.

Data processing

The data on peptides masses were exported in a format suitable for submission to the database search program, Mascot (Matrix Science Ltd, London, UK). The peaklists were searched against *Homo sapiens* entries in the SwissProt database. High scores in the database search would indicate a likely match (confirmed and qualified by operator inspection). The protein identification for this study was undertaken at Australian Proteome Analysis Facility (APAF) the infrastructure provided by the Australian Government through the National Collaborative Research Infrastructure Strategy (NCRIS).

Appendix II: Detail of the proteins identified from HT-29 cell line

Spot No.	Protein name (Protein ID)	Alternative names	Primary cellular location	Genes	Molecular function
HT18	NPM (PO6748)	Nucleophosmin, Nucleolar phosphoprotein B23, Nucleolar protein NO38 and Numatrin	Nucleus, cytoskeleton	NPM1	Involved in diverse cellular processes such as ribosome biogenesis, centrosome duplication, protein chaperoning, histone assembly, cell proliferation, and regulation of tumor suppressors p53/TP53 and ARF. Binds ribosome presumably to drive ribosome nuclear export. Associated with nucleolar ribonucleoprotein structures and bind single-stranded nucleic acids. Acts as a chaperonin for the core histones H3, H2B and H4. Stimulates APEX1 endonuclease activity on apurinic/apyrimidinic (AP) double-stranded DNA but inhibits APEX1 endonuclease activity on AP single-stranded RNA. May exert a control of APEX1 endonuclease activity within nucleoli devoted to repair AP on rDNA and the removal of oxidized rRNA molecules. In concert with BRCA2, regulates centrosome duplication. Regulates centriole duplication: phosphorylation by PLK2 is able to trigger centriole replication. Negatively regulates the activation of EIF2AK2/PKR and suppresses apoptosis through inhibition of EIF2AK2/PKR autophosphorylation. Antagonizes the inhibitory effect of ATF5 on cell proliferation and relieves ATF5-induced G2/M blockade. In complex with MYC enhances the transcription of MYC target genes

HT22	ACTB (P60709)	Actin cytoplasmic 1 protein,	Cytoskeleton	ACTB	Actins are highly conserved proteins that are involved in various types of cell motility and are ubiquitously expressed in all eukaryotic cells.
HT31	TBB5 (P07437)	Tubulin beta chain protein, Tubulin beta-5 chain	Cytoskeleton	TUBB	Tubulin is the major constituent of microtubules. It binds two moles of GTP, one at an exchangeable site on the beta chain and one at a non-exchangeable site on the alpha chain.
HT39	HSP7C (P11142)	Heat shock cognate 71 kDa protein	Cell membrane Nucleus nucleolus Cytoplasm Melanosome	HSPA8	Molecular chaperone implicated in a wide variety of cellular processes, including protection of the proteome from stress, folding and transport of newly synthesized polypeptides, activation of proteolysis of misfolded proteins and the formation and dissociation of protein complexes. Plays a pivotal role in the protein quality control system, ensuring the correct folding of proteins, the re-folding of misfolded proteins and controlling the targeting of proteins for subsequent degradation. This is achieved through cycles of ATP binding, ATP hydrolysis and ADP release, mediated by co-chaperones. The co-chaperones have been shown to not only regulate different steps of the ATPase cycle of HSP70, but they also have an individual specificity such that one co-chaperone may promote folding of a substrate while another may promote degradation. The affinity of HSP70 for polypeptides is regulated by its nucleotide bound state. In the ATP-bound form, it has a low affinity for substrate proteins. However, upon hydrolysis of the ATP to ADP, it undergoes a conformational change that increases its affinity for substrate proteins. HSP70 goes through repeated cycles

					of ATP hydrolysis and nucleotide exchange, which permits cycles of substrate binding and release. The HSP70-associated co-chaperones are of three types: J-domain co-chaperones HSP40s (stimulate ATPase hydrolysis by HSP70), the nucleotide exchange factors (NEF) such as BAG1/2/3 (facilitate conversion of HSP70 from the ADP-bound to the ATP-bound state thereby promoting substrate release), and the TPR domain chaperones such as HOPX and STUB1. Acts as a repressor of transcriptional activation. Inhibits the transcriptional coactivator activity of CITED1 on Smad-mediated transcription. Component of the PRP19-CDC5L complex that forms an integral part of the spliceosome and is required for activating pre-mRNA splicing. May have a scaffolding role in the spliceosome assembly as it contacts all other components of the core complex. Binds bacterial lipopolysaccharide (LPS) and mediates LPS-induced inflammatory response, including TNF secretion by monocytes. Participates in the ER-associated degradation (ERAD) quality control pathway in conjunction with J domain-containing co-chaperones and the E3 ligase STUB1.
HT55	K2CB (P04259)	Keratin, type II cytoskeletal 6B, Cytokeratin-6B, Keratin-6B, Type-II keratin Kb10	Cytoskeleton Keratin Filament Cytosol Reactome Extracellular region or Secreted	KRT6B	There are at least six isoforms of human type II keratin-6 (K6). There are two types of cytoskeletal and microfibrillar keratin, I (acidic) and II (neutral to basic) (40-55 and 56-70 kDa, respectively).

			Extracellular Exosome		
HT134	GSTP1 (P09211)	Glutathione S-transferase P, GST class-pi, GSTP1-1	Mitochondrion Nucleus Cytoplasm	GSTP1	Conjugation of reduced glutathione to a wide number of exogenous and endogenous hydrophobic electrophiles. Regulates negatively CDK5 activity via p25/p35 translocation to prevent neurodegeneration.

Appendix III: Detail of the protein identified from CACO-2 cell line

Spot No.	Protein name (Protein ID)	Alternative names	Primary cellular location	Genes	Molecular function
CA35	K2CB (P P04259)	Keratin, type II cytoskeletal 6B, Cytokeratin-6B, Keratin-6B, Type-II keratin Kb10	Cytoskeleton Keratin Filament Cytosol Reactome Extracellular region or Secreted Extracellular Exosome	KRT6B	There are at least six isoforms of human type II keratin-6 (K6). There are two types of cytoskeletal and microfibrillar keratin, I (acidic) and II (neutral to basic) (40-55 and 56-70 kDa, respectively).
CA37	HSP7C (P11142)	Heat shock cognate 71 kDa protein	Cell membrane Nucleus nucleolus Cytoplasm Melanosome	HSPA8	Molecular chaperone implicated in a wide variety of cellular processes, including protection of the proteome from stress, folding and transport of newly synthesized polypeptides, activation of proteolysis of misfolded proteins and the formation and dissociation of protein complexes. Plays a pivotal role in the protein quality control system, ensuring the correct folding of proteins, the re-folding of misfolded proteins and controlling the targeting of proteins for subsequent degradation. This is achieved through cycles of ATP binding, ATP hydrolysis and ADP release, mediated by co-chaperones. The co-chaperones have been shown to not only regulate different steps of the ATPase cycle of HSP70, but they also have an individual specificity such that one co-chaperone may promote folding of a substrate while another may promote degradation. The affinity of HSP70 for polypeptides is regulated by its

					nucleotide bound state. In the ATP-bound form, it has a low affinity for substrate proteins. However, upon hydrolysis of the ATP to ADP, it undergoes a conformational change that increases its affinity for substrate proteins. HSP70 goes through repeated cycles of ATP hydrolysis and nucleotide exchange, which permits cycles of substrate binding and release. The HSP70-associated co-chaperones are of three types: J-domain co-chaperones HSP40s (stimulate ATPase hydrolysis by HSP70), the nucleotide exchange factors (NEF) such as BAG1/2/3 (facilitate conversion of HSP70 from the ADP-bound to the ATP-bound state thereby promoting substrate release), and the TPR domain chaperones such as HOPX and STUB1. Acts as a repressor of transcriptional activation. Inhibits the transcriptional coactivator activity of CITED1 on Smad-mediated transcription. Component of the PRP19-CDC5L complex that forms an integral part of the spliceosome and is required for activating pre-mRNA splicing. May have a scaffolding role in the spliceosome assembly as it contacts all other components of the core complex. Binds bacterial lipopolysaccharide (LPS) and mediates LPS-induced inflammatory response, including TNF secretion by monocytes. Participates in the ER-associated degradation (ERAD) quality control pathway in conjunction with J domain-containing co-chaperones and the E3 ligase STUB1.
CA39	GRP78 (P11021)	78 kDa glucose-regulated protein,	Endoplasmic reticulum	GRP78	Plays a role in facilitating the assembly of multimeric protein complexes inside the endoplasmic reticulum.

		Endoplasmic reticulum lumenal Ca(2+)-binding protein grp78, Heat shock 70 kDa protein 5, Immunoglobulin heavy chain-binding protein	Melanosome Cytoplasm		Involved in the correct folding of proteins and degradation of misfolded proteins via its interaction with DNAJC10, probably to facilitate the release of DNAJC10 from its substrate.
CA53	PSB6 (B8BZW7)	Proteasome subunit beta type-6	Nucleus Cytoplasm	PSB6	Component of the 20S core proteasome complex involved in the proteolytic degradation of most intracellular proteins. This complex plays numerous essential roles within the cell by associating with different regulatory particles. Associated with two 19S regulatory particles, forms the 26S proteasome and thus participates in the ATP-dependent degradation of ubiquitinated proteins. The 26S proteasome plays a key role in the maintenance of protein homeostasis by removing misfolded or damaged proteins that could impair cellular functions, and by removing proteins whose functions are no longer required. Associated with the PA200 or PA28, the 20S proteasome mediates ubiquitin-independent protein degradation. This type of proteolysis is required in several pathways including spermatogenesis (20S-PA200 complex) or generation of a subset of MHC class I-presented antigenic peptides (20S-PA28 complex). Within the 20S core complex, PSMB6 displays a peptidylglutamyl-hydrolizing activity also termed postacidic or caspase-

					like activity, meaning that the peptides bond hydrolysis occurs directly after acidic residues.
CA85	COF1 (P23528)	Cofilin-1, 18 kDa phosphoprotein, Cofilin, non-muscle isoform	Plasma membrane Cytoskeleton Nucleus	CFL1, CFL	Binds to F-actin and exhibits pH-sensitive F-actin depolymerizing activity. Regulates actin cytoskeleton dynamics. Important for normal progress through mitosis and normal cytokinesis. Plays a role in the regulation of cell morphology and cytoskeletal organization. Required for the up-regulation of atypical chemokine receptor ACKR2 from endosomal compartment to cell membrane, increasing its efficiency in chemokine uptake and degradation.
CA125	IDHC (O75874)	Isocitrate dehydrogenase [NADP] cytoplasmic, Cytosolic NADP-isocitrate dehydrogenase, NADP(+)-specific ICDH, Oxalosuccinate decarboxylase	Peroxisome Cytoplasm	IDH1	IDHC enzymes are include three enzymes IDH1, IDH2 and IDH3. IDH1 and IDH2 converts isocitrate to 2-ketoglutarate and as a result of NADPH is produces. This NADPH produced from isocitrate dehydrogenase 1 is involved in the breakdown of fats for energy, and it also protects cells from ROS (potentially harmful molecules called reactive oxygen species).
CA166	K1C18	Cytokeratin-18 , Keratin-18, Cell proliferation-inducing gene 46 protein	Nucleus Perinuclear region	KRT18	Involved in the uptake of thrombin-antithrombin complexes by hepatic cells (By similarity). When phosphorylated, plays a role in filament reorganization. Involved in the delivery of mutated CFTR to the plasma membrane. Together with KRT8, is involved in interleukin-6 (IL-6)-mediated barrier protection.